

Nucleoside Analogue Containing Nanoparticle for Therapeutic Management of Leukemia

Thesis submitted by

Manisheeta Ray

Doctor of Philosophy (Science)

School of Materials Science & Nanotechnology

Faculty of Interdisciplinary Studies, Law & Management (FISLM)

Jadavpur University

Kolkata-700032

India

2025

JADAVPUR UNIVERSITY
KOLKATA – 700032, INDIA
REGISTRATION NUMBER- S-21/381/22

1. TITLE OF THE THESIS:

Nucleoside Analogue Containing Nanoparticle for Therapeutic Management of Leukemia

2. NAME, DESIGNATION & INSTITUTION OF SUPERVISOR:

Dr. Biswajit Mukherjee
Professor
Department of Pharmaceutical Technology
Jadavpur University
Kolkata: 700032

3. LIST OF PUBLICATION (RELATED TO THESIS):

- ❖ Ray, M., Al Hoque, A., Chatterjee, S., Adhikary, S., Paul, S., Mukherjee, B., & Bhattacharya, A. (2025). Clofarabine-loaded aptamer-conjugated biodegradable nanoparticle successfully targeted CD117 overexpressed HL60 cells and potentially induced apoptosis. *Heliyon*.

4. LIST OF OTHER PUBLICATIONS:

- ❖ Adhikary, S., Al Hoque, A., Ray, M., Pal, P., Chaudhuri, M. G., & Dey, R. (2024). Tailored Transdermal Drug Delivery System for Pain Management: Development and Evaluation of Clonidine Hydrochloride/Sodium Montmorillonite Composite Patch. *BioNanoScience*, 14(2), 1651-1664.
- ❖ Mallick, S., Barman, M., Mukherjee, B., Halder Hota, S., Ray, M., (2023). Future Prospects of Nano-Therapeutics in Cancer Treatment. *Novel Molecular Oncotargets and Nano-Oncotherapeutics* (Chapter: 16). Cambridge Scholars Publishing.
- ❖ Adhikary, S., Al Hoque, A., Ray, M., Paul, S., Hossain, A., Goswami, S., & Dey, R. (2023). Investigation of paracetamol entrapped nanoporous silica nanoparticles in transdermal drug delivery system. *Applied Biochemistry and Biotechnology*, 195(8), 4712-4727.
- ❖ Mukherjee, B., Dutta, L., Kumari, L., Rajagopalan, M., Bhattacharya, S., Ray, M., & Chakraborty, S. (2022). Nonionic surfactant nanovesicles for cosmeceutical applications. In *Nanocosmeceuticals* (pp. 327-345). Academic Press.
- ❖ Mukherjee, B., Rajagopalan, M., Chakraborty, S., Ghosh, P., Ray, M., Sen, R., & Ehsan, I. (2022). Hepatocellular carcinoma: diagnosis, molecular pathogenesis, biomarkers, and conventional therapy. In *Nanotherapeutics for the Treatment of Hepatocellular Carcinoma* (pp. 1-97). Bentham Science Publishers.
- ❖ Mukherjee, B., Kumari, L., Ehsan, I., Ghosh, P., Banerjee, S., Chakraborty, S., ... & Sahoo, R. (2021). Guar gum-based nanomaterials in drug delivery and biomedical applications. In *Biopolymer-based nanomaterials in drug delivery and biomedical applications* (pp. 143-164). Academic Press.
- ❖ Mukherjee, B., Sengupta, S., Banerjee, S., Dhara, M., Al Hoque, A., Kumari, L., ... & Mukherjee, A. (2020). Transdermal Nanomedicines for Reduction of Dose and Site-Specific Drug Delivery. *Nano Medicine and Nano Safety: Recent Trends and Clinical Evidences*, 175-211.

5. LIST OF PATENTS: NIL

6. LIST OF PRESENTATIONS IN NATIONAL /INTERNATIONAL CONFERENCE:

- ❖ Presented a poster at the National Seminar on “Advancing Healthcare Through Pharmaceutical and Biomedical Applications” in 2024 at the Department of Pharmaceutical Technology, Jadavpur University.
- ❖ Paper presentation under the auspices of METALLIX'24, the annual national symposium for Metallurgical and Material Engineering department, Jadavpur University (2024).
- ❖ Certified for presenting a paper at the International Seminar on Modern Medicine and Rational Use of Medicine-A Challenge in 2025 organized by IAPST, CARPS (JU), CDMU and WBVHA.
- ❖ Certified Best Oral Presentation for presenting a paper at the International Conference HEALTHMEDICON 2025 on Unveiling Opportunities in Global Healthcare Landscape: Scientific Advancements, Innovations & Recent Trends in collaboration with Universiti of Teknologi MARA (UiTM), Malaysia.
- ❖ Certified Best Oral Presentation for presenting paper at the National Seminar on Drugs and Biologics: Discovery, Development and Clinical Evaluation, Central University of Kerala (2025), Kasaragod, Periyekulam, Kerala.

STATEMENT OF ORIGINALITY

I, Miss Manisheeta Ray, registered on 26th September 2022, hereby declare that the thesis entitled “**Nucleoside Analogue Containing Nanoparticle for Therapeutic Management of Leukemia**” embodies the results of my original research work and an extensive literature review carried out as part of my doctoral studies.

I affirm that all information presented in this thesis has been obtained and documented in accordance with prevailing academic standards and ethical guidelines. Wherever the work of others has been cited or used, it has been appropriately acknowledged and referenced.

Furthermore, I declare that this thesis has been subjected to plagiarism screening using iThenticate software, in compliance with the “Policy on Anti-Plagiarism, Jadavpur University, 2019.” The overall similarity index of the thesis stands at 7%, which is within the acceptable limit as per the University norms.

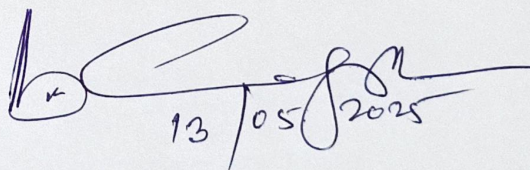
Manisheeta Ray

Signature of Candidate:

Date: 13/05/2025

Certified by Supervisor:

(Signature with date and seal)

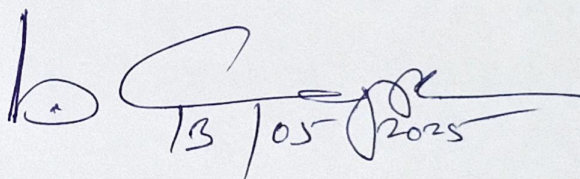

13/05/2025

Professor (Dr.) Biswajit Mukherjee
Department of Pharmaceutical Technology
Jadavpur University
Kolkata-700032, India

CERTIFICATE FROM THE SUPERVISOR

This is to certify that the thesis entitled “**Nucleoside Analogue Containing Nanoparticle for Therapeutic Management of Leukemia**”, submitted by Miss Manisheetta Ray for the award of the PhD (Science) degree at Jadavpur University, is the result of her original research carried out under the supervision of Prof. (Dr.) Biswajit Mukherjee. It is further certified that neither this thesis nor any part of it has been submitted previously for the award of any degree, diploma, or other academic award elsewhere.

Signature of Supervisor:

Handwritten signature of Professor (Dr.) Biswajit Mukherjee, including the date 13/05/2025.

Date:

Professor (Dr.) Biswajit Mukherjee
Department of Pharmaceutical Technology
Jadavpur University
Kolkata-700032, India



ACKNOWLEDGEMENT

The completion of my Ph.D. journey marks a significant milestone in my academic and personal life, and it would have not been possible without the support, encouragement, and contributions of many individuals. I take this opportunity to express my sincere gratitude to all those who have been part of this important chapter.

First and foremost, I would like to express my deepest gratitude to my supervisor, **Prof. (Dr.) Biswajit Mukherjee**, Department of Pharmaceutical Technology, Jadavpur University, for his constant guidance, encouragement, and valuable suggestions throughout the course of my research. Coming from a background in Botany, both at the undergraduate and postgraduate levels, the transition to the field of Pharmaceutics was undoubtedly challenging. However, Prof. Mukherjee's unwavering support, patient mentorship, and belief in my abilities made this transition much smoother. He never allowed me to feel out of place due to my academic background, and his constant reassurance strengthened my confidence to take on new challenges and broaden my horizons.

I would like to sincerely thank **Dr. Saptarshi Chatterjee**, Assistant Professor, Department of Microbiology, School of Life Science & Biotechnology, Adamas University, for kindly providing access to the cell culture laboratory, which was essential for carrying out key parts of my experimental work. His timely support and encouragement have been greatly helpful in the smooth progress of my research.

My heartfelt appreciation goes to **Dr. Amitava Sengupta**, Senior Principal Scientist, CSIR-IICB TRUE, Kolkata for generously providing the cell line necessary for my experiments. His support played a crucial role in enabling important aspects of my project.

I am also thankful to **Dr. Sourav Sarkar**, Professor, former Director, School of Materials Science and Nanotechnology, Jadavpur University, and **Dr. Mahua Ghosh Chowdhury**, Director and Associate Professor, School of Materials Science and Nanotechnology, for their assistance and support during my Ph.D. registration and administrative formalities. Their timely help ensured that necessary procedures were completed efficiently, allowing me to focus on my research without administrative hurdles.

I would like to extend my heartfelt thanks to all my labmates for their continuous support, collaboration, and friendship throughout this journey. I would sincerely thank all my fellow lab members for creating an environment that felt like a home away from home. I am especially

grateful to **Dr. Ashique Al Hoque** and **Dr. Sourav Adhikary** for their constant support, valuable suggestions, and generous help in various aspects of my work. I also sincerely thank my lab seniors **Dr. Apala Chakraborty**, **Dr. Samrat Chakraborty**, **Dr. Ramkrishna Sen**, **Dr. Leena Kumari**, and **Dr. Iman Ehsan** for their guidance, encouragement, and positive spirit.

I would also like to extend my heartfelt gratitude to Prof. Mukherjee's family, **Mrs. Dipa Mukherjee (Madam)**, his daughter **Mrs. Alankar Mukherjee (Pinky)**, and his son **Mr. Avinaba Mukherjee (Gullu)** for their warmth and kindness. Their affectionate gestures and the welcoming environment they created made me feel at home. Their support, has been a comforting and motivating presence throughout my journey.

Above all, I express my deepest and most heartfelt gratitude to my parents, **Dr. Rajat Ray** and **Mrs. Madhumita Ray**, whose unconditional love, support, and sacrifices have been the foundation of all my achievements. I am especially indebted to my father, Dr. Rajat Ray, who, through his association with Adamas University, extended invaluable indirect support in facilitating access to certain research-related resources, easing many practical aspects of my work. Beyond his professional contributions, his unwavering financial support and constant encouragement gave me the strength to overcome every hurdle along the way. His silent yet powerful presence has been a pillar of strength, and I owe a great part of this journey's success to his sacrifices and belief in my dreams. My mother's endless patience, unconditional love, and emotional support have been equally vital, silently inspiring me to persevere even through the most challenging times.

Finally, I extend my sincere thanks to everyone who, directly or indirectly, contributed to my academic journey. Every piece of advice, every word of encouragement, and every gesture of support has left a lasting impact on me and my work.

With deep respect and sincere gratitude,

Manisheeta Ray

PREFACE

The research work presented in this thesis, submitted for the award of the Doctor of Philosophy (Science), has been carried out under the supervision of Prof. (Dr.) Biswajit Mukherjee at the Department of Pharmaceutical Technology, Jadavpur University, Kolkata.

The present study, entitled “Nucleoside Analogue Containing Nanoparticle for Therapeutic Management of Leukemia”, is based on the development of a novel targeted drug delivery system aimed at addressing the challenges in the treatment of leukemia therapy. Acute myeloid leukemia (AML) is a form of leukemia and is a malignant disorder of the hematopoietic system, which continues to cause therapeutic difficulties due to drug resistance, systemic toxicity, and non-specific distribution of chemotherapeutic agents. Conventional treatment approaches often compromise healthy tissues, leading to severe side effects and suboptimal outcomes.

To overcome these limitations, this research focuses on the design and formulation of poly(lactic-co-glycolic acid) (PLGA) nanoparticles encapsulating clofarabine, a potent nucleoside analogue used in leukemia treatment. The novelty of the study lies in the functionalization of these nanoparticles with a single-stranded DNA aptamer specific for the CD117 (c-Kit) receptor, which is overexpressed on AML cells.

This thesis details the systematic formulation and optimization of the aptamer-conjugated clofarabine-loaded PLGA nanoparticles (Apt-CNP), followed by comprehensive characterization through various physicochemical techniques to confirm particle size, surface charge, drug encapsulation efficiency, and aptamer conjugation. Furthermore, biological evaluations were conducted to assess cellular uptake, cytotoxicity, and targeted efficacy against leukemia cells, thereby demonstrating the enhanced therapeutic potential and specificity of the developed nanoparticle system compared to the free drug.

By combining the approaches of nanotechnology and pharmaceutical formulation, this research aims to improve the therapeutic approach for leukemia by addressing the drawbacks of conventional chemotherapy. The findings presented in this thesis demonstrate a promising nanoparticle-based drug delivery system that offers enhanced selectivity towards leukemia cells, reduce systemic toxicity, and the potential to overcome existing challenges in the treatment of AML. The outcomes of this study are expected to enrich the field of drug delivery and support ongoing efforts to develop more effective treatment options for hematological cancers.

LIST OF ABBREVIATIONS

Abs	Absorbance
AFM	Atomic Force Microscopy
AML	Acute Myeloid Leukemia
ALL	Acute Lymphoblastic Leukemia
ANOVA	Analysis of Variance
Apt-CNP	Aptamer-Conjugated Clofarabine-Encapsulated PLGA Nanoparticles
AUC	Area Under the Curve
AUMC	Area Under the Moment Curve
CAR	Chimeric Antigen Receptor
CD117 (c-KIT)	Cluster of Differentiation 117
CML	Chronic Myeloid Leukemia
CLL	Chronic Lymphocytic Leukemia
CNP	Clofarabine-Encapsulated PLGA Nanoparticles
CRS	Cytokine Release Syndrome
°C	Degree Celsius
DCM	Dichloromethane
DLS	Dynamic Light Scattering
DMSO	Dimethyl Sulfoxide
DNA	Deoxyribonucleic Acid
EDC	1-Ethyl-3-(3-dimethylaminopropyl)carbodiimide
EFS	Event-Free Survival
ELISA	Enzyme-Linked Immunosorbent Assay
EPR	Enhanced Permeation and Retention
FACS	Fluorescence Activated Cell Sorter
FBS	Fetal Bovine Serum
FESEM	Field Emissions Scanning Electron Microscopy
FITC	Fluorescein Isothiocyanate
FTIR	Fourier Transform Infrared Spectroscopy
g	Gram

G-CSF	Granulocyte-Colony Stimulating Factor
GVL	Graft-Versus-Leukemia
HR-TEM	High-Resolution Transmission Electron Microscopy
HSCT	Hematopoietic Stem Cell Transplantation
IC ₅₀	Half Maximal Inhibitory Concentration
ICH	International Council of Harmonization
IV	Intravenous Administration
KBr	Potassium Bromide
K _D	Dissociation Constant
LC-MS/MS	Liquid Chromatography & Mass Spectroscopy
MAbs	Monoclonal Antibodies
MDR	Multidrug Resistance
MDS	Myelodysplastic Syndrome
MPN	Myeloproliferative Neoplasm
MRT	Mean Residence Time
MTT	3-(4,5-Dimethylthiazol-2-Yl)-2,5-Diphenyltetrazolium Bromide
mg	Milligram
ml	Millilitre
NHS	N-hydroxysuccinimide
NK	Natural Killer
nM	Nanomolar
nm	Nanometre
OS	Overall Survival
PBMC	Peripheral Blood Mononuclear Cells
PBS	Phosphate-Buffered Saline
PDB	Protein Data Bank
PEG	Poly(Ethylene Glycol)
PFS	Progression-Free Survival
PGA	Poly(Glycolic Acid)
PLA	Poly(lactic Acid)

PLGA	Poly(Lactic-Co-Glycolic Acid)
RH	Relative Humidity
RPMI	Roswell Park Memorial Institute medium
SCF	Stem Cell Factor
SCT	Stem Cell Transplantation
SELEX	Systematic Evolution of Ligands by Exponential Enrichment
US-FDA	United States-Food and Drug Administration
VEGF	Vascular Endothelial Growth Factor
λ_{\max}	Wavelength of Maximum Absorbance
μg	Microgram
μL	Microlitre
μM	Micromolar

LIST OF CONTENTS

	Page No.
❖ Chapter 1: Introduction	1-25
• Overview of Leukemia and Acute Myeloid Leukemia (AML).....	2-3
• Pathogenesis and Risk Factors of AML.....	4-6
• Symptoms of AML.....	6-9
• Diagnosis of Acute Myeloid Leukemia (AML).....	9-10
• Treatment Strategies for Acute Myeloid Leukemia (AML).....	11-13
• Clofarabine: A Nucleoside Analogue in Leukemia Treatment.....	13-15
• Use of PLGA Nanoparticles: Vehicle for Drug Delivery.....	15-17
• Ligand-Conjugated Drug Delivery for Targeted Therapy.....	17-19
• Future Directions and Emerging Strategies in AML Therapy.....	19
• References.....	20-25
❖ Chapter 2: Literature Review	26-57
• Overview and Molecular Basis of AML.....	27-28
• Types and Sub-Types of AML.....	28
• Current Treatment and Limitations.....	29-31
• Exploring Various Nanoformulations for AML.....	31-32
• PLGA as a Versatile Drug Delivery Vehicle in Cancer Therapy.....	31-35
• Clofarabine in AML Therapy: Mechanisms, Stability, and Emerging Clinical Perspectives.....	35-37
• Aptamers and Antibodies as Ligands in Leukemia Therapy.....	37-40
• Targeting Various Bioreceptors for AML therapy.....	41-41
• CD117- A Promising Biomarker for AML Therapy.....	44
• CD117 Activated Signaling Pathways.....	44-45
• CD117-Expressing Cell Lines: A Promising Tool for AML Research and Targeted Therapy.....	45-47
• CD117-Targeted Aptamer-Conjugated PLGA Nanoparticles: A Novel Strategy for Drug Delivery in AML.....	48
• References.....	49-57
❖ Chapter 3: Objectives and Plan of Work	58-62
❖ Chapter 4: Materials and Equipment	63-67
❖ Chapter 5: Methodology	68-83
• Calibration Curve of Clofarabine.....	69
• Preparation of Clofarabine-Encapsulated PLGA Nanoparticles (CNP)....	69-70
• Preparation of FITC Tagged Clofarabine-Encapsulated PLGA Nanoparticles.....	70
• Drug-Excipients Interaction Study Using Fourier Transform Infrared Spectroscopy (FTIR).....	71
• Analysis of Aptamer and CD117 (c-KIT) Interactions by Molecular Docking.....	71-72
• Aptamer Conjugation on the Surface of Nanoparticles (Apt-CNP)	72-73
• Agarose Gel Electrophoresis.....	73

• Drug Loading and Entrapment Efficiency Study.....	73
• Atomic Force Microscopy (AFM).....	74
• In Vitro Drug Release Study.....	74-45
• Particle Size Distribution and Zeta Potential.....	75
• Field Emissions Scanning Electron Microscopy (FESEM).....	75
• Stability Study of the Nanoparticle.....	76
• High-Resolution Transmission Electron Microscopy (HR-TEM)	76
• In Vitro Cell Cytotoxicity Assay.....	76-77
• In Vitro Cellular Uptake Study.....	77-78
• Cellular Apoptosis Assay.....	78-79
• Mitochondrial Membrane Depolarization Study by JC-1.....	79
• In vivo Pharmacokinetic Activity in Normal Mice.....	79-80
• Statistical analysis.....	80
• References.....	81-83
❖ Chapter 6: Results	84-109
• The Absorption Spectrum of Clofarabine.....	85
• Calibration Curve of Clofarabine.....	85-86
• Drug-Excipients Interaction Study by FTIR.....	86-87
• Analysis of aptamer-CD117 (c-KIT) interactions by molecular docking.....	87-89
• Attachment of aptamer to the surface of nanoparticles.....	89-90
• Percentage of encapsulation efficiency and average drug loading of the formulation.....	90-91
• Measurement of Particle Size Distribution and Zeta Potential and Stability data of the nanoparticles.....	91-92
• Surface morphology of nanoparticle by Field Emissions Scanning Electron Microscopy (FESEM).....	92-93
• Stability Study of the Experimental Nanoparticle.....	94-95
• Internal morphology by transmission electron microscopy (HR-TEM) ...	95-96
• Atomic force microscopy (AFM).....	96-97
• In vitro drug release study.....	97-98
• Apt-CNP had variable IC50 values in HL60 and U937 cells, and non-toxic to Peripheral Blood Mononuclear Cells (PBMC).....	98-100
• FITC-Apt-CNP showed maximum cellular internalization in vitro among the treatment groups.....	101-103
• Apt-CNP treatment showed maximum cellular apoptosis in HL60 cells.....	103-105
• Apt-CNP treatment predominantly enhanced mitochondrial membrane depolarization.....	105-106
• In Vivo Pharmacokinetic Study.....	106-108
• References.....	109
❖ Chapter 7: Discussion	110-126
• Reference.....	124-126
❖ Chapter 8: Conclusion	127-129
❖ Chapter 9: Summary	130-132
❖ Annexure	

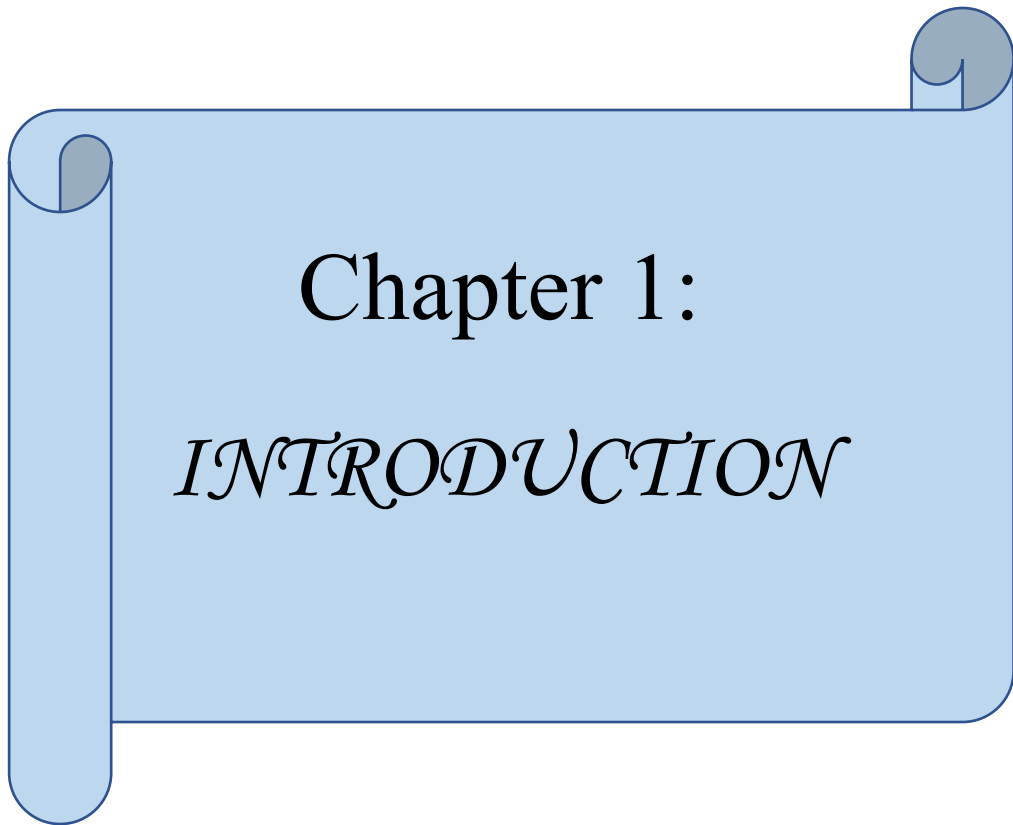
LIST OF FIGURES

Figure No.	Description	Page No.
Chapter 1: Introduction		
Figure 1.1.	Origin of Acute Myeloid Leukemia	4
Figure 1.2.	Symptoms of Acute Myeloid Leukemia	7
Chapter 3: Objectives and Plan of Work		
Figure 3.1.	Graphical Abstract representing the plan of work	62
Chapter 6: Results		
Figure 6.1.	The UV absorption maxima of clofarabine in PBS buffer 7.4	85
Figure 6.2.	Calibration Curve of Clofarabine at 263nm	86
Figure 6.3.	Drug excipient interaction study results obtained through FTIR spectroscopy	87
Figure 6.4.A.	Aptamer-CD117 receptor interactions by hydrogen bonding through in silico molecular docking	89
Figure 6.4.B.	Aptamer-CD117 receptor hydrophobic interactions through in silico molecular docking	89
Figure 6.5.	Agarose gel electrophoresis confirming the conjugation of aptamer to the drug-loaded nanoparticle	90
Figure 6.6.	Particle size measurement of CNP and Apt-CNP by Dynamic Light Scattering (DLS)	91
Figure 6.7.A.	Zeta potential value of CNP	92
Figure 6.7.B.	Zeta potential value of Apt-CNP	92
Figure 6.8.A.	FESEM image of freshly prepared nanoformulations	93
Figure 6.8.B.	FESEM image of freshly prepared nanoformulations	93
Figure 6.9.	Stability Study of the Experimental Nanoparticle	94
Figure 6.10.A	Internal morphology by transmission electron microscopy (HR-TEM)	96
Figure 6.10.B	Atomic force microscopy (AFM)	96
Figure 6.11.	In vitro drug release study of the experimental nanoformulations	98

Figure 6.12.	In vitro cell cytotoxicity assay of the experimental nanoformulations on HL60 cells	99
Figure 6.13.	In vitro cell cytotoxicity assay of the experimental nanoformulations on U937 cells	100
Figure 6.14.	In vitro cell cytotoxicity assay of the experimental nanoformulations on PBMC cells	100
Figure 6.15.	In vitro cellular uptake study of the experimental nanoformulations on HL60 and U937 cells by using flow cytometer	102
Figure 6.16.	Cellular apoptosis assay of the nanoformulations on HL60 and U937 cells by using flow cytometer	104
Figure 6.17.	Cellular mitochondrial membrane depolarisation study by using JC-1 on HL60 cells	106
Figure 6.18.	In vivo pharmacokinetic profile of the experimental nanoformulations on normal mice	108

LIST OF TABLES

Table No.	Description	Page No.
Chapter 6: Results		
Table 1.	Aptamer-CD117 (c-KIT) binding using molecular docking technique	88
Table 2.	Regression coefficient (R ²) values of in vitro drug release data employed in various kinetic models	97
Table 3.	Pharmacokinetic parameters of experimental nanoformulations	107



Chapter 1:

INTRODUCTION

1. Introduction

1.1. Overview of Leukemia and Acute Myeloid Leukemia (AML)

Leukemia holds significant emotional and societal impact due to its relatively high prevalence and often poor survival rates. It is the most common form of cancer in children and ranks among the top 15 most prevalent cancers in adults, according to the World Health Organization. It is a hematological malignancy indicated by the uncontrolled proliferation of abnormal white blood cells, originating primarily in the bone marrow (Shafat et al., 2017). This overproduction of immature or dysfunctional leukocytes interferes with the bone marrow's ability to produce healthy blood cells, resulting in a range of symptoms related to anemia, immunosuppression, and bleeding disorders. Leukemia can be broadly classified into acute, (which progresses quickly) and chronic forms, (which progresses slowly). The types of acute leukemia involves, Acute Myeloid Leukemia (AML) and Acute Lymphoblastic Leukemia (ALL). The types of chronic leukemia involves, Chronic Myeloid Leukemia (CML), Chronic Lymphocytic Leukemia (CLL). Acute leukemias, such as AML, advances rapidly and requires immediate intervention. Leukemia is considered particularly challenging cancer to treat due to its aggressive nature, complexity, and resistance mechanisms. Despite advances in chemotherapy, stem cell transplantation, and targeted therapies, the prognosis remains dismal for many patients, especially older adults or those with relapsed or refractory disease. One of the primary difficulties lies in its rapid progression rate. In AML, the myeloid lineage is specifically affected, leading to the accumulation of poorly differentiated myeloid cells (Figure 1.1) in the bone marrow and peripheral blood (Obeagu et al., 2021). Genetic mutations within hematopoietic stem cells, often triggered by environmental exposures (e.g., chemicals like benzene, prior chemotherapy or radiation), initiate the leukemogenic process. Leukemia originates in the bone marrow, affecting the body's blood-forming system, which complicates treatment as the disease is spread throughout the bloodstream rather than being localized, making surgical options unfeasible. Traditional chemotherapy, although effective in reducing leukemic cells, often results in severe side effects like myelosuppression, hepatotoxicity, and immunosuppression, due to its impact on both cancerous and healthy rapidly dividing cells (Liu et al., 2021). Moreover, leukemia cells can develop drug resistance over time, either through genetic mutations or alterations in cell signaling pathways, leading to relapsed or refractory disease. Many leukemia patients also have underlying health conditions that limit

their ability to tolerate high-intensity treatments, further complicating therapeutic options. The variability in genetic mutations among patients with leukemia adds another layer of complexity, as each mutation can influence treatment response and prognosis differently (Vecchio et al., 2013). These factors highlight the need for more targeted approaches, such as personalized medicine and ligand-conjugated drug delivery systems, which offer potential for more effective and safer leukemia treatments by selectively targeting cancer cells while sparing healthy ones. With the advancement of chemotherapy, stem cell transplantation, and targeted therapies the outcomes have improved, still, AML remains difficult to treat due to its aggressive nature, high relapse rates, and drug resistance. Current research focuses on developing targeted therapies, such as ligand-conjugated nanoparticles that deliver drugs directly to leukemia cells, minimizing systemic toxicity and overcoming resistance, which is an approach that shows promise in enhancing therapeutic efficacy and reducing adverse effects (Mauro et al., 2009).

AML is a malignancy originating in the bone marrow, the spongy interior of bones responsible for producing new blood cells. AML primarily impacts the myeloid lineage of blood cells, which are precursors to various mature blood cells, comprising red blood cells, white blood cells, and platelets (Bullinger et al., 2017). This disease is marked by the fast proliferation of abnormal white blood cells which accumulate in the bone marrow, hindering the production of the normal blood cells. Unlike the typical slow progression of chronic leukemias, AML advances swiftly and can become life-threatening within a short timeframe if left untreated. It specifically targets the myeloid cell line, encompassing cells that would normally differentiate into granulocytes (neutrophils, eosinophils, and basophils), monocytes, erythrocytes (red blood cells), and megakaryocytes (platelet-producing cells). The prognosis for AML varies significantly based on factors such as the patient's overall health, age, certain genetic mutations present in the leukemia cells, and the cancer's responsiveness to treatment (Estey, 2020). Although advances in treatment have improved outcomes, AML remains a challenging disease to treat due to its aggressive nature (Döhner et al., 2022).

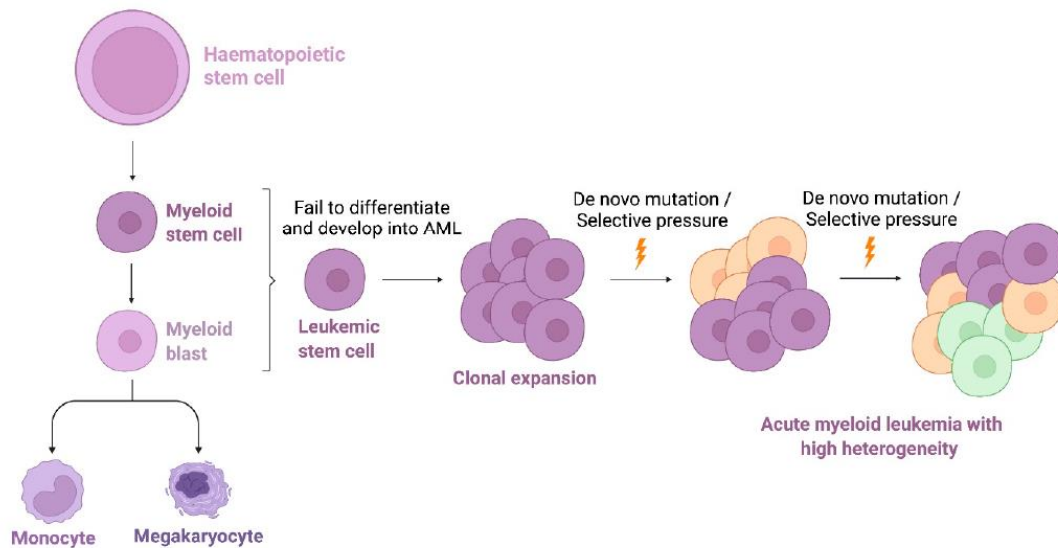


Figure 1.1: Origin of Acute Myeloid Leukemia (Xiang et al., 2022)

1.2. Pathogenesis and Risk Factors of AML

AML can develop due to genetic mutations in the DNA of immature blood cells. The risk of AML is increased by previous chemotherapy or radiation therapy (Obeagu et al., 2021). Exposure to tobacco smoke, which contains benzene and other carcinogens, is also a contributing factor. Prolonged exposure to certain chemicals, notably benzene, has been associated with an elevated risk of AML. Additionally, preexisting blood disorders, such as myelodysplastic syndromes, can progress to AML (Steensma et al., 2003). A family history of leukemia or other blood cancers further increases the susceptibility to this disease.

1.2.1. Genetic Mutations and Susceptibility

The development of AML is linked to genetic mutations in hematopoietic stem cells, which are responsible for generating all types of blood cells. These mutations may be spontaneous or inherited, and they alter the normal processes of cell division and differentiation. The mutations frequently involve genes responsible for regulating cell growth, apoptosis, and DNA repair mechanisms. For example, abnormalities in genes such as *FLT3*, *NPM1*, and *CEBPA* have been commonly observed in AML patients. Some mutations occur randomly without a clear external trigger, others may be induced by environmental or lifestyle factors (Taskesen et al., 2011).

1.2.2. Previous Chemotherapy and Radiation Therapy

A significant risk factor for AML is prior exposure to chemotherapy or radiation therapy, commonly used in the treatment of other cancers (Morton et al., 2013). Alkylating agents and topoisomerase II inhibitors, two classes of chemotherapy drugs, are particularly associated with therapy-related AML (t-AML). These treatments, while effective against the initial cancer, can inadvertently damage the DNA of normal hematopoietic cells, leading to secondary malignancies such as AML. Similarly, radiation therapy, which uses high-energy radiation to eradicate cancer cells, can cause mutations in the bone marrow cells, raising the likelihood of developing AML (Radivoyevitch et al., 2016).

1.2.3. Tobacco Smoke and Benzene Exposure

Lifestyle and environmental exposures also play a significant role in increasing the risk of AML. Tobacco smoke is a well-documented carcinogen that contains benzene and other harmful chemicals (Hecht, 2002). Benzene, a volatile organic compound found in cigarette smoke, industrial emissions, and certain household products, is particularly harmful to the bone marrow. Prolonged benzene exposure can cause DNA damage and interfere with normal hematopoiesis, significantly elevating the risk of leukemia, including AML (McHale et al., 2012). Workers in industries such as chemical manufacturing, oil refining, and shoe production, where benzene exposure is more likely, are at an increased risk of developing this disease.

1.2.4. Preexisting Blood Disorders

Certain preexisting hematological conditions can predispose individuals to AML. Myelodysplastic syndromes (MDS), a group of disorders characterized by ineffective blood cell production and dysplasia, are known to progress to AML in approximately 30% of cases (Saygin & Godley, 2021). Similarly, other blood disorders, such as myeloproliferative neoplasms (MPNs), can also transform into AML over time. The progression from these pre-leukemic conditions to full-blown AML underscores the importance of regular monitoring and early intervention for individuals diagnosed with such disorders.

1.2.5. Family History and Genetic Predisposition

A family history of leukemia or other blood cancers is another significant risk factor for AML. Certain hereditary syndromes, such as Li-Fraumeni syndrome, Fanconi anemia, and familial platelet disorder, are associated with an increased risk of leukemia (Rafei & DiNardo, 2019). These conditions often involve inherited mutations in genes that regulate cell division and DNA repair, making individuals more susceptible to developing AML. Additionally, studies have shown that first-degree relatives of AML patients have a slightly elevated risk of developing the disease themselves, highlighting the role of genetic predisposition in its etiology (Churpek et al., 2013).

1.2.6. Other Contributing Factors

In addition to the aforementioned risk factors, age and gender also influence the likelihood of developing AML. The disease is frequent in older adults, with the average age of diagnosis being around 68 years. This is partly due to the cumulative exposure to environmental toxins and the natural decline in DNA repair mechanisms with age (Saygin & Godley, 2021). Moreover, while AML affects both men and women, it is slightly more prevalent in men, possibly due to higher exposure to occupational and environmental risk factors (Rafei & DiNardo, 2019).

1.3. Symptoms of AML

AML represents a diverse range of clinical symptoms, primarily resulting from the infiltration of abnormal leukemia cells into the bone marrow and their interference with normal hematopoiesis. The resulting disruption of normal hematopoiesis leads to a wide array of clinical symptoms, many of which significantly impact the daily lives of patients. These symptoms originate from the deficiencies in the production of healthy blood cells, which includes red blood cells (RBCs), white blood cells (WBCs), and platelets, as well as the infiltration of leukemic cells into various tissues (Figure 1.2). Clinical presentation of AML varies across patients, but several hallmark symptoms are consistently observed (Adhikary et al., 2025).

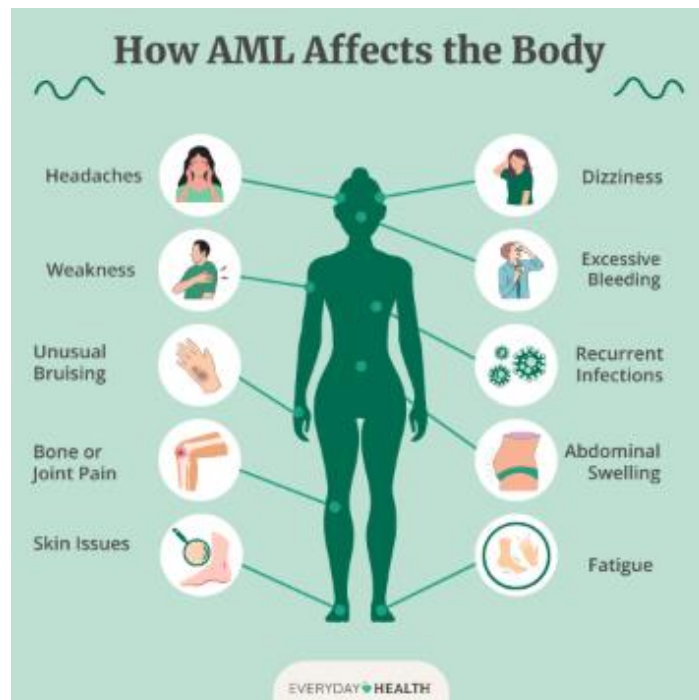


Figure 1.2: Symptoms of Acute Myeloid Leukemia

(<https://www.everydayhealth.com/leukemia/acute-myeloid-leukemia-aml-cancer-refractory-relapsed-prognosis-symptoms-treatment-more>)

1.3.1. Fatigue and Anemia

One of the most prominent symptoms of AML is fatigue, which is closely associated with anemia, a condition characterized by an insufficient number of functional red blood cells. The deficiency of RBCs leads to reduced oxygen delivery to tissues and organs, manifesting as persistent tiredness, reduced physical stamina, and a sense of general weakness. These symptoms often escalate with disease progression, resulting in significant limitations in a patient's ability to carry out routine activities. Anemia in AML is multifactorial in origin, arising from both the suppression of normal erythropoiesis by leukemic infiltration and the competition for nutrients between leukemic cells and healthy hematopoietic cells (Steele & Narendran, 2012).

1.3.2. Increased susceptibility to infections

Another defining feature of AML is an increased susceptibility to infections, which results from a marked reduction in the number and functionality of normal white blood cells. These immune cells play a critical role in defending the body against pathogens, and their depletion creates a

state of immunosuppression. Patients with AML often experience recurrent infections, ranging from mild respiratory tract infections to severe, life-threatening systemic infections such as sepsis. The compromised immune defense in AML patients also contributes to prolonged recovery periods and heightened vulnerability to opportunistic pathogens (Chandran et al., 2012).

1.3.3. Thrombocytopenia and Frequent Bleeding

In addition to anemia and immunosuppression, thrombocytopenia or a reduced platelet count is another hallmark of AML. Platelets are essential for normal blood clotting, and their deficiency predisposes patients to easy bruising and spontaneous bleeding. Common manifestations of thrombocytopenia in AML include frequent nosebleeds (epistaxis), bleeding gums, and the appearance of petechiae, which are pinpoint red or purple spots on the skin caused by subcutaneous bleeding. These bleeding episodes may occur spontaneously or with minimal trauma and can be quite challenging to control, posing a serious risk to the patient's overall health (Kohli et al., 2022).

1.3.4. Bone Pain and Bone Marrow Infiltration

Another symptom frequently reported by AML patients is bone pain, which occurs due to the invasion of leukemic cells into the bone marrow and the surface of bones. This pain is typically localized to long bones, such as those in the legs and arms, and may also affect the ribs and spine. The severity of bone pain can range from mild discomfort to debilitating pain that significantly limits mobility and quality of life. Bone pain in AML patients is often accompanied by tenderness and a feeling of pressure in the affected areas, reflecting the expansion of leukemic cell masses within the marrow (Hamid, 2013).

1.3.5. Systemic Symptoms: Fever and Night Sweats

Systemic symptoms such as fever and night sweats are also commonly observed in AML and are indicative of the body's inflammatory response to the disease. Fever may be a direct consequence of the release of inflammatory cytokines by leukemic cells or may result from underlying infections, given the immune-compromised state of the patient. Night sweats, which are episodes of excessive sweating during sleep, can be particularly distressing, as they disrupt rest and contribute to overall fatigue and malaise. While these symptoms are not unique to

AML and can occur in other malignancies, their presence often raises suspicion of an underlying hematologic or oncologic disorder (Hamid, 2013).

1.3.6. Impact on Quality of Life and Importance of Early Diagnosis

The combination of these symptoms—anemia-related fatigue, infection susceptibility, bleeding tendencies, bone pain, fever, and night sweats—creates a complex clinical picture that significantly affects the physical and emotional well-being of AML patients (Kohli et al., 2022). Beyond the physical manifestations, these symptoms often result in psychological distress, including anxiety and depression, due to the uncertainty and challenges associated with the disease. Early recognition and understanding of these symptoms are critical for prompt diagnosis and initiation of appropriate treatment strategies. Timely intervention not only helps in alleviating these debilitating symptoms but also improves the prognosis and quality of life for individuals affected by AML.

1.4. Diagnosis of Acute Myeloid Leukemia

Diagnosis of AML can be achieved through several methods that includes blood tests, which assess abnormal levels of blood cells; bone marrow aspiration and biopsy, which involve examining bone marrow cells for abnormalities; and genetic testing, which identifies specific genetic mutations that can inform treatment strategies (Percival et al., 2017).

1.4.1. Hematological Assessments

Complete Blood Count (CBC)

Evaluates the counts of red blood cells (RBCs), white blood cells (WBCs), and platelets. A marked reduction in RBCs and platelets, along with an abnormal increase or decrease in WBCs, may indicate AML.

Peripheral Blood Smear

It involves microscopic examination of blood cells to identify the presence of blast cells (immature white blood cells). Leukemic blasts exhibit morphological abnormalities such as an increased nucleus-to-cytoplasm ratio and the presence of Auer rods (rod-shaped cytoplasmic inclusions found in the cytoplasm of myeloid blast cells).

1.4.2. Bone Marrow Evaluation

Bone Marrow Aspiration

A sample of liquid bone marrow is extracted, typically from the iliac crest, for cytological and immunophenotypic analysis.

Bone Marrow Biopsy

A solid core of bone marrow is obtained to assess cellularity, infiltration of leukemic cells, and architectural abnormalities.

Flow Cytometry

It utilized to determine the immunophenotypic profile of cells based on surface and cytoplasmic markers, aiding in the classification of AML subtypes.

1.4.3. Cytogenetic and Molecular Analysis

Conventional Karyotyping

It detects chromosomal aberrations such as translocations, deletions, and inversions that are characteristic of AML.

Fluorescence In Situ Hybridization (FISH)

It identifies specific genetic translocations by using fluorescently labeled probes targeting chromosomal regions of interest.

Polymerase Chain Reaction (PCR) and Next-Generation Sequencing (NGS)

It detects molecular mutations in genes such as *FLT3*, *NPM1*, and *CEBPA*, which have prognostic and therapeutic implications.

Minimal Residual Disease (MRD) Assessment

It is employed post-treatment to detect residual leukemic cells through high-sensitivity techniques like quantitative PCR (qPCR) and multiparametric flow cytometry.

All these diagnostic methodologies collectively provide a comprehensive evaluation of AML, facilitating accurate classification and personalized treatment strategies.

1.5. Treatment Strategies for Acute Myeloid Leukemia

The treatment options for AML include several approaches like supportive care, which involves managing symptoms and side effects through blood transfusions and antibiotics; chemotherapy, the primary treatment option for AML, typically administered in phases (induction, consolidation, and maintenance); stem cell transplant, which replaces diseased bone marrow with healthy stem cells; and targeted therapy, which uses drugs to target the leukemic cells to specifically target genetic mutations or abnormal proteins within the leukemia cells (Kantarjian et al., 2021).

1.5.1. Chemotherapy

Chemotherapy remains the primary treatment option for AML, aiming to eliminate leukemic cells through cytotoxic agents administered in multiple phases (Liu, 2021). The initial phase, known as induction therapy, is designed to achieve complete remission by rapidly reducing the leukemic load. The standard regimen, commonly referred to as the "7+3" protocol, consists of dual chemotherapy drugs, e.g., cytarabine administered continuously for seven days along with an anthracycline for three days. In high-risk cases, targeted agents like *FLT3* inhibitors may be incorporated to improve outcomes. Following induction, consolidation therapy is implemented to eradicate residual leukemia cells and minimize relapse risk (Jimenez-Chillon et al., 2024). High-dose cytarabine is frequently employed, particularly in younger patients with favorable prognostic markers. For those with intermediate or high-risk cytogenetics, allogeneic stem cell transplantation is often recommended during this phase. In some cases, maintenance therapy is introduced to prolong remission, especially in older patients or those ineligible for intensive treatment. Hypomethylating agents like azacitidine and decitabine are commonly used in this setting to suppress leukemia progression while maintaining a better quality of life (Estey, 2013). Although chemotherapy remains highly effective, its associated toxicities include myelosuppression, increased infection risk, drug resistance and high disease relapse rates necessitate careful patient monitoring and supportive care throughout treatment.

1.5.2. Stem Cell Transplantation (SCT)

Stem cell transplantation (SCT) serves as a potentially curative option for AML, particularly for patients at high risk of relapse or those who do not achieve sustained remission with

chemotherapy alone. The procedure involves replacing diseased bone marrow with healthy hematopoietic stem cells, which can be derived from either the patient (autologous SCT) or a compatible donor (allogeneic SCT). Autologous transplantation, where the patient's own stem cells are collected and reinfused after high-dose chemotherapy, is typically reserved for patients in remission who are not candidates for allogeneic transplantation (Cornelissen & Blaise, 2016). In contrast, allogeneic transplantation, which utilizes stem cells from a matched sibling, unrelated donor, or haploidentical donor, offers a graft-versus-leukemia (GVL) effect, wherein donor immune cells recognize and eliminate residual leukemia cells (Gyurkocza & Sandmaier, 2014). Furthermore, this approach also carries risks, such as graft-versus-host disease (GVHD), where the donor's immune system attacks the recipient's healthy tissues. To mitigate these complications, patients undergoing allogeneic SCT require immunosuppressive therapy post-transplant (Zeiser & Blazar, 2017). Despite its challenges and high treatment costs, SCT remains one of the most effective treatment strategies for AML, significantly improving long-term survival in appropriately selected patients.

1.5.3. Targeted Therapy

Targeted therapy in AML focuses on inhibiting specific molecular pathways that drive leukemogenesis, thereby reducing toxicity to normal cells. One of the most significant advancements in this area is the development of *FLT3* inhibitors such as midostaurin and gilteritinib, which are particularly effective in patients harboring *FLT3* mutations, a marker associated with aggressive disease progression (Short et al., 2019). Similarly, *IDH* inhibitors such as ivosidenib (*IDH1* inhibitor) and enasidenib (*IDH2* inhibitor) target metabolic abnormalities caused by mutations in the isocitrate dehydrogenase (IDH) genes, thereby restoring normal hematopoiesis. Another class of targeted agents includes BCL-2 inhibitors such as venetoclax, which promotes apoptosis in leukemia cells and is often combined with hypomethylating agents for elderly or unfit patients. Additionally, monoclonal antibodies like gemtuzumab ozogamicin, a CD33-directed antibody-drug conjugate, selectively bind to leukemia cells expressing CD33, delivering cytotoxic agents directly to malignant cells. CD117 (c-KIT), a transmembrane tyrosine kinase receptor highly expressed in certain AML subtypes, has also emerged as a promising therapeutic target. Inhibitors such as dasatinib and avapritinib are being explored for their potential to suppress aberrant c-KIT signaling, which is implicated in leukemic cell proliferation and survival. These therapies, either as standalone treatments or

in combination with conventional chemotherapy, offer promising outcomes in specific AML subtypes, improving remission rates while minimizing adverse effects (Sheikh et al., 2022).

1.5.4. Supportive Care

Supportive care plays a vital role in the overall management of AML, addressing disease-related complications and mitigating the adverse effects of intensive treatments like chemotherapy and stem cell transplantation. One of the primary supportive measures is blood transfusion therapy, which helps managing anemia and thrombocytopenia that are common consequences of bone marrow failure. Red blood cell transfusions improve oxygen delivery, reducing fatigue and weakness, while platelet transfusions prevent bleeding episodes in thrombocytopenic patients. Another critical component is infection control, as AML patients, particularly those undergoing chemotherapy, are highly susceptible to infections due to prolonged neutropenia. Prophylactic and therapeutic administration of broad-spectrum antibiotics, antifungals, and antivirals is essential in reducing infection-related morbidity and mortality. Additionally, growth factor support, such as granulocyte-colony stimulating factor (G-CSF), is sometimes used to accelerate neutrophil recovery following chemotherapy, minimizing infection risk. Beyond medical interventions, supportive care also includes nutritional support, pain management, and psychological counseling to improve the patient's overall well-being. By integrating these supportive strategies, clinicians can enhance treatment tolerability, reduce complications, and improve the quality of life for AML patients throughout their treatment journey (Izak & Bussel, 2014).

1.6. Clofarabine: A Nucleoside Analogue in Leukemia Treatment

Clofarabine, a second-generation purine nucleoside analogue, has emerged as a critical chemotherapeutic agent for the treatment of acute leukemias, particularly ALL and AML (Zhenchuk et al., 2009). Structurally derived from fludarabine and cladribine, clofarabine exhibits enhanced stability and efficacy in targeting leukemic cells. Its mechanism of action primarily involves the inhibition of key enzymes essential for DNA replication and repair, ultimately leading to apoptosis. Despite its efficacy, the clinical use of clofarabine is associated with significant challenges, including toxicity and the development of drug resistance, which limit its broader therapeutic application.

1.6.1. Mechanism of Action

Clofarabine exerts its cytotoxic effects through multiple pathways, primarily by inhibiting ribonucleotide reductase (RNR), an essential enzyme responsible for deoxyribonucleotide triphosphate (dNTP) synthesis. By depleting the dNTP pool, clofarabine disrupts DNA synthesis, thereby inhibiting the proliferation of rapidly dividing leukemia cells. Additionally, clofarabine directly interferes with DNA polymerases, leading to premature chain termination during DNA replication. This results in the accumulation of DNA damage and ultimately triggers apoptosis in leukemia cells. Another crucial mechanism involves mitochondrial disruption, where clofarabine alters mitochondrial membrane potential, promoting the activation of caspase-dependent pathways that lead to programmed cell death (Dasari et al., 2016). These mechanisms collectively make clofarabine an effective agent in effecting leukemic cells, particularly in cases of refractory or relapsed leukemia.

1.6.2. Efficacy in Hematologic Malignancies

Clofarabine has demonstrated promising efficacy in both pediatric and adult patients with relapsed or refractory acute leukemias. It has been accepted for pediatric patients having ALL who have failed at least two prior treatment regimens, showing significant improvement in remission rates. In AML, clofarabine has been evaluated as a monotherapy and in combination with other agents such as cytarabine, particularly in older patients or those who are unfit for intensive chemotherapy. Clinical trials have highlighted its role in achieving remission and improving survival outcomes in high-risk leukemia patients (Zhenchuk et al., 2009). However, despite these advantages, clofarabine's broad-spectrum cytotoxicity remains a concern, necessitating careful patient selection and dose optimization to balance efficacy with tolerability.

1.6.3. Toxicity and Adverse Effects

One of the major limitations of clofarabine therapy is its dose-dependent toxicity, which affects both malignant and healthy cells. Among its most concerning adverse effects is myelosuppression, leading to profound neutropenia, thrombocytopenia, and anemia, thereby increasing the risk of life-threatening infections and bleeding complications. Additionally, clofarabine has been linked to hepatotoxicity, with elevated liver enzymes and hepatocellular

damage observed in some patients. Nephrotoxicity is another significant concern, as clofarabine is primarily excreted via the kidneys, leading to renal impairment, particularly in patients with preexisting kidney dysfunction. Furthermore, gastrointestinal toxicity, characterized by severe nausea, vomiting, diarrhea, and mucositis, often compromises the patient's overall quality of life. The occurrence of these toxicities underscores the need for supportive care measures, including hydration, prophylactic antimicrobial therapy, and dose adjustments in patients with compromised organ function (Jhaveri et al., 2014).

1.6.4. Drug Resistance and Limitations

Despite its potent anti-leukemic activity, long-term use of clofarabine has been associated with the development of drug resistance, reducing its effectiveness in refractory cases. One of the key mechanisms of resistance involves alterations in nucleoside transporters, which reduce clofarabine uptake into leukemic cells, thereby decreasing intracellular drug concentrations. Additionally, overexpression of anti-apoptotic proteins, such as BCL-2 and MCL-1, can hinder apoptosis, allowing leukemia cells to evade clofarabine-induced cell death. Moreover, mutations in DNA repair pathways may enable leukemic cells to counteract the DNA damage caused by clofarabine, further contributing to resistance (Kantarjian et al., 2007). To mitigate these challenges, combination therapies incorporating BCL-2 inhibitors (e.g., venetoclax) or other targeted agents are being explored to enhance clofarabine's efficacy and overcome resistance mechanisms. One approach is to conjugate clofarabine with specific ligands, such as an aptamer or an antibody, that selectively binds to biomarkers overexpressed on the surface of cancer cells.

1.7. Use of PLGA Nanoparticles: Vehicle for Drug Delivery

The development of nanocarrier-based drug delivery systems has gained significant attention in oncology, particularly for the treatment of hematological malignancies such as AML and ALL. Among various nanocarriers, poly(lactic-co-glycolic acid) (PLGA) nanoparticles have emerged as a promising platform for the targeted delivery of chemotherapeutic agents, including clofarabine. This strategy offers several advantages, including sustained drug release, improved bioavailability, reduced systemic toxicity, and enhanced therapeutic efficacy (Bala et al., 2004). By encapsulating clofarabine within PLGA nanoparticles, its therapeutic index can

be significantly improved, minimizing off-target effects while ensuring efficient drug accumulation at the tumor site.

1.7.1. Advantages of PLGA Nanoparticles

Sustained and Controlled Drug Release

One of the major limitations of conventional chemotherapy is its short plasma half-life, necessitating frequent dosing, which can lead to dose-dependent toxicities. PLGA nanoparticles offer a controlled and sustained drug release profile, ensuring prolonged therapeutic activity while reducing peak plasma concentrations that contribute to systemic toxicity. This controlled release mechanism helps maintain optimal drug levels in circulation, enhancing overall treatment efficacy (Danhier et al., 2012).

Targeted Drug Delivery and Tumor Accumulation

PLGA nanoparticles can be functionalized with targeting ligands, monoclonal antibodies, or aptamers to facilitate active targeting of leukemic cells (Cheng et al., 2007). One of the most relevant targets in AML is CD117 (c-KIT), a transmembrane tyrosine kinase receptor overexpressed on leukemic stem cells. By conjugating anti-CD117 aptamers or antibodies onto the nanoparticle surface, the system can achieve selective binding to AML cells, ensuring precise drug delivery while sparing normal hematopoietic cells. This targeted approach significantly enhances therapeutic efficacy by increasing drug accumulation in leukemic cells and reducing systemic toxicity.

Reduction of Off-Target Toxicity

Clofarabine, while highly effective against leukemia cells, also affects rapidly dividing healthy cells, leading to severe myelosuppression, hepatotoxicity, nephrotoxicity, and gastrointestinal toxicity. The use of PLGA nanoparticles for its delivery helps prevent premature drug release in systemic circulation, thereby reducing off-target toxicity (Jan et al., 2021). This is particularly beneficial for leukemia patients who are often immunocompromised and at risk of severe infections and organ damage due to conventional chemotherapy.

Overcoming Drug Resistance

One of the significant challenges in leukemia therapy is the development of drug resistance, which reduces treatment efficacy over time (Wang et al., 2014). Mechanisms of resistance to clofarabine include altered nucleoside transporter expression, upregulation of anti-apoptotic proteins (BCL-2, MCL-1), and enhanced DNA repair pathways. PLGA nanoparticle-based delivery can help overcome resistance by:

- Increasing intracellular drug concentration, ensuring that adequate levels of clofarabine reach leukemic cells.
- Co-encapsulation of clofarabine with chemosensitizers such as BCL-2 inhibitors (e.g., venetoclax) to promote apoptosis.
- Enhancing endocytosis-mediated drug uptake, bypassing nucleoside transporters involved in drug resistance.

Improved Pharmacokinetics and Biodistribution

PLGA nanoparticles enhance the stability and solubility of clofarabine, preventing its rapid degradation and clearance from circulation (Domaratzki et al., 2009). Their nanoscale size (typically 100–200 nm) allows for enhanced permeation and retention (EPR) effect, facilitating passive accumulation in leukemic tissues. Additionally, surface modifications such as PEGylation (polyethylene glycol coating) help prolong circulation time by reducing opsonization and clearance by the reticuloendothelial system (RES).

1.8. Ligand-Conjugated Drug Delivery for Targeted Therapy

The development of ligand-conjugated drug delivery systems has revolutionized targeted therapy by enhancing drug specificity toward diseased cells while minimizing adverse effects (Srinivasarao et al., 2017). This approach employs various ligands, such as antibodies and aptamers, to facilitate precise drug targeting, particularly in conditions like AML. By improving drug localization at the site of action, ligand-mediated drug delivery optimizes therapeutic efficacy and significantly reduces systemic toxicity.

1.8.1. Advantages of Aptamer-Based Targeting

Among the various ligands utilized in targeted drug delivery, aptamers have gained considerable attention due to their unique properties. Often referred to as synthetic monoclonal antibodies, aptamers are short, single-stranded oligonucleotides that can bind to specific molecular targets with high affinity and selectivity. Compared to traditional monoclonal antibodies, aptamers offer several advantages, including enhanced stability, cost-effectiveness, and lower immunogenicity. Their ability to fold into intricate three-dimensional structures allows them to interact precisely with target molecules, making them an excellent choice for drug conjugation (Giudice et al., 2020).

1.8.2. Reduced Immunogenicity and Enhanced Specificity

Aptamers exhibit minimal immunogenicity, which is a crucial advantage for clinical applications (Zhao et al., 2015). Unlike antibodies, which can trigger unwanted immune responses, aptamers do not provoke significant immune activation, thereby reducing the risk of hypersensitivity reactions. Furthermore, their ability to bind selectively to target cells, such as AML cells overexpressing specific biomarkers, enhances drug delivery precision. This specificity ensures that therapeutic agents are directed primarily to diseased cells while sparing healthy tissues, thereby improving treatment outcomes and reducing off-target effects.

1.8.3. Stability and Cost-Effectiveness

One of the key benefits of aptamers is their superior stability under various physiological conditions. Unlike protein-based antibodies, aptamers remain structurally intact over prolonged periods, reducing the likelihood of degradation and loss of function. Additionally, the chemical synthesis of aptamers is relatively inexpensive and does not require the use of cell culture systems, making large-scale production more feasible and economically viable (Hidding, 2017).

The integration of aptamers in ligand-conjugated drug delivery systems holds immense potential for advancing targeted therapies, particularly in hematologic malignancies like AML. Their high stability, cost-effectiveness, minimal immunogenicity, and exceptional specificity make them a promising alternative to traditional monoclonal antibodies. By leveraging these advantages, aptamer-conjugated drug delivery systems can significantly enhance the efficacy

and safety of anticancer treatments, paving the way for more precise and effective therapeutic interventions.

1.9. Future Directions and Emerging Strategies in AML Therapy

AML remains a highly aggressive hematologic malignancy with poor survival outcomes, particularly in relapsed or refractory cases. Conventional chemotherapy, despite its effectiveness, is associated with significant toxicity, drug resistance, and high relapse rates. The emergence of targeted therapies and nanotechnology-based drug delivery systems provides a promising avenue for overcoming these limitations. The future perspectives of AML treatment are shifting towards personalized and targeted strategies, highlighting the significance of customized medicine and its incorporation into standard clinical practice. Personalized medicine focuses on adapting therapies to the specific genetic, epigenetic, and molecular features of each patient's leukemia cells.

While clofarabine remains a valuable tool in leukemia therapy, its limitations, including toxicity and drug resistance, underscore the need for more precise and safer delivery methods. Ligand-conjugated, nanoparticle-based targeted therapy offers a promising avenue for enhancing the therapeutic efficacy of clofarabine, reducing its toxic side effects, and overcoming resistance, thus improving patient outcomes.

This study explores the development of aptamer-conjugated clofarabine-loaded PLGA nanoparticles, a novel drug delivery system aimed at selectively targeting floated AML cells overexpressing the CD117 (c-KIT) receptor. By leveraging the high specificity and affinity of aptamers, this approach enhances clofarabine's therapeutic efficacy while minimizing systemic toxicity. The PLGA nanoparticle platform enables controlled drug release, improving drug stability, circulation time, and cellular uptake. This targeted delivery system holds the potential to reduce off-target effects, enhance treatment response, and overcome drug resistance mechanisms associated with standard chemotherapy.

The findings of this study provide a scientific foundation for the development of ligand-conjugated nanotherapeutics in AML treatment. Further preclinical and clinical investigations are necessary to validate the efficacy, biodistribution, pharmacokinetics, and safety profile of this delivery system.

1.10. References

- Adhikary, K., Ganguly, K., Roy, N., Bar, P., Mahapatra, S., & Maiti, R. (2025). Updated insights on clinical diagnosis and targeted therapy of acute myeloid leukaemia (AML): A molecular approach. *Chemical Biology Letters*, 12(2), 1262-1262. <https://doi.org/10.62110/sciencein.cbl.2025.v12.1262>
- Bala, I., Hariharan, S., & Kumar, M. R. (2004). PLGA nanoparticles in drug delivery: the state of the art. *Critical Reviews™ in Therapeutic Drug Carrier Systems*, 21(5). DOI: 10.1615/CritRevTherDrugCarrierSyst.v21.i5.20
- Bullinger, L., Döhner, K., & Döhner, H. (2017). Genomics of acute myeloid leukemia diagnosis and pathways. *Journal of clinical oncology*, 35(9), 934-946. <https://doi.org/10.1200/JCO.2016.71.2208>
- Chandran, R., Hakki, M., & Spurgeon, S. (2012). Infections in leukemia. *Sepsis-an ongoing and significant challenge*, 334-68. <http://dx.doi.org/10.5772/50193>
- Cheng, J., Teply, B. A., Sherifi, I., Sung, J., Luther, G., Gu, F. X., Nissenbaum, E. L., Moreno, A. R., Langer, R., & Farokhzad, O. C. (2007). Formulation of functionalized PLGA-PEG nanoparticles for in vivo targeted drug delivery. *Biomaterials*, 28(5), 869-876. <https://doi.org/10.1016/j.biomaterials.2006.09.047>
- Churpek, J. E., Lorenz, R., Nedumgottil, S., Onel, K., Olopade, O. I., Sorrell, A., Owen, C. J., Bertuch, A. A., & Godley, L. A. (2013). Proposal for the clinical detection and management of patients and their family members with familial myelodysplastic syndrome/acute leukemia predisposition syndromes. *Leukemia & lymphoma*, 54(1), 28-35. <https://doi.org/10.3109/10428194.2012.701738>
- Cornelissen, J. J., & Blaise, D. (2016). Hematopoietic stem cell transplantation for patients with AML in first complete remission. *Blood*, 127(1), 62-70. <https://doi.org/10.1182/blood-2015-07-604546>
- Danhier, F., Ansorena, E., Silva, J. M., Coco, R., Le Breton, A., & Pr at, V. (2012). PLGA-based nanoparticles: an overview of biomedical applications. *Journal of controlled release*, 161(2), 505-522. <https://doi.org/10.1016/j.jconrel.2012.01.043>
- Dasari, A., Choi, J. S., & Berdis, A. J. (2016). Chemotherapeutic intervention by inhibiting DNA polymerases. In *DNA Repair in Cancer Therapy* (pp. 179-224). Academic Press. <https://doi.org/10.1016/B978-0-12-803582-5.00007-3>

Döhner, H., Estey, E., Grimwade, D., Amadori, S., Appelbaum, F. R., Büchner, T., Dombret, h., Ebert, B. L., Fenaux, P., Larson, R. A., Levine, R. L., Lo-Coco, F., Naoe, T., Niederwieser, D., Ossenkoppele, G. J., Sanz, M., Sierra, J., Tallman, M. S., Tien, H. F., Wei, A. H., & Löwenberg, B. (2022). Diagnosis and management of AML in adults: 2022 ELN recommendations from an international expert panel. *Blood*, *140*(12), 1345-1377. <https://doi.org/10.1182/blood-2016-08-733196>

Domaratzki, R. E. (2009). *A chitosan nanoparticle carrier for delivery of the anticancer drug cladribine*. Library and Archives Canada= Bibliothèque et Archives Canada, Ottawa. ISBN: 97804944260670494426063.

Estey, E. H. (2013). Epigenetics in clinical practice: the examples of azacitidine and decitabine in myelodysplasia and acute myeloid leukemia. *Leukemia*, *27*(9), 1803-1812. <https://doi.org/10.1038/leu.2013.173>

Estey, E. H. (2020). Acute myeloid leukemia: 2021 update on risk-stratification and management. *American journal of hematology*, *95*(11), 1368-1398. <https://doi.org/10.1002/ajh.25975>

Everyday Health. (n.d.). *Acute myeloid leukemia (AML): Symptoms, treatment & prognosis*. Retrieved February 18, 2025, from <https://www.everydayhealth.com/leukemia/acute-myeloid-leukemia-aml-cancer-refractory-relapsed-prognosis-symptoms-treatment-more/#resources>

Giudice, V., Mensitieri, F., Izzo, V., Filippelli, A., & Selleri, C. (2020). Aptamers and antisense oligonucleotides for diagnosis and treatment of hematological diseases. *International journal of molecular sciences*, *21*(9), 3252. <https://doi.org/10.3390/ijms21093252>

Gyurkocza, B., & Sandmaier, B. M. (2014). Conditioning regimens for hematopoietic cell transplantation: One size does not fit all. *Blood*, *124*(3), 344–353. <https://doi.org/10.1182/blood-2014-02-514778>

Hamid, G. A. (2013). Acute leukemia clinical presentation. *Leukemia*, *75*. <http://dx.doi.org/10.5772/53531>

Hecht, S. S. (2002). Tobacco smoke carcinogens and breast cancer. *Environmental and molecular mutagenesis*, *39*(2-3), 119-126. <https://doi.org/10.1002/em.10071>

Hidding, J. (2017). A therapeutic battle: Antibodies vs. Aptamers. *Nanosci. Master Progr*, *109*, 1-20.

Izak, M., & Bussel, J. B. (2014). Management of thrombocytopenia. *F1000prime reports*, *6*. <https://doi.org/10.12703/P6-45>

Jan, N., Madni, A., Rahim, M. A., Khan, N. U., Jamshaid, T., Khan, A., Jabar, A., Khan, S., & Shah, H. (2021). In vitro anti-leukemic assessment and sustained release behaviour of cytarabine loaded biodegradable polymer based nanoparticles. *Life Sciences*, 267, 118971. <https://doi.org/10.1016/j.lfs.2020.118971>

Jhaveri, K. D., Chidella, S., Allen, S. L., & Fishbane, S. (2014). Clofarabine-induced kidney toxicity. *Journal of Oncology Pharmacy Practice*, 20(4), 305-308. <https://doi.org/10.1177/1078155213504976>

Jimenez-Chillon, C., Dillon, R., & Russell, N. (2024). Optimal post-remission consolidation therapy in patients with AML. *Acta Haematologica*, 147(2), 147-158. <https://doi.org/10.1159/000535457>

Kantarjian, H. M., Kadia, T. M., DiNardo, C. D., Welch, M. A., & Ravandi, F. (2021). Acute myeloid leukemia: Treatment and research outlook for 2021 and the MD Anderson approach. *Cancer*, 127(8), 1186-1207. <https://doi.org/10.1002/cncr.33477>

Kantarjian, H. M., Jeha, S., Gandhi, V., Wess, M., & Faderl, S. (2007). Clofarabine: past, present, and future. *Leukemia & lymphoma*, 48(10), 1922-1930. <https://doi.org/10.1080/10428190701545644>

Kohli, V. K., Kohli, C., & Singh, A. (2022). Hematopathology of Red Blood Cells and White Blood Cells. In *Comprehensive Multiple-Choice Questions in Pathology: A Study Guide* (pp. 53-67). Cham: Springer International Publishing. https://doi.org/10.1007/978-3-031-08767-7_8

Liu, H. (2021). Emerging agents and regimens for AML. *Journal of hematology & oncology*, 14(1), 49. <https://doi.org/10.1186/s13045-021-01062-w>

Liu, Y. Q., Wang, X. L., He, D. H., & Cheng, Y. X. (2021). Protection against chemotherapy- and radiotherapy-induced side effects: A review based on the mechanisms and therapeutic opportunities of phytochemicals. *Phytomedicine*, 80, 153402. <https://doi.org/10.1016/j.phymed.2020.153402>

Mauro, M. J., & Deininger, M. W. (2009). Management of drug toxicities in chronic myeloid leukaemia. *Best practice & research clinical haematology*, 22(3), 409-429. <https://doi.org/10.1016/j.beha.2009.06.001>

McHale, C. M., Zhang, L., & Smith, M. T. (2012). Current understanding of the mechanism of benzene-induced leukemia in humans: implications for risk assessment. *Carcinogenesis*, 33(2), 240-252. <https://doi.org/10.1093/carcin/bgr297>

Morton, L. M., Dores, G. M., Tucker, M. A., Kim, C. J., Onel, K., Gilbert, E. S., & Fraumeni, J., Curtis, R. E. (2013). Evolving risk of therapy-related acute myeloid leukemia following cancer chemotherapy among adults in the United States, 1975-2008. *Blood, The Journal of the American Society of Hematology*, *121*(15), 2996-3004. <https://doi.org/10.1182/blood-2012-08-448068>

Obeagu, E. I., & Babar, Q. (2021). Acute Myeloid Leukaemia (AML): The Good, the Bad, and the Ugly. *Int. J. Curr. Res. Med. Sci*, *7*(7), 29-41.

Percival, M. E., Lai, C., Estey, E., & Hourigan, C. S. (2017). Bone marrow evaluation for diagnosis and monitoring of acute myeloid leukemia. *Blood reviews*, *31*(4), 185-192. <https://doi.org/10.1016/j.blre.2017.01.003>

Radvoyevitch, T., Sachs, R. K., Gale, R. P., Molenaar, R. J., Brenner, D. J., Hill, B. T., Kalaycio, M. E., Carraway, H. E., Mukherjee, S., Sekeres, M. A., & Maciejewski, J. P. (2016). Defining AML and MDS second cancer risk dynamics after diagnoses of first cancers treated or not with radiation. *Leukemia*, *30*(2), 285-294. <https://doi.org/10.1038/leu.2015.258>

Rafei, H., & DiNardo, C. D. (2019). Hereditary myeloid malignancies. *Best Practice & Research Clinical Haematology*, *32*(2), 163-176. <https://doi.org/10.1016/j.beha.2019.05.001>

Rafiei, P., & Haddadi, A. (2017). Docetaxel-loaded PLGA and PLGA-PEG nanoparticles for intravenous application: pharmacokinetics and biodistribution profile. *International journal of nanomedicine*, 935-947. <https://doi.org/10.2147/IJN.S121881>

Saygin, C., & Godley, L. A. (2021). Genetics of myelodysplastic syndromes. *Cancers*, *13*(14), 3380. <https://doi.org/10.3390/cancers13143380>

Shafat, M. S., Gnanaswaran, B., Bowles, K. M., & Rushworth, S. A. (2017). The bone marrow microenvironment—Home of the leukemic blasts. *Blood reviews*, *31*(5), 277-286. <https://doi.org/10.1016/j.blre.2017.03.004>

Sheikh, E., Tran, T., Vranic, S., Levy, A., & Bonfil, R. D. (2022). Role and significance of c-KIT receptor tyrosine kinase in cancer: A review. *Bosnian journal of basic medical sciences*, *22*(5), 683. <https://doi.org/10.17305/bjbms.2021.7399>

Short, N. J., Kantarjian, H., Ravandi, F., & Daver, N. (2019). Emerging treatment paradigms with FLT3 inhibitors in acute myeloid leukemia. *Therapeutic Advances in Hematology*, *10*, 2040620719827310. <https://doi.org/10.1177/2040620719827310>

Srinivasarao, M., & Low, P. S. (2017). Ligand-targeted drug delivery. *Chemical reviews*, *117*(19), 12133-12164. <https://doi.org/10.1021/acs.chemrev.7b00013>

Steele, M., & Narendran, A. (2012). Mechanisms of defective erythropoiesis and anemia in pediatric acute lymphoblastic leukemia (ALL). *Annals of hematology*, *91*, 1513-1518. <https://doi.org/10.1007/s00277-012-1475-5>

Steensma, D. P., & Tefferi, A. (2003). The myelodysplastic syndrome (s): a perspective and review highlighting current controversies. *Leukemia research*, *27*(2), 95-120. [https://doi.org/10.1016/S0145-2126\(02\)00098-X](https://doi.org/10.1016/S0145-2126(02)00098-X)

Taskesen, E., Bullinger, L., Corbacioglu, A., Sanders, M. A., Erpelinck, C. A., Wouters, B. J., Luytgaarde, S. C., Damm, F., Krauter, J., Ganser, A., Schlenk, R. F., Löwenberg, B., Delwel, R., Döhner, H., Valk, P.A., & Döhner, K. (2011). Prognostic impact, concurrent genetic mutations, and gene expression features of AML with CEBPA mutations in a cohort of 1182 cytogenetically normal AML patients: further evidence for CEBPA double mutant AML as a distinctive disease entity. *Blood, The Journal of the American Society of Hematology*, *117*(8), 2469-2475. <https://doi.org/10.1182/blood-2010-09-307280>

Vecchio, L., Etet, P. F. S., Kipanyula, M. J., Krampera, M., & Kamdje, A. H. N. (2013). Importance of epigenetic changes in cancer etiology, pathogenesis, clinical profiling, and treatment: what can be learned from hematologic malignancies?. *Biochimica et Biophysica Acta (BBA)-Reviews on Cancer*, *1836*(1), 90-104. <https://doi.org/10.1016/j.bbcan.2013.04.001>

Wang, H., Zhao, Y., Wang, H., Gong, J., He, H., Shin, M. C., Yang, V. C., & Huang, Y. (2014). Low-molecular-weight protamine-modified PLGA nanoparticles for overcoming drug-resistant breast cancer. *Journal of controlled release*, *192*, 47-56. <https://doi.org/10.1016/j.jconrel.2014.06.051>

Xiang, W., Lam, Y. H., Periyasamy, G., & Chuah, C. (2022). Application of high throughput technologies in the development of acute myeloid leukemia therapy: Challenges and progress. *International Journal of Molecular Sciences*, *23*(5), 2863. <https://doi.org/10.3390/ijms23052863>

Zeiser, R., & Blazar, B. R. (2017). Pathophysiology of acute graft-versus-host disease and therapeutic targets. *New England Journal of Medicine*, *377*(22), 2167-2179. DOI: 10.1056/nejmra1609337vol. 377 NO. 22

Zhang, X., Jia, X., Tong, W., Chen, H., Lei, N., Li, G., Tai, J., & Li, P. (2022). Quantification of clofarabine in urine and plasma by LC-MS/MS: suitable for PK study and TDM in pediatric patients with relapsed or refractory ALL. *RSC advances*, *12*(51), 33091-33098. <https://doi.org/10.1039/D2RA05843J>

Zhao, N., Pei, S. N., Qi, J., Zeng, Z., Iyer, S. P., Lin, P., & Tung, C. H., Zu, Y. (2015). Oligonucleotide aptamer-drug conjugates for targeted therapy of acute myeloid leukemia. *Biomaterials*, 67, 42-51. <https://doi.org/10.1016/j.biomaterials.2015.07.025>

Zhenchuk, A., Lotfi, K., Juliusson, G., & Albertioni, F. (2009). Mechanisms of anti-cancer action and pharmacology of clofarabine. *Biochemical pharmacology*, 78(11), 1351-1359. <https://doi.org/10.1016/j.bcp.2009.06.094>



Chapter 2:

LITERATURE REVIEW

2.1. Overview and Molecular Basis of AML

AML is a highly aggressive type of hematological malignancy that originates from genetic mutations impairing the normal differentiation of hematopoietic stem and progenitor cells (Obeagu et al., 2021). These mutations result in a clonal expansion of immature myeloid blasts, leading to their accumulation in the bone marrow and peripheral blood, eventually causing bone marrow failure. The molecular pathogenesis of AML is complex, involving genetic and epigenetic alterations that disrupt crucial regulatory processes. Mutations in transcription factors, signaling pathways, and epigenetic regulators play a vital role in leukemogenesis (Eriksson et al., 2015). For instance, mutations in genes regulating signaling pathways such as *FLT3* and *RAS* are frequently observed, contributing to uncontrolled proliferation and survival of leukemic blasts. *FLT3* internal tandem duplications (*FLT3-ITD*) are among the most common mutations in AML and are associated with a poor prognosis due to their aggressive clinical behavior (Müller et al., 2020). Similarly, mutations in epigenetic regulators, including DNA methyltransferase 3A (*DNMT3A*) and isocitrate dehydrogenase 1/2 (*IDH1/2*), alter the epigenome, affecting gene expression and promoting leukemic transformation. Dysregulation of these genes disrupts the normal hematopoietic differentiation program, favoring the expansion of immature myeloid cells at the expense of healthy blood cell development. Clinically, AML manifests with symptoms of bone marrow failure, including anemia, thrombocytopenia, and neutropenia, resulting from the suppression of normal hematopoiesis (Hamid et al., 2013). Anemia comes with fatigue, pallor, and shortness of breath, while thrombocytopenia leads to an increased risk of bleeding and bruising. Neutropenia renders patients highly susceptible to infections. The combination of genetic mutations, impaired hematopoietic differentiation, and resultant clinical manifestations underpins the aggressive nature of AML, necessitating an in-depth understanding of its pathogenesis for the development of targeted therapies.

As explained by (Vainchenker and Kralovics, 2017), the genetic landscape of classical myeloproliferative neoplasms (MPNs) is primarily driven by mutations in *JAK2*, *CALR*, and *MPL*, which result in abnormal activation of the cytokine receptor/JAK2 signaling pathway and downstream effectors like STAT proteins. The *JAK2V617F* mutation, the most common among these, activates erythropoietin, granulocyte colony-stimulating factor, and MPL receptors, leading to diseases such as polycythemia vera (PV), essential thrombocythemia

(ET), and primary myelofibrosis (PMF). In contrast, *CALR* and *MPL* mutations are restricted to MPL activation, primarily associated with ET and PMF. Other mutations in genes involved in epigenetic regulation (*TET2*, *DNMT3A*, *EZH2*, *ASXL1*) and RNA splicing are common in PMF and contribute to disease progression and hematological abnormalities like anemia or pancytopenia. Besides somatic mutations, factors such as germline predisposition, chronic inflammation, and aging also influence MPN pathogenesis.

2.2. Types and Sub-Types of AML

AML can be classified into distinct subtypes based on genetic, cytogenetic, and morphological factors as described by the World Health Organization (WHO) and French-American-British (FAB) classification systems. The WHO classification includes four major types: AML with recurrent genetic mutations, AML associated with myelodysplasia-related alterations, therapy-related AML (t-AML), and AML not otherwise specified (NOS) (Kansal, 2019). AML with recurrent genetic abnormalities is defined by specific chromosomal translocations and mutations such as t(8;21)(RUNX1-RUNX1T1), inv(16)(CBFB-MYH11), and t(15;17)(PML-RARA), which characterizes acute promyelocytic leukemia (APL) with distinct therapeutic implications (Yang et al., 2017). AML with myelodysplasia-related changes is associated with a history of myelodysplastic syndrome (MDS) or dysplasia in multiple cell lineages and is linked to poor prognostic mutations such as ASXL1, TP53, and complex karyotypes. According to (Godley et al., 2008), therapy-related AML occurs as a late complication of chemotherapy or radiotherapy and frequently shows adverse cytogenetic abnormalities like del(5q) or del(7q), with a poor prognosis. AML not otherwise specified (NOS) includes cases that do not fit into the above categories and are classified based on morphology and cytochemistry using the FAB classification. (Øystein et al., 2024) has described FAB subtypes range from M0 to M7, including M1 (AML with minimal differentiation), M2 (AML with maturation), M4 (acute myelomonocytic leukemia), and M7 (acute megakaryoblastic leukemia). Among these, M3 (APL) stands out due to its favorable response to targeted therapy with all-trans retinoic acid (ATRA), while subtypes such as M6 (acute erythroid leukemia) and M7 are associated with poor outcomes. Accurate classification of AML subtypes is crucial for prognostication and treatment selection, given their significant differences in clinical presentation and therapeutic response.

2.3. Current Treatment and Limitations

The current treatment approach for AML primarily consists of intensive induction chemotherapy with a combination of dual drugs like cytarabine and anthracycline, commonly known as the "7+3" regimen, followed by hematopoietic stem cell transplantation (HSCT) in eligible patients (Diaz et al., 2024). This treatment strategy aims to achieve complete remission and prevent disease relapse. While initial remission rates range from 60% to 80% in younger patients, long-term outcomes remain poor, with a significant proportion experiencing relapse. The prognosis is particularly dismal in older patients or those with high-risk genetic mutations, where treatment options are limited, and overall survival rates are markedly reduced. The primary limitations of conventional AML therapies stem from their high toxicity and non-specific mechanisms of action (Zhao et al., 2022). Chemotherapeutic agents not only target leukemic blasts but also cause significant damage to healthy hematopoietic cells, resulting in severe adverse effects such as myelosuppression, cardiotoxicity, and increased susceptibility to life-threatening infections. Furthermore, the emergence of drug resistance remains a significant obstacle in the treatment of AML, greatly contributing to treatment failure and disease relapse (Zhang et al., 2019). Drug resistance in AML is driven by various mechanisms, including genetic mutations that alter drug targets, enhance survival pathways, or inactivate apoptotic signaling, thereby promoting leukemic cell survival despite chemotherapy. Mutations in genes such as *FLT3*, *TP53*, and *NRAS* are associated with resistance to standard chemotherapeutic agents, reducing their efficacy (McMahon et al., 2019). Among the most well-characterized mechanisms of drug resistance in AML involves the overexpression of ATP-binding cassette (ABC) transporters, particularly P-glycoprotein (P-gp), encoded by the MDR1 (multidrug resistance 1) gene. P-gp functions as an energy-dependent efflux pump, actively transporting chemotherapeutic agents such as anthracyclines and vinca alkaloids out of leukemic cells, thereby lowering intracellular drug concentrations and reducing cytotoxic effects. The upregulation of P-gp is frequently observed in relapsed or refractory AML and is associated with a poor prognosis (Kolk et al., 2002). This overexpression not only diminishes the efficacy of chemotherapy but also complicates subsequent treatment attempts, as resistant leukemic clones dominate the disease progression. The combination of genetic mutations and P-gp-mediated drug efflux makes AML highly refractory to conventional treatments, underscoring

the need for novel therapeutic strategies targeting these resistance pathways to improve clinical outcomes.

According to Crossnohere et al. (2019), a national survey conducted by the Leukemia & Lymphoma Society highlighted the prevalence and severity of short-term side effects such as nausea, vomiting, diarrhea, hair loss, mouth sores, and infections, as well as long-term complications like organ dysfunction, cognitive impairment (chemobrain), fatigue, and neuropathy. Among 1182 participants, 87% reported severe short-term effects, and 33% experienced severe long-term effects. Hair loss and fatigue were the most common side effects. The study also found that caregivers were more likely to report severe long-term effects, including organ dysfunction and neuropathy, compared to patients. These findings emphasize the need for developing fewer toxic therapies to reduce the burden of AML treatment and improve patients' quality of life.

Immunotherapy has emerged as a promising treatment strategy for AML, offering advantages over traditional therapies like chemotherapy. As explained by Tan et al. (2020) it can boost the immune system's capacity to recognize and destroy cancer cells, potentially improving progression-free survival (PFS) and overall survival (OS). Innovative approaches such as immune checkpoint inhibitors, monoclonal antibodies, and chimeric antigen receptor (CAR) T-cell therapy have shown encouraging results in clinical trials. Combination therapies are being explored to boost efficacy while minimizing adverse effects. However, despite its potential, immunotherapy has limitations. The unpredictable nature of immune responses can lead to severe adverse reactions, such as cytokine release syndrome (CRS) and immune-related toxicity, which may be life-threatening in some cases. Additionally, high treatment costs, variability in patient responses, and the lack of universal biomarkers to predict outcomes remain significant challenges. Therefore, personalized immunotherapy approaches, tailored to the patient's tumor profile and immune status, are essential to maximize therapeutic benefits and reduce risks.

Recent research into the underlying mechanisms of AML has significantly improved our knowledge of the disease. Cytogenetic and molecular abnormalities are key factors in predicting response to chemotherapy and long-term outcomes. Beyond their role in prognosis, these abnormalities serve as potential therapeutic targets. Advances like next-generation sequencing have driven the development of new treatments, particularly small molecules

targeting specific molecular pathways in AML. Several new agents, including tyrosine kinase inhibitors, immune checkpoint inhibitors, monoclonal and bispecific T-cell engager antibodies, metabolic drugs, and pro-apoptotic agents, are being tested in clinical trials. The best results are frequently achieved by combining these targeted therapies with standard chemotherapy (Kayser et al., 2018).

2.4. Exploring Various Nanoformulations for AML

Several nanoformulations have been explored for the treatment of AML, each offering unique advantages. Liposomes enhance drug solubility and circulation time Immordino et al. (2006), while micelles improve the delivery of hydrophobic drugs (Matsumura & Kataoka, 2009). Dendrimers provide precise drug loading and release control due to their branched structure Yiyun & Tongwen, (2005), and gold nanoparticles offer excellent photothermal properties for combination therapies (Huang et al., 2008). Despite these innovations, PLGA nanoparticles stand out due to their biocompatibility, biodegradability, and sustained drug release properties Danhier et al. (2012), ensuring controlled drug delivery with minimal systemic toxicity. These advantages make PLGA an ideal choice for drug encapsulation, allowing for targeted therapy and reduced off-target effects, especially in floated AML cells.

Nanomedicine offers a promising alternative through nanocarrier-based drug delivery systems, which can enhance targeting, reduce side effects, and repurpose old drugs for new uses. This study explored by Gundersen et al. (2016), involves liposomal and PLGA-based nanoparticles for AML therapy. The nanoparticles were characterized for size, morphology, drug-loading capacity, cellular uptake, and cytotoxicity. Both liposomes and PLGA nanoparticles were under 400 nm, making them suitable for systemic delivery. AML cells efficiently internalized both types of nanoparticles, with PLGA nanoparticles showing successful chlorpromazine (CPZ) loading and sustained release over 72 hours, resulting in significant cytotoxicity. However, liposomes showed limited encapsulation for peptide drugs and no conclusive cytotoxic effects. Attempts to use liposomes for siRNA delivery showed some potential, but no significant gene silencing effect. Overall, the study highlights the potential of nanoparticle-based systems in developing targeted AML therapies and repurposing existing drugs.

Nanotechnology has brought significant advancements in cancer diagnosis and treatment. Nanoparticles serve as efficient drug delivery systems by enhancing drug stability, availability,

and retention at the target site. They can penetrate tissues, cross cancer cell membranes, and selectively target cancer cells, reducing toxicity to healthy cells. Nanoparticles improve intracellular drug concentration through endocytosis, leading to higher drug accumulation at the tumor site compared to normal tissues (Soni et al., 2015).

The work done by Poonia et al. (2024) involves nanotechnology offering a promising alternative by improving drug delivery and reducing side effects. For example, CPX351 (VYXEOS™), an FDA-approved liposomal formulation of doxorubicin and cytarabine, Poonia et al. (2024) has shown better therapeutic outcomes compared to traditional treatments. Current research is focusing on various nanocarriers for delivering multiple drugs, helping to improve drug targeting, address chemoresistance, and enhance pharmacokinetics. Their work highlights how nanotechnology-based combination therapies can revolutionize AML treatment and offer more effective solutions.

The review article by Wu et al. (2024) focuses on different types of nanoparticles used in AML treatment, such as liposomes, polymeric nanoparticles, micelles, dendrimers, and also inorganic nanoparticles. Strategies to improve targeted delivery, including ligand conjugation, biomimetic nanotechnology, and bone marrow targeting, are also highlighted for their potential to overcome drug resistance. The role of nanomedicine in supporting immunotherapy is explored as well, along with the advantages and challenges of moving nanomedicine from preclinical to clinical use.

In the review by Soni et al. (2015), various nanocarriers like polymeric nanoparticles, micelles, solid lipid nanoparticles, and liposomes are used to deliver anti-cancer drugs selectively. They can encapsulate both water- and fat-soluble drugs, with controlled drug release based on time or environmental conditions. Polymeric nanoparticles made from biodegradable materials such as polylactic acid (PLA) and poly(lactic-co-glycolic acid) (PLGA) ensure sustained drug release with better efficacy and fewer side effects. To overcome limitations like rapid clearance by the immune system or poor brain penetration, surface modification of nanoparticles is crucial. Poly(ethylene glycol) (PEG) coating extends their circulation time, while modified nanoparticles can cross the blood-brain barrier through endocytosis, enabling targeted brain drug delivery.

2.5. PLGA as a Versatile Drug Delivery Vehicle in Cancer Therapy

Nanoparticles are versatile drug delivery systems suitable for almost all routes of administration. Over time, both natural and synthetic polymers have been widely explored for nanoparticle preparation. Among these, poly(lactic acid) (PLA), poly(glycolic acid) (PGA), and their copolymer poly(lactic-co-glycolic acid) (PLGA) have gained significant recognition due to their excellent biocompatibility and biodegradability. Nanoparticles serve as effective carriers for various drug classes, including anticancer agents, immunomodulators, hormones, and macromolecules such as nucleic acids, proteins, and antibodies. Advancements in traditional preparation techniques, along with the development of novel methods, have expanded the options for formulating drug-loaded nanoparticles. Each preparation method has its own set of advantages and limitations. However, one of the main challenges is maintaining nanoparticle stability after preparation. This is often addressed through freeze-drying to preserve particle integrity (Bala et al., 2004). Nanoparticles can also be designed for site-specific drug delivery, where their targeting efficiency is influenced by factors such as particle size, surface charge, surface modification, and hydrophobicity. The in vivo performance of nanoparticles depends on their morphological properties, surface chemistry, and molecular weight. Careful optimization of these factors, along with appropriate selection of the target site and administration route, can help overcome some of the challenges associated with delivering new therapeutic molecules.

According to the review of Sharma et al. (2016), nanocarriers made from biocompatible and biodegradable polymers approved by the US FDA and EMA are being explored for the controlled delivery of different therapeutic agents. Among these polymers, poly(lactic-co-glycolic acid) (PLGA) is the most widely used. PLGA stands out due to its beneficial features, including controlled and sustained drug release, low toxicity, biocompatibility with cells and tissues, long-term use in biomedical applications, prolonged circulation time, and the ability to deliver drugs to specific targets.

According to the work done by Huanbutta et al. (2016), drug delivery systems offer an effective strategy to overcome multidrug resistance in AML cells, and these systems can be targeted to AML cells by attaching specific molecules, such as folate (FOL), which binds to folate receptors that are selectively expressed in about 70% of AML patients.

Decitabine (DAC), a DNA methyltransferase inhibitor, is commonly used to treat AML. However, it has poor chemical stability, requiring a complex dosing regimen, and causes significant side effects. This study aimed to develop and evaluate new DAC-loaded nanoparticles (NPs) using PLGA-PEG-FOL for targeted drug delivery to AML cells. Two preparation strategies were explored: attaching FOL to pre-synthesized PLGA-PEG nanoparticles and synthesizing PLGA-PEG-FOL copolymer, followed by nanoparticle preparation using the double emulsion solvent diffusion method. Characterization using NMR and FTIR confirmed the successful synthesis of PLGA-PEG-FOL. The nanoparticles were spherical, with an average size of less than 284 nm, a narrow size distribution (polydispersity index < 0.25), negative surface charge (-41.7 to -17.8 mV), and drug encapsulation efficiency ranging from 5.64% to 15.51%. These results indicate that PLGA-PEG-FOL nanoparticles are a promising system for delivering DAC specifically to AML cells (Huanbutta et al., 2016).

Poly(lactic-co-glycolic acid) (PLGA) is widely used as a drug delivery vehicle in cancer treatment due to its biodegradability, biocompatibility, and controlled drug release properties. Being a biodegradable polymer approved by the U.S. Food and Drug Administration (FDA), PLGA gradually breaks down into lactic and glycolic acids, which are naturally metabolized by the body, minimizing toxicity (Dutta et al., 2018). It provides sustained and targeted drug release, enhancing therapeutic efficacy while reducing systemic toxicity. In blood cancers such as AML, PLGA nanoparticles can improve drug solubility and stability, allowing efficient delivery of chemotherapeutic agents directly to cancer cells. Functionalization of PLGA with targeting ligands, such as antibodies, peptides, or aptamers Dutta et al. (2018) further enables specific targeting of cancer cells, sparing healthy cells and reducing adverse effects. Additionally, PLGA nanoparticles can be co-loaded with multiple drugs or combined with imaging agents, offering potential for theranostic applications (Tonbul et al., 2019). These properties make PLGA a promising vehicle for developing novel therapies aimed at improving outcomes in hematological malignancies.

PLGA nanoparticles enhance the drug's stability and control its release, ensuring sustained drug availability at the tumor site. This targeted delivery improves the drug's therapeutic index while minimizing systemic toxicity. The nanoscale size of PLGA nanoparticles facilitates passive targeting through the enhanced permeability and retention (EPR) effect, allowing better accumulation in AML tissues. Moreover, surface modification of PLGA nanoparticles can

further improve drug delivery by enhancing cellular uptake and prolonging circulation time. Combining clofarabine with PLGA nanoparticles not only reduces off-target effects but also enhances its therapeutic efficacy, making it a highly suitable candidate for advanced AML treatment strategies (Huang et al., 2021). Additionally, PLGA nanoparticles can be functionalized with ligands or antibodies to target specific biomarkers, enhancing the selective uptake by floated leukemia cells and improving therapeutic outcomes.

2.6. Clofarabine in AML Therapy: Mechanisms, Stability, and Emerging Clinical Perspectives

Clofarabine, a second-generation purine nucleoside analog, plays a significant role in AML therapy due to its dual mechanism of action—DNA chain termination and inhibition of ribonucleotide reductase, resulting in potent anti-leukemic activity. Clofarabine is designed to combine the beneficial properties of fludarabine and cladribine while overcoming their limitations. It works by blocking ribonucleotide reductase and DNA polymerase, reducing the levels of intracellular deoxynucleoside triphosphates essential for DNA replication. Compared to its predecessors, clofarabine is more stable due to increased resistance to deamination and phosphorolysis and has a stronger affinity for deoxycytidine kinase (dCyd), which plays a crucial role in nucleoside phosphorylation. The first Phase I clinical trial of clofarabine began in 1993, targeting patients with hematologic and solid malignancies. Since then, clofarabine has shown significant antitumor activity as a single agent in both pediatric and adult acute leukemia. Its ability to enhance the effects of other established antileukemic drugs, especially cytarabine, has led to the exploration of combination regimens. Current research continues to assess its role in treating acute leukemia, myelodysplastic syndrome, and solid tumors.

However, in a clinical trial study conducted by Löwenberg et al. (2017), clofarabine showed antileukemic activity in AML, but its effectiveness in younger adults as a part of frontline therapy with standard chemotherapy is yet to be thoroughly evaluated. In this study, two induction regimens were compared in newly diagnosed AML or high-risk myelodysplastic syndrome (MDS) patients aged 18–65 years. The regimens included idarubicin-cytarabine (Cycle I) and amsacrine-cytarabine (Cycle II), with or without clofarabine (10 mg/m² on days 1–5 of both cycles). Consolidation treatment consisted of chemotherapy alone or combined with hematopoietic stem cell transplantation.

The primary endpoint was event-free survival (EFS), with other clinical outcomes and toxicities were also assessed. A total of 402 and 393 evaluable patients were randomized to the control and clofarabine treatment arms, respectively. Complete remission rates were similar (89%) between both groups but were achieved faster in the clofarabine group (66% vs. 75% after Cycle I). After a median follow-up of 36 months, there were no significant differences in overall survival or EFS between the control group (EFS: 35% at 4 years) and the clofarabine group (EFS: 38%). Subgroup analysis showed that clofarabine improved overall survival and EFS in patients with intermediate-risk AML proving that, clofarabine appears to improve survival outcomes in specific intermediate-risk AML subgroups, but its general benefit in frontline treatment remains limited.

Clofarabine is particularly effective in targeting rapidly proliferating AML cells and is often used in relapsed or refractory cases (Zhenchuk et al., 2009). Despite its therapeutic potential, clofarabine's clinical use is limited by poor aqueous solubility, rapid plasma clearance, and systemic toxicity, leading to adverse effects. This often results in dose-limiting toxicities, including severe myelosuppression, hepatotoxicity, and gastrointestinal complications. Clofarabine also lacks tumor specificity, leading to significant off-target effects and damage to healthy tissues.

Another report by Faderl et al. (2006), involves the prognosis for patients over 60 with AML remains poor, with low remission rates and limited survival. The phase 2 study evaluated clofarabine and cytarabine in patients aged 50 and above with non-treated AML. Clofarabine (40 mg/m²) was given as a 1-hour intravenous infusion for 5 days (days 2–6), followed by cytarabine (1 g/m²) as a 2-hour infusion for 5 days (days 1–5). Among 60 patients, 48% had secondary AML, 50% had abnormal karyotypes, and 21% showed FLT3 mutations.

The overall response rate was 60% (52% complete response [CR] and 8% CR with incomplete platelet recovery (CRp). Four patients (7%) died during induction. Most side effects were mild (grade 2 or lower), including diarrhea, vomiting, nausea, skin reactions, mucositis, liver issues, and infusion-related symptoms. Myelosuppression was common. While clofarabine plus cytarabine showed good response rates, it did not significantly improve survival compared to other regimens. Further studies are needed to optimize this combination for older AML patients.

Clofarabine, which is a second-generation purine nucleoside analog, has already shown significant anti-leukemic activity, but its clinical utility is often limited by short plasma half-life, poor selectivity, and dose-dependent toxicities. Encapsulation in poly-lactic-glycolic acid (PLGA) nanoparticles offers a promising solution to overcome these challenges. PLGA, being biocompatible and biodegradable, ensures the controlled and sustained release of clofarabine, reducing the need for frequent dosing and enhancing patient compliance (de la Torre et al., 2020). This delivery system helps improve clofarabine's stability, preventing premature degradation in the bloodstream and increasing its bioavailability (Zhang et al., 2017).

2.7. Aptamers and Antibodies as Ligands in Leukemia Therapy

Aptamers and antibodies are widely used as targeting ligands in leukemia therapy due to their high specificity and strong binding affinity for cell surface markers on leukemic cells. Antibodies are Y-shaped proteins that recognize specific antigens, such as CD33, CD117, or CD123, which are commonly overexpressed in leukemia cells (Rodriguez et al., 2023). They have been extensively utilized in the development of targeted therapies, including antibody-drug conjugates (ADCs) and bispecific T-cell engagers (BiTEs), enabling selective delivery of therapeutic agents to cancer cells while minimizing damage to healthy tissues (Ramos & Grover, 2017). However, their large size, potential immunogenicity, and high production cost are notable limitations.

In contrast, aptamers are short single-stranded DNA or RNA molecules that adopt into specific three-dimensional shapes, enabling them to bind to target molecules with high precision (Sun et al., 2014). Due to their smaller size and non-immunogenic nature, aptamers offer several advantages over antibodies. They can penetrate tumors more efficiently and are easier to modify for conjugation with nanoparticles or therapeutic agents (Girotti et al., 2020). Aptamers targeting CD117, a key biomarker in AML, have shown promising results in selective drug delivery, improving drug accumulation in leukemic cells and reducing off-target toxicity (Giudice et al., 2020).

The combination of aptamers or antibodies with nanoparticle-based delivery systems further enhances therapeutic efficacy by providing controlled drug release and precise targeting. Both ligands play a crucial role in improving the therapeutic index of anticancer drugs, offering new possibilities for personalized and targeted leukemia therapy. However, ongoing research is

essential to optimize their clinical application and address challenges such as stability and large-scale production.

Research shows that many human cancers, including AML, follow a cancer stem cell model. This means cancer is driven by a small population of self-renewing cancer stem cells, known as leukemia stem cells (LSCs). To fully cure the disease, these cancer stem cells must be eliminated. Monoclonal antibodies have become promising treatments due to their ability to target specific antigens with minimal side effects. To target AML LSCs, scientists focus on identifying antigens that are present on LSCs but not on normal blood stem cells. Key antigens identified include CD123, CD44, CLL-1, CD96, CD47, CD32, and CD25. Monoclonal antibodies against CD44, CD123, and CD47 have shown effectiveness in experimental models and could offer new hope for AML treatment (Majeti et al., 2011).

Monoclonal antibodies targeting cancer cell surface proteins have shown significant success in treating solid tumors and lymphoid cancers. However, their effectiveness in AML is less established. Anti-CD33 antibodies, including unconjugated forms, antibody-drug conjugates (ADCs), and radioisotope-linked antibodies, have been tested for decades but failed to become standard treatments due to limited efficacy. Advances in antibody engineering, drug-linker technology, and identification of new targets like CD123, Clec12A, and CD47 have renewed interest in antibody-based AML therapies. Re-engineered anti-CD33 antibodies and T cell-engaging antibodies offer promising new options for AML treatment (Garfin et al., 2016).

Despite the promise of antibody-based therapies in targeting AML, several limitations restrict their success. One of the primary challenges is off-target toxicity. Most antibodies, including those targeting CD33, bind to antigens also expressed on normal hematopoietic cells, causing significant damage to healthy tissues and resulting in severe myelosuppression (Jilani et al., 2002; Pagel et al., 2011). Antibody-drug conjugates (ADCs) face issues of stability and controlled drug release. Premature release of the cytotoxic payload in circulation can lead to systemic toxicity, while incomplete release at the tumor site reduces therapeutic efficacy. The large molecular size of antibodies also limits tissue penetration, preventing efficient delivery to all cancerous cells within the bone marrow microenvironment, which can result in incomplete leukemic cell elimination and disease relapse rate (Frankel et al., 2000).

Furthermore, the production of monoclonal antibodies is expensive and involves complex cell culture procedures and purification processes (Beck & Reichert, 2013). Immunogenicity is another concern, as patients may develop anti-drug antibodies, reducing the efficacy of therapy over time (Hansel et al., 2010). These drawbacks underscore the need for alternative molecular tools with higher specificity, lower immunogenicity, and improved pharmacokinetics.

Aptamers, on the other hand, offers a promising alternative for AML treatment. Their small size allows better tissue penetration and better reach to the leukemic microenvironment (Fu et al., 2020). Aptamers are chemically synthesized, making them more cost-effective with consistent quality compared to antibodies (Ellington & Szostak, 1990). Unlike antibodies, aptamers exhibit minimal immunogenicity, significantly lowering the risk of adverse immune responses (Keefe et al., 2010). They can be easily modified to improve stability and bioavailability while maintaining high specificity and binding affinity for target antigens.

Aptamers have been developed for over 30 years through the SELEX process (Systematic Evolution of Ligands by Exponential Enrichment), first introduced by Tuerk and Gold in 1990 (Tuerk & Gold, 1990). This method is used to select short DNA or RNA molecules that can bind specifically to target proteins for diagnostic and therapeutic applications. The SELEX process involves three main steps: incubation of DNA or RNA molecules with the target protein, selection of molecules that bind well to the protein, and amplification of the best-binding molecules for multiple cycles until highly specific aptamers are obtained. For RNA aptamers, the bound RNA is strengthened using RT-PCR, converted back to DNA, and then transcribed to RNA for further selection rounds.

In recent years, various advanced SELEX methods have been developed to improve efficiency and reliability. These include Cell-SELEX, which targets whole cells, Capillary Electrophoresis-SELEX (CE-SELEX) for faster selection, Microfluidic-SELEX (M-SELEX) for high-throughput selection (Shangguan et al., 2006), and IP-SELEX, which enhances specificity and affinity by incorporating immunoprecipitation. Each method has its advantages and disadvantages. For instance, IP-SELEX increases specificity by focusing on real protein interactions without needing cell cultures or protein purification before SELEX. However, this method is more time-consuming compared to the other standard SELEX process. Overall, these

advancements aim to make aptamer selection more precise and efficient for various biomedical applications (Nur et al., 2021).

Cell surface proteins play key roles in cancer development. Understanding how these proteins are expressed on tumor cells is essential for studying cancer progression. This requires molecular probes that can specifically bind to these surface proteins. Such probes are valuable for cancer diagnosis, classification, and treatment. Aptamers, which are synthetic DNA or RNA molecules offer a solution by binding to proteins, peptides, and small molecules with high precision and strong affinity. Using a method called cell-based SELEX, (Sefah et al., 2009), selected DNA aptamers by exposing live AML cells to several rounds of selection. These aptamers were able to specifically recognize AML cells with dissociation constants (Kd) in the nanomolar range. Among the selected aptamers, KH1C12 (Sequence: ATCCAGAGTGACGCAGCATGCCCTAGTTACTACTACTCTTTTTAGCAAACGCCCTC GCTTTGGACACGGTGGCTTAGT) showed high selectivity for the AML cell line (HL60) compared to control cell lines (K562 and NB4) and could even detect AML cells in bone marrow aspirate samples. Two other aptamers, KK1B10 (Sequence: ATCCAGAGTGACGCAGCAGATCAGTCTATCTTCTCCTGATGGGTTCCATTTATAGG TGAAGCTGGACACGGTGGCTTAGT) and KK1D04 (Sequence: ATCCAGAGTGACGCAGCACAAAGTCTCTTCGGCGCGAATCAGTTCATCTTTCCCT GATGGGGGTGGACACGGTGGCTTAGT), were found to bind to markers related to monocytic differentiation. These results suggest that these aptamers can serve as useful tools for analyzing protein expression on leukemia cells, providing a basis for more accurate classification and molecular studies of leukemia.

2.8. Targeting Various Bioreceptors for AML therapy

In the treatment of acute myeloid leukemia, aptamers offer a targeted approach by selectively binding to overexpressed cell surface biomarkers on leukemic cells, minimizing damage to healthy tissues. Several targeting strategies have been developed using aptamers to inhibit key molecular pathways, facilitate drug delivery, and enhance the therapeutic efficiency.

CD44, CD123, and CD33 are among the most promising targets for aptamer-based therapeutics in AML due to their key roles in disease progression and resistance. One significant targeting strategy in AML involves CD33, a well-known surface marker highly expressed on myeloid

blasts. CD33-specific aptamers are designed to deliver cytotoxic agents directly to leukemic cells, reducing systemic toxicity and improving therapeutic outcomes (Zhou et al., 2020). Aptamer-drug conjugates have shown considerable potential in increasing the precision of chemotherapy, especially in combination therapies. Another important target is CD123, the alpha subunit of the interleukin-3 receptor, which plays a critical role in the survival of leukemia stem cells (Sun et al., 2019). Aptamers targeting CD123 have been explored for eliminating these resistant subpopulations, which are a major cause of relapse in AML. A novel approach has been the use of CD44-specific aptamers, focusing on disrupting the interactions between leukemic stem cells and their microenvironment. CD44 is involved in cell adhesion and homing, and blocking this receptor has been shown to enhance the efficacy of conventional chemotherapy (Noga et al 2023). Targeting CD44 with aptamers may sensitize leukemic cells to treatment by preventing their attachment to protective niches in the bone marrow. In addition to cell surface receptors, nucleolin, a multifunctional protein present on the plasma membrane of AML cells, has been targeted using the AS1411 aptamer. This approach disrupts critical cellular processes such as DNA replication and transcription, ultimately inducing cell death. Furthermore, vascular endothelial growth factor (VEGF) is a key regulator of angiogenesis in AML. VEGF-targeting aptamers have been investigated for their ability to inhibit the formation of new blood vessels that support leukemic cell proliferation and survival (Li et al., 2016).

Combining aptamers with nanoparticles or liposomes has further expanded the range of targeting strategies. Aptamer-functionalized nanoparticles can be used to deliver drugs, siRNA, or imaging agents to leukemic cells, enhancing specificity and therapeutic efficiency. This multifunctional approach provides the potential for simultaneous treatment and monitoring of disease progression. While clinical translation remains challenging due to issues like aptamer stability and delivery efficiency, continuous advancements in chemical modifications and nanocarrier systems are improving the clinical feasibility of these therapies.

2.9. CD117- A Promising Biomarker for AML Therapy

CD117, also known as the c-kit proto-oncogene, is found in several normal and cancerous blood cells. In healthy bone marrow, about half of the CD34+ precursor cells (which give rise to blood cells) express CD117, particularly those committed to becoming red blood cells, granulocytes, monocytes, and platelets. Strong CD117 expression is also seen in bone marrow

mast cells, a small group of NK (natural killer) cells, and early T-cell precursors (prothymocytes). This shows that CD117 is mainly present in the myeloid cell lineage but can also be found in a limited number of lymphoid cells.

In acute leukemias, CD117 was initially linked to AML, but it has also been observed in some cases of T-cell acute lymphoblastic leukemia (T-ALL), though it is rarely present in B-cell ALL. Additionally, about one-third of multiple myeloma patients and those with related plasma cell disorders show CD117 expression in their abnormal plasma cells. The role of CD117 in predicting disease outcomes is not yet fully understood. However, analyzing CD117 alongside other markers may help track minimal residual disease (MRD) in patients with AML and multiple myeloma, allowing for better monitoring after treatment (Escribano et al., 1998).

AML cells are very similar to the normal cells they originate from the hematopoietic stem and progenitor cells (HSPCs), which makes it difficult to find a unique marker to target only the leukemia cells. Since it's hard to differentiate them, the researchers, Myburgh et al. (2020) suggest using CAR T-cell therapy to attack both healthy and cancerous HSPCs by targeting CD117, a receptor found on these cells. This method would kill most of the immature blood cells (both healthy and malignant) but spare mature blood cells. After this therapy, patients would need a transplant of healthy stem cells to restore normal blood cell production. They created CAR T-cells from healthy donors and AML patients that successfully killed CD117-positive cells (both healthy and cancerous) in lab experiments. In mice, these CAR T-cells eliminated human CD117-positive cells but left CD117-negative cells untouched. In mice with AML, the CAR T-cells completely destroyed the leukemia. To stop the CAR T-cells after treatment, they used a combination of antithymocyte globulin, (ATG) and rituximab, which helped remove the CAR T-cells from the body. This study provides the first evidence that CD117-targeting CAR T-cells can be a potential therapy for AML.

Several new therapeutic targets, including CD117, FR β , CD93, and TIM3, are currently being tested in preclinical trials using animal models to evaluate their safety and effectiveness. Preclinical studies on CD117 are ongoing, but a significant challenge is that CD117 is highly expressed on hematopoietic stem and progenitor cells. This makes CD117-targeted CAR-T therapy risky, as it can severely suppress blood cell formation. To address this, Myburgh et al. 2020 proposed a three-step approach for immunotherapy: first, using CD117 CAR-T cells to

eliminate both AML cells and original HSPCs; second, stopping the clearance effects; and finally, transplanting healthy HSPCs.

In a mouse model, CD117 CAR-T treatment successfully eliminated both healthy and leukemic cells, followed by recovery of normal blood cell production after depleting CAR-T cells with anti-thymocyte globulin and rituximab, along with hematopoietic stem cell transplantation (HSCT). While these results are promising, *in vitro* studies showed that low levels of target antigen expression and loss of the antigen due to therapeutic pressure can limit the full effectiveness of CAR-T cells. Therefore, further research is needed to understand both the potential and limitations of CD117 CAR-T therapy, especially how antigen loss might impact future clinical trials (Shao et al., 2023).

Current treatment for AML involves chemotherapy to induce remission, followed by more chemotherapy or stem cell transplantation. However, since most AML patients are older (60s–70s), many cannot tolerate chemotherapy due to severe side effects like infections, bone marrow suppression, and heart toxicity. Therefore, safer and more effective treatments are needed. An ideal therapy would specifically target AML cells without harming normal cells. Since CD117 is present on 70% of AML cells, it is a promising target for developing such therapies.

Aptamers, which are short single-stranded DNA or RNA molecules acting like chemical antibodies, binding to specific targets with high affinity. They are easy to produce, modify, and have low immunogenicity. In this study, by Zhao et al. (2013), a DNA aptamer specific for CD117 was developed using a hybrid SELEX method. Sequencing revealed a dominant aptamer sequence with 80% frequency. Flow cytometry and microscopy confirmed that the aptamer binds only to CD117-expressing AML cells and not to CD117-negative control cell lines (U937, CA46, 468, and LNCap). The aptamer also blocked anti-CD117 antibody binding, showing it directly targets CD117.

For therapy, an aptamer-drug conjugate (Apt-MTX) was created by linking the CD117 aptamer to the chemotherapy drug methotrexate (MTX). In mixed cultures of CD117+ leukemic cells (HEL) and CD117- cells (U937), Apt-MTX selectively targeted CD117+ cells without affecting the others. At a low concentration of 10 nM, Apt-MTX killed 60% of CD117+ cells, whereas free MTX had no effect. This study by Zhao et al. (2013) suggests that aptamer-drug conjugates

could offer a new, highly specific treatment for AML, complementing existing antibody-drug therapies.

Oligonucleotide aptamers are short DNA or RNA sequences that can uniquely bind to biomarkers on cancer cells. They can also be easily modified with other molecules for personalized treatments. In this study by Zhao et al. (2015), researchers have developed a single-strand DNA aptamer that targets CD117, a biomarker highly expressed on AML cells. They found that the aptamer had a G-rich core region that forms a stable structure called a G-quadruplex, which is important for its function. Experiments showed that the aptamer could bind specifically to CD117 proteins from cell samples and attach to AML cells (both lab-grown and patient-derived) with high binding strength. Once bound, the aptamer was internalized into the AML cells.

To create a targeted AML treatment, the researchers combined the aptamer with methotrexate (MTX), a drug commonly used in AML chemotherapy, forming an Apt-MTX conjugate. This conjugate specifically inhibited the growth of AML cells, caused the cells to undergo apoptosis (programmed cell death), and stopped them in the G1 phase of the cell cycle. Importantly, the Apt-MTX conjugate did not affect cells that didn't express CD117. When tested on bone marrow samples from AML patients, it selectively killed AML cells while leaving healthy cells unharmed. These results suggest that Apt-MTX could be a promising targeted therapy for AML with minimal side effects, and it also opens up new possibilities for developing other targeted cancer treatments through chemical synthesis (Zhao et al., 2015).

2.10. CD117 Activated Signaling Pathways

CD117 is activated when a stem cell factor (SCF) dimer binds to its extracellular region. Normally, CD117 exists as a single unit on the cell surface, while SCF exists as a dimer outside the cell. When SCF binds to CD117, it causes the receptor to form a homodimer, leading to autophosphorylation at specific tyrosine sites in its intracellular domain (Cardoso et al., 2017). This phosphorylation activates several key signaling pathways, including *JAK/STAT*, *RAS/MAP* kinase, *PI3* kinase, *PLC γ* , and *SRC* pathways (Linnekin et al., 1999). These pathways work together to promote cell survival, growth, differentiation, and movement. After autophosphorylation, CD117 is quickly tagged by SOCS6 for internalization and degradation.

2.10.1. JAK/STAT Pathway

This pathway helps in cell growth and differentiation. When SCF binds to CD117, *JAK2* is activated, leading to the phosphorylation of *STAT* proteins (*STAT1*, 2, or 5). These phosphorylated *STATs* move to the nucleus and trigger gene transcription for cell proliferation (Weiler et al., 1996).

2.10.2. RAS/MAP Kinase Pathway

CD117 activation recruits adaptor proteins like Grb2, Shc, and SHP2, which activate Ras—a key protein in this pathway. Ras activates a cascade involving Raf, MEK, and ERK, which regulates cell growth, differentiation, apoptosis, and movement (Yasuda et al., 2008).

2.10.3. PI3-Kinase/Akt Pathway

This pathway promotes cell survival by activating *Akt* and mTOR. *Akt* blocks pro-apoptotic factors like BAD, ensuring cell survival. It also plays a role in SCF-driven cell movement (Ueda et al., 2002).

2.10.4. SRC Pathway

CD117 strongly activates *SRC* family kinases (SFK), such as Lyn and Fyn. These kinases promote cell growth by activating CDK2 and phosphorylating Rb. Lyn can also regulate the *PI3K/Akt* pathway, though its mechanism is not fully understood (Sette et al., 2002).

2.10.5. PLC γ Pathway

PLC γ interacts with phosphorylated CD117 and breaks down PIP2 into DAG and IP3. DAG activates PKC, while IP3 increases Ca²⁺ release. Together, they regulate cell survival, growth, and adhesion, contributing to cancer progression (Lennartsson et al., 2005).

2.11. CD117-Expressing Cell Lines: A Promising Tool for AML Research and Targeted Therapy

CD117, also known as c-Kit, is a transmembrane tyrosine kinase receptor that plays a crucial role in hematopoiesis, stem cell maintenance, and cellular signaling (Rosu-Myles et al., 2007). Its overexpression is frequently observed in acute myeloid leukemia and is associated with disease progression, poor prognosis, and resistance to treatment (Beghini et al., 2004). Several

AML cell lines, including HL-60, Kasumi-1, and MOLM-13, are widely used in research to model CD117 overexpression and to develop targeted therapeutic strategies.

Cell lines expressing CD117 serve as a promising tool for studying AML, given that this transmembrane receptor tyrosine kinase is frequently overexpressed in AML cells. CD117 plays a critical role in cell proliferation, differentiation, and survival, making it an essential biomarker for identifying AML subtypes and developing targeted therapeutic strategies (Zhou et al., 2015). Among various cell lines, HL60 and Kasumi-1 are widely utilized to model CD117-positive AML, offering a reliable model for understanding disease mechanisms and evaluating novel drug delivery approaches. The expression of CD117 not only aids in disease diagnosis but also provides an opportunity for selective targeting in therapy, potentially minimizing systemic toxicity and improving treatment outcomes (Wang et al., 2019). Furthermore, CD117-based targeting strategies are being explored in experimental models to enhance the therapeutic drug delivery systems, such as aptamer-conjugated nanoparticles, for AML therapy (Zhang et al., 2021).

2.11.1. Cell Lines with CD117 Overexpression

HL-60 cells, derived from a patient with promyelocytic leukemia, are known to express CD117, particularly during differentiation into granulocytes or macrophages. This makes them a valuable model for studying the role of CD117 in AML pathogenesis and apoptosis (Birnie, 1998). Kasumi-1 cells, established from a patient with AML harboring the t(8;21) translocation, exhibit high levels of CD117 expression and are commonly used to evaluate targeted therapies involving CD117 inhibitors. MOLM-13, derived from a patient with FLT3-ITD-positive AML, also expresses CD117 and serves as a critical model for drug screening and the investigation of leukemogenesis (Quentmeier et al., 2003). Other CD117-positive AML cell lines include HEL, KG-1, and TF-1, all of which have varying levels of CD117 expression depending on their differentiation status and mutation profile.

2.11.2. Cell Lines Lacking CD117 Overexpression

In contrast, certain AML cell lines lack significant CD117 expression and serve as negative controls or models for CD117-independent AML subtypes. For instance, THP-1 cells, which are derived from a patient with monocytic leukemia, show minimal CD117 expression and are

more commonly used to study monocyte and macrophage differentiation. NB4 cells, derived from a patient with acute promyelocytic leukemia (APL), are also largely negative for CD117. These cells are often employed in studies related to APL and the effects of retinoic acid treatment rather than CD117-targeted therapies (Lanotte et al., 1991). U937 cells, another monocytic leukemia cell line, similarly lack CD117 expression and are used in research focusing on apoptosis, immune response, and signal transduction pathways (Sundström & Nilsson, 1976).

2.11.3. Role of CD117 in Apoptosis and Differentiation

The differential expression of CD117 in these cell lines is pivotal for understanding AML heterogeneity and therapeutic responses. For example, in HL-60 cells, the induction of apoptosis during neutrophil differentiation correlates with changes in the expression of apoptosis-regulating genes such as bak, bfl-1, and caspases (Mollinedo et al., 2008). These gene expression patterns are similar to those observed in mature neutrophils, where CD117 expression also diminishes as cells undergo apoptosis. Studies show that inhibiting caspase activity or overexpressing anti-apoptotic genes like BCL-2 can delay apoptosis in HL-60 cells without affecting their differentiation potential, suggesting a tightly regulated balance between differentiation and cell death in neutrophil development (Shen et al., 2013).

2.11.4. Clinical Implications and Future Directions

The contrasting roles of CD117-positive and CD117-negative cell lines offer valuable insights into the molecular mechanisms underlying AML and highlight the potential for targeted therapies. CD117 inhibitors, such as imatinib and dasatinib, have shown promise in preclinical models and clinical trials, particularly in patients with *FLT3* or c-Kit mutations (Giles et al., 2003). Understanding how these inhibitors affect various AML subtypes can aid in developing more personalized and effective treatment strategies. Moreover, the use of nanoparticle-based drug delivery systems targeting CD117 offers new opportunities for improving therapeutic outcomes while minimizing off-target effects (Zhang et al., 2021).

2.12. CD117-Targeted Aptamer-Conjugated PLGA Nanoparticles: A Novel Strategy for Drug Delivery in AML

The development of PLGA nanoparticles conjugated with a CD117-specific aptamer and loaded with clofarabine represents a pioneering strategy in targeted drug delivery for AML. Unlike conventional chemotherapy, which lacks selectivity and often results in systemic toxicity and multidrug resistance, this innovative system harnesses the biocompatibility and controlled drug release properties of PLGA nanoparticles while enhancing specificity through aptamer-based targeting. The CD117 receptor, a crucial biomarker overexpressed in AML cells, allows precise recognition and binding of the aptamer, ensuring selective drug accumulation at the cancer site. This targeted delivery approach minimizes off-target effects, reducing toxicity to healthy tissues while improving therapeutic efficacy. Additionally, the encapsulation of clofarabine within PLGA nanoparticles enables sustained drug release, which may enhance intracellular drug retention and prolong anti-leukemic activity. The rationale behind this approach is to overcome the limitations of free clofarabine administration, such as rapid systemic clearance and dose-dependent toxicity, by offering a sustained, tumor-specific drug delivery system. The expected outcomes include increased drug bioavailability, enhanced cellular uptake by leukemic cells, and a potential reduction in side effects, ultimately improving treatment outcomes in AML.

Looking ahead, the integration of nanotechnology with molecular targeting opens new avenues for targeted medicine in AML. Future research could explore the optimization of nanoparticle formulation to further enhance drug loading efficiency and release kinetics. Additionally, combining aptamer-conjugated PLGA nanoparticles with other therapeutic agents, such as small-molecule inhibitors or immunotherapies, may offer synergistic effects, improving treatment response. Investigating the biodistribution and pharmacokinetics of this delivery system through *in vivo* studies will be critical in advancing toward clinical translation. Furthermore, advancements in aptamer engineering, including modifications to enhance stability and resistance to nuclease degradation, could improve the therapeutic potential of this platform. As targeted medicine continues to evolve, this novel approach holds promise in not only refining AML treatment but also serving as a versatile model for targeted drug delivery in other hematological malignancies and solid tumors (Ding et al., 2020; Noga et al., 2023).

2.13. References:

- Bala, I., Hariharan, S., & Kumar, M. N. V. R. (2004). PLGA nanoparticles in drug delivery: The state of the art. *Critical Reviews™ in Therapeutic Drug Carrier Systems*, 21(5). DOI: 10.1615/CritRevTherDrugCarrierSyst.v21.i5.20
- Beck, A., & Reichert, J. M. (2013, September). Approval of the first biosimilar antibodies in Europe: a major landmark for the biopharmaceutical industry. In *MAbs* (Vol. 5, No. 5, pp. 621-623). Taylor & Francis. <https://doi.org/10.4161/mabs.25864>
- Beghini, A., Ripamonti, C. B., & Roversi, G. (2004). *c-Kit mutations in core-binding factor leukemias*. *Haematologica*, 89(8), 971–973. <https://doi.org/10.1182/blood.V95.2.726>
- Birnie, G. D. (1988). The HL60 cell line: a model system for studying human myeloid cell differentiation. *The British journal of cancer. Supplement*, 9, 41.
- Bruserud, Ø., Selheim, F., Hernandez-Valladares, M., & Reikvam, H. (2024). Monocytic differentiation in acute myeloid leukemia cells: Diagnostic criteria, biological heterogeneity, mitochondrial metabolism, resistance to and induction by targeted therapies. *International Journal of Molecular Sciences*, 25(12), 6356. <https://doi.org/10.3390/ijms25126356>
- Cardoso, H. J., Figueira, M. I., & Socorro, S. (2017). The stem cell factor (SCF)/c-KIT signalling in testis and prostate cancer. *Journal of cell communication and signaling*, 11, 297-307. <https://doi.org/10.1007/s12079-017-0399-1>
- Cheng, Y., Xu, Z., Ma, M., & Xu, T. (2008). Dendrimers as drug carriers: Applications in different routes of drug administration. *Journal of Pharmaceutical Sciences*, 97(1), 123–143. <https://doi.org/10.1002/jps.21079>
- Crossnohere, N. L., Richardson, D. R., Reinhart, C., O'Donoghue, B., Love, S. M., Smith, B. D., & Bridges, J. F. P. (2019). Side effects from acute myeloid leukemia treatment: Results from a national survey. *Current Medical Research and Opinion*, 35(11), 1965–1970. <https://doi.org/10.1080/03007995.2019.1631149>
- Danhier, F., Ansorena, E., Silva, J. M., Coco, R., Le Breton, A., & Pr at, V. (2012). PLGA-based nanoparticles: An overview of biomedical applications. *Journal of Controlled Release*, 161(2), 505–522. <https://doi.org/10.1016/j.jconrel.2012.01.043>
- de la Torre, P., P erez-Lorenzo, M. J., Alc azar-Garrido,  ., & Flores, A. I. (2020). Cell-based nanoparticles delivery systems for targeted cancer therapy: lessons from anti-angiogenesis treatments. *Molecules*, 25(3), 715. <https://doi.org/10.3390/molecules25030715>

- Ding, Y., Sun, Z., Tong, Z., Zhang, S., Min, L., & Fu, Y. (2020). Aptamer-functionalized nanoparticles for targeted drug delivery in cancer therapy. *International Journal of Molecular Sciences*, 21(3), 872. <https://doi.org/10.3389/fmolb.2020.00193>
- Dutta, D., Chakraborty, A., Mukherjee, B., & Gupta, S. (2018). Aptamer-conjugated apigenin nanoparticles to target colorectal carcinoma: A promising safe alternative of colorectal cancer chemotherapy. *ACS Applied Bio Materials*, 1(5), 1538–1556. <https://doi.org/10.1021/acsabm.8b00441>
- Ellington, A. D., & Szostak, J. W. (1990). In vitro selection of RNA molecules that bind specific ligands. *nature*, 346(6287), 818-822. <https://doi.org/10.1038/346818a0>
- Eriksson, A., Lennartsson, A., & Lehmann, S. (2015). Epigenetic aberrations in acute myeloid leukemia: Early key events during leukemogenesis. *Experimental Hematology*, 43(8), 609–624. <https://doi.org/10.1016/j.exphem.2015.05.009>
- Escribano, L., Ocqueteaub, M., Almeida, J., Orfao, A., & Migue, J. F. S. (1998). Expression of the c-kit (CD117) molecule in normal and malignant hematopoiesis. *Leukemia & lymphoma*, 30(5-6), 459-466. <https://doi.org/10.3109/10428199809057558>
- Faderl, S., Verstovsek, S., Cortes, J., Ravandi, F., Beran, M., Garcia-Manero, G., Ferrajoli, A., Estrov, Z., O'Brien, S., Koller, C., Giles, F. J., Wierda, W., Kwari, M., & Kantarjian, H. M. (2006). Clofarabine and cytarabine combination as induction therapy for acute myeloid leukemia (AML) in patients 50 years of age or older. *Blood*, 108(1), 45-51. <https://doi.org/10.1182/blood-2005-08-3294>
- Frankel, A. E., Sievers, E. L., & Scheinberg, D. A. (2000). Cell surface receptor-targeted therapy of acute myeloid leukemia: a review. *Cancer biotherapy & radiopharmaceuticals*, 15(5), 459-476. <https://doi.org/10.1089/cbr.2000.15.459>
- Fu, Z., & Xiang, J. (2020). Aptamers, the nucleic acid antibodies, in cancer therapy. *International Journal of Molecular Sciences*, 21(8), 2793. <https://doi.org/10.3390/ijms21082793>
- Garfin, P. M., & Feldman, E. J. (2016). Antibody-based treatment of acute myeloid leukemia. *Current hematologic malignancy reports*, 11, 545-552. <https://doi.org/10.1007/s11899-016-0349-7>
- Ghanem, H., Jabbour, E., Faderl, S., Ghandhi, V., Plunkett, W., & Kantarjian, H. (2010). Clofarabine in leukemia. *Expert review of hematology*, 3(1), 15-22. <https://doi.org/10.1586/ehm.09.70>

- Giles, F. J., Albitar, M., & Thomas, D. A. (2003). *Targeting c-Kit in AML: Emerging treatment strategies*. *Cancer*, 98(8), 1605–1613.
- Girotti, A., Escalera-Anzola, S., Alonso-Sampedro, I., González-Valdivieso, J., & Arias, F. J. (2020). Aptamer-functionalized natural protein-based polymers as innovative biomaterials. *Pharmaceutics*, 12(11), 1115. <https://doi.org/10.3390/pharmaceutics12111115>
- Giudice, V., Mensitieri, F., Izzo, V., Filippelli, A., & Selleri, C. (2020). Aptamers and antisense oligonucleotides for diagnosis and treatment of hematological diseases. *International journal of molecular sciences*, 21(9), 3252. <https://doi.org/10.3390/ijms21093252>
- Godley, L. A., & Larson, R. A. (2008). Therapy-related myeloid leukemia. In *Seminars in Oncology* (Vol. 35, No. 4, pp. 418–429). WB Saunders. <https://doi.org/10.1053/j.seminoncol.2008.04.012>
- Gundersen, E. T. (2016). *The production and characterization of drug-loaded liposomal and PLGA nanocarriers for targeted treatment of acute myeloid leukemia* (Master's thesis, The University of Bergen). <https://hdl.handle.net/1956/12587>
- Hamid, G. A. (2013). Acute leukemia clinical presentation. *Leukemia*, 75. <http://dx.doi.org/10.5772/53531>
- Hansel, T. T., Kropshofer, H., Singer, T., Mitchell, J. A., & George, A. J. (2010). The safety and side effects of monoclonal antibodies. *Nature reviews Drug discovery*, 9(4), 325-338. <https://doi.org/10.1038/nrd3003>
- Huanbutta, K., Teixeira, M., Gonçalves, V., Tiritan, E., & Pinto, M. M. M. (2016). Development of targeted polymeric nanoparticles for acute myeloid leukaemia. *Advanced Science, Engineering and Medicine*, 8(1), 68–74. <https://doi.org/10.1166/asem.2016.1804>
- Huang, X., Jain, P. K., El-Sayed, I. H., & El-Sayed, M. A. (2008). Plasmonic photothermal therapy (PPTT) using gold nanoparticles. *Lasers in Medical Science*, 23, 217–228. <https://doi.org/10.1007/s10103-007-0470-x>
- Huang, Z., Qiu, L., Zhang, T., & Tan, W. (2021). Integrating DNA nanotechnology with aptamers for biological and biomedical applications. *Matter*, 4(2), 461-489. <https://doi.org/10.1016/j.matt.2020.11.002>
- Immordino, M. L., Dosio, F., & Cattel, L. (2006). Stealth liposomes: Review of the basic science, rationale, and clinical applications, existing and potential. *International Journal of Nanomedicine*, 1(3), 297–315. <https://doi.org/10.2147/DIJN.1.S633>

- Jilani, I., Estey, E., Huh, Y. O., et al. (2002). Differences in CD33 intensity between normal myeloid precursors and acute myeloid leukemia blasts. *Implications for targeted therapy. Blood*. <https://doi.org/10.1309/1WMW-CMXX-4WN4-T55U>
- Kansal, R. (2019). Classification of acute myeloid leukemia by the revised fourth edition World Health Organization criteria: A retrospective single-institution study with appraisal of the new entities of acute myeloid leukemia with gene mutations in *NPM1* and biallelic *CEBPA*. *Human Pathology*, *90*, 80–96. <https://doi.org/10.1016/j.humpath.2019.04.020>
- Kayser, S., & Levis, M. J. (2018). Advances in targeted therapy for acute myeloid leukaemia. *British Journal of Haematology*, *180*(4), 484–500. <https://doi.org/10.1111/bjh.15032>
- Keefe, A. D., Pai, S., & Ellington, A. (2010). Aptamers as therapeutics. *Nature reviews Drug discovery*, *9*(7), 537-550. <https://doi.org/10.1038/nrd3141>
- Lanotte, M., Martin-Thouvenin, V., Najman, S., Balerini, P., Valensi, F., & Berger, R. (1991). NB4, a maturation inducible cell line with *t(15;17)* marker isolated from a human acute promyelocytic leukemia. *Blood*, *77*(5), 1080–1086. <https://doi.org/10.1182/blood.V77.5.1080.1080>
- Lennartsson, J., Jelacic, T., Linnekin, D., & Shivakrupa, R. (2005). Normal and oncogenic forms of the receptor tyrosine kinase kit. *Stem cells*, *23*(1), 16-43. <https://doi.org/10.1634/stemcells.2004-0117>
- Li, F., Lu, J., & Dong, Q. (2016). VEGF-targeting aptamers and their potential therapeutic applications in cancer. *Journal of Molecular Medicine*, *94*(8), 861–872. <https://www.proquest.com/dissertations-theses/material-toolbox-advanced-therapeutics/docview/2492667704/se-2?accountid=16284>
- Linnekin, D. (1999). Early signaling pathways activated by c-Kit in hematopoietic cells. *The international journal of biochemistry & cell biology*, *31*(10), 1053-1074. [https://doi.org/10.1016/S1357-2725\(99\)00078-3](https://doi.org/10.1016/S1357-2725(99)00078-3)
- Löwenberg, B., Pabst, T., Maertens, J., Van Norden, Y., Biemond, B. J., Schouten, H. C., Spertini, O., Vellenga, E., Graux, C., Havelange, V., Greef, G. E., Weerdt, O., Legdeur, M. C., Kuball, J., Marwijk Kooy, M., Gjertsen, B.T., Lavrencic, M. J., Lammeren-Venema, D.V., Hodossy, B., Breems, D.A., Chalandon, Y., Passweg, J., Valk, P., Manz, M.G., & Ossenkoppele, G. J. (2017). Therapeutic value of clofarabine in younger and middle-aged (18-65 years) adults with newly diagnosed AML. *Blood, The Journal of the American Society of Hematology*, *129*(12), 1636-1645. <https://doi.org/10.1182/blood-2016-10-740613>

- Majeti, Ravindra. "Monoclonal antibody therapy directed against human acute myeloid leukemia stem cells." *Oncogene* 30, no. 9 (2011): 1009-1019. <https://doi.org/10.1038/onc.2010.511>
- Matsumura, Y., & Kataoka, K. (2009). Preclinical and clinical studies of anticancer agent-incorporating polymer micelles. *Cancer Science*, 100(4), 572–579. <https://doi.org/10.1111/j.1349-7006.2009.01103.x>
- McMahon, C. M., Ferng, T., Canaani, J., Wang, E. S., Morrissette, J. J. D., Eastburn, D. J., Pellegrino, M., et al. (2019). Clonal selection with RAS pathway activation mediates secondary clinical resistance to selective FLT3 inhibition in acute myeloid leukemia. *Cancer Discovery*, 9(8), 1050–1063. <https://doi.org/10.1158/2159-8290.CD-18-1453>
- Mollinedo, F., López-Pérez, R., & Gajate, C. (2008). Differential gene expression patterns coupled to commitment and acquisition of phenotypic hallmarks during neutrophil differentiation of human leukaemia HL-60 cells. *Gene*, 419(1-2), 16-26. <https://doi.org/10.1016/j.gene.2008.04.015>
- Müller, J. P., & Schmidt-Arras, D. (2020). Novel approaches to target mutant FLT3 leukaemia. *Cancers*, 12(10), 2806. <https://doi.org/10.3390/cancers12102806>
- Myburgh, R., Kiefer, J. D., Russkamp, N. F., Magnani, C. F., Nuñez, N., Simonis, A., Pfister, S., Wilk, C. M., Friemel, J., Müller, A. M., Becher, B., Münz, C., Broek, M., Neri, D., & Manz, M. G. (2020). Anti-human CD117 CAR T-cells efficiently eliminate healthy and malignant CD117-expressing hematopoietic cells. *Leukemia*, 34(10), 2688-2703. <https://doi.org/10.1038/s41375-020-0818-9>
- Noga, M., Milan, J., Frydrych, A., & Jurowski, K. (2023). Toxicological aspects, safety assessment, and green toxicology of silver nanoparticles (AgNPs)—critical review: state of the art. *International Journal of Molecular Sciences*, 24(6), 5133. <https://doi.org/10.3390/ijms24065133>
- Nur, Y., Gaffar, S., Hartati, Y. W., & Subroto, T. (2021). Applications of electrochemical biosensor of aptamers-based (APTASENSOR) for the detection of leukemia biomarker. *Sensing and Bio-Sensing Research*, 32, 100416. <https://doi.org/10.1016/j.sbsr.2021.100416>
- Obeagu, E. I., & Babar, Q. (2021). *Acute myeloid leukaemia (AML): The good, the bad, and the ugly*. *International Journal of Current Research in Medical Sciences*, 7(7), 29–41.
- Pagel, J. M., et al. (2011). Targeting CD33 in acute myeloid leukemia. *Blood Reviews*.

- Poonia, N., Jadhav, N. V., Mamatha, D., Garg, M., Kabra, A., Bhatia, A., Ojha, S., Lather, V., & Pandita, D. (2024). Nanotechnology-assisted combination drug delivery: A progressive approach for the treatment of acute myeloid leukemia. *Therapeutic Delivery*, *15*(11), 893–910. <https://doi.org/10.1080/20415990.2024.2394012>
- Quentmeier, H., Reinhardt, J., & Zaborski, M. (2003). *MOLM-13: A model for FLT3-mutated acute myeloid leukemia*. *Leukemia Research*, *27*(6), 567–571.
- Ramos, T. L., & Grover, S. P. (2017). Antibody-drug conjugates: A new frontier in cancer therapy. *Clinical Cancer Research*, *23*(3), 622–631. <https://doi.org/10.1016/j.ymthe.2024.07.028>
- Rodriguez-Sevilla, J. J., Adema, V., Garcia-Manero, G., & Colla, S. (2023). Emerging treatments for myelodysplastic syndromes: biological rationales and clinical translation. *Cell Reports Medicine*, *4*(2). <https://doi.org/10.1016/j.xcrm.2023.100940>
- Roman Diaz, J. L., Vazquez Martinez, M., & Khimani, F. (2024). New approaches for the treatment of AML beyond the 7+3 regimen: Current concepts and new approaches. *Cancers*, *16*(3), 677. <https://doi.org/10.3390/cancers16030677>
- Rosu-Myles, M., Taylor, B. J., & Wolff, L. (2007). *CD117 signaling in stem cell biology and leukemogenesis*. *Stem Cell Reviews*, *3*(2), 157–166.
- Sefah, K., Tang, Z. W., Shangguan, D. H., Chen, H., Lopez-Colon, D., Li, Y., Parekh, P., Martin, J., Meng, L., Phillips, J. A., Kim, Y. M., Tan, W. H. (2009). Molecular recognition of acute myeloid leukemia using aptamers. *Leukemia*, *23*(2), 235-244. <https://doi.org/10.1038/leu.2008.335>
- Sette, C., Paronetto, M. P., Barchi, M., Bevilacqua, A., Geremia, R., & Rossi, P. (2002). Tr-kit-induced resumption of the cell cycle in mouse eggs requires activation of a Src-like kinase. *The EMBO Journal*. <https://doi.org/10.1093/emboj/cdf553>
- Shangguan, D., Li, Y., Tang, Z., Cao, Z. C., Chen, H. W., Mallikaratchy, P., Sefah, K., Yang, C. J., & Tan, W. (2006). Aptamers evolved from live cells as effective molecular probes for cancer study. *Proceedings of the National Academy of Sciences*, *103*(32), 11838–11843. <https://doi.org/10.1073/pnas.0602615103>
- Shao, R., Li, Z., Xin, H., Jiang, S., Zhu, Y., Liu, J., Huang, R., Xu, K., & Shi, X. (2023). Biomarkers as targets for CAR-T/NK cell therapy in AML. *Biomarker Research*, *11*(1), 65. <https://doi.org/10.1186/s40364-023-00501-9>

- Sharma, S., Parmar, A., Kori, S., & Sandhir, R. (2016). PLGA-based nanoparticles: A new paradigm in biomedical applications. *Trends in Analytical Chemistry*, 80, 30–40. <https://doi.org/10.1016/j.trac.2015.06.014>
- Shen, H., Yu, C., & Wang, Y. (2013). *Caspase regulation in HL-60 cell apoptosis during differentiation*. *Journal of Hematologic Research*, 14(3), 89–97. <https://doi.org/10.5246/jcps.2013.02.026>
- Soni, G., & Yadav, K. S. (2015). Applications of nanoparticles in treatment and diagnosis of leukemia. *Materials Science and Engineering: C*, 47, 156–164. <https://doi.org/10.1016/j.msec.2014.10.043>
- Sun, H., Zu, Y., & Deng, Y. (2019). CD123-specific aptamers for leukemia stem cell targeting and elimination. *Leukemia Research*, 82, 1–10.
- Sundström, C., & Nilsson, K. (1976). *Establishment and characterization of a human histiocytic lymphoma cell line (U937)*. *International Journal of Cancer*, 17(5), 565–577. <https://doi.org/10.1002/ijc.2910170504>
- Sun, H., Zhu, X., & Lu, P. (2014). Recent advances in aptamer-based therapeutics and applications in leukemia therapy. *Leukemia Research*, 38(5), 528–535.
- Tan, S., Li, D., & Zhu, X. (2020). Cancer immunotherapy: Pros, cons and beyond. *Biomedicine & Pharmacotherapy*, 124, 109821. <https://doi.org/10.1016/j.biopha.2020.109821>
- Tonbul, H., Sahin, A., Tavukcuoglu, E., Esendagli, G., & Capan, Y. (2019). Combination drug delivery with actively-targeted PLGA nanoparticles to overcome multidrug resistance in breast cancer. *Journal of Drug Delivery Science and Technology*, 54, 101380. <https://doi.org/10.1016/j.jddst.2019.101380>
- Tuerk, C., & Gold, L. (1990). Systematic evolution of ligands by exponential enrichment: RNA ligands to bacteriophage T4 DNA polymerase. *Science*, 249(4968), 505–510. <https://doi.org/10.1126/science.2200121>
- Ueda, S., Mizuki, M., Ikeda, H., Tsujimura, T., Matsumura, I., Nakano, K., Daino, H., Honda, Z., Sanoyama, J., Shibayama, H., Sugarahara, H., Machii, T., & Kanakura, Y. (2002). Critical roles of c-Kit tyrosine residues 567 and 719 in stem cell factor-induced chemotaxis: contribution of src family kinase and PI3-kinase on calcium mobilization and cell migration. *Blood, The Journal of the American Society of Hematology*, 99(9), 3342–3349. <https://doi.org/10.1182/blood.V99.9.3342>

- Vainchenker, W., & Kralovics, R. (2017). Genetic basis and molecular pathophysiology of classical myeloproliferative neoplasms. *Blood*, *129*(6), 667–679. <https://doi.org/10.1182/blood-2016-10-695940>
- van der Kolk, D. M., de Vries, E. G. E., Müller, M., & Vellenga, E. (2002). The role of drug efflux pumps in acute myeloid leukemia. *Leukemia & Lymphoma*, *43*(4), 685–701. <https://doi.org/10.1080/10428190290016773>
- Wang, X., Zhou, H., & Zheng, J. (2021). CD44 aptamers and their role in targeting leukemia stem cells. *Hematology Reports*, *13*(1), 75–84.
- Wang, J., Li, Z., & Chen, X. (2019). *Targeting CD117 for acute myeloid leukemia therapy: Advances and challenges*. *Experimental Hematology*, *47*(4), 123–136.
- Weiler, S. R., Mou, S., DeBerry, C. S., Keller, J. R., Ruscetti, F. W., Ferris, D. K., Longo, D. L., & Linnekin, D. (1996). JAK2 is associated with the c-kit proto-oncogene product and is phosphorylated in response to stem cell factor. <https://doi.org/10.1182/blood.V87.9.3688.bloodjournal8793688>
- Wu, X., Wang, F., Yang, X., Gong, Y., Niu, T., Chu, B., Qu, Y., & Qian, Z. (2024). Advances in drug delivery systems for the treatment of acute myeloid leukemia. *Small*, *20*(42), 2403409.
- Yang, J. J., Park, T. S., & Wan, T. S. K. (2017). Recurrent cytogenetic abnormalities in acute myeloid leukemia. In *Cancer Cytogenetics: Methods and Protocols* (pp. 223–245). https://doi.org/10.1007/978-1-4939-6703-2_19
- Yasuda, T., & Kurosaki, T. (2008). Regulation of lymphocyte fate by Ras/ERK signals. *Cell Cycle*, *7*(23), 3634–3640. <https://doi.org/10.4161/cc.7.23.7103>
- Zhang, Y., Huang, C., & Liu, F. (2021). *Nanoparticle-based approaches for AML targeted therapy: Role of CD117 biomarker*. *Molecular Cancer Therapeutics*, *20*(2), 201–214.
- Zhang, J., Gu, Y., & Chen, B. (2019). Mechanisms of drug resistance in acute myeloid leukemia. *OncoTargets and Therapy*, *12*, 1937–1945. <https://doi.org/10.2147/OTT.S191621>
- Zhang, X., Wang, W., & Yuan, S. (2017). Strategies for improving the delivery and bioavailability of anticancer drugs using nanoparticles. *Journal of Drug Delivery Science and Technology*, *40*, 55–67.
- Zhao, X., Liu, H. Q., Wang, L. N., Yang, L., & Liu, X. (2022). Current and emerging molecular and epigenetic disease entities in acute myeloid leukemia and a critical assessment of their

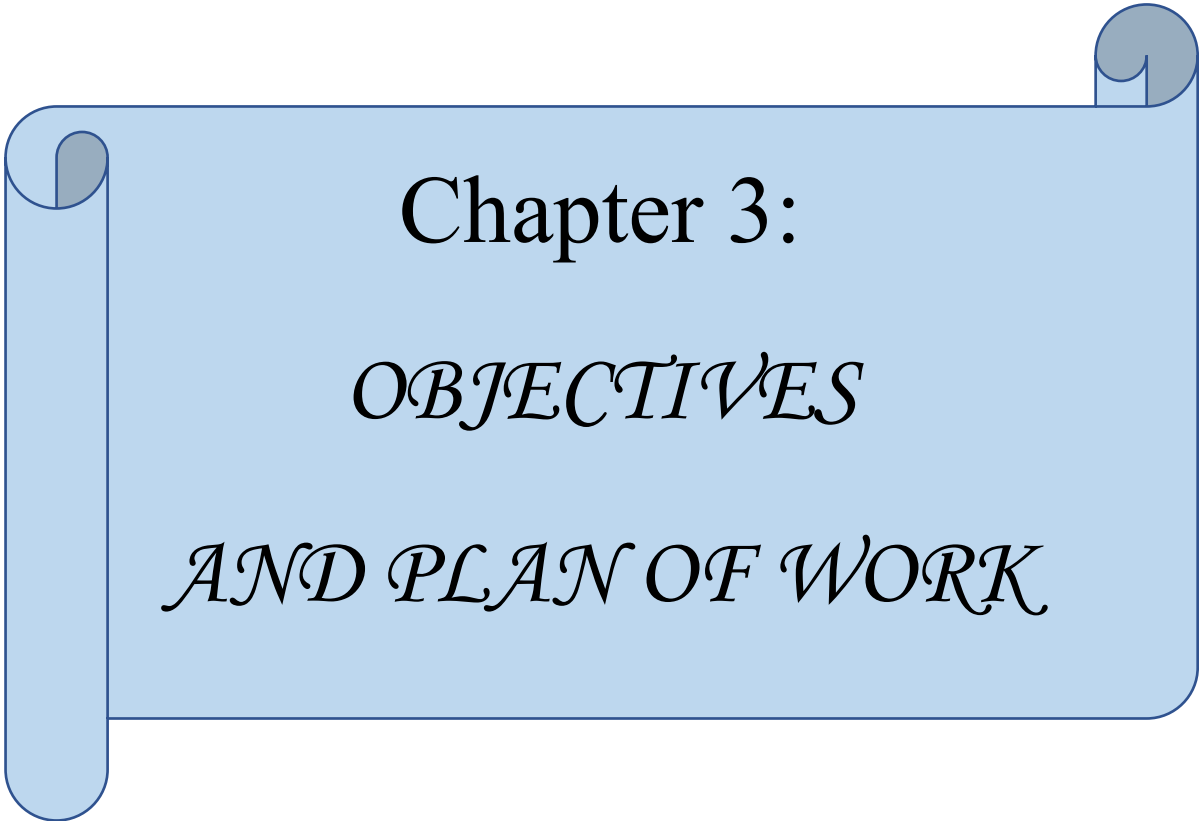
therapeutic modalities. In *Seminars in Cancer Biology* (Vol. 83, pp. 121–135). Academic Press. <https://doi.org/10.1016/j.semcancer.2020.11.010>

Zhao, N., Pei, S. N., Qi, J., Lin, P., & Zu, Y. (2013). Targeted therapy of acute myeloid leukemia by A CD117-specific aptamer-drug-conjugate. <https://doi.org/10.1182/blood.V122.21.1446.1446>

Zhao, N., Pei, S. N., Qi, J., Zeng, Z., Iyer, S. P., Lin, P., Tung, C. H., & Zu, Y. (2015). Oligonucleotide aptamer-drug conjugates for targeted therapy of acute myeloid leukemia. *Biomaterials*, 67, 42-51. <https://doi.org/10.1016/j.biomaterials.2015.07.025>

Zhenchuk, A., Lotfi, K., Juliusson, G., & Albertioni, F. (2009). Mechanisms of anti-cancer action and pharmacology of clofarabine. *Biochemical Pharmacology*, 78(11), 1351–1359. <https://doi.org/10.1016/j.bcp.2009.06.094>

Zhou, J., Rossi, J. J., & Shigdar, S. (2020). CD33-targeted aptamers: Emerging tools for AML therapy. *Journal of Clinical Oncology*, 38(15), 1711–1718.



Chapter 3:
OBJECTIVES
AND PLAN OF WORK

3.1. Objectives of the Study:

Acute myeloid leukemia remains one of the most aggressive forms of leukemia, with a high rate of relapse and poor prognosis despite advancements in conventional chemotherapy. Clofarabine, a nucleoside analogue, is widely used in AML treatment due to its ability to inhibit ribonucleotide reductase and disrupt DNA synthesis in cancer cells. However, its clinical application is often limited due to severe systemic toxicity, non-specific distribution, and the development of drug resistance. Current treatment strategies, including chemotherapy and stem cell transplantation, are associated with significant adverse effects, necessitating the exploration of more targeted and efficient drug delivery systems.

Previous research has investigated nanoparticle-based drug delivery systems to improve chemotherapy outcomes. Among these, poly(lactic-co-glycolic acid), PLGA nanoparticles have been extensively studied due to their biocompatibility, biodegradability, and ability to provide controlled drug release. Studies have shown that encapsulating chemotherapeutic drugs within PLGA nanoparticles can reduce systemic toxicity and improve drug bioavailability. However, a major limitation observed in this study is the lack of selective targeting, leading to non-specific uptake by healthy hematopoietic cells and rapid clearance by the mononuclear phagocyte system. While antibody-conjugated nanoparticles have been explored to enhance targeting, challenges such as high immunogenicity, complex production processes, and stability issues hinder their clinical translation.

The key gap in the previous research lies in the limited exploration of aptamer-conjugated nanoparticles for AML treatment. Although aptamers have gained attention as targeting ligands due to their high specificity, stability, lower immunogenicity, and cost-effectiveness compared to antibodies, their potential in directing drug-loaded nanoparticles to AML cells has not been fully utilized. Specifically, while CD117 (c-KIT) is well-recognized as a biomarker overexpressed in leukemic stem and progenitor cells, very few studies have leveraged CD117-specific aptamers for targeted drug delivery in AML. Existing research primarily focuses on aptamers for diagnostic applications or as standalone therapeutic agents, rather than integrating them into a nanoparticle-based system for enhanced drug delivery.

To bridge this gap, this study aims to develop an innovative nanoparticle-based drug delivery system that specifically targets AML cells. PLGA nanoparticles have been extensively

investigated as biodegradable and biocompatible carriers that enable controlled and sustained drug release, thereby reducing systemic toxicity and enhancing therapeutic outcomes. However, to achieve selective targeting, a ligand-based approach is necessary. Among various ligands, aptamers have emerged as promising candidates due to their high specificity, stability, lower immunogenicity compared to antibodies, and cost-effectiveness. The CD117 (c-KIT) receptor is overexpressed in a significant subset of AML cells, making it an ideal target for aptamer-based delivery strategies.

This study hypothesizes that by conjugating a CD117-specific aptamer to clofarabine-loaded PLGA nanoparticles (Apt-CNP), the therapeutic efficacy of clofarabine should significantly enhance while reducing off-target side effects. The selective targeting of leukemia cells should allow for higher intracellular drug concentrations at the tumor site, reducing systemic toxicity and minimizing the damage to healthy hematopoietic cells. Additionally, the sustained release properties of PLGA nanoparticles could ensure prolonged drug retention in circulation, reducing the need for frequent dosing and potentially overcoming drug resistance mechanisms that often arise due to rapid drug metabolism and clearance.

By integrating nanotechnology with aptamer-based targeting, this study aims to develop a novel and effective strategy for AML treatment that not only improves patient outcomes but also contributes to the broader field of precision medicine. The findings from this research could pave the way for future clinical applications, offering a more efficient and safer alternative to conventional chemotherapy for AML patients.

3.2. Plan of Work

3.2.1. Literature Review and Conceptualization

- Studied leukemia and AML, nanoparticle drug delivery involving PLGA and nanoliposomes, and aptamer-based drug targeting.
- Identified CD117 as a suitable target after reviewing various other biomarkers for targeting.

3.2.2. Synthesis and Characterization of Nanoparticles

- Formulated clofarabine-loaded PLGA nanoparticles using the multiple emulsion solvent evaporation method.
- Surface morphology analysis of all the experimental nanoparticles by FESEM, HR-TEM, and AFM
- Characterized nanoparticles for particle size (DLS), charge (zeta potential), drug loading and encapsulation efficiency, in vitro drug release profile and in vivo pharmacokinetic activity.

3.2.3. Aptamer Conjugation and Validation

- Conjugated CD117-specific aptamer to nanoparticles using EDC/NHS method.
- Evaluated the aptamer binding affinity to the nanoparticle surface by molecular docking study.
- Confirmed successful conjugation of the aptamer onto the nanoparticle surface by agarose gel electrophoresis.

3.2.4. In Vitro and In Vivo Studies

- Conducted cytotoxicity assays by using an MTT on AML cells, HL60 cells (CD117 positive), U937 cells (CD117 negative) and normal peripheral blood mononuclear cells (PBMC).
- Studied cellular uptake studies on CD117 positive as well as CD117 negative cells using flow cytometry.
- Performed cellular apoptosis analysis using Annexin V/PI staining on CD117 positive and CD117 negative cells.
- Performed mitochondrial membrane depolarisation study using JC-1 on HL60 cells (CD117 positive).
- Performed in vivo pharmacokinetic activity on normal male Swiss albino mice.

3.2.5. Data Analysis and Interpretation

- Analyzed experimental results statistically.
- Compared findings with previous studies.

3.2.6. Thesis Writing and Publication

- Documented research findings.
- Presented findings at an international seminar.

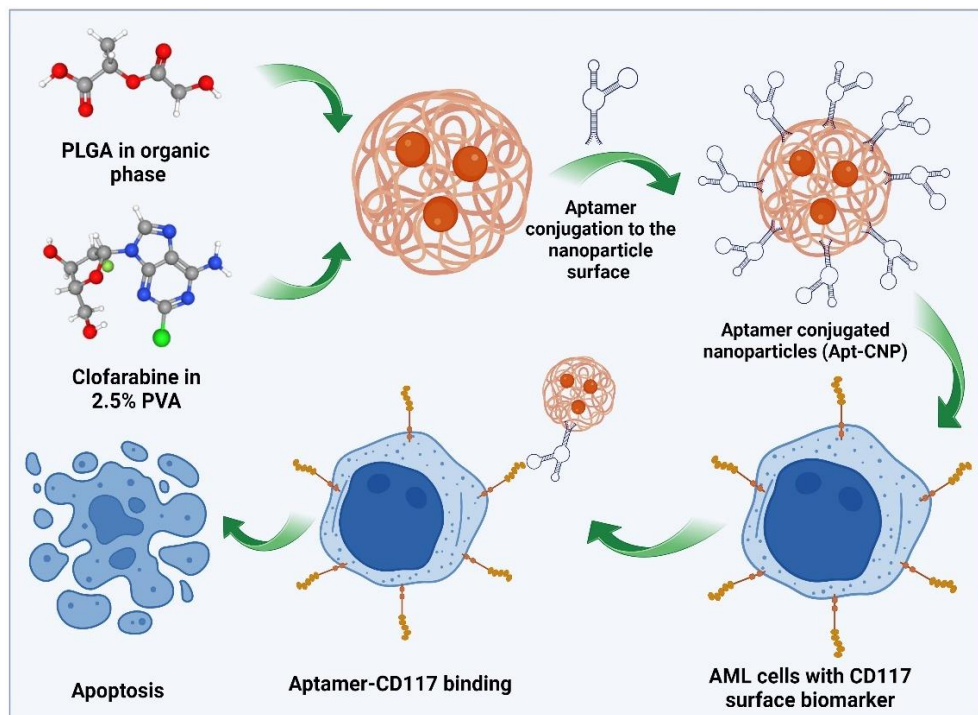
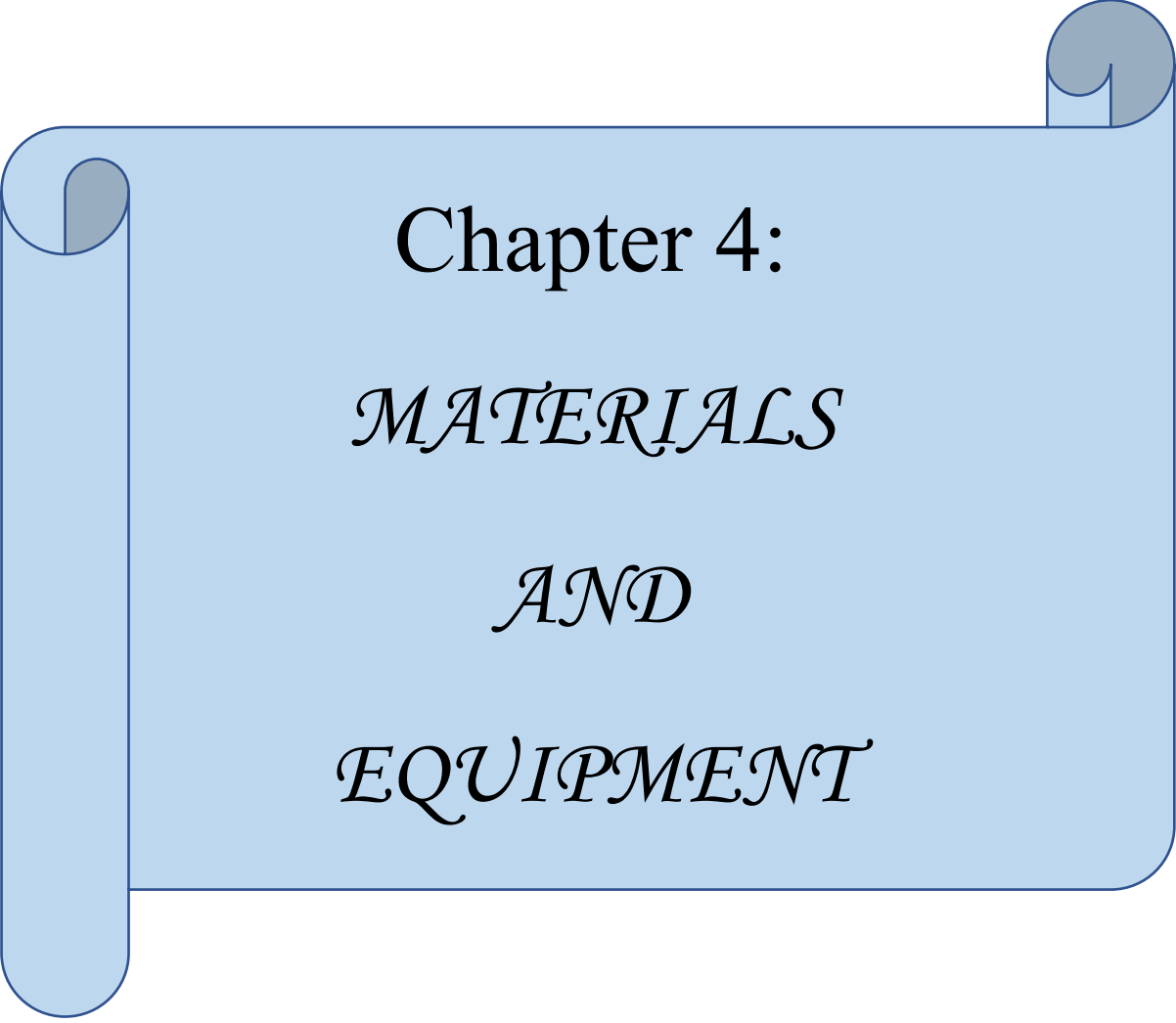


Figure 3.1. Graphical Abstract representing the plan of work.



Chapter 4:
MATERIALS
AND
EQUIPMENT

4. Materials and Equipment

4.1. Chemicals used in the study

Table 4.1. List of materials/chemicals used in the study

Serial No.	Name	Source
1.	Acetonitrile	Merck Life Science Pvt. Ltd, Bengaluru, India.
2.	CD117 DNA aptamer	India Integrated DNA Technologies, Bengaluru, India.
3.	Clofarabine	TCI Chemicals, Chennai, India.
4.	Dichloromethane (DCM)	Merck Life Science Pvt. Ltd, Bengaluru, India.
5.	Dimethylsulfoxide (DMSO)	Merck Life Science Pvt. Ltd, Bengaluru, India.
6.	1-(3-Dimethylaminopropyl)-3-ethylcarbodiimide hydrochloride (EDC)	Himedia Laboratories Pvt. Ltd., Maharashtra, Mumbai, India.
7.	Ethyl acetate	Merck Life Science Pvt. Ltd, Bengaluru, India India.
8.	Ethylene diamene tetra acetic acid (EDTA)	Merck Life Science Pvt. Ltd, Bengaluru, India
9.	Fetal bovine serum (FBS)	HiMedia Laboratories, Mumbai, India.
10.	Fluorescein isothiocyanate (FITC)	Sisco Research Laboratories Pvt. Ltd. (SRL), India.
11.	FITC annexin V/dead cell apoptosis kit	Thermo Fisher Scientific, Waltham, MA, USA.
12.	3-(4,5-Dimethylthiazol-2-yl)-2,5-diphenyltetrazolium bromide (MTT)	Sigma-Aldrich Co., St Louis, MO, USA.
13.	N-Hydroxysuccinimide (NHS)	Himedia Laboratories Pvt. Ltd., Mumbai, India.
14.	Penicillin-Streptomycin	HiMedia Laboratories, Mumbai, India.

15.	Phosphate buffer saline pH-7.4	Sigma-Aldrich Co, St Louis, MO, USA.
16.	Polylactic co-glycolic acid (ratio, 75:25; molecular weight, 4,000-15,000 Da) [Acid-terminated]	Sigma-Aldrich Co, St Louis, MO, USA.
17.	Potassium dihydrogen phosphate	Merck Life Science Pvt. Ltd, Bengaluru, India
18.	Polyvinyl alcohol (PVA)	HiMedia Laboratories, Mumbai, India.
19.	Roswell Park Memorial Institute Medium (RPMI 1640)	Thermo Fisher Scientific, Waltham, USA
20.	Water for HPLC	Merck Life Sc. Pvt. Ltd., Mumbai, Maharashtra, India.
21.	5,5',6,6' -Tetrachloro-1,1',3,3' -tetraethyl benzimidazolylcarbocyanine iodide (JC-1)	Invitrogen, Carlsbad, CA, USA

4.2. Cell lines used in this study

Table 4.2. The source of cell lines used in the study

Human Cells	Source
HL60 (human acute promyelocytic leukemia)	National Centre for Cell Sciences, Pune, India.
U937 (human monocytic leukemia cells)	CSIR-Indian Institute of Chemical Biology-TRUE (Translational Research Unit of Excellence), Kolkata, India.

4.3. Animals used in this study

Table 4.3. Source of animals used in the study

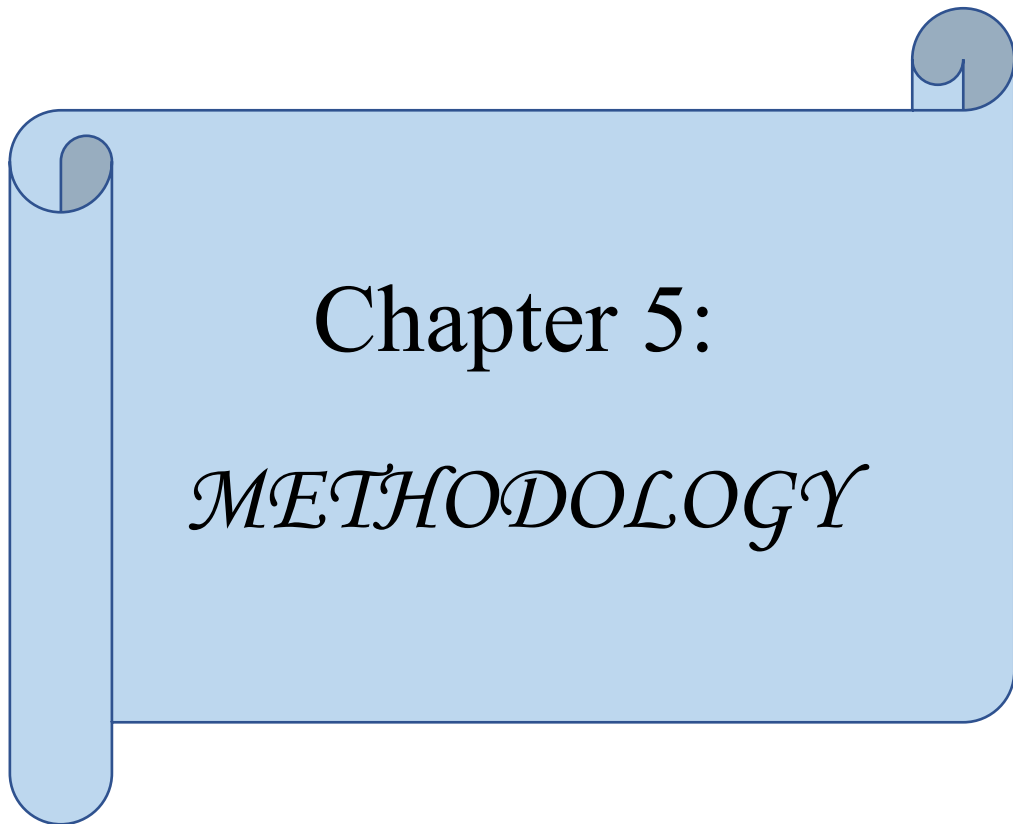
Animals	Source
Male Swiss Albino mice	National Institute of Nutrition (NIN), Hyderabad, Telangana, India.

4.4. Instruments

Table 4.4. List of instruments and equipments used in the study

Serial No.	Name	Source
1.	Bath sonicator	Trans-O-Sonic, Mumbai, India.
2.	Biosafety cabinet (Class II)	Esco Lifesciences, Singapore.
3.	CO ₂ incubator	Thermo Fisher Scientific, Waltham, USA
4.	Cold centrifuge	HERMLE Labortechnik GmbH, Wehingen, Germany
5.	Digital pH meter (EUTECH)	Thermo Fisher Scientific India Pvt. Ltd., Hiranandani Business Park, Mumbai India.
6.	Digital weigh balance	Sartorius Corporate Administration, Otto-Brenner-Straße 20, Goettingen, Germany.
7.	FTIR instrument	FTIR Shimadzu Corporation, Japan.
8.	Normal Freezer	LG double door, Yeouido-dong, Seoul, South Korea.
9.	-80° C Freezer (Model no U410-86)	New Brunswick Scientific, Eppendorf House, Arlington Business Park, Stevenage, UK.
10.	High speed homogenizer	IKA Laboratory Equipment, Model T10B Ultras-Turrax, Staufen, Germany.
11.	Laboratory Freeze Dryer (lyophilizer)	Instrumentation India, Kolkata, India.
12.	Magnetic stirrer	Remi Sales & Engineering Ltd, Ganesh Chandra Avenue, Bando House, Dharmatala, Kolkata, India.

13.	0.22 μ Membrane filter	Merck Life Science Pvt. Ltd, Mumbai, India.
14.	Microplate reader	Spectromax, Japan
15.	Particle size and zetasizer	Zetasizer nano ZS 90, Malvern Zetasizer Limited, Malvern, UK.
16.	Field Emission Scanning Electron microscope	FESEM Joel JSM-7600 F, Tokyo, Japan.
17.	Transmission electron microscope	TEM, JEOL JEM-2010, JEOL, USA.
18.	LC-MS instrument	Agilent 6545 Q-TOF LC/MS system
19.	UV-VIS spectrophotometer	LI-295 UV VIS Single Beam, Lasany International, India
20.	Vortex mixture	Remi Sales & Engineering Ltd, Ganesh Chandra Avenue, Bando House, Dharmatala, Kolkata, India
21.	Flow cytometer	BD FACS Cell sorter, B.D. Biosciences, San Diego, CA
22.	Flow cytometer	BD LSRFortessa™ Cell Analyzer B.D. Biosciences, San Diego, CA



Chapter 5:
METHODOLOGY

5. Methodology

5.1. Calibration Curve of Clofarabine

A stock solution of clofarabine was prepared by accurately weighing 1 mg of the drug and dissolving it in 1 mL of distilled water to achieve a concentration of 1000 µg/mL. The solution was vortexed thoroughly to ensure complete dissolution followed by sonication. Subsequently, a series of dilutions was prepared from the stock solution using distilled water to obtain working concentrations ranging from 20-1000 µg/mL. To determine the maximum absorption wavelength (λ_{max}) of clofarabine, 1 µg/mL solution was scanned over a wavelength range of 200-600 nm using a UV-Vis spectrophotometer (LI-295 UV VIS Single Beam Spectrophotometer). The highest absorbance was observed at 263 nm, which was recorded as λ_{max} . The absorbance of the prepared standard solutions was measured at 263 nm against a blank (distilled water) using a 1 cm quartz cuvette in a UV-Vis spectrophotometer. A calibration curve was generated by plotting concentration (µg/mL) on the X-axis and absorbance on the Y-axis. The linear regression equation and correlation coefficient (R^2) were determined to evaluate the linearity of the method (Prasad et al., 2018; Ehsan et al., 2022). The developed calibration curve for clofarabine using UV-Vis spectroscopy demonstrated a reliable and reproducible quantification approach.

5.2. Preparation of Clofarabine-Encapsulated PLGA Nanoparticles (CNP)

Clofarabine-loaded poly(lactic-co-glycolic acid) (PLGA) nanoparticles (CNP) were synthesized using multiple-emulsion solvent evaporation technique, a well-established method for encapsulating hydrophilic and hydrophobic drugs in polymeric nanocarriers (Chakraborty et al., 2020 ; Iqbal et al., 2015). PLGA with a lactic acid to glycolic acid ratio of 75:25 (50 mg) was dissolved in a 3 mL organic phase comprising of dichloromethane (DCM) and acetone mixture in a 1:1 (v/v) ratio. Aqueous polyvinyl alcohol (PVA) solutions at 1.5% and 2.5% (w/v) were prepared separately by dissolving PVA in Milli-Q water under continuous stirring and heating at 50°C to ensure complete dissolution. Clofarabine (5 mg), the active pharmaceutical ingredient, was dispersed in the 2.5% PVA solution to form a hydrophilic drug-containing aqueous phase. To initiate the emulsification process, the PLGA organic solution was homogenized with the drug-loaded 2.5% PVA solution at 6000 rpm for 5 to 7 minutes using an Ultra-Turrax homogenizer (IKA Laboratory Equipment, Germany), generating a primary

water-in-oil (W/O) emulsion. Subsequently, this primary emulsion was transferred into 1.5% PVA solution and homogenized for an additional 10 minutes, forming a stable water-in-oil-in-water (W/O/W) double emulsion. To enhance nanoparticle stability and achieve uniform size distribution, the resulting emulsion was sonicated for 30 minutes, followed by overnight magnetic stirring to facilitate solvent evaporation. To remove large aggregates and obtain a homogeneous nanoparticle suspension, an initial centrifugation step was performed at 5000 rpm for 5 minutes. The supernatant, containing well-dispersed nanoparticles, was further subjected to ultracentrifugation at 16,000 rpm for 45 minutes to pellet the nanoparticles. The collected nanoparticles were washed thrice with deionized water to eliminate residual PVA and any unencapsulated drug, with each washing step followed by centrifugation at 16,000 rpm for 10 minutes. For long-term stability and prevention of nanoparticle aggregation, the purified nanoparticles were subjected to a pre-freezing step at -20°C for 9 hours, ensuring preservation of their structural integrity before lyophilization. Finally, the nanoparticles were freeze-dried using a laboratory-scale lyophilizer (Instrumentation India, Kolkata, India) for 8 hours, yielding a dry powder formulation suitable for subsequent characterization and biomedical applications. This optimized multiple-emulsion solvent evaporation technique ensures high drug encapsulation efficiency, controlled particle size, and improved stability, making the resulting nanoparticles highly suitable for targeted drug delivery applications in leukemia therapy.

5.3. Preparation of FITC Tagged Clofarabine-Encapsulated PLGA Nanoparticles

Fluorescein isothiocyanate (FITC)-tagged PLGA nanoparticles were prepared using the same multiple-emulsion solvent evaporation method as described previously (Chakraborty et al., 2020). To facilitate fluorescence-based tracking and imaging, 100 µL of a FITC solution in ethanol (0.4% w/v) was incorporated into the organic phase containing the polymer and drug prior to the homogenization step. The addition of FITC did not alter the primary emulsification, secondary emulsification, or subsequent processing steps, ensuring that the overall nanoparticle synthesis protocol remained unchanged. After preparation, FITC-labeled nanoparticles underwent the same purification process, including sequential centrifugation and washing with deionized water, to remove any free FITC or unencapsulated components. The nanoparticles were then pre-frozen at -20°C and lyophilized as described earlier to obtain a dry formulation for further analysis. This approach enables the production of fluorescently labeled

nanoparticles suitable for cellular uptake studies, biodistribution analysis, and real-time imaging in drug delivery research.

5.4. Drug-Excipients Interaction Study Using Fourier Transform Infrared Spectroscopy (FTIR)

Fourier Transform Infrared (FTIR) spectroscopy was used to investigate potential interactions between clofarabine and various excipients, ensuring the chemical integrity and compatibility of the drug within the nanoparticle formulation (Dutta et al., 2018). FTIR is a well-established analytical technique used to detect changes in chemical bonds and functional groups, allowing for the assessment of potential chemical interactions. To assess the chemical compatibility, FTIR spectra were recorded for pure clofarabine, PVA, PLGA, physical mixtures, drug-loaded nanoparticles, blank nanoparticles, and aptamer-conjugated nanoparticles. Spectroscopic analysis was conducted using an FTIR spectrophotometer (Model: Prestige 22, Shimadzu, Japan) under an inert atmosphere to prevent unwanted interactions with environmental moisture and gases. Samples were prepared by thoroughly mixing with potassium bromide (KBr) in an appropriate ratio, followed by compression into transparent KBr pellets using a hydraulic press. The spectral measurements were performed within a wavenumber range of 4000–400 cm^{-1} , ensuring comprehensive analysis of characteristic absorption bands associated with functional groups in the formulation components. The obtained spectra were compared to detect potential shifts, broadening, or disappearance of peaks, which could indicate hydrogen bonding, electrostatic interactions, or other molecular changes. This comparative analysis provided a deeper understanding of the physicochemical behavior of clofarabine within the polymeric matrix, ensuring formulation stability and effectiveness in targeted drug delivery applications.

5.5. Analysis of Aptamer and CD117 (c-KIT) Interactions by Molecular Docking

To investigate the molecular interactions between the aptamer and CD117 (c-KIT), an *in silico* docking study was performed. The receptor, CD117 (c-KIT), was selected as the target protein due to its specific affinity for the designed aptamer. The crystal structure of CD117 (PDB ID: 6GQJ) was obtained from the RCSB (Research Collaboratory for Structural Bioinformatics) Protein Data Bank (PDB) (Al Hoque et al., 2023). The three-dimensional structure of the DNA aptamer was generated by incorporating the 79-base-pair DNA sequence into Discovery Studio

Visualizer 2021. The structure was then converted into PDB format to facilitate molecular docking analysis. Prior to docking, the receptor was prepared by removing water molecules and adding polar hydrogen atoms and partial atomic charges to ensure accurate interaction modelling. Similarly, the aptamer molecule underwent preparation using Discovery Studio Visualizer 2021 to optimize its structural conformation for docking studies. For the molecular docking analysis, HDockLite, a widely used blind docking software, was employed to assess the binding interactions between the aptamer and the tyrosine-protein kinase KIT protein (Yan et al., 2020). The docking results were subsequently analyzed and visualized using Biovia Discovery Studio 2021 (BIOVIA Discovery Studio - BIOVIA, Dassault Systèmes®, Vélizy-Villacoublay, France), which provided a detailed representation of the molecular interactions, including hydrogen bonding, van der Waals forces, and electrostatic interactions. This docking study provided valuable information on the binding affinity and interaction sites of the aptamer with CD117, supporting its potential as a targeted therapeutic agent in AML treatment.

5.6. Aptamer Conjugation on the Surface of Nanoparticles (Apt-CNP)

A 3'-amino and phosphorothioate backbone-modified aptamer was successfully conjugated onto a clofarabine-loaded PLGA nanoparticle (CNP) formulation using the well-established EDC/NHS (1-Ethyl-3-(3-dimethylaminopropyl)carbodiimide/N-hydroxysuccinimide) coupling method (Farokhzad et al., 2006). This method facilitates the formation of stable amide bonds between the carboxyl-functionalized nanoparticle surface and the amino-modified aptamer, ensuring efficient bioconjugation. To begin the conjugation process, CNPs were dissolved in distilled water at a concentration of 5 mg/mL. The nanoparticle suspension was then incubated with 200 mM EDC and 100 mM NHS for 30 minutes at 25°C, allowing for the activation of carboxyl groups on the nanoparticle surface. Following activation, excess EDC/NHS was carefully removed by washing the nanoparticles with DNase- and RNase-free water, thereby preventing any unintended crosslinking or hydrolysis of reactive intermediates. Meanwhile, the aptamer solution was prepared by adjusting the concentration to 2.50 µM. To ensure proper folding and structural integrity, the aptamer was subjected to a denaturation-renaturation cycle, where it was heated to 85°C for 10 minutes, followed by ice cooling for another 10 minutes. This step is essential for restoring the aptamer's specific three-dimensional conformation, which is critical for its target recognition and binding capabilities. The renatured aptamer was then added to the activated CNP suspension and incubated under continuous

rotation for 6 hours to allow for efficient conjugation. Post-reaction, the resulting aptamer-CNP bioconjugates were thoroughly washed with deionized water, ensuring the removal of any unbound aptamer, residual reactants, or byproducts. This optimized conjugation strategy resulted in a stable and functionally active aptamer-nanoparticle complex, making it highly suitable for further characterization and application in targeted drug delivery systems. By leveraging the specificity of the aptamer towards CD117 (c-KIT)-expressing leukemia cells, this formulation holds significant potential for enhancing the precision and efficacy of AML therapy while minimizing off-target side effects.

5.7. Agarose Gel Electrophoresis

Agarose gel electrophoresis provides a rapid and qualitative method to assess aptamer conjugation by detecting mobility shifts in the gel (Shahriari et al., 2021). When aptamers successfully attach to nanoparticles, their migration pattern differs from that of free aptamers and non-conjugated nanoparticles, serving as an indication of successful conjugation (Al Hoque et al., 2023). In this study, both aptamer-conjugated nanoparticles (Apt-CNP) and non-conjugated drug-loaded nanoparticles were analyzed alongside a DNA ladder and free aptamers as controls. The electrophoresis was carried out on a 2% agarose gel at 100V for 30 minutes. To visualize the base pairs (bp), the gel was stained with 0.5 mg/mL ethidium bromide, allowing for clear differentiation of the bands and confirmation of aptamer attachment.

5.8. Drug Loading and Entrapment Efficiency Study

The drug loading and entrapment efficiency of the nanoformulation were assessed by dissolving 2 mg of the nanoparticles in 2 mL of an acetonitrile and water solution (80:20) and incubating the mixture for 3-4 hours in a Somax Incubator Shaker (China). This process ensured thorough dispersion of the formulation, allowing for accurate measurement of drug content. Drug loading was determined by calculating the percentage of the drug encapsulated within the nanoparticles relative to the total nanoparticle weight, using the formula:

$$\text{Drug loading (Practical) (\%)} = \frac{\text{Quantity of drug present in nanoparticles} \times 100}{\text{Quantity of nanoparticles taken}}$$

$$\text{Entrapment efficiency (\%)} = \frac{\text{Practical drug loading} \times 100}{\text{Theoretical drug loading}}$$

5.9. Atomic Force Microscopy (AFM)

Atomic Force Microscopy (AFM) was employed to conduct a detailed surface characterization of the samples at the nanometer scale. To prepare the samples, they were initially dissolved in Milli-Q water and subjected to vortexing to ensure uniform dispersion. This was followed by a sonication process to break down any aggregates and achieve a homogeneous suspension. The prepared solution was then carefully cast onto coverslips to form a thin, transparent layer. These samples were subsequently left to air dry for approximately eight hours to allow for proper film formation. Once dried, the samples were analyzed using AFM (5500 Agilent Technologies, USA) in tapping mode, which provided high-resolution imaging of the surface morphology while minimizing potential damage to the delicate structures (Herdiana et al., 2022).

5.10. In Vitro Drug Release Study

The in vitro drug release study was employed to evaluate the release profile of the drug from the nanoparticles under physiological conditions, providing valuable insight into how the formulation might behave within the human body (Kumari et al., 2023; Adhikary et al., 2023). To ensure reliability and reproducibility, the study was performed in triplicate over a period of 30 days using phosphate-buffered saline (PBS) at pH 7.4, which mimics the physiological environment. Precisely measured amounts of drug-loaded nanoparticles were incubated in PBS buffer at a controlled temperature of $37^{\circ}\text{C} \pm 0.5^{\circ}\text{C}$, maintained within an incubator shaker to ensure uniform conditions throughout the study. At predetermined time intervals, pre-labeled sample aliquots were collected and subjected to centrifugation at 16,000 rpm for 30 minutes to separate the nanoparticles from the supernatant. The collected supernatants were then analyzed using UV-Vis spectroscopy at a wavelength of 263 nm to determine the amount of drug released over time. This approach allowed for a systematic evaluation of the release kinetics, which is critical for understanding the drug delivery potential of the nanoparticles.

The data from this study were plotted to test various kinetic models, namely, zero-order ($C = k_0 t$), first-order ($\log C = \log C_0 - k_1 t/2.303$), Higuchi ($Q = k\sqrt{t}$), and Korsmeyer-Peppas ($Mt/M_{\infty} = Kt^n$) (Pattnaik et al., 2012). The zero-order model indicates drug release independent of drug concentration, promoting slow release. The first-order model shows the release rate linearly related to the remaining drug concentration. The Higuchi model explains drug release

regulated by diffusion from a drug matrix. The Korsmeyer-Peppas model's "n" values characterize the release mechanism: $n \leq 0.45$ (Fickian diffusion), $0.45 < n < 0.89$ (non-Fickian diffusion), $n = 0.89$ (case II transport), and $n > 0.89$ (super case II transport) (Ehsan et al., 2022).

5.11. Particle Size Distribution and Zeta Potential

Particle size distribution and zeta potential analysis are essential for nanoparticle characterization, stability, drug release, and cellular uptake. A uniform particle size ensures consistent performance, while zeta potential determines colloidal stability by measuring surface charge and electrostatic repulsion (Chakraborty et al., 2020). A negative zeta potential prevents aggregation, ensuring a stable suspension. In this study, the particle size and zeta potential of CNP and Apt-CNP were analyzed using a Malvern Zetasizer Nano-ZS 90 (Malvern Instruments, UK). Samples were dispersed in Milli-Q water, vortexed to break aggregates, and sonicated for uniform dispersion. Particle size was measured by dynamic light scattering (DLS), while electrophoretic light scattering determined zeta potential.

5.12. Field Emissions Scanning Electron Microscopy (FESEM)

The morphological characteristics of the developed nanoformulation were analyzed using a field emission scanning electron microscope (FESEM), which provides ultra-high-resolution imaging in the nanometer range (Dutta et al., 2018). This advanced imaging technique enables a detailed examination of surface morphology, particle size, shape, and distribution, facilitating a comprehensive understanding of the formulation's physical properties. The use of lower accelerating voltages in FESEM minimizes the risk of sample degradation, making it particularly suitable for imaging delicate nanoparticles. To prepare the sample for imaging, the nanoformulation was carefully deposited onto carbon tape affixed to an aluminum stub. It was then coated with a thin, 5 nm layer of platinum using a platinum coater to enhance conductivity and improve image resolution. The coated sample was subsequently visualized using a JEOL JSM-7600F FESEM (Japan), allowing for precise morphological assessment crucial for evaluating the quality and stability of the nanoformulation.

5.13. Stability Study of the Nanoparticle

We proceeded stability with the Apt-CNP only, as this was the formulation of our experimental interest. We have evaluated the particle surface morphology using FESEM of the Apt-CNP nanoformulation after storage at 4-8°C in a refrigerator, and at 30°C with 75% relative humidity (RH) and at 40°C with 75% RH for 45 days, by particle size analysis for the samples stored at 30°C and 40°C, and FESEM analysis for all the three samples. Drug loading was also checked.

5.14. High-Resolution Transmission Electron Microscopy (HR-TEM)

High-Resolution Transmission Electron Microscopy (HR-TEM) is an advanced imaging technique that provides a detailed view of nanoparticle structures, allowing for a comprehensive understanding of their internal morphology, surface features, and the distribution of encapsulated drugs within the polymeric matrix. This advanced analytical method plays a crucial role in assessing the structural integrity and homogeneity of nanoparticle formulations, which are essential factors in determining their suitability for targeted drug delivery applications. In this study, HR-TEM was employed to investigate the internal morphology and drug distribution within the synthesized nanoparticles. The nanoparticles were first suspended in Milli-Q water to ensure uniform dispersion, and a small droplet of the suspension was carefully placed onto a 300-mesh copper grid. The sample was then left to air-dry for 12 hours to allow for proper adhesion and solvent evaporation, ensuring optimal imaging conditions. HR-TEM analysis was performed using the JEOL JEM 2100 HR instrument (Tokyo, Japan), which provided high-resolution images that facilitated a deeper understanding of nanoparticle architecture and drug encapsulation patterns. This detailed characterization is crucial for optimizing nanoparticle formulations and enhancing their performance in targeted drug delivery applications (Dutta et al., 2018).

5.15. In Vitro Cell Cytotoxicity Assay

AML cells (HL-60 and U937) were cultured under controlled conditions to ensure optimal growth and maintain experimental consistency. The cells were grown in RPMI 1640 medium, supplemented with 10% fetal bovine serum (FBS) to provide essential nutrients, along with 50 µg/ml streptomycin and 50 IU/mL penicillin G to prevent bacterial contamination. The cultures were maintained at 37°C in a humidified incubator with a 5% CO₂ atmosphere, creating an ideal physiological environment for cell proliferation. To sustain continuous exponential

growth and preserve cell viability, subculturing was carried out every 72 hours. Peripheral Blood Mononuclear Cells (PBMC) were isolated from anticoagulated blood (blood with anticoagulants) through density gradient centrifugation using Ficoll-Hypaque (Dutta et al., 2015). An equal volume of Ficoll-Hypaque was carefully mixed with the anticoagulated blood and centrifuged at $400 \times g$ for 30 minutes, allowing the separation of different blood components. The PBMCs were then collected from the distinct interface between the plasma and Ficoll layers, thoroughly washed with phosphate-buffered saline (PBS) to remove residual contaminants, and resuspended in fresh RPMI 1640 medium to ensure their viability for subsequent experiments.

For cytotoxicity assessment, approximately $1.0\text{--}1.20 \times 10^6$ PBMCs were seeded in 96-well plates, each well containing 100 μL of RPMI 1640 medium, and incubated for 48 hours with the experimental formulations. Following the incubation period, 20 μL of MTT solution (5 mg/ml in PBS) was introduced to each well and further incubated for 4 hours to enable the viable cells to metabolize the MTT reagent into insoluble formazan crystals. These crystals were then dissolved in 100 μL of dimethyl sulfoxide (DMSO) to facilitate optical density measurements. The absorbance was recorded at 540 nm using an ELISA reader (Bio-Rad, CA, USA), providing quantitative data on cell viability and proliferation following treatment.

$$\text{Mean percentage viability} = \frac{\text{Mean specific absorbance of treated cells} \times 100}{\text{Mean specific absorbance of untreated cells}}$$

IC₅₀ values were determined using OriginPro software, with experiments conducted in triplicate (Dutta et al., 2018; Aravind et al., 2012).

5.16. In Vitro Cellular Uptake Study

Cells were cultured under strictly controlled conditions to ensure optimal growth, viability, and experimental consistency throughout the study. This investigation was aimed to evaluate the cellular uptake of drug-loaded nanoparticles (CNP) and aptamer-conjugated nanoparticles (Apt-CNP) by HL-60 and U937 cells to assess their potential for targeted drug delivery in leukemia treatment. Since neither formulation exhibited cytotoxicity in Peripheral Blood Mononuclear Cells (PBMC) within the tested concentration range, PBMCs were excluded from further studies. To facilitate tracking and quantification of nanoparticle internalization, fluorescently labeled nanoparticles were synthesized by encapsulating fluorescein isothiocyanate (FITC) within the nanoparticles, following the same preparation process as

previously described. Additionally, the surface of FITC-labeled nanoparticles was functionalized with an aptamer using the EDC/NHS conjugation technique, as detailed earlier. Flow cytometry was employed to quantitatively analyze the internalization of these fluorescently tagged nanoparticles within the leukemia cells. HL-60 cells treated with CNP and Apt-CNP were incubated for 12 and 24 hours, after which they were harvested by centrifugation, thoroughly washed with ice-cold phosphate-buffered saline (PBS) to remove unbound nanoparticles, resuspended in PBS, and subjected to flow cytometric analysis to determine the extent of nanoparticle uptake. Similarly, U937 cells were cultured under identical conditions as HL-60 cells and exposed to fluorescently labeled CNP and Apt-CNP for 24 hours. Following incubation, U937 cells were also collected, washed with ice-cold PBS to eliminate residual nanoparticles, resuspended in PBS, and analyzed using flow cytometry to measure nanoparticle uptake. The uptake efficiency of nanoparticles in U937 cells was directly compared to that in HL-60 cells, enabling an evaluation of differential internalization between the two leukemia cell lines. Flow cytometry, a highly sensitive and quantitative technique, provided precise measurements of cellular internalization, offering valuable data on the efficiency of targeted drug delivery and the potential of Apt-CNP for enhanced leukemia treatment (Dutta et al., 2018; Al hoque et al., 2023; Fathi et al., 2022).

5.17. Cellular Apoptosis Assay

Annexin V-FITC is commonly used to detect and quantify apoptosis by identifying the translocation of phosphatidylserine (PS) from the inner to the outer plasma membrane. This assay utilizes Annexin V, which has a high affinity for PS and is conjugated with fluorescein isothiocyanate (FITC) to enable fluorescence-based detection. In this study, HL60 cells were treated with the IC₅₀ concentrations of the free drug, CNP, Apt-CNP for 24 hours at 37°C. Following treatment, the cells were harvested by centrifugation, resuspended in binding buffer, and adjusted to a concentration of 1×10^6 cells in 100 μ L. Subsequently, 5 μ L of Annexin V-FITC was added to the cell suspension, and the mixture was incubated in the dark for 15 minutes. After incubation, the cells were diluted with the binding buffer to a final volume of 500 μ L, followed by the addition of 5 μ L of propidium iodide (PI) to differentiate viable from non-viable cells. The samples were then analyzed using a flow cytometer, specifically measuring fluorescence in the FITC (B530-A) and PI (YG586-A) channels. Additionally, U937 cells were subjected to the same experimental conditions in RPMI 1640 medium to compare

the apoptosis-inducing effects across different cell lines. The results were visualized using a four-quadrant plot, which allowed for the classification of cells into live, early apoptotic, late apoptotic, and dead populations based on their staining patterns (Jan et al., 2021; Farahzadi et al., 2023).

5.18. Mitochondrial Membrane Depolarization Study by JC-1

Mitochondrial membrane depolarization was investigated using JC-1 dye, a widely used fluorescent probe for assessing mitochondrial membrane potential (Dutta et al., 2024). JC-1 dye selectively accumulates in mitochondria, where it exhibits potential-dependent fluorescence. At high membrane potential, JC-1 forms J-aggregates, which emit red fluorescence, in contrast, when the membrane potential is low, JC-1 remains in its monomeric form, emitting green fluorescence. A shift from red to green fluorescence indicates a loss of mitochondrial membrane potential, a hallmark of apoptosis.

Since Apt-CNP demonstrated the highest efficacy in HL60 cells, this cell line was selected for the investigation. HL60 cells were seeded at a density of 2.8×10^4 cells/mL and treated with IC_{50} concentrations of the free drug, CNP, and Apt-CNP for 24 hours at 37°C. Following treatment, cells were washed with ice-cold PBS to remove residual compounds, incubated with JC-1 dye for 20 minutes to allow mitochondrial staining, and subsequently collected by centrifugation. The fluorescence intensity of JC-1 was then analyzed using a flow cytometer with FACS Diva software to assess mitochondrial membrane depolarization in response to the treatments (Chen et al., 2004).

5.19. In vivo Pharmacokinetic Activity in Normal Mice

Pharmacokinetic studies were conducted in male Swiss albino mice (body weight 25–30 g) following intravenous (IV) administration of free clofarabine (10 mg/kg), clofarabine-loaded nanoparticles (CNP), and aptamer-conjugated clofarabine-loaded nanoparticles (Apt-CNP). Mice were randomly divided into three groups and received IV injections of free drug, clofarabine, CNP, and Apt-CNP at an equivalent drug dose. All animal experiments were performed with prior approval from the Animal Ethics Committee (AEC), Jadavpur University, Kolkata, India (Ref No: AEC/PHARM/1705/04A/2020, Dated: 05.03.2020).

At predefined time points (0.08, 0.25, 0.5, 1, 2, 4, 6, 8, 10, 24, and 48 h post-administration), two mice per group were sacrificed, and blood samples were drawn into heparin coated tubes.

Plasma was separated by centrifugation at 10,000 rpm for 10 min at 4°C. For plasma sample preparation, 0.1 mL of plasma was mixed with 1 mL of ice-cold acetonitrile-methanol mixture, vortexed, and centrifuged. The resulting clear supernatant was combined with 100 µL of water and analyzed using tandem liquid chromatography-mass spectrometry (LC–MS/MS).

LC–MS/MS analysis was carried out using a Shimadzu Model 20AC liquid chromatograph coupled to an AB SCIEX API4000 mass spectrometer, with data acquisition through Analyst 1.6 software. Chromatographic separation was achieved using a YMC Triat C18 column (30 × 2.1 mm, 5 µm) and a gradient elution technique. The mobile phases consisted of (A) 0.1% formic acid in water and (B) 0.1% formic acid in a methanol: acetonitrile: water (45:45:10) mixture, with a flow rate of 0.8 mL/min, injection volume of 20 µL, and total run time of 3.0 min. Pharmacokinetic parameters, including C_{max} (Maximum Plasma Concentration), T_{max} (Time to Reach Maximum Plasma Concentration), AUC (Area Under the Time Curve), T_{1/2} (Half-life), MRT (Mean Residence Time), V_d (Volume of Distribution), and clearance, were determined using non-compartmental analysis with Python (Matplotlib library, version 3.6.3) (Kumari et al., 2023).

5.20. Statistical analysis

All experiments were conducted in triplicate to ensure the reliability and reproducibility of the results. Data obtained from these experiments were expressed as mean values along with their corresponding standard deviations (mean ± SD) to represent the variability within the dataset. For statistical analysis, Student's *t*-test was employed to compare differences between two groups, while one-way analysis of variance (ANOVA) was used to assess statistical significance across multiple groups prior. A significance level (*p*-value) was set to determine the reliability of the observed differences. To visually represent the data, graphical plots and images were generated using specialized software tools. Origin 2021 was utilized for creating high-quality scientific graphs, enabling detailed visualization of trends and differences among experimental groups. Additionally, BIOVIA Discovery Studio Visualizer (BIOVIA—Dassault Systèmes®, Vélizy-Villacoublay, France) was employed for molecular modeling and structural visualization, facilitating in-depth analysis of molecular interactions.

5.20. References

- Adhikary, S., Al Hoque, A., Ray, M., Paul, S., Hossain, A., Goswami, S., & Dey, R. (2023). Investigation of paracetamol entrapped nanoporous silica nanoparticles in transdermal drug delivery system. *Applied Biochemistry and Biotechnology*, 195(8), 4712-4727. <https://doi.org/10.1007/s12010-023-04576-w>
- Al Hoque, A., Dutta, D., Paul, B., Kumari, L., Ehsan, I., Dhara, M., ... & Ganguly, S. (2023). Δ PSap4# 5 surface-functionalized abiraterone-loaded nanoparticle successfully inhibits carcinogen-induced prostate cancer in mice: a mechanistic investigation. *Cancer Nanotechnology*, 14(1), 73. <https://doi.org/10.1007/s12010-023-04576-w>
- Aravind, A., Varghese, S. H., Veerananarayanan, S., Mathew, A., Nagaoka, Y., Iwai, S., ... & Kumar, D. S. (2012). Aptamer-labeled PLGA nanoparticles for targeting cancer cells. *Cancer Nanotechnology*, 3, 1-12. <https://doi.org/10.1007/s12645-011-0024-6>
- Chakraborty, S., Dlie, Z. Y., Chakraborty, S., Roy, S., Mukherjee, B., Besra, S. E., ... & Sen, R. (2020). Aptamer-functionalized drug nanocarrier improves hepatocellular carcinoma toward normal by targeting neoplastic hepatocytes. *Molecular Therapy-Nucleic Acids*, 20, 34-49. <https://doi.org/10.1016/j.omtn.2020.01.034>
- Chen, J. C., Zhang, X., Singleton, T. P., & Kiechle, F. L. (2004). Mitochondrial membrane potential change induced by Hoechst 33342 in myelogenous leukemia cell line HL-60. *Annals of Clinical & Laboratory Science*, 34(4), 458-466.
- Dutta, D., Al Hoque, A., Paul, B., Park, J. H., Chowdhury, C., Quadir, M., ... & Mukherjee, B. (2024). EpCAM-targeted betulinic acid analogue nanotherapy improves therapeutic efficacy and induces anti-tumorigenic immune response in colorectal cancer tumor microenvironment. *Journal of Biomedical Science*, 31(1), 81. <https://doi.org/10.1186/s12929-024-01069-8>
- Dutta, D., Chakraborty, A., Mukherjee, B., & Gupta, S. (2018). Aptamer-conjugated apigenin nanoparticles to target colorectal carcinoma: a promising safe alternative of colorectal cancer chemotherapy. *ACS Applied Bio Materials*, 1(5), 1538-1556. <https://doi.org/10.1021/acsabm.8b00441>
- Dutta, D., Sarkar, A., Chakraborty, B., Chowdhury, C., & Das, P. (2015). Induction of apoptosis by a potent Betulinic acid derivative in Human colon carcinoma HT-29 cells. *International Journal of Scientific and Research Publications*, 5(2), 1-7.

- Ehsan, I., Kumari, L., Sen, R., Al Hoque, A., Mukherjee, B., Mukherjee, A., ... & Bhattacharya, S. (2022). J591 functionalized paclitaxel-loaded PLGA nanoparticles successfully inhibited PSMA overexpressing LNCaP cells. *Journal of Drug Delivery Science and Technology*, 75, 103689. <https://doi.org/10.1016/j.jddst.2022.103689>
- Farahzadi, R., Sanaat, Z., Movassaghpour-Akbari, A. A., Fathi, E., & Montazersaheb, S. (2023). Investigation of L-carnitine effects on CD44+ cancer stem cells from MDA-MB-231 breast cancer cell line as anti-cancer therapy. *Regenerative Therapy*, 24, 219-226. <https://doi.org/10.1016/j.reth.2023.06.014>
- Farokhzad, O. C., Cheng, J., Teply, B. A., Sherifi, I., Jon, S., Kantoff, P. W., ... & Langer, R. (2006). Targeted nanoparticle-aptamer bioconjugates for cancer chemotherapy in vivo. *Proceedings of the National Academy of Sciences*, 103(16), 6315-6320. <https://doi.org/10.1073/pnas.0601755103>
- Fathi, E., Azarbad, S., Farahzadi, R., Javanmardi, S., & Vietor, I. (2022). Effect of rat bone marrow derived-mesenchymal stem cells on granulocyte differentiation of mononuclear cells as preclinical agent in cellbased therapy. *Current Gene Therapy*, 22(2), 152-161. <https://doi.org/10.2174/1566523221666210519111933>
- Herdiana, Y., Wathoni, N., Shamsuddin, S., & Muchtaridi, M. (2022). Drug release study of the chitosan-based nanoparticles. *Heliyon*, 8(1). <https://doi.org/10.1016/j.heliyon.2021.e08674>
- Iqbal, M., Zafar, N., Fessi, H., & Elaissari, A. (2015). Double emulsion solvent evaporation techniques used for drug encapsulation. *International journal of pharmaceutics*, 496(2), 173-190. <https://doi.org/10.1016/j.ijpharm.2015.10.057>
- Jan, N., Madni, A., Rahim, M. A., Khan, N. U., Jamshaid, T., Khan, A., ... & Shah, H. (2021). In vitro anti-leukemic assessment and sustained release behaviour of cytarabine loaded biodegradable polymer based nanoparticles. *Life Sciences*, 267, 118971. <https://doi.org/10.1016/j.lfs.2020.118971>
- Kumari, L., Ehsan, I., Mondal, A., Al Hoque, A., Mukherjee, B., Choudhury, P., ... & Ghosh, P. (2023). Cetuximab-conjugated PLGA nanoparticles as a prospective targeting therapeutics for non-small cell lung cancer. *Journal of Drug Targeting*, 31(5), 521-536. <https://doi.org/10.1080/1061186X.2023.2199350>
- Pattnaik, G., Sinha, B., Mukherjee, B., Ghosh, S., Basak, S., Mondal, S., & Bera, T. (2012). Submicron-size biodegradable polymer-based didanosine particles for treating HIV at early stage: an in vitro study. *Journal of Microencapsulation*, 29(7), 666-676. <https://doi.org/10.3109/02652048.2012.680509>

Prasad, A. R., & Ratna, J. V. (2018). Development and validation of a simple UV-spectrophotometric method for the determination of ciprofloxacin HCL present in taste masked drug resin complex. *Int. J. Appl. Pharm*, 10(3), 37-41.

Shahriari, M., Taghdisi, S. M., Abnous, K., Ramezani, M., & Alibolandi, M. (2021). Self-targeted polymersomal co-formulation of doxorubicin, camptothecin and FOXM1 aptamer for efficient treatment of non-small cell lung cancer. *Journal of Controlled Release*, 335, 369-388. <https://doi.org/10.1016/j.jconrel.2021.05.039>

Yan, Y., Tao, H., He, J., & Huang, S. Y. (2020). The HDock server for integrated protein–protein docking. *Nature protocols*, 15(5), 1829-1852. <https://doi.org/10.1016/j.jconrel.2021.05.039>



Chapter 6:

RESULTS

6. Results

6.1. The Absorption Spectrum of Clofarabine

The maximum absorption wavelength (λ_{\max}) of clofarabine was determined using a UV-Vis spectrophotometer with the UV Professional V1.39.0 software. The study was conducted in a phosphate-buffered saline (PBS) solution with a pH of 7.4 to stimulate physiological conditions. The absorbance spectrum of clofarabine revealed a distinct peak at 263 nm (Figure 6.1), indicating its λ_{\max} . This characteristic wavelength is crucial for accurately quantifying the drug concentration in analytical solution through the spectrophotometric method.

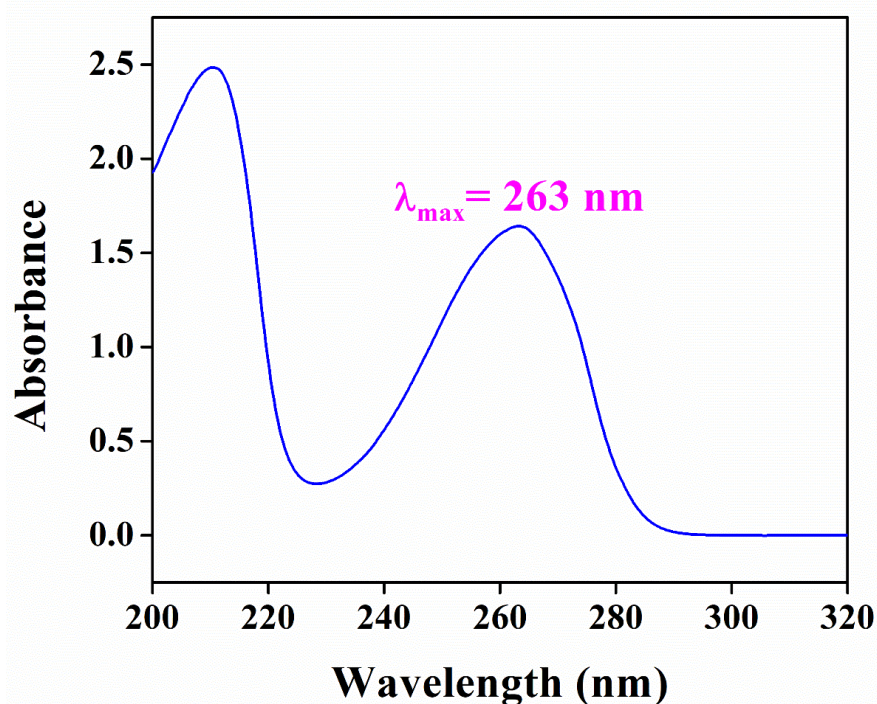


Figure 6.1. The UV absorption maxima of clofarabine in PBS buffer 7.4.

6.2. Calibration Curve of Clofarabine

To study *in vitro* drug release and drug loading in the developed nanoparticles, a calibration curve for clofarabine was prepared using PBS (pH 7.4). Absorbance readings were taken at 263 nm for drug concentrations ranging from 20 $\mu\text{g/mL}$ to 100 $\mu\text{g/mL}$ (including 20, 30, 40, 50, 60, 70, 80, 90, and 100 $\mu\text{g/mL}$). The calibration curve showed a strong linear relationship between absorbance and drug concentration, with high regression coefficient value, $R^2 = 0.992$ confirming the accuracy of the measurement. The calibration curve is illustrated in Figure 6.2.

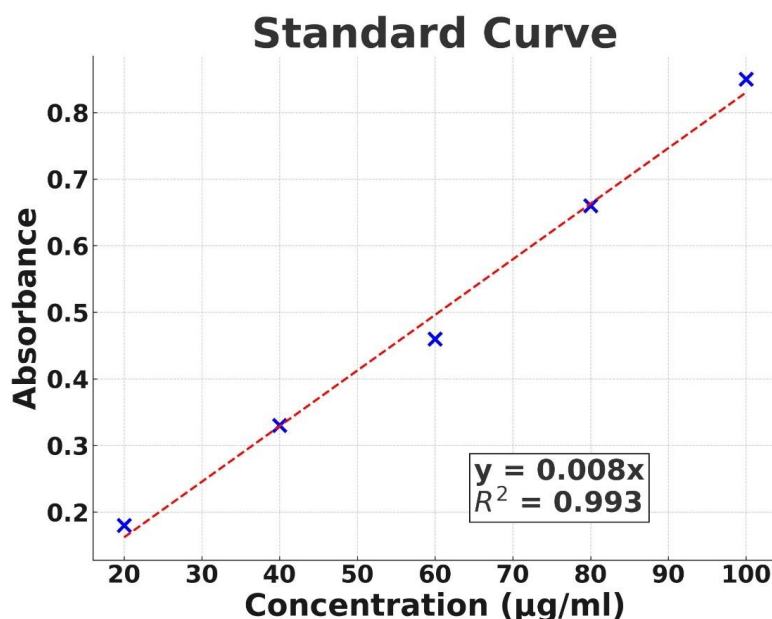


Figure 6.2. Calibration Curve of Clofarabine at 263nm.

6.3. Drug-Excipients Interaction Study by FTIR

FTIR studies were conducted to assess potential chemical interactions between clofarabine and the excipients, PVA and PLGA, as shown in Figure 6.3. The FTIR spectra of PLGA displayed characteristic absorption peaks at 3650 cm^{-1} (O–H stretching), 2935 cm^{-1} (asymmetric stretching of $-\text{CH}_2-$), and 1735 cm^{-1} (C=O stretching of the carboxylic acid group), while pure clofarabine exhibited distinct peaks at 3466.08 cm^{-1} (O-H stretching), 3113.19 cm^{-1} (N-H stretching), 1624.06 cm^{-1} (C=C stretching), 1581.62 cm^{-1} (C=N stretching), 1066.35 cm^{-1} (C-O stretching), 1244.08 cm^{-1} (C-N stretching), and 704.01 cm^{-1} (C-Cl stretching). The FTIR spectra of the drug-loaded nanoparticles (CNP) and aptamer-conjugated nanoparticles (Apt-CNP) retained the characteristic peaks of clofarabine, confirming that the drug's chemical structure remained intact within these formulations. Additionally, new peaks corresponding to the polymeric components were observed, verifying the successful incorporation of PLGA and PVA into the nanoparticles. Notably, in the Apt-CNP formulation, a peak at 1635 cm^{-1} was observed, indicating the formation of amide bond, which suggests successful conjugation of aptamer on to the nanoparticle surface. These findings collectively confirm the structural stability of clofarabine within the nanoformulations and provide evidence for the successful attachment of the aptamer, which is crucial for targeted drug delivery (Song et al., 2020 ; Dutta et al., 2018).

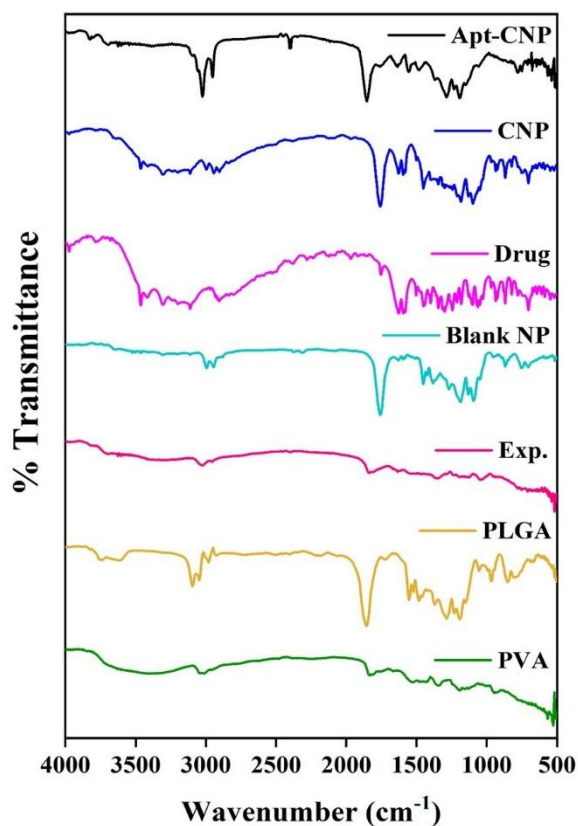


Figure 6.3. Drug excipient interaction study results obtained through FTIR spectroscopy.

6.4. Analysis of aptamer-CD117 (c-KIT) interactions by molecular docking

A molecular docking study was conducted to evaluate the affinity and interactions between the 79 bp DNA aptamer and the CD117 (c-KIT) protein, providing a detailed understanding of their binding mechanism (Al Hoque et al., 2023). The docking analysis revealed that various nucleotide bases of the aptamer effectively formed bonds with different amino acid residues of the receptor protein, as illustrated in Figure 6.4.A and Figure 6.4.B. A diverse range of interactions, including electrostatic, hydrophobic, and hydrogen bonding, were identified, as summarized in Table 6.2.1. They include guanine (DG 38), guanine (DG 39), guanine (DG 40), guanine (DG 41), guanine (DG 42), guanine (DG 43), adenine (DA 46), adenine (DA 47), cytosine (DC 48), guanine (DG 49), guanine (DG 50), guanine (DG 51), guanine (DG 57), guanine (DG 58), thymine (DT 59), and thymine (DT 60). These interactions occurred with various amino acid residues of the receptor protein, such as threonine (THR 594), leucine (LEU 595), glycine (GLY 596), alanine (ALA 597), glycine (GLY 598), alanine (ALA 599), lysine (LYS 626), histidine (HIS 630), serine (SER 631), threonine (THR 632), glutamic acid (GLU

633), arginine (ARG 634), asparagine (ASN 680), arginine (ARG 683), aspartic acid (ASP 816), lysine (LYS 818), asparagine (ASN 819), aspartic acid (ASP 820), serine (SER 821), aspartic acid (ASP 825), glycine (GLY 827), asparagine (ASN 828), alanine (ALA 829), arginine (ARG 686), aspartic acid (ASP 687), glutamic acid (GLU 688), phenylalanine (PHE 689), valine (VAL 690), proline (PRO 691), phenylalanine (PHE 763), glutamic acid (GLU 893), and tyrosine (TYR 894). The docking score revealed a value of -250.95, suggesting a strong binding affinity between the ligand and receptor.

Table 1. Aptamer-CD117 (c-KIT) binding using molecular docking technique

Name of the receptor	Protein Data Bank (PDB) code	DNA aptamer sequence	Docking Score	Interacting residues	Interaction type
CD117 receptor, tyrosine-protein kinase KIT	6GQJ	5'- GAGGCATACC AGCTTATTATT GGGGCCGGG GCAAGGGGG GGGGTACCGT GGTAGGACAG ATAGTAAGTG CAATCTGCGA A-3'	-250.95	THR 594, LEU 595, GLY 596, ALA 597, GLY 598, ALA 599, LYS 626, HIS 630, SER 631, THR 632, GLU 633, ARG 634, ASN 680, ARG 683, ASP 816, LYS 818, ASN 819, ASP 820, SER 821, ASP 825, GLY 827, ASN 828, ALA 829, ARG 686, ASP 687, GLU 688, PHE 689, VAL 690, PRO 691, PHE 763, GLU 893 and TYR 894.	electrostatic, hydrophobic interactions, hydrogen bonding

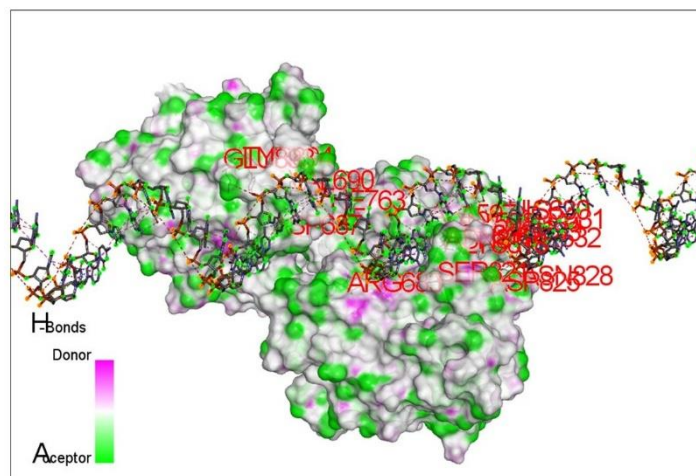


Figure 6.4.A. Aptamer-CD117 receptor interactions by hydrogen bonding through in silico molecular docking.

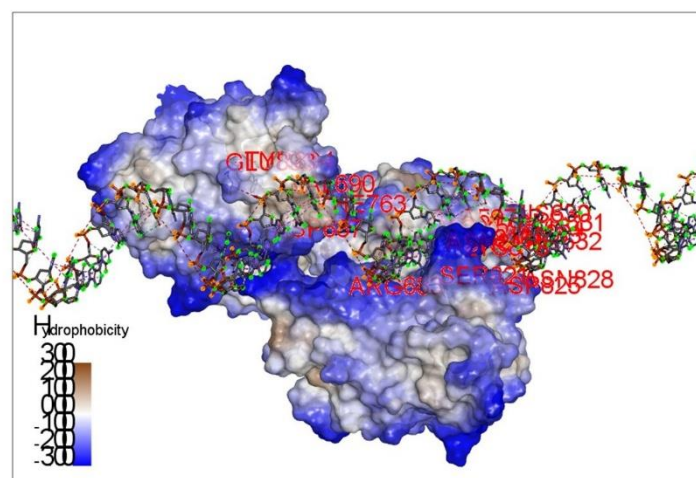


Figure 6.4.B. Aptamer-CD117 receptor hydrophobic interactions through in silico molecular docking.

6.5. Attachment of aptamer to the surface of nanoparticles

Agarose gel electrophoresis was employed to verify the successful attachment of the CD117-specific DNA aptamer to the nanoparticle surface (Dhara et al., 2023). As depicted in Figure 6.5, the free 79-base pair aptamer exhibited distinct migration through the gel, aligning with the 100-bp marker on the conventional DNA ladder. In contrast, the aptamer-conjugated nanoparticle formulation (Apt-CNP) remained localized within the loading well, as evidenced

by fluorescence band. This lack of migration is indicative of the aptamer being firmly attached to the nanoparticle surface, preventing its free movement through the gel matrix. The nonconjugated nanoparticles (CNP) did not produce any visible band in the well, further highlighting the absence of the aptamer in this formulation. The observed gel electrophoresis findings, in conjunction with FTIR data, robustly confirmed the successful conjugation of the aptamer to the nanoparticle surface.

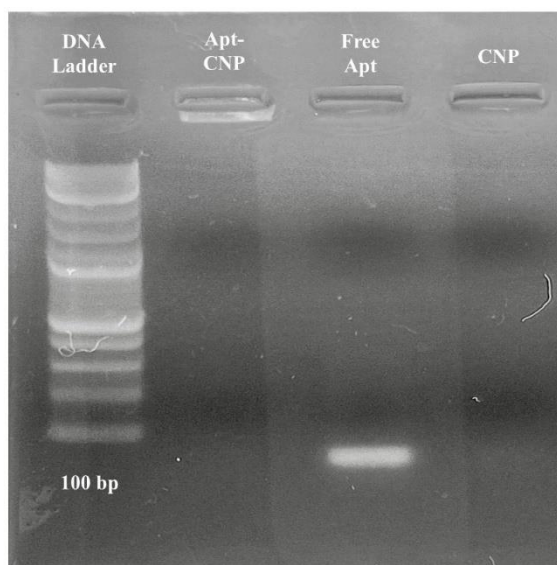


Figure 6.5. Agarose gel electrophoresis confirming the conjugation of aptamer to the drug-loaded nanoparticle.

6.6. Percentage of encapsulation efficiency and average drug loading of the formulation

The clofarabine-loaded PLGA nanoparticle (CNP) formulation exhibited an average drug loading of $23.63 \pm 0.593\%$, with a notable encapsulation efficiency of 70.92% . In comparison, the aptamer-conjugated nanoparticles (Apt-CNP) demonstrated a mean drug loading of $21.78 \pm 0.482\%$, along with an encapsulation efficiency of 69.86% . To assess stability, Apt-CNP formulations were stored under varying conditions, refrigerated at $4-8^{\circ}\text{C}$, and at elevated temperatures of 30°C and 40°C with 75% relative humidity (RH) for 45 days. The results showed that drug loading remained relatively close across all the above-mentioned experimental conditions. Specifically, refrigerated Apt-CNP retained a drug loading of

22.99±0.671%, while storage at 30°C and 40°C for (mentioned duration) resulted in drug loadings of 21.27±0.358% and 20.96±0.432%, respectively. These findings indicate that the Apt-CNP formulation maintained its drug-loading capacity effectively, even under stress conditions of higher temperature and humidity.

6.7. Measurement of Particle Size Distribution and Zeta Potential and Stability data of the nanoparticles

The zeta potential and particle size distribution of the formulations were assessed using the dynamic light scattering (DLS) method. The average hydrodynamic diameter (d_H or $d.nm$) values for CNP and Apt-CNP were 154.7 nm and 175.2 nm, respectively (Figure 6.6). The aptamer conjugation led to an approximate 20% increase in the size of the Apt-CNP, indicating successful conjugation. The zeta potential values of CNP and Apt-CNP were -10.9 mV and -15.9 mV, respectively (Figures 6.7.A and 6.7.B), suggesting increased negative surface charge upon aptamer conjugation.

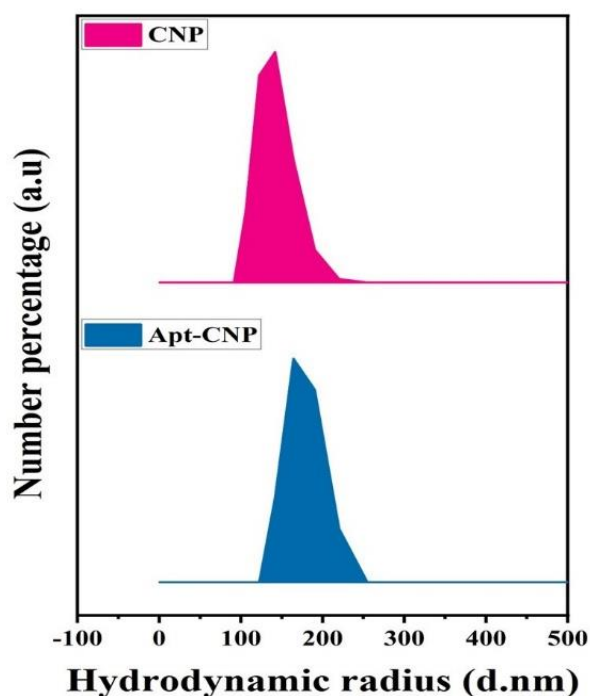


Figure 6.6. Particle size measurement of CNP and Apt-CNP by Dynamic Light Scattering (DLS).

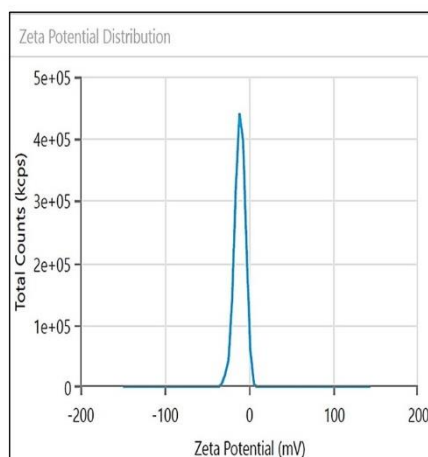


Figure 6.7.A. Zeta potential value of CNP.

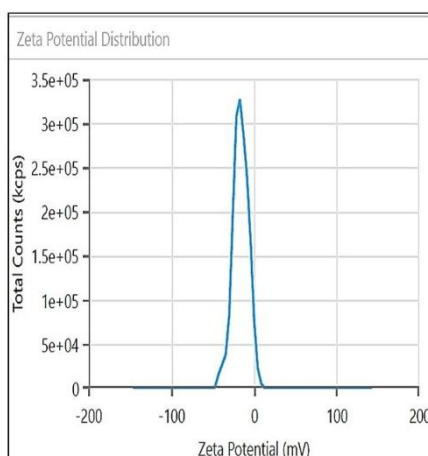


Figure 6.7.B. Zeta potential value of Apt-CNP.

6.8. Surface morphology of nanoparticle by Field Emissions Scanning Electron Microscopy (FESEM)

Field Emission Scanning Electron Microscopy (FESEM) analysis of the CNP and the Apt-CNP revealed that both formulations exhibited smooth, spherical surfaces with a well-distributed morphology (Figure 6.8.A and Figure 6.8.B). The particles maintained a consistent and homogenous size distribution, with the hydrodynamic diameter of CNPs ranging from 100 to 250 nm. The smooth and spherical morphology of both nanoparticle formulations ensures

optimal cellular uptake and interaction, which is critical for the targeted drug delivery system being developed.

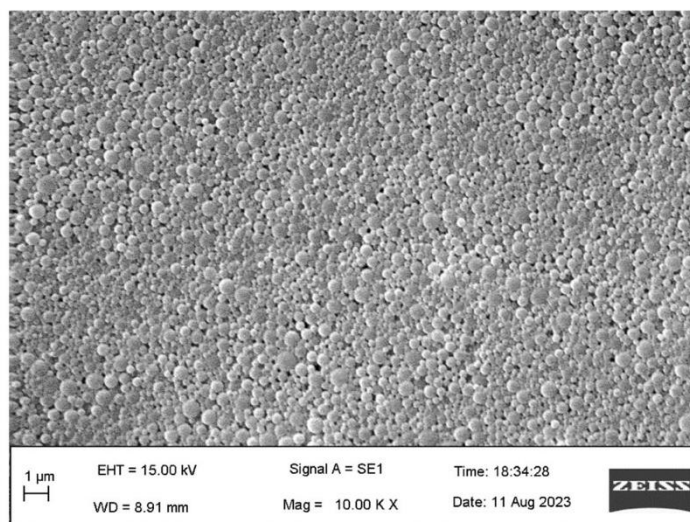


Figure 6.8.A. FESEM image of freshly prepared CNP.

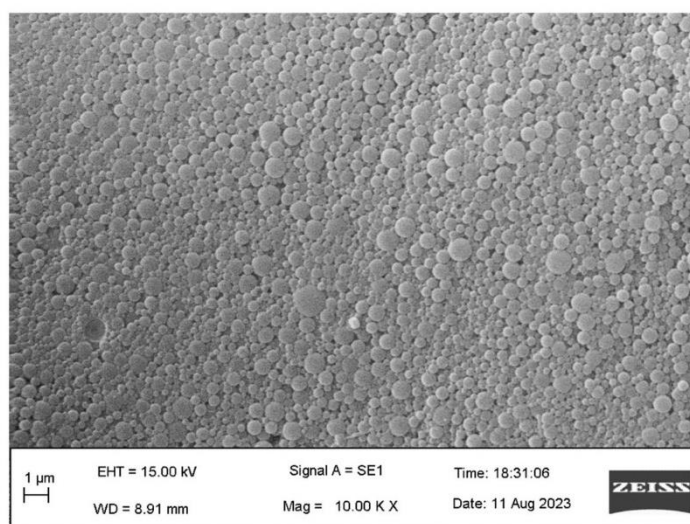


Figure 6.8.B. FESEM image of freshly prepared Apt-CNP.

6.9. Stability Study of the Experimental Nanoparticle

In this study, only Apt-CNP was selected for further experiments as it is the formulation of experimental interest. There was no significant morphological change observed between CNP and Apt-CNP when stored at 4-8°C (Figure 6.9.A). However, formulations stored at 30°C and 40°C with 75% relative humidity (RH) for 45 days (Figures 6.9.D and 6.9.E) exhibited an increase in dH, likely due to particle agglomeration and deformation under the accelerated storage conditions. This observation highlights the impact of higher temperature and humidity on the stability of Apt-CNP, emphasizing the need for optimal storage conditions to maintain particle integrity.

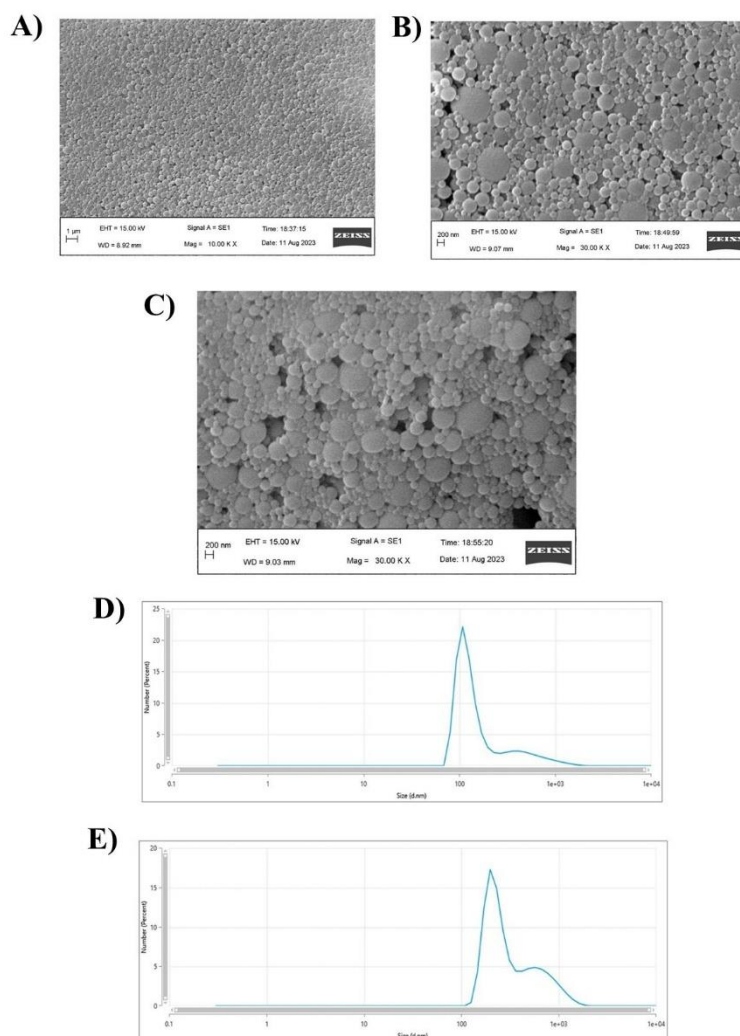


Figure 6.9. A) Represents FESEM image of Apt-CNP stored at 4-8 °C (in a refrigerator) for 45 days. B) Represents FESEM image of Apt-CNP stored at 30°C with 75% RH for 45 days. C) Represents FESEM image of Apt-CNP stored at 40°C with 75% RH for 45 days. D) Represents Particle size distribution of Apt-CNP at 30°C with 75% RH for 45 days. E) Represents Particle size distribution of Apt-CNP at 40°C with 75% RH for 45 days.

The stability studies of CNP and Apt-CNP conducted at accelerated storage conditions of 30°C and 40°C with 75% relative humidity (RH) for 45 days revealed significant morphological changes (Figure 6.9.B and Figure 6.9.C). FESEM analysis demonstrated that prolonged exposure to elevated temperatures and high humidity led to noticeable deformation of the nanoparticles, along with the occurrence of nanoparticle aggregation. These changes in morphology are likely attributable to the softening of the PLGA polymer matrix under stress conditions. However, drug content did not vary significantly.

6.10. Internal morphology by transmission electron microscopy (HR-TEM)

High-Resolution Transmission Electron Microscopy (HR-TEM) analysis was performed to investigate the internal morphology of the CNP and Apt-CNP. The HR-TEM images (and 6.10.B) revealed that both formulations exhibited spherical nanoparticles. Figure 6.10.A showed appearance of the nanoparticles in which, clofarabine particles were distributed in the polymer matrix, indicating encapsulation of the drug within the PLGA nanoparticles. Further, Figure 6.10 B showed darker surface, of Apt-CNP probably due to the incorporation of large amount of aptamers. Additionally, the spherical morphology observed under HR-TEM aligns with the findings from FESEM analysis, reinforcing the stability and integrity of the nanoparticle formulations.

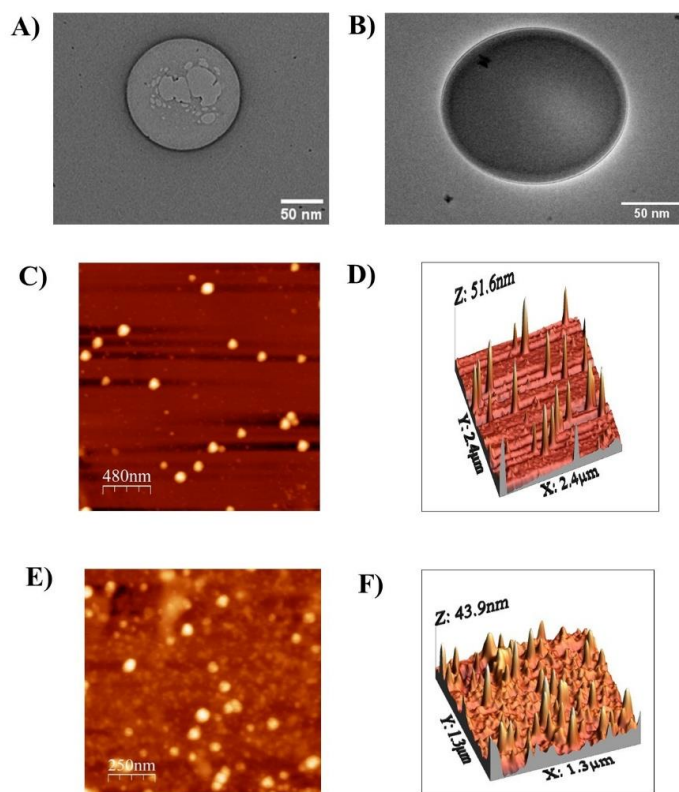


Figure 6.10. A) Represents HR-TEM image of freshly prepared CNP, showing drug particles were inside the CNP. B) Represents HR-TEM image of freshly prepared Apt-CNP, showing dark surface for the incorporation of a large amount of aptamer. C) Represents two-dimensional AFM image of CNP. D) Represents three-dimensional AFM image of CNP. E) Represents two-dimensional AFM image of Apt-CNP. F) Represents three-dimensional AFM image of Apt-CNP.

6.11. Atomic force microscopy (AFM)

Atomic force microscopy (AFM) imaging was performed to analyze the morphology of the clofarabine-loaded PLGA nanoparticles (CNP) and the aptamer-conjugated nanoparticles (Apt-CNP), as shown in Figure 6.10.C, Figure 6.10.D, Figure 6.10. E and Figure 6.10.F respectively. The AFM images were captured in both flattened topography and three-dimensional modes to provide a comprehensive view of the nanoparticle surface characteristics. The analysis revealed that both CNP and Apt-CNP exhibited a well-defined spherical shape with a smooth surface morphology. The preservation of the spherical geometry following aptamer conjugation indicates that the aptamer surface conjugation on to the

nanoparticle surface did not compromise the structural integrity of the nanoparticles. These findings suggest that the aptamer conjugation step was successful while maintaining the desired physicochemical properties of the nanoparticles, which is crucial for ensuring consistent drug delivery performance.

6.12. In vitro drug release study

In vitro clofarabine release studies from both CNP and Apt-CNP formulations were conducted using phosphate-buffered saline (PBS) at pH 7.4, which closely mimics the physiological pH of human blood, providing a biologically relevant environment for this study (Kumari et al., 2023). The cumulative drug release percentages of CNP and Apt-CNP reached $81.15 \pm 3.036\%$ and $92.45 \pm 3.208\%$, respectively, over a 680-hour study period (Figure 6.11). To analyze the release kinetics, the drug release data were analyzed into various kinetic models, including zero-order, first-order, Higuchi, and Korsmeyer–Peppas models (Adhikary et al., 2023). The regression coefficient (R^2) values for each model were calculated, and the results (Table 2) demonstrated that the Korsmeyer–Peppas model provided the best fit for both formulations, suggesting that the drug release mechanism predominantly followed this model. Moreover, the release exponent (n) values obtained from the Korsmeyer–Peppas model indicated a Fickian diffusion mechanism, highlighting that the drug release from the nanoparticles was primarily governed by diffusion through the polymer matrix.

Table: 2. Regression coefficient (R^2) values of in vitro drug release data employed in various kinetic models.

Kinetic Models	Formulations	
	CNP	Apt-CNP
Zero Order	$R^2 = 0.8594$	$R^2 = 0.7309$
First Order	$R^2 = 0.9309$	$R^2 = 0.8901$
Higuchi Model	$R^2 = 0.9554$	$R^2 = 0.8668$
Korsmeyer-Peppas Model	$R^2 = 0.9899$	$R^2 = 0.9576$
	$n = 0.2$	$n = 0.12$

R^2 = regression coefficient and n = release exponent (obtained from the Korsmeyer-Peppas kinetic equation)

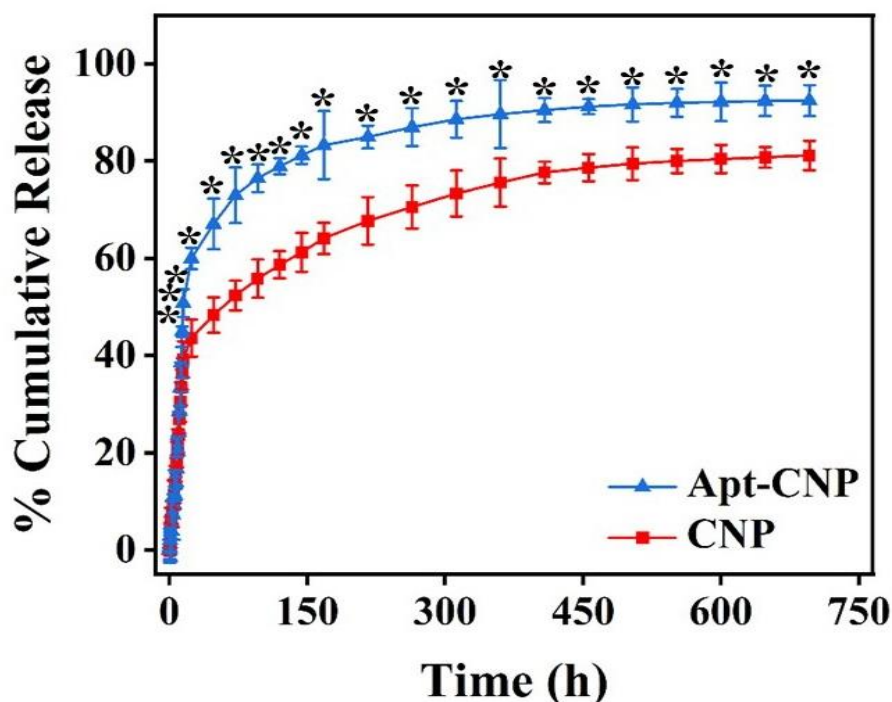


Figure 6.11. In vitro drug release of Apt-CNP and CNP (data show mean \pm SD, n= 3; * indicates $p < 0.05$ when compared with CNP treated group).

6.13. Apt-CNP had variable IC_{50} values in HL60 and U937 cells, and non-toxic to Peripheral Blood Mononuclear Cells (PBMC)

The cytotoxic effects of clofarabine and the developed nanoparticle formulations were evaluated on HL60 cells, U937 cells and PBMC (Peripheral Blood Mononuclear) cells using an MTT assay to determine cell viability. These specific cell lines were selected to evaluate the targeted cytotoxic efficacy of the formulations against CD117 overexpressing HL60 cells (Acute Myeloid Leukemia model), assess off-target effects on U937 cells (CD117-negative myeloid lineage), and determine biocompatibility with normal human PBMC cells. Among the tested formulations, Apt-CNP exhibited the highest toxicity against HL60 cells, demonstrating the lowest IC_{50} value (Figure 6.12). The IC_{50} of free clofarabine was found to be 2.14 μ M, whereas the nanoformulations showed a marked improvement in potency. Specifically, the IC_{50} values for CNP and Apt-CNP were significantly reduced to 1.30 μ M and 1.07 μ M, respectively.

When tested on U937 cells, a similar trend of enhanced efficacy with the nanoparticle formulations was observed, but to a lesser extent. The IC_{50} values for clofarabine, CNP, and

Apt-CNP were 2.31 μM , 1.81 μM , and 1.77 μM , respectively (Figure 6.13). The modest improvement in cytotoxicity with Apt-CNP over CNP in U937 cells indicates that the targeting advantage of the aptamer is likely limited by the absence of expression of the CD117 biomarker in these cells.

Furthermore, the safety profile of the formulations was assessed in normal Peripheral Blood Mononuclear Cells. Interestingly, none of the formulations produced IC_{50} values in PBMCs (Figure 6.14), suggesting minimal cytotoxicity. This highlights the favorable selectivity of the nanoparticle formulations, offering potent anticancer activity while sparing non-cancerous cells.

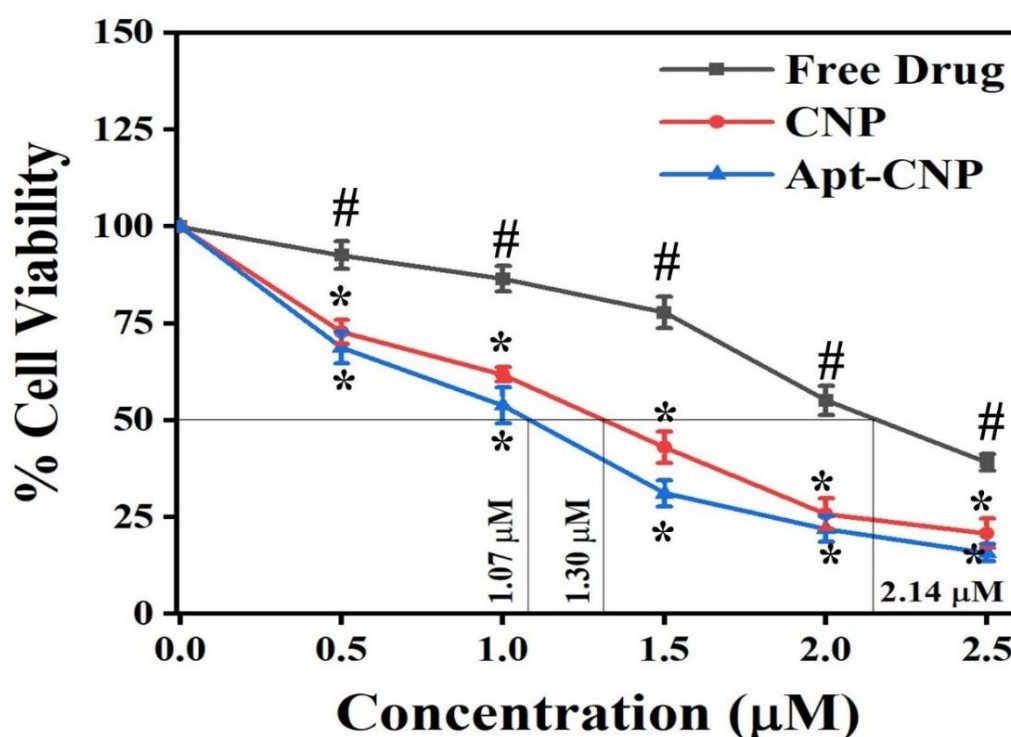


Figure 6.12. In vitro cell cytotoxicity assay of the experimental nanoformulations by using MTT on HL60 cells.

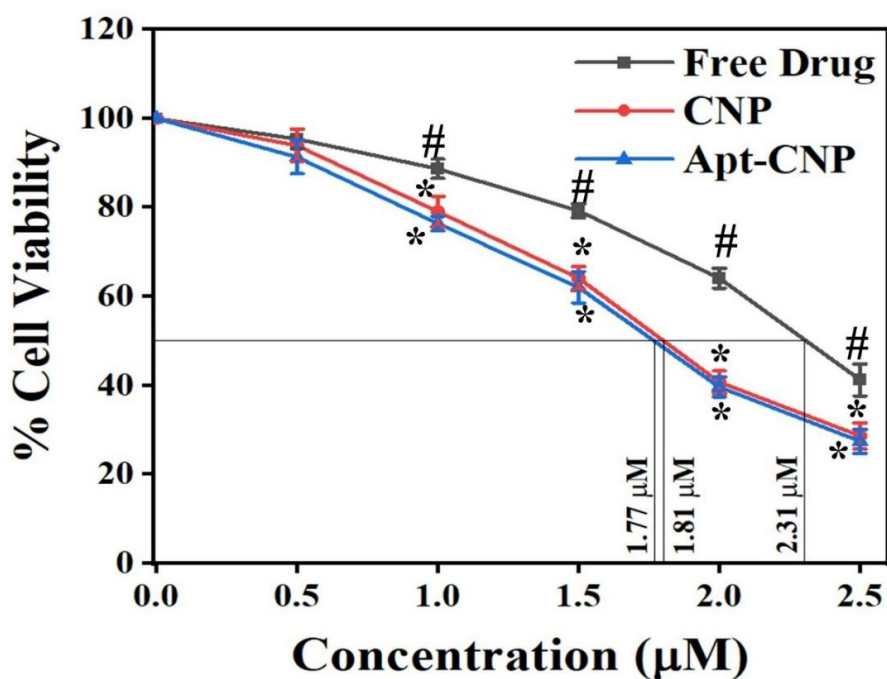


Figure 6.13. In vitro cell cytotoxicity assay of the experimental nanoformulations by using MTT on U937 cells.

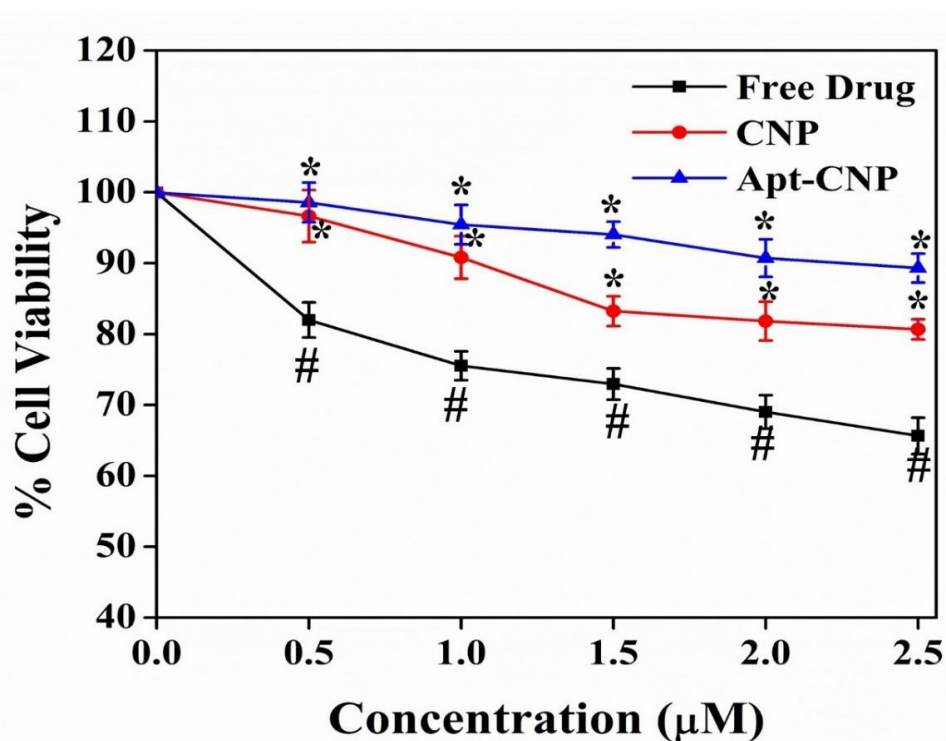


Figure 6.14. In vitro cell cytotoxicity assay of the experimental nanoformulations by using MTT on PBMC cells.

6.14. FITC-Apt-CNP showed maximum cellular internalization in vitro among the treatment groups

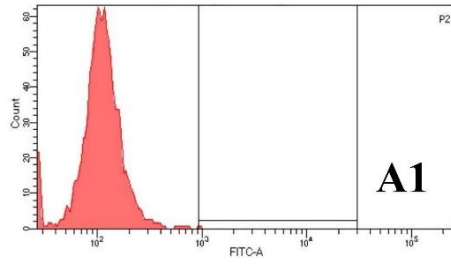
In vitro cellular uptake studies were conducted using flow cytometry to evaluate the internalization efficiency of FITC-labeled nanoformulations, CNP and Apt-CNP, in HL60 and U937 cells. The study aimed to assess the targeting capability of the aptamer-conjugated nanoparticles (Apt-CNP) compared to the non-targeted formulation (CNP).

HL60, a human promyelocytic leukemia cell line, is extensively utilized in biomedical research, particularly in hematopoiesis, myeloid leukemia, and cell differentiation studies (Dutta et al., 2024). These cells are characterized by their rapid proliferation in suspension culture, making them an ideal model for investigating differentiation, apoptosis, drug resistance, and targeted drug delivery mechanisms in leukemia research. On the other hand, U937 cells, derived from human histiocytic lymphoma, serve as a well-established model for leukemia and monocytic differentiation studies (Harris et al., 1985).

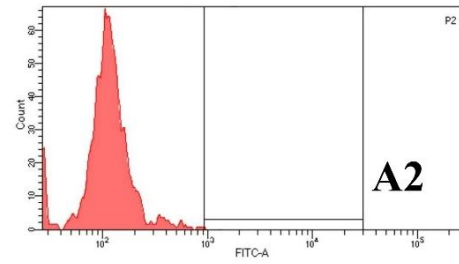
Upon treatment of HL60 cells with FITC-labeled CNP and Apt-CNP for 12 and 24 hours, a significant enhancement in cellular uptake was observed with the Apt-CNP formulation compared to CNP. Flow cytometric analysis revealed a pronounced increase in internalization for Apt-CNP-treated cells compared to the untreated control (Figure 6.15 A1 and Figure 6.15 A2). After 12 hours of incubation, CNP achieved 73.2% cellular uptake (Figure 6.15 B1), whereas Apt-CNP demonstrated a marked higher uptake of 90.6% (Figure 6.15 C1). After 24 hours, the internalization efficiency further increased, with CNP reaching 82.9% uptake (Figure 6.15 B2) and Apt-CNP achieving 95.6% (Figure 6.15 C2). The significant enhancement in cellular uptake with Apt-CNP highlights the role of the CD117-specific aptamer in facilitating targeted delivery and promoting nanoparticle internalization in HL60 cells. The aptamer's specificity likely contributed to the increased association with the conjugation of CD117-overexpressed on HL60 cell surface, enabling more efficient endocytosis of the nanoformulation. In contrast, the uptake study in U937 cells showed comparable internalization rates for both CNP (88.4%) and Apt-CNP (86.2%) after 24 hours of treatment (Figure 6.15, D-F). The absence of a significant difference between the formulations, CNP and Apt-CNP, suggests nonspecific uptake mechanisms in U937 cells. This observation is consistent with the lack of CD117 overexpression in U937 cells, limiting the aptamer-mediated targeting advantage of Apt-CNP. These findings underscore the targeted delivery potential of Apt-CNP in CD117-positive leukemia models, enhancing cellular uptake and offering a promising strategy in leukemia treatment.

HL60

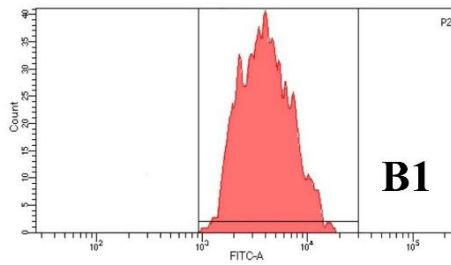
CONTROL 12h



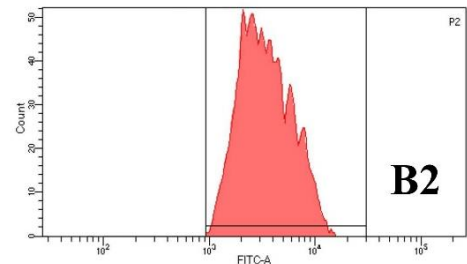
CONTROL 24h



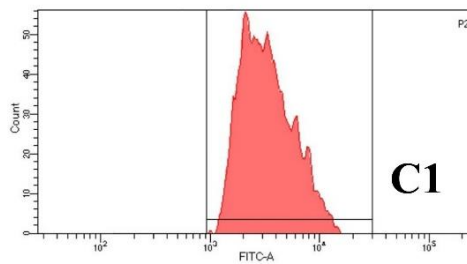
CNP 12h



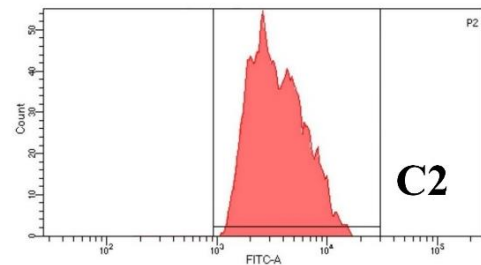
CNP 24h



APT-CNP 12h

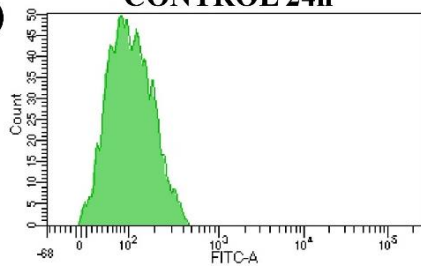


APT-CNP 24h

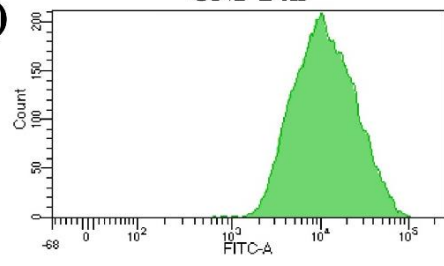


U937

(D) CONTROL 24h



(E) CNP 24h



(F) Apt-CNP 24h

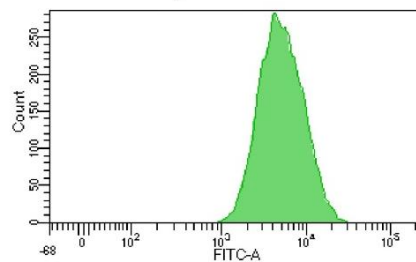


Figure 6.15. In vitro HL60/ U937 cellular uptake of the experimental formulations. A1 and A2 represent untreated control HL60 cells for 12 hours and 24 hours, respectively. B1 and B2 represent CNP data for 12 hours and 24 hours treatment, respectively. C1 and C2 represent data of Apt-CNP treatment for 12 hours and 24 hours, respectively. D U937 control cells without treatment at 24 hours. E U937 cells received CNP treatment for 24 hours. F U937 cells received Apt-CNP treatment for 24 hours.

6.15. Apt-CNP treatment showed maximum cellular apoptosis in HL60 cells

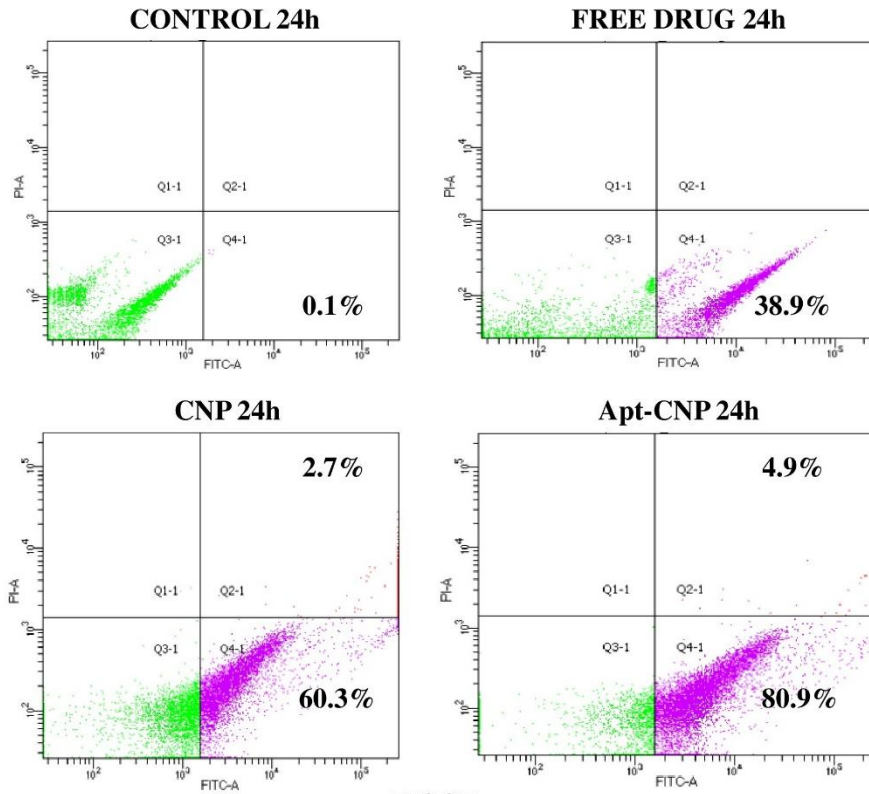
The apoptosis-inducing potential of the free drug, CNP, and Apt-CNP was evaluated in HL60 and U937 cells using the Annexin V-FITC/PI dual staining method, followed by flow cytometric analysis. This assay differentiates between early apoptotic, late apoptotic, and necrotic cell populations, offering a comprehensive assessment of the formulations' effectiveness in promoting programmed cell death.

In HL60 cells, a human promyelocytic leukemia cell line with overexpression of the CD117 biomarker, a marked increase in apoptotic induction was observed with Apt-CNP treatment compared to the free drug and CNP. After 24 hours of treatment, the early apoptotic population was 38.9% for the free drug, 60.3% for CNP, and a remarkable 80.9% for Apt-CNP (Figure 6.16 A). Additionally, Apt-CNP treatment exhibited the highest late apoptotic population among all the experimental groups at 4.4%. This enhancement in both early and late apoptosis underscores the potent chemotherapeutic potential of Apt-CNP, attributed to its targeted delivery and increased cellular internalization in CD117-positive HL60 cells. In contrast, the apoptosis assay in U937 cells, which do not overexpress the CD117 biomarker, revealed a distinct pattern. The early and late apoptotic populations for the free drug were 25.2% and 10.3%, respectively. Treatment with CNP led to early apoptosis of 61.4% and late apoptosis of 7.4%. Interestingly, Apt-CNP treatment resulted in 55.4% early apoptosis and 18.5% late apoptosis (Figure 6.16 B). Although Apt-CNP demonstrated apoptosis induction, the difference compared to CNP was not as pronounced as in HL60 cells. This reduced efficacy in U937 cells can be attributed to the absence of specific CD117-mediated targeting, leading to a more nonspecific interaction and uptake of the nanoparticles.

The observed differential apoptosis induction between HL60 and U937 cells aligns with the expected trend that the extent of apoptosis depends on CD117 expression levels. These findings highlight the selective efficacy of Apt-CNP in targeting CD117-positive leukemia cells while minimizing off-target effects in non-target cells.

HL60

(A)



U937

(B)

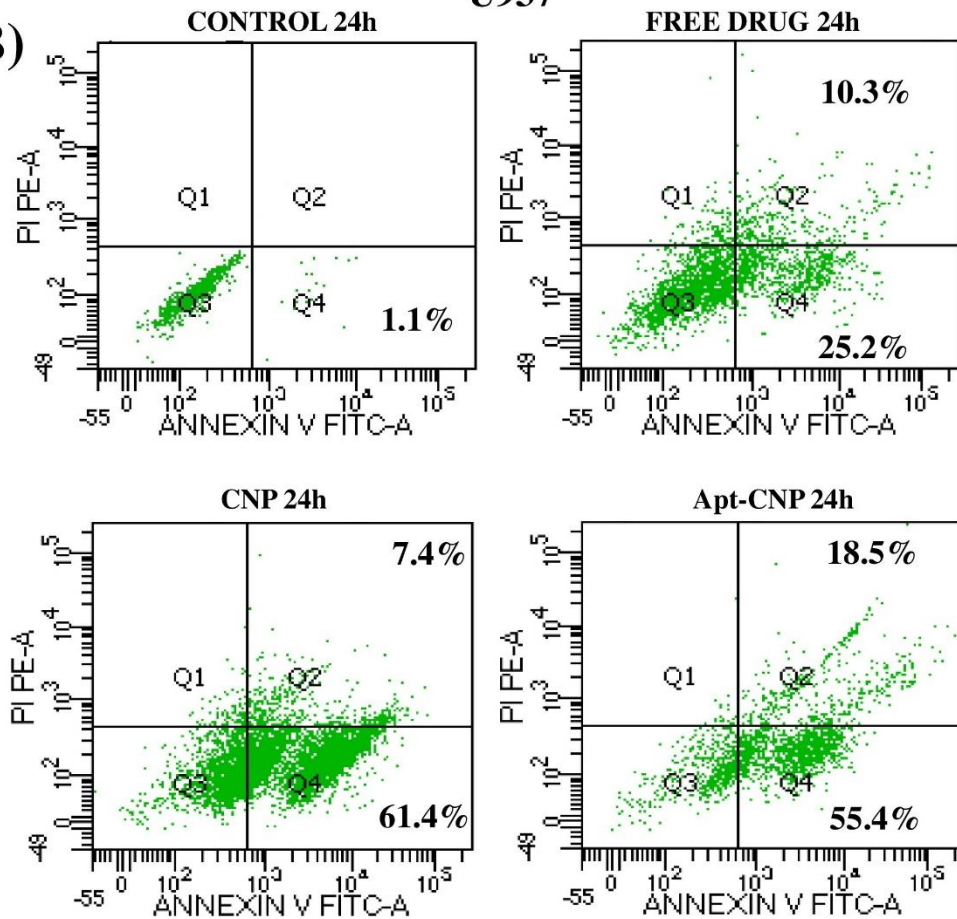


Figure 6.16. Cellular apoptosis and cellular internalization of the experimental treatments on HL 60/ U937 cells using flow cytometer. (A) In vitro cellular apoptosis study through Annexin V-FITC/PI on HL60 cells. (B) In vitro cellular apoptosis study through Annexin V-FITC/PI on U937 cells

6.16. Apt-CNP treatment predominantly enhanced mitochondrial membrane depolarization

Since Apt-CNP demonstrated higher efficacy in HL60 cells compared to U937 cells, the impact of Apt-CNP on mitochondrial membrane polarization was specifically evaluated in HL60 cells using the JC-1 dye assay. This assay measures mitochondrial membrane potential, an important indicator of cellular health and apoptosis. The JC-1 dye exists as monomers (green fluorescence) in depolarized mitochondria, while it forms aggregates (red fluorescence) in healthy, polarized mitochondria.

Following 24 hours of treatment, the percentages of JC-1 monomer (indicating mitochondrial depolarization) were 58.6% for free clofarabine, 77.4% for CNP, and a remarkable 90.6% for Apt-CNP (Figure 6.17, A-D). The substantial increase in the depolarized mitochondrial cell population upon Apt-CNP treatment reflects its potent ability to induce mitochondrial dysfunction, a key hallmark of apoptosis. The observed increase in JC-1 monomer fluorescence with Apt-CNP treatment aligns well with the cellular apoptosis data, demonstrating a consistent and robust apoptotic effect. The enhanced efficacy of Apt-CNP in disrupting mitochondrial membrane potential further supports its targeted action and improved apoptotic induction in CD117-positive HL60 cells. These findings reinforce the potential of Apt-CNP as a promising therapeutic strategy for targeting AML cells through the induction of mitochondrial mediated apoptosis.

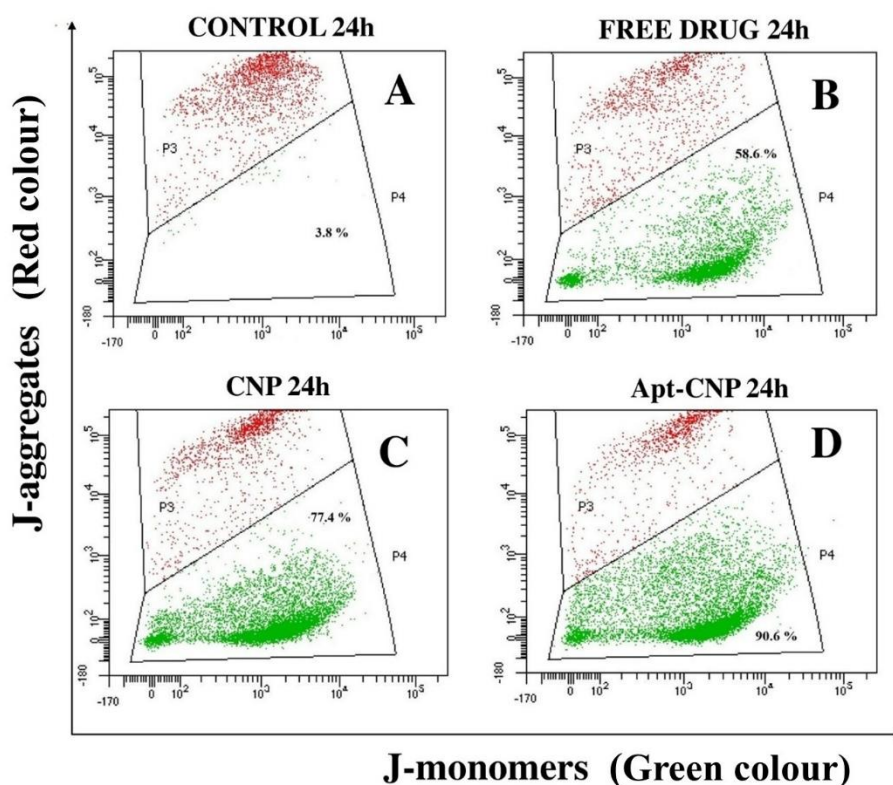


Figure 6.17. Cellular mitochondrial membrane depolarisation of HL60 cells, receiving experimental treatments using flow cytometer. A) Control B) Free drug treatment for 24 hours C) CNP treatment for 24 hours D) Apt-CNP treatment for 24 hours.

6.17. In Vivo Pharmacokinetic Study

The pharmacokinetic parameters of free clofarabine, clofarabine-loaded nanoparticles (CNP), and aptamer-conjugated nanoparticles (Apt-CNP) were evaluated following intravenous (IV) administration at a dose of 10 mg/kg in male Swiss Albino mice (Table 3). The dose was selected based on commonly used ranges in preclinical pharmacokinetic studies to ensure detectable plasma levels while avoiding toxicity, and to allow comparative evaluation of free drug and the experimental nanoparticle formulations (Zhenchuk et al., 2009). The free drug exhibited a rapid decline in plasma concentration, with a high C_{max} (5000 ± 400 ng/mL) reached at $T_{max} = 0.08 \pm 0.00$ h, followed by fast elimination ($T_{1/2} = 2.5 \pm 0.3$ h) and high clearance ($CL = 35 \pm 4$ mL/h).

In contrast, CNP and Apt-CNP displayed sustained drug release, with T_{max} delayed to 0.25 ± 0.05 h. The $T_{1/2}$ was significantly prolonged for CNP (6.8 ± 0.5 h) and Apt-CNP (7.6 ± 0.6 h),

while clearance was reduced (8 ± 1 mL/h for CNP, 7 ± 1 mL/h for Apt-CNP), indicating slower drug elimination. The AUC_{last} values for CNP ($25,000 \pm 2000$ ng·h/mL) and Apt-CNP ($30,000 \pm 2500$ ng·h/mL) were markedly higher than that of free clofarabine ($10,000 \pm 900$ ng·h/mL), suggesting improved systemic exposure (Figure 6.18). Additionally, AUMC and MRT were significantly increased, confirming prolonged circulation and sustained drug availability.

Overall, the results indicate that the desired experimental nanoparticle formulations, particularly Apt-CNP, enhance the pharmacokinetic profile of the drug by increasing systemic retention and reducing clearance, which may improve therapeutic efficacy.

Table: 3 Pharmacokinetic parameters of Clofarabine, (Free drug), Clofarabine nanoparticles (CNP), and Aptamer-conjugated Clofarabine nanoparticles (Apt-CNP) in Swiss Albino mice following intravenous (IV) administration (10 mg/kg).

Parameter	Free Drug	CNP	Apt-CNP
C _{max} (ng/mL)	5000 ± 400	4300 ± 300*	4400 ± 350*
T _{max} (h)	0.08 ± 0.00	0.25 ± 0.05*	0.25 ± 0.05*
AUC _{last} (ng·h/mL)	10,000 ± 900	25,000 ± 2000*	30,000 ± 2500*
AUC _{0-∞} (ng·h/mL)	11,000 ± 1000	28,000 ± 2200*	34,000 ± 2800*
AUMC (ng·h ² /mL)	35,000 ± 3000	250,000 ± 10,000*	360,000 ± 20,000*
T _{1/2} (h)	2.5 ± 0.3	6.8 ± 0.5*	7.6 ± 0.6*
MRT (h)	3.5 ± 0.4	10.5 ± 1.2*	12.0 ± 1.3*
V _d (mL)	400 ± 40	125 ± 10*	115 ± 10*
Clearance (mL/h)	35 ± 4	8 ± 1*	7 ± 1*

Data represent mean ± SD (n=3). Statistical analysis was performed using one-way ANOVA followed by Tukey's post-test ($p < 0.05$) compared against the Free Drug group. Data marked with (*) indicates significant differences compared to the Free Drug group.

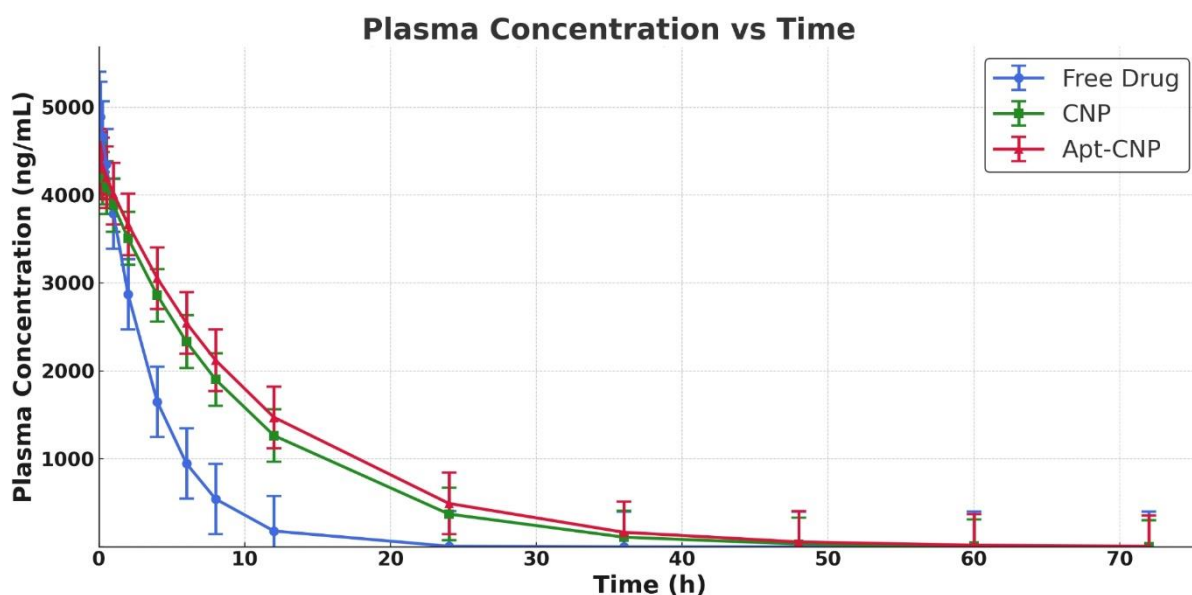
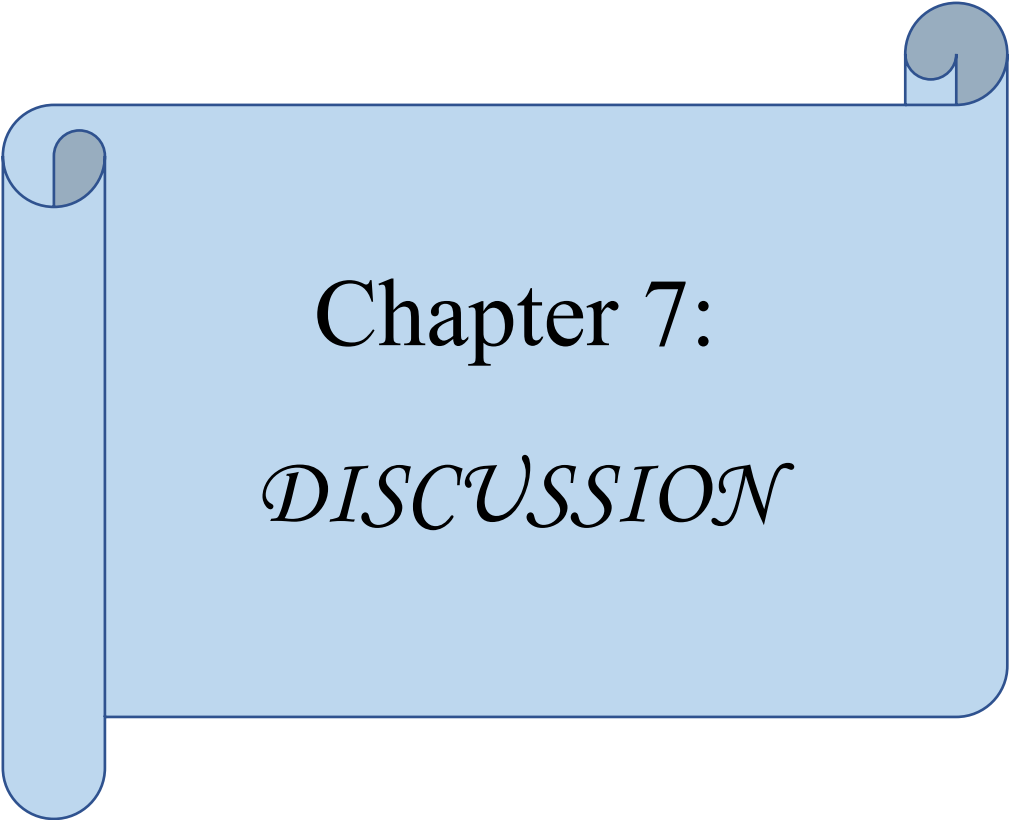


Figure 6.18. The pharmacokinetic profile of the “Free drug” “CNP”, and “Apt-CNP” was evaluated in Swiss Albino mice by measuring the concentration of clofarabine and experimental formulations in the bloodstream over time. The results were plotted as per the data represented in Table 3.

6.18. References

- Adhikary, S., Al Hoque, A., Ray, M., Paul, S., Hossain, A., Goswami, S., & Dey, R. (2023). Investigation of paracetamol entrapped nanoporous silica nanoparticles in transdermal drug delivery system. *Applied Biochemistry and Biotechnology*, 195(8), 4712-4727. <https://doi.org/10.1007/s12010-023-04576-w>
- Al Hoque, A., Dutta, D., Paul, B., Kumari, L., Ehsan, I., Dhara, M., Mukherjee, B., Quadir, M., Kaiparettu, B. A., Laha, S., & Ganguly, S. (2023). ΔPSap4# 5 surface-functionalized abiraterone-loaded nanoparticle successfully inhibits carcinogen-induced prostate cancer in mice: a mechanistic investigation. *Cancer Nanotechnology*, 14(1), 73. <https://doi.org/10.1186/s12645-023-00223-5>
- Dhara, M., Al Hoque, A., Sen, R., Dutta, D., Mukherjee, B., Paul, B., & Laha, S. (2023). Phosphorothioated amino-AS1411 aptamer functionalized stealth nanoliposome accelerates bio-therapeutic threshold of apigenin in neoplastic rat liver: a mechanistic approach. *Journal of Nanobiotechnology*, 21(1), 28. <https://doi.org/10.1186/s12951-022-01764-4>
- Dutta, D., Chakraborty, A., Mukherjee, B., & Gupta, S. (2018). Aptamer-conjugated apigenin nanoparticles to target colorectal carcinoma: a promising safe alternative of colorectal cancer chemotherapy. *ACS applied bio materials*, 1(5), 1538-1556. <https://doi.org/10.1021/acsabm.8b00441>
- Harris, P., & Ralph, P. (1985). Human leukemic models of myelomonocytic development: a review of the HL-60 and U937 cell lines. *Journal of leukocyte biology*, 37(4), 407-422. <https://doi.org/10.1002/jlb.37.4.407>
- Kumari, L., Ehsan, I., Mondal, A., Al Hoque, A., Mukherjee, B., Choudhury, P., et al. (2023). Cetuximab-conjugated PLGA nanoparticles as a prospective targeting therapeutics for non-small cell lung cancer. *Journal of Drug Targeting*, 31(5), 521-536. <https://doi.org/10.1080/1061186X.2023.2199350>
- Song, Y., Cong, Y., Wang, B., & Zhang, N. (2020). Applications of Fourier transform infrared spectroscopy to pharmaceutical preparations. *Expert opinion on drug delivery*, 17(4), 551-571. <https://doi.org/10.1080/17425247.2020.1737671>
- Zhenchuk, A., Lotfi, K., Juliusson, G., & Albertioni, F. (2009). Mechanisms of anti-cancer action and pharmacology of clofarabine. *Biochemical pharmacology*, 78(11), 1351-1359. <https://doi.org/10.1016/j.bcp.2009.06.094>



Chapter 7:
DISCUSSION

In this study, we have used poly(lactic-co-glycolic acid) (PLGA), a biocompatible, biodegradable, and US FDA-approved polymer, along with a short DNA aptamer that is non-toxic and exhibits minimal immunogenicity (Zhao et al., 2015; Chakraborty et al., 2020). This strategic combination was designed to facilitate efficient in vitro targeted drug delivery while mitigating cytotoxic effects on healthy cells, primarily due to the negligible uptake of the targeted formulation by non-cancerous cells. The primary objective of this approach was to achieve preferential accumulation of aptamer-conjugated clofarabine-loaded PLGA nanoparticles (Apt-CNP) in AML cells overexpressing CD117, thereby enhancing therapeutic specificity.

HL60 cells were selected for this study as they serve as a well-established in vitro model for AML, offering a relevant and reliable system to evaluate the efficacy of the targeted drug delivery strategy (Aravind et al., 2012). Notably, CD117 is overexpressed in approximately 70% of AML subtypes, including HL60 cells. While this protein is also present in certain normal cells, it is not significantly overexpressed in them. Given that a substantial proportion of AML cases exhibit CD117 overexpression, it was chosen as the primary target for this study.

Successful development of this formulation could provide a targeted therapeutic approach for AML subtypes characterized by CD117 overexpression. Furthermore, this platform holds potential for broader applications by modifying the aptamer to target other overexpressed proteins in AML, thereby expanding the scope of aptamer-based targeted drug delivery strategies for hematological malignancies.

Fourier-transform infrared (FTIR) spectroscopy was employed to analyze potential chemical interactions between clofarabine and the excipients used in the formulation (Dutta et al., 2018). The results demonstrated that no significant chemical interactions occurred between the drug and the excipients, thereby preserving the stability and structural integrity of clofarabine within the nanoparticle system. The FTIR spectra of both clofarabine-loaded nanoparticles (CNP) and aptamer-conjugated clofarabine-loaded nanoparticles (Apt-CNP) exhibited characteristic peaks corresponding to clofarabine, confirming that the drug's chemical structure remained unchanged in these formulations. This observation suggests that the drug was successfully encapsulated without undergoing any chemical modifications, ensuring its therapeutic efficacy.

Moreover, the spectra of both nanoformulations showed the presence of drug-specific peaks alongside polymer-associated peaks, further validating the incorporation of clofarabine within the nanoparticles. Notably, in the Apt-CNP formulation, a distinct peak at 1635 cm^{-1} was observed, which is indicative of amide bond formation. This peak signifies the successful conjugation of the aptamer to the nanoparticle surface, thereby confirming its attachment through a covalent linkage. The presence of this peak is particularly significant, as it validates the effective functionalization of the nanoparticles with the aptamer, a critical aspect of targeted drug delivery.

These findings confirm that the excipients used in the formulation are chemically compatible with clofarabine, making them suitable for use in nanoparticle-based drug delivery systems. Additionally, the presence of the aptamer-binding peak in Apt-CNP further reinforces the successful conjugation of the aptamer, which is essential for achieving targeted delivery to CD117-overexpressing AML cells.

The molecular docking study was conducted to evaluate the binding affinity and interactions between the DNA aptamer and the CD117 (c-KIT) receptor, providing a detailed understanding of the specificity and stability of the aptamer-receptor complex. The results revealed that the nucleotide bases of the aptamer formed strong interactions with multiple amino acid residues of the CD117 receptor, establishing a highly stable complex. These interactions included electrostatic forces, hydrophobic interactions, and weak hydrogen bonding, highlighting the intricate and multifaceted nature of the binding mechanism.

Notably, the amino acid residues involved in these interactions were not confined solely to the receptor's active binding pocket but extended to other functionally significant regions of the CD117 receptor. This widespread interaction pattern suggests that the aptamer engages with the receptor at multiple sites, further reinforcing its high binding affinity. The docking score of -250.95 reflects the remarkable stability of the aptamer-CD117 complex, demonstrating the aptamer's strong and selective binding capability. This high binding affinity is particularly significant for its role in targeted drug delivery, as it ensures precise recognition of the CD117 biomarker overexpressed on AML cells, specifically HL60 cells. The selective binding of the Apt-CNP to CD117 receptor confirms that these nanoparticles can efficiently target AML cells, facilitating precise drug delivery while minimizing off-target interactions. By directing the

therapeutic payload specifically to cancerous cells, this targeted drug delivery approach significantly enhances drug accumulation at the tumor site, thereby improving therapeutic efficacy. Overall, the molecular docking analysis provides strong evidence of the aptamer's high binding affinity to CD117, reinforcing its potential as a targeting ligand for AML therapy (Al Hoque et al., 2023; Yan et al., 2020).

Agarose gel electrophoresis was employed to confirm the successful conjugation of the CD117-specific DNA aptamer onto the surface of PLGA nanoparticles. This technique exploits the differential migration of nucleic acid and nanoparticle-aptamer conjugates under an electric field, allowing the assessment of molecular interactions between the aptamer and nanoparticles (Chakraborty et al., 2020).

The free DNA aptamer, being a single-stranded oligonucleotide, migrates faster through the agarose gel due to its smaller size and negative charge. In contrast, the aptamer-conjugated nanoparticles (Apt-CNPs) exhibit reduced electrophoretic mobility, appearing as a band with significantly less migration compared to the free aptamer. The fluorescence observed in the Apt-CNP loading well provides a direct indication of the aptamer's attachment to the nanoparticle surface. This is because the presence of the heavier nanoparticle complex restricts the movement of the aptamer, thereby localizing fluorescence to the loading well rather than dispersing along the gel matrix.

Further confirmation of aptamer conjugation was obtained through FTIR analysis. It provides molecular-level insights by detecting specific functional groups and chemical bonds involved in the conjugation process. The spectrum of Apt-CNP demonstrated characteristic absorption peaks corresponding to the chemical interactions between the aptamer and the nanoparticle surface. Shifts in peak positions, along with the emergence of new bands indicative of phosphate and amide bond formations, further validated the presence of covalent or electrostatic interactions between the DNA aptamer and the PLGA nanoparticles (Estévez et al., 2010; Chang et al., 2011).

The average drug loading and percentage encapsulation efficiency results indicate that both formulations achieved substantial drug loading and good encapsulation efficiency. This suggests that the nanoparticles effectively encapsulated and retained the drug within their polymeric matrix, ensuring a controlled and sustained release profile. The high encapsulation

efficiency further highlights the stability of the formulation, minimizing drug loss during the preparation process (Kumari et al., 2023).

The morphological characteristics of CNP and Apt-CNP were evaluated using Field Emission Scanning Electron Microscopy (FESEM), which confirmed that both formulations exhibited a spherical shape with smooth surface morphologies and are closely distributed. The absence of surface irregularities suggests that the synthesis and surface modification processes did not introduce significant roughness, a crucial factor in maintaining biocompatibility and minimizing nonspecific interactions in biological environments. The well-defined spherical shape further indicates uniform particle formation, which is essential for achieving consistent drug delivery performance.

High-Resolution Transmission Electron Microscopy (HR-TEM) imaging provided additional insights into the internal structure of the nanoparticles, revealing that the drug was homogeneously distributed within the nanoparticle matrix. This uniform internal morphology is indicative of efficient drug encapsulation, reducing the likelihood of drug aggregation and ensuring a controlled release profile. The presence of a well-defined core-shell structure further supports the stability of the formulation.

Atomic Force Microscopy (AFM) was employed to analyze the three-dimensional surface topology and particle distribution. The AFM images demonstrated that the nanoparticles were well-separated, with a narrow size distribution, confirming the monodispersity of the formulations. Additionally, the absence of pinholes or structural deformities in the nanoparticles further validates the integrity of the formulation, ensuring its suitability for biomedical applications. These findings collectively confirm that the developed nanoparticles possess favorable physicochemical characteristics, which are critical for their functionality as an efficient drug delivery system.

Dynamic Light Scattering (DLS) was utilized to analyze the particle size distribution and zeta potential of the nanoparticles. The results indicated an approximate 20% increase in particle size upon aptamer conjugation, suggesting successful surface modification of the nanoparticles. This size increase is expected due to the presence of aptamers on the nanoparticle surface.

The zeta potential values provided crucial insights into the stability of the nanoparticle suspensions. The observed negative zeta potential values for both CNP and Apt-CNP formulations suggest the presence of moderate electrostatic repulsion between nanoparticles, preventing aggregation and ensuring prolonged colloidal stability in aqueous suspensions. It has been reported that nanoparticles with zeta potential values exceeding ± 30 mV exhibit strong electrostatic repulsion, leading to highly stable suspensions (Champion et al., 2007). However, since the zeta potential values of the developed nanoparticles were moderately negative, special care must be taken to prevent aggregation over extended storage periods. To maintain optimal stability, the nanoparticles should be stored in powder form at the refrigerated condition (2–8°C) and reconstituted in an aqueous medium prior to use. These findings highlight the importance of surface charge in determining nanoparticle stability and reinforce the need for appropriate storage conditions to preserve formulation integrity.

The stability study of CNP and Apt-CNP formulations was conducted under different storage conditions to assess their morphological and physicochemical stability over time. Samples, which were stored at 4–8°C retained their morphology and drug content consistently throughout the study, demonstrating their stability under refrigerated conditions. In contrast, nanoparticles stored at elevated temperatures of 30°C with 75% relative humidity (RH) and 40°C with 75% RH for 45 days exhibited significant morphological changes.

Higher temperatures induced polymer softening, leading to nanoparticle aggregation and an increase in particle size. These changes compromised the stability of the formulations, indicating that temperatures exceeding 30°C negatively impact nanoparticle integrity. These findings highlight the necessity of maintaining storage temperatures between 2–8°C to preserve the physical and chemical stability of the nanoparticles, ensuring their efficacy and shelf life for potential therapeutic applications (Al Hoque et al., 2023; Kumari et al., 2023).

An *in vitro* drug release study was conducted for both CNP and Apt-CNP formulations using phosphate-buffered saline (PBS) at pH 7.4 as the release medium as it is a blood mimicking medium. This experimental setup facilitated the evaluation of drug release kinetics in an environment relevant to the human body (Dhara et al., 2023). The cumulative drug release profile was monitored over a period of 680 hours, revealing that the Apt-CNP formulation exhibited a higher overall drug release percentage compared to CNP. Both nanoparticle

formulations demonstrated a biphasic release pattern, characterized by an initial burst release followed by sustained drug release. The rapid initial release is attributed to the diffusion of drug molecules localized near the nanoparticle surface, whereas the prolonged release phase is governed by the gradual diffusion of the drug from the nanoparticle core. The presence of surface-bound aptamers on the Apt-CNP formulation likely modulated drug-polymer interactions, potentially reducing the binding affinity between the drug and the PLGA matrix. This alteration in interaction dynamics facilitated an enhanced diffusion rate, leading to a comparatively faster drug release from the Apt-CNP system. These findings underscore the influence of aptamer conjugation on drug release kinetics, contributing to an optimized drug delivery profile for targeted therapeutic applications.

To further understand the drug release mechanism, the release data were analyzed using various kinetic models, including zero-order, first-order, Higuchi, and Korsmeyer–Peppas models (Pattnaik et al., 2012). The regression coefficient (R^2) values obtained for each model were compared to determine the best fit, while the release exponent (n) values from the Korsmeyer–Peppas model provided insights into the underlying drug release mechanism.

The analysis revealed that the drug release from both CNP and Apt-CNP formulations predominantly followed the Korsmeyer–Peppas model, as evidenced by the highest R^2 values. This suggests that the drug release is governed by a combination of diffusion and polymer relaxation mechanisms rather than a purely concentration-dependent (first-order) or time-independent (zero-order) release profile. Furthermore, the n -values indicated that the release mechanism adhered to Fickian diffusion, implying that drug molecules primarily diffused through the polymer matrix without significant polymer chain relaxation. The Fickian diffusion-based release profile is particularly advantageous for achieving sustained drug release, as it ensures a predictable and controlled drug release rate over time. The slightly higher drug release from Apt-CNP compared to CNP can be attributed to the presence of aptamers on the nanoparticle surface, which may have altered drug-polymer interactions and facilitated a more efficient drug diffusion process.

In the cellular internalization study, the uptake of FITC-labeled CNP and aptamer-conjugated FITC-Apt-CNP by HL60 leukemia cells was evaluated after 12 and 24 hours of treatment. A substantial increase in the internalization of Apt-CNP compared to CNP alone underscores the

pivotal role of the aptamer in facilitating targeted nanoparticle delivery. The aptamer, specifically designed to recognize the CD117 receptor overexpressed on HL60 leukemia cells, significantly enhanced the internalization of the nanoformulation, demonstrating its efficacy in receptor-mediated uptake.

In contrast, a significant lower uptake of Apt-CNP was observed in U937 cells, which do not overexpress CD117. This discrepancy highlights the specificity of the aptamer for CD117, reinforcing its role in selective targeting. The distinct differences in uptake between HL60 and U937 cells provide strong evidence for the aptamer's selectivity in CD117-expressing leukemia cells, emphasizing the potential of Apt-CNP in developing a targeted therapeutic approach for AML.

Compared to non-targeted CNP, Apt-CNP exhibited a significantly improved ability to deliver the therapeutic formulation directly to HL60 leukemia cells, which predominantly express CD117. Interestingly, HL60 cells, which share morphological and functional characteristics with neutrophils, exhibited efficient uptake of Apt-CNP. This could be attributed to the phagocytic nature of these cells, allowing for enhanced recognition and internalization of Apt-CNP due to the aptamer's strong affinity for CD117. The close interaction between the aptamer-functionalized nanoparticles and the CD117 receptor likely facilitated greater nanoparticle accumulation within the target cells.

Previous studies have suggested that aptamer-conjugated PLGA nanoparticles can enter cells through receptor-mediated endocytosis and micropinocytosis (Wan et al. 2019; Liu et al. 2009; Shishparenok et al. 2023; Yallapu et al. 2014). Receptor-mediated endocytosis is a highly specific mechanism wherein Apt-CNP bind to the CD117 receptor on HL60 leukemia cells, triggering cellular uptake via clathrin or caveolae-mediated pathways. This interaction facilitates the internalization of nanoparticles into endosomes and lysosomes, where the drug is subsequently released. The receptor-specific nature of this pathway enhances targeting efficiency while minimizing off-target effects in non-CD117-expressing cells. On the other hand, micropinocytosis is a non-specific fluid-phase endocytosis mechanism that allows cells to engulf extracellular fluid, including nanoparticles. This process is particularly relevant in phagocytic and cancerous cells, which often exhibit increased micropinocytic activity (Stow et al., 2020). The combination of these two internalization pathways suggests that both specific

and non-specific uptake mechanisms contribute to the efficient delivery of Apt-CNP. However, receptor-mediated endocytosis remains the primary mechanism ensuring selective targeting of CD117-overexpressing HL60 cells while significantly reducing uptake in CD117-negative cells such as U937. Understanding these mechanisms is crucial for optimizing nanoparticle design, improving drug loading and release kinetics, and ultimately enhancing the therapeutic efficacy of Apt-CNP in AML treatment.

This aptamer-mediated targeted approach not only improved cellular uptake but also holds promise for enhancing the therapeutic efficacy of the drug while minimizing off-target effects. The specificity of Apt-CNP for CD117-overexpressing leukemia cells positions it as a highly effective strategy for AML treatment, potentially improving drug delivery efficiency and therapeutic outcomes.

IC₅₀, or the half-maximal inhibitory concentration, is a fundamental pharmacological parameter that quantifies the concentration of a substance required to inhibit a specific biological function or target by 50% (Kazakova et al., 2022). In the context of evaluating the cytotoxicity of a compound in cancer cells, a lower IC₅₀ value signifies greater potency, as it indicates that a minimal concentration of the compound is sufficient to achieve significant inhibitory effects.

The MTT assay is a widely used method for assessing cell viability and cytotoxicity, measuring the minimal concentration of a substance necessary to reduce cell viability by 50% (Dutta et al., 2018). This method provides a reliable measure of the compound's efficacy at lower doses. In this study, MTT assay results revealed the superior therapeutic potential of Apt-CNP in HL60 cells, demonstrating its efficacy as a targeted drug delivery system for CD117-overexpressing AML cells.

The research examined the impact of both free drug and the experimental nanoparticle formulations on cell viability across three different cell types, HL60 cells, U937 cells, and normal peripheral blood mononuclear cells (PBMC). The findings indicated that Apt-CNP nanoparticles exhibited the highest cytotoxicity against HL60 cells, as reflected by the lowest IC₅₀ values. Specifically, the IC₅₀ value for the CNP formulation in HL60 cells was determined to be 1.30 μ M, whereas the Apt-CNP formulation exhibited an even lower IC₅₀ value of 1.07

μM . This reduction in IC_{50} suggests enhanced potency and targeted action of the Apt-CNP formulation against HL60 cells.

In the case of U937 cells, the Apt-CNP formulation did not show a significant improvement in cytotoxicity compared to the CNP formulation. This outcome corroborates the absence of CD117 expression in U937 cells, confirming that the aptamer-mediated delivery system is highly specific to CD117-overexpressing cells such as HL60. The selective action of Apt-CNP underscores the specificity of the formulation in targeting CD117-positive AML cells while sparing non-target cells.

Furthermore, the absence of cytotoxicity in PBMCs highlights the favorable safety profile of the Apt-CNP nanoformulation. This finding is particularly significant, as it suggests minimal off-target effects and preservation of normal cell viability. The selective cytotoxic action of Apt-CNP against HL60 cells, combined with its non-toxic nature towards normal PBMCs, establishes its potential as an effective and targeted therapeutic approach for AML treatment.

Apoptosis, or programmed cell death, is a fundamental process essential for maintaining cellular homeostasis and is a key mechanism exploited by anticancer agents to eliminate malignant cells (Pistritto et al., 2016). In this study, the apoptotic potential of clofarabine, CNP, and Apt-CNP was evaluated. The findings underscore the selective effectiveness of Apt-CNP in inducing apoptosis in HL60 leukemia cells, which overexpress the CD117 receptor. Among the tested formulations, Apt-CNP exhibited the most potent apoptotic effect, significantly surpassing both free clofarabine and CNP in triggering apoptosis. Notably, a higher proportion of HL60 cells treated with Apt-CNP entered early apoptosis, with a substantial fraction also progressing to late-stage apoptosis. This suggests that Apt-CNP effectively induces apoptotic cell death, highlighting its potential as a promising chemotherapeutic agent with strong cytotoxic activity.

To assess apoptosis, Annexin V-FITC staining was employed. It is a well-established method that detects phosphatidylserine (PS) externalization on the cell membrane, which is an early hallmark of apoptosis (Yedjou et al., 2010; N'Guessan, 2020). In healthy cells, PS is confined to the inner leaflet of the plasma membrane. However, during apoptosis, PS translocates to the outer leaflet, where it binds to Annexin V, a calcium-dependent phospholipid-binding protein. This binding, detected through flow cytometry, enables the distinction between early apoptotic

(Annexin V-positive, PI-negative) and late apoptotic or necrotic cells (Annexin V-positive, PI-positive). The results demonstrated that Apt-CNP treatment resulted in the highest percentage of Annexin V-positive cells, indicating highest apoptosis induction in CD117-overexpressing HL60 cells.

In contrast, U937 cells, which lack CD117 expression, did not exhibit a comparable increase in apoptosis following Apt-CNP treatment. This reinforces the specificity of the aptamer-mediated targeting mechanism, as Apt-CNP did not induce significant apoptosis beyond that observed with CNP. The selective apoptotic response in HL60 cells highlights the therapeutic precision of Apt-CNP, minimizing off-target cytotoxic effects, which is an essential factor for enhancing cancer treatment efficacy while reducing systemic toxicity. These findings emphasize the potential of Apt-CNP as a targeted therapeutic strategy against CD117-positive leukemia. The ability of Apt-CNP to selectively induce apoptosis through aptamer-mediated binding and internalization suggests its strong potential for further preclinical and clinical development in cancer therapy.

Mitochondrial membrane potential is a critical indicator of cellular health and apoptosis, making it a key target for assessing the efficacy of anticancer therapies. JC-1, a cationic lipophilic dye, is widely utilized to monitor mitochondrial membrane potential alterations (Al Hoque et al., 2023; Fathi et al., 2022; Sivandzade et al., 2019). The dye exhibits potential-dependent accumulation within mitochondria, allowing for a fluorescence-based distinction between healthy and depolarized mitochondria. Under normal physiological conditions, when the mitochondrial membrane potential is high, JC-1 aggregates within the mitochondria and emits red fluorescence (J-aggregates). However, in depolarized or dysfunctional mitochondria, JC-1 remains in its monomeric form in the cytoplasm, and emits green fluorescence. This shift from red to green fluorescence serves as a reliable indicator of mitochondrial membrane depolarization, a hallmark of apoptosis.

In this study, JC-1 staining was employed to assess mitochondrial dysfunction following treatment with free clofarabine, CNP, and Apt-CNP in HL60 cells. The results revealed that Apt-CNP induced the highest degree of mitochondrial membrane depolarization compared to both free clofarabine and CNP. This suggests that Apt-CNP exerts a stronger apoptotic effect by compromising mitochondrial integrity. The loss of mitochondrial membrane potential

disrupts ATP production, increases reactive oxygen species (ROS) generation, and triggers the release of pro-apoptotic factors such as cytochrome c, ultimately activating the intrinsic apoptotic pathway.

The pronounced mitochondrial dysfunction observed in HL60 cells treated with Apt-CNP underscores its enhanced cytotoxic efficacy through targeted drug delivery. The aptamer-mediated targeting of CD117-overexpressing HL60 cells likely facilitates higher intracellular uptake of Apt-CNP, leading to sustained mitochondrial damage and subsequent apoptosis. Notably, this effect was not observed to the same extent with CNP or free clofarabine, reinforcing the role of aptamer-mediated selectivity in improving therapeutic outcomes. The ability of Apt-CNP to induce mitochondrial membrane depolarization more effectively than conventional formulations highlights its potential as a promising therapeutic strategy for leukemia treatment. By selectively targeting CD117-positive leukemia cells and inducing mitochondrial dysfunction, Apt-CNP represents a valuable approach for developing advanced anticancer therapeutics.

HL60 cells were selected here for this study due to their well-characterized model for AML and their high expression of the CD117 (c-Kit) receptor, which serves as the target for Apt-CNP. Since CD117 plays a crucial role in leukemic cell proliferation and survival, its overexpression in HL60 cells makes them an ideal system for evaluating the targeted efficacy of Apt-CNP (Yedjou et al., 2010; Zhou et al., 2015). The selective binding of the aptamer to CD117 ensures efficient internalization of the nanoparticle formulation, leading to enhanced mitochondrial dysfunction and apoptosis. In contrast, U937 cells, which lack significant CD117 expression, were used as a control to confirm the specificity of Apt-CNP's targeting mechanism. The preferential apoptotic response observed in HL60 cells further validates the effectiveness of Apt-CNP in selectively eliminating CD117-overexpressing leukemia cells, reinforcing its potential as a targeted therapeutic strategy.

The data obtained from U937 cells reveal a distinct pattern, underscoring the nonspecific interaction of the tested formulations in the absence of CD117 expression. While both CNP and Apt-CNP were taken up by U937 cells to some extent, their cytotoxic effects and apoptosis induction were comparatively moderate, with no substantial difference between the two formulations. This indicates that, in the absence of CD117-mediated targeting, Apt-CNP does

not exhibit significantly enhanced therapeutic efficacy over CNP. The lack of a pronounced differential effect in U937 cells further reinforces the specificity of the aptamer for CD117-overexpressing cells, such as HL60.

Since the differences in apoptosis induction between CNP and Apt-CNP in U937 cells were minimal, further investigations were not pursued. Given that JC-1 staining primarily serves as an indicator of mitochondrial dysfunction associated with apoptosis, conducting this assay in U937 cells was unlikely to yield additional meaningful insights, as these cells lack CD117 expression and thus were not selectively targeted by the Apt-CNP. However, the absence of JC-1 data for U937 cells does not affect the overall conclusions of the study. The findings clearly illustrate that Apt-CNP exerts a selective apoptotic effect in HL60 cells, driven by its specific interaction with CD117. This reinforces the aptamer-mediated targeting mechanism and highlights the potential of Apt-CNP as a precise and effective therapeutic strategy for CD117-positive leukemia, with reduced off-target effects.

The pharmacokinetic behaviour of clofarabine improved significantly upon nanoparticle incorporation, particularly with aptamer conjugation, highlighting the benefits of nanocarrier-based drug delivery. Free clofarabine exhibited a rapid rise in plasma concentration followed by swift elimination, indicative of high systemic clearance and short half-life. In contrast, CNP and Apt-CNP demonstrated a more controlled pharmacokinetic profile. The delayed T_{max} suggests slower drug release, preventing sharp plasma peaks that can cause toxicity. The prolonged half-life and reduced clearance indicate improved systemic retention and bioavailability. The reduced renal elimination observed with CNP and Apt-CNP is likely due to the sustained drug release.

Among the formulations, Apt-CNP showed the most favorable pharmacokinetics, with the highest systemic exposure and longest circulation time. The increased AUC_{last} suggests enhanced systemic drug availability, which could improve therapeutic efficacy. Aptamer conjugation may contribute to this by enabling receptor-mediated interactions, reducing non-specific clearance, and enhancing targeted delivery, which is particularly advantageous in leukemia treatment.

The increased MRT and AUMC values (Table 3) further support prolonged circulation, ensuring sustained drug availability. This enhanced pharmacokinetic profile could translate into improved therapeutic outcomes with reduced dosing frequency, enhancing patient compliance.

Due to certain experimental limitations, we were unable to evaluate the targeted therapeutic potential of Apt-CNP in an in vivo setting. However, in vivo studies using suitable animal models, such as xenograft techniques, would be valuable for further validating the efficacy and specificity of Apt-CNP in targeting AML. These models would help assess biodistribution, pharmacokinetics, and overall therapeutic performance within a physiological environment.

Additionally, in vitro experiments can be further refined by incorporating normal blood cells alongside AML cancer cells. This approach would allow for a better assessment of Apt-CNP's ability to selectively target leukemic cells while sparing healthy hematopoietic cells, providing a more comprehensive evaluation of its targeted delivery mechanism. Such studies would contribute to a deeper understanding of its potential for clinical translation and further support its development as a precise and effective therapeutic strategy for AML treatment.

7.1. References

- Al Hoque, A., Dutta, D., Paul, B., Kumari, L., Ehsan, I., Dhara, M., Mukherjee, B., Quadir, M., Kaiparettu, B. A., Laha, S., & Ganguly, S. (2023). Δ PSap4# 5 surface-functionalized abiraterone-loaded nanoparticle successfully inhibits carcinogen-induced prostate cancer in mice: a mechanistic investigation. *Cancer Nanotechnology*, *14*(1), 73. <https://doi.org/10.1186/s12645-023-00223-5>
- Aravind, A., Varghese, S. H., Veeranarayanan, S., Mathew, A., Nagaoka, Y., Iwai, S., Fukuda T., Hasumura T., Yoshida Y., Maekawa T & Kumar, D. S. (2012). Aptamer-labeled PLGA nanoparticles for targeting cancer cells. *Cancer Nanotechnology*, *3*, 1-12. <https://doi.org/10.1007/s12645-011-0024-6>
- Chakraborty, S., Dlie, Z. Y., Chakraborty, S., Roy, S., Mukherjee, B., Besra, S. E., Dewanjee, S., Mukherjee, A., Ojha, P. K., Kumar, V., & Sen, R. (2020). Aptamer-functionalized drug nanocarrier improves hepatocellular carcinoma toward normal by targeting neoplastic hepatocytes. *Molecular Therapy Nucleic Acids*, *20*, 34-49. <https://doi.org/10.1016/j.omtn.2020.01.034>
- Champion, J. A., Katare, Y. K., & Mitragotri, S. (2007). Particle shape: a new design parameter for micro-and nanoscale drug delivery carriers. *Journal of controlled release*, *121*(1-2), 3-9. <https://doi.org/10.1016/j.jconrel.2007.03.022>
- Chang, M., Yang, C. S., & Huang, D. M. (2011). Aptamer-conjugated DNA icosahedral nanoparticles as a carrier of doxorubicin for cancer therapy. *ACS nano*, *5*(8), 6156-6163. <https://doi.org/10.1021/nn200693a>
- Dhara, M., Al Hoque, A., Sen, R., Dutta, D., Mukherjee, B., Paul, B., & Laha, S. (2023). Phosphorothioated amino-AS1411 aptamer functionalized stealth nanoliposome accelerates bio-therapeutic threshold of apigenin in neoplastic rat liver: a mechanistic approach. *Journal of Nanobiotechnology*, *21*(1), 28. <https://doi.org/10.1186/s12951-022-01764-4>
- Dutta, D., Chakraborty, A., Mukherjee, B., & Gupta, S. (2018). Aptamer-conjugated apigenin nanoparticles to target colorectal carcinoma: a promising safe alternative of colorectal cancer chemotherapy. *ACS applied bio materials*, *1*(5), 1538-1556. <https://doi.org/10.1021/acsabm.8b00441>
- Estévez, M. C., Huang, Y. F., Kang, H., O'Donoghue, M. B., Bamrungsap, S., Yan, J., Chen, X., & Tan, W. (2010). Nanoparticle–aptamer conjugates for cancer cell targeting and detection. *Cancer Nanotechnology: Methods and Protocols*, 235-248. https://doi.org/10.1007/978-1-60761-609-2_16

- Fathi, E., Azarbad, S., Farahzadi, R., Javanmardi, S., & Vietor, I. (2022). Effect of rat bone marrow derived-mesenchymal stem cells on granulocyte differentiation of mononuclear cells as preclinical agent in cellbased therapy. *Current Gene Therapy*, 22(2), 152-161. <https://doi.org/10.2174/1566523221666210519111933>
- Kazakova, R. R., & Masson, P. (2022). Quantitative measurements of pharmacological and toxicological activity of molecules. *Chemistry*, 4(4), 1466-1474. <https://doi.org/10.3390/chemistry4040097>
- Kumari, L., Ehsan, I., Mondal, A., Al Hoque, A., Mukherjee, B., Choudhury, P., Sengupta, A., Sen, R., & Ghosh, P. (2023). Cetuximab-conjugated PLGA nanoparticles as a prospective targeting therapeutics for non-small cell lung cancer. *Journal of Drug Targeting*, 31(5), 521-536. <https://doi.org/10.1080/1061186X.2023.2199350>
- Liu, J., Kopeckova, P., Bühler, P., Wolf, P., Pan, H., Bauer, H., Beile, U. E., & Kopecek, J. (2009). Biorecognition and subcellular trafficking of HPMA copolymer– anti-PSMA antibody conjugates by prostate Cancer cells. *Molecular pharmaceutics*, 6(3), 959-970. <https://doi.org/10.1021/mp8002682>
- N'Guessan, K. F. (2020). *Phosphatidylserine Externalization in Pancreatic Ductal Adenocarcinoma: Elucidating Mechanisms of Regulation for Combination Therapy* (Doctoral dissertation, University of Cincinnati).
- Pattnaik, G., Sinha, B., Mukherjee, B., Ghosh, S., Basak, S., Mondal, S., & Bera, T. (2012). Submicron-size biodegradable polymer-based didanosine particles for treating HIV at early stage: an in vitro study. *Journal of Microencapsulation*, 29(7), 666-676. <https://doi.org/10.3109/02652048.2012.680509>
- Pistritto, G., Trisciuglio, D., Ceci, C., Garufi, A., & D'Orazi, G. (2016). Apoptosis as anticancer mechanism: function and dysfunction of its modulators and targeted therapeutic strategies. *Aging (albania NY)*, 8(4), 603. <https://doi.org/10.18632/aging.100934>
- Shishparenok, A. N., Furman, V. V., & Zhdanov, D. D. (2023). DNA-based nanomaterials as drug delivery platforms for increasing the effect of drugs in tumors. *Cancers*, 15(7), 2151. <https://doi.org/10.3390/cancers15072151>
- Sivandzade, F., Bhalerao, A., & Cucullo, L. (2019). Analysis of the mitochondrial membrane potential using the cationic JC-1 dye as a sensitive fluorescent probe. *Bio-protocol*, 9(1), e3128-e3128. DOI:10.21769/BioProtoc.3128

Stow, J. L., Hung, Y., & Wall, A. A. (2020). Macropinocytosis: Insights from immunology and cancer. *Current opinion in cell biology*, 65, 131-140. <https://doi.org/10.1016/j.ceb.2020.06.005>

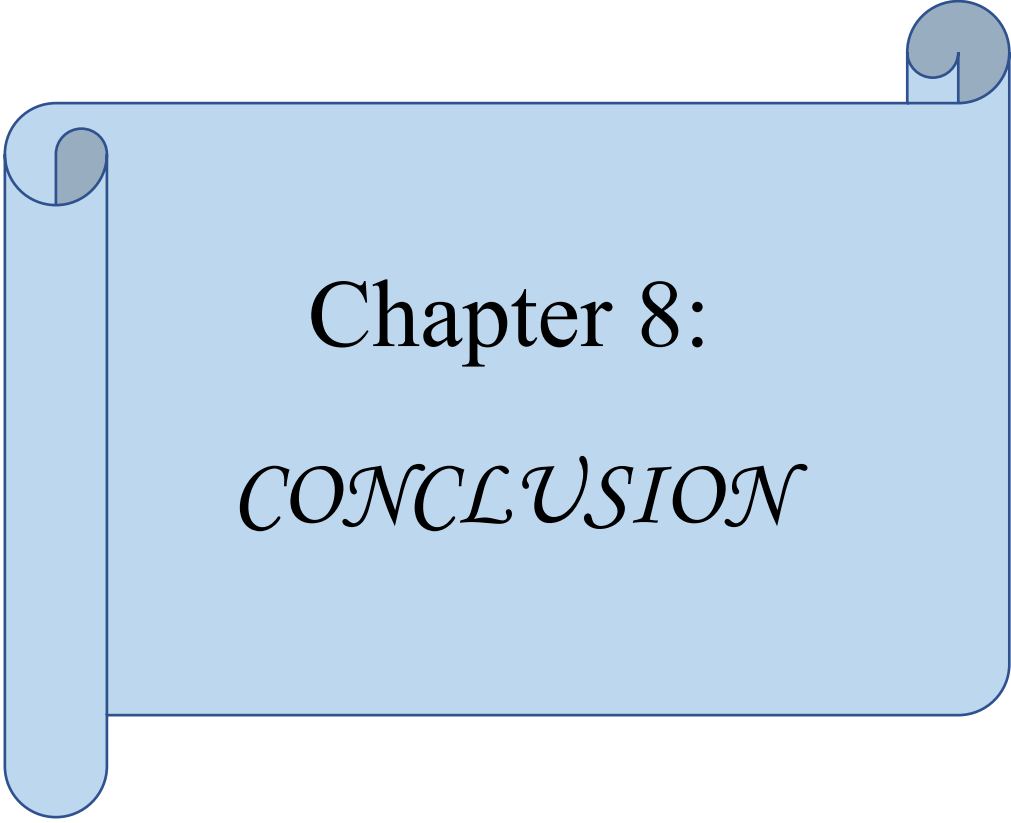
Wan, L. Y., Yuan, W. F., Ai, W. B., Ai, Y. W., Wang, J. J., Chu, L. Y., Zhang, Y. Q., & Wu, J. F. (2019). An exploration of aptamer internalization mechanisms and their applications in drug delivery. *Expert opinion on drug delivery*, 16(3), 207-218. <https://doi.org/10.1080/17425247.2019.1575808>

Yallapu, M. M., Khan, S., Maher, D. M., Ebeling, M. C., Sundram, V., Chauhan, N., Ganju, A., Balakrishna, S., Gupta, B. K., Zafar, N., Jaggi, M., & Chauhan, S. C. (2014). Anti-cancer activity of curcumin loaded nanoparticles in prostate cancer. *Biomaterials*, 35(30), 8635-8648. <https://doi.org/10.1016/j.biomaterials.2014.06.040>

Yan, Y., Tao, H., He, J., & Huang, S. Y. (2020). The HDOCK server for integrated protein–protein docking. *Nature protocols*, 15(5), 1829-1852. <https://doi.org/10.1038/s41596-020-0312-x>

Yedjou, C., Tchounwou, P., Jenkins, J., & McMurray, R. (2010). Basic mechanisms of arsenic trioxide (ATO)-induced apoptosis in human leukemia (HL-60) cells. *Journal of hematology & oncology*, 3, 1-9. <https://doi.org/10.1186/1756-8722-3-28>

Zhao, N., Pei, S. N., Qi, J., Zeng, Z., Iyer, S. P., Lin, P., Tung, C. H., & Zu, Y. (2015). Oligonucleotide aptamer-drug conjugates for targeted therapy of acute myeloid leukemia. *Biomaterials*, 67, 42-51. <https://doi.org/10.1016/j.biomaterials.2015.07.025>



Chapter 8:
CONCLUSION

The present study demonstrates that CD117-specific aptamer-conjugated clofarabine-loaded PLGA nanoparticles (Apt-CNP) significantly enhance cellular internalization in HL60 leukemia cells, which overexpress CD117, compared to non-conjugated formulations. This aptamer-mediated targeting strategy facilitated efficient drug delivery, leading to improved intracellular accumulation of the therapeutic agent and superior *in vitro* therapeutic efficacy. By leveraging the high specificity of aptamer-receptor interactions, the Apt-CNP system ensures a more selective uptake of the drug by malignant cells, minimizing non-specific drug distribution and associated cytotoxic effects on healthy cells.

The selective targeting capability of Apt-CNP underscores the advantages of aptamer-functionalized nanoparticles in modern drug delivery approaches, particularly in enhancing drug specificity and reducing adverse effects often observed with conventional chemotherapy. Traditional chemotherapy for AML is often hindered by systemic toxicity, rapid drug clearance, and off-target interactions, leading to undesirable side effects and limited therapeutic efficacy. In contrast, the Apt-CNP formulation effectively addresses these challenges by ensuring precise localization of the therapeutic agent within leukemia cells, thereby increasing treatment efficacy while reducing systemic toxicity.

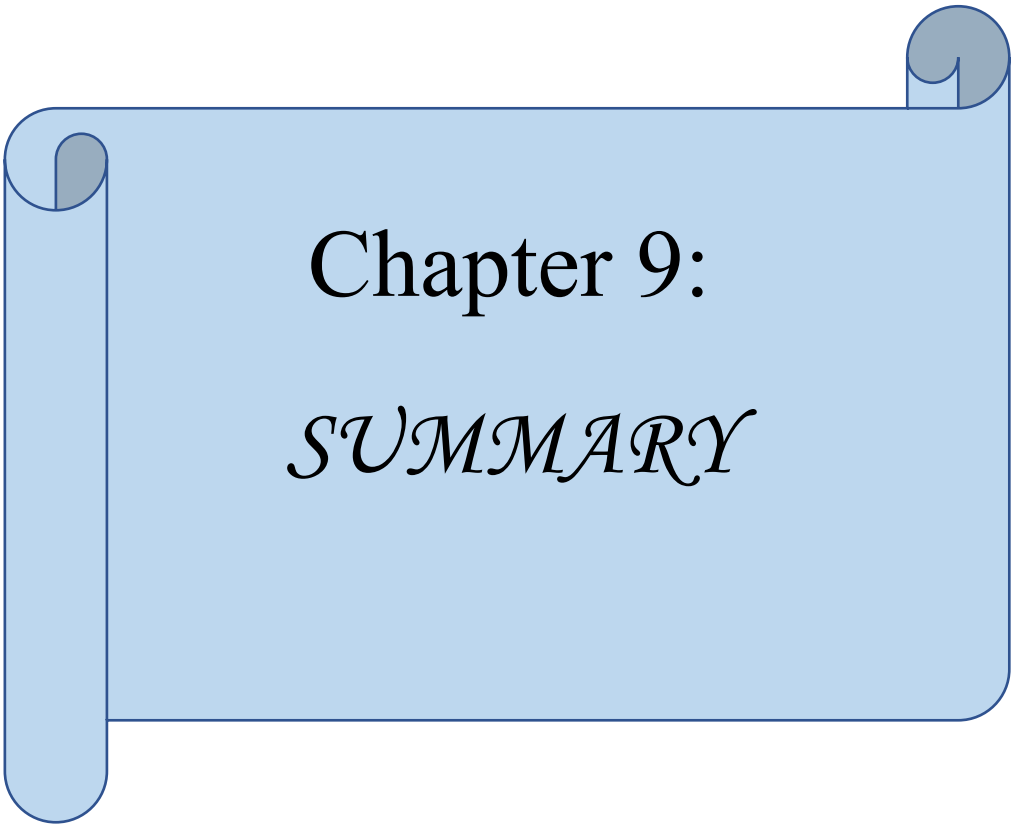
Beyond the promising *in vitro* findings, the results of this study highlight the broader potential of aptamer-functionalized nanoparticulate drug delivery systems as a transformative approach for AML treatment. The ability to engineer nanoparticles with ligand specificity opens new avenues for personalized and targeted cancer therapy. This targeted strategy not only enhances drug accumulation in cancerous cells but also holds promise for overcoming multidrug resistance, a significant obstacle in leukemia treatment. Furthermore, by tuning the physicochemical properties of PLGA nanoparticles, such as size, surface charge, and release kinetics, Apt-CNP can be optimized to maximize therapeutic benefits.

While these *in vitro* results provide compelling evidence of the efficacy of Apt-CNP, further studies are necessary to validate its therapeutic potential *in vivo*. Future investigations should focus on preclinical animal models to evaluate the pharmacokinetics, biodistribution, tumor penetration, and overall treatment efficacy of the Apt-CNP system in a physiological setting. Understanding the circulation time and bioavailability of the nanoparticles in systemic circulation will be crucial for predicting their translational applicability. Additionally, assessing

the immunogenicity and potential off-target effects in vivo provide key insights into the safety profile of the aptamer-functionalized nanoparticles.

Moreover, exploring the possibility of combining this aptamer-mediated drug delivery approach with other therapeutic modalities could further enhance its clinical applicability. Integrating Apt-CNP with immunotherapy, targeted small-molecule inhibitors, or combination chemotherapy regimens may result in synergistic effects, improving overall treatment outcomes for AML patients. Such combinatorial strategies could be particularly beneficial in overcoming drug resistance mechanisms, thereby offering a more robust and durable therapeutic response.

In summary, this novel aptamer-functionalized nanoplatform represents a significant advancement in AML-targeted therapy. By offering precise drug delivery, improved therapeutic outcomes, and a reduced side-effect profile, it paves the way for the development of innovative nanoparticle-based treatments for leukemia and other hematologic malignancies. The results gained from this study could be instrumental in guiding future research efforts aimed at translating aptamer-conjugated nanoparticles into viable clinical applications, ultimately contributing to more effective and safer therapeutic options for AML and beyond.



AML is a highly aggressive hematological malignancy characterized by the clonal expansion of immature myeloid cells within the bone marrow and peripheral blood. Despite advancements in chemotherapeutic strategies, the treatment of AML continues to pose significant clinical challenges, including systemic toxicity, non-specific drug distribution, and the emergence of drug resistance in patients. In response to these limitations, this research focuses on designing a targeted drug delivery system employing polymeric nanoparticles for site-specific delivery of chemotherapeutics to AML cells, thereby enhancing therapeutic efficacy and minimizing adverse effects.

The present study explores the formulation and evaluation of PLGA (poly lactic-co-glycolic acid) nanoparticles encapsulating clofarabine, which is a second-generation purine nucleoside analog, approved for the treatment of relapsed or refractory leukemia. PLGA was chosen due to its FDA-approved status, excellent biocompatibility, and sustained-release capabilities, which are particularly beneficial for maintaining therapeutic drug levels over extended periods of time. To achieve active targeting, the surface of these nanoparticles was conjugated with a single-stranded DNA aptamer that specifically recognizes CD117 (c-Kit), a transmembrane tyrosine kinase receptor that is overexpressed in AML blast cells, especially in the HL60 cell line used as the disease model in this study.

The research was divided into several phases. Initially, PLGA nanoparticles were formulated using the multiple emulsion solvent evaporation technique, optimized for size, surface charge, drug entrapment efficiency, and controlled release kinetics. Clofarabine encapsulation was confirmed through spectroscopic techniques. The next step involved the conjugation of the CD117 aptamer to the surface of PLGA nanoparticles via EDC/NHS mediated covalent coupling linkage. Successful conjugation was confirmed by agarose gel electrophoresis based on electrophoretic mobility shifts and further supported by changes in zeta potential and particle size.

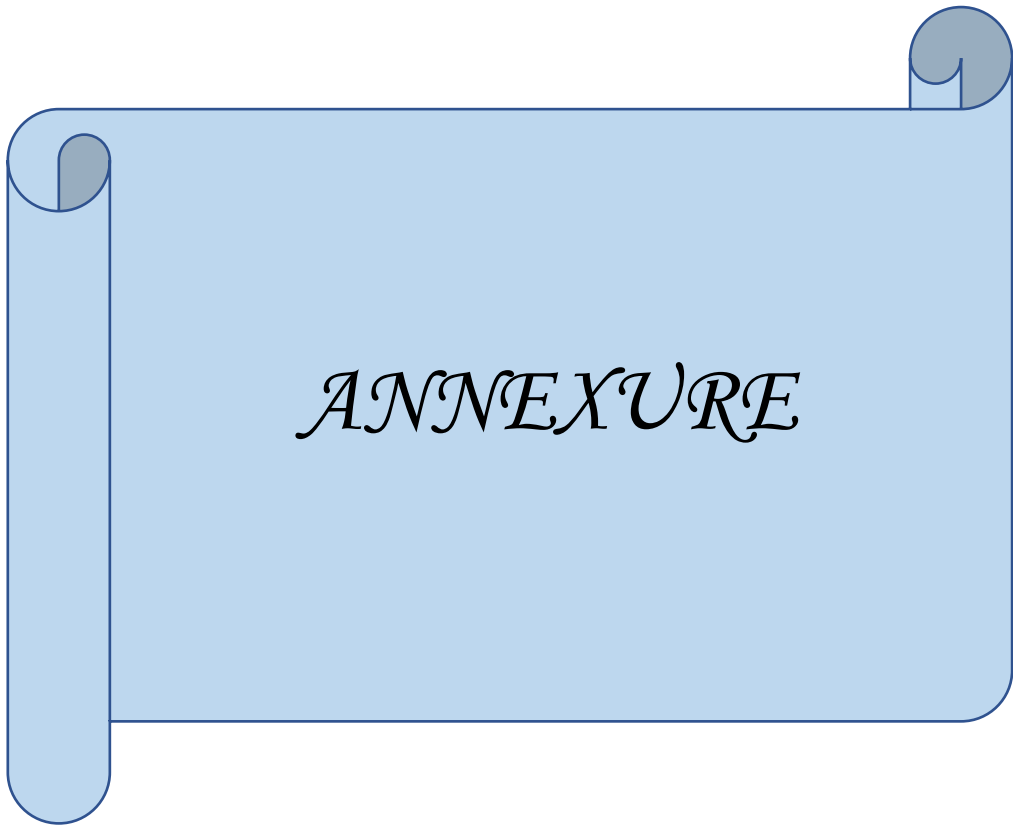
The developed aptamer-conjugated clofarabine-loaded PLGA nanoparticles (Apt-CNP) were then subjected to a series of *in vitro* biological evaluations CD117 positive as well as CD117 negative leukemia cells. Cellular uptake studies demonstrated a significantly enhanced internalization of Apt-CNP in CD117-expressing HL60 cells compared to non-conjugated nanoparticles, validating the targeting specificity of the aptamer. MTT assays and apoptosis

studies confirmed that Apt-CNP induced a higher degree of cytotoxicity and apoptosis in leukemic cells, suggesting improved therapeutic performance due to this targeted delivery and sustained drug release.

Furthermore, hemocompatibility studies confirmed the biosafety of the nanoparticulate system, and stability studies under physiological conditions demonstrated satisfactory shelf-life potential. The combination of passive targeting (via enhanced permeation and retention effect) and active targeting (via aptamer-receptor interaction) positions this formulation as a robust and innovative strategy for AML treatment.

In conclusion, this thesis presents a promising nano-therapeutic platform for the targeted treatment of AML that offers multiple advantages over conventional chemotherapy. The aptamer-functionalized PLGA nanoparticles not only ensure selective delivery of clofarabine to leukemic cells but also reduce collateral damage to healthy tissues, thereby overcoming major limitations of existing therapies. By integrating principles of nanotechnology, molecular targeting, and pharmaceutical science, the work paves the way for the development of patient-specific, precision drug delivery systems in hematological malignancies.

This study also opens avenues for further preclinical evaluations and eventual clinical translation. Future directions may include *in vivo* validation in xenograft mice models, pharmacokinetic profiling, and possible expansion to other hematological cancers expressing CD117. These findings lay the groundwork for a next-generation targeted therapeutic approach, contributing meaningfully to the advancement of translational research in oncology and nanomedicine.



ANNEXURE

Dr. Biswajit Mukherjee

M.Pharm., Ph.D., F.I.C., F.I.C.S.
Professor in Pharmaceutics
Coordinator, QIP Nodal Cell (Pharmacy)
Coordinator,
Centre for Advance Research in Pharmaceutical Sciences,
Jadavpur University, Kolkata
Former DAAD Fellow (Germany) and Ex-guest Scientist,
German Cancer Research Center (DKFZ)
Heidelberg, Germany
Indo-Hungarian Education Exchange Fellow,
Budapest, Hungary
Former Fellow Scientist, School of Pharmacy,
University of London, London, U.K.
Ex. Biotechnology Overseas Associate,
Department of Biotechnology
(Government of India) and worked in DKFZ
Heidelberg, Germany



Professor and Former Head
Department of Pharmaceutical Technology
JADAVPUR UNIVERSITY
Kolkata - 700 032, India
Phone : +91-33-2414 6677 / 2414 6666 ext. 2588
Resi. : +91-33-2427 6026
Fax : +91-33-2414 6677 (0)
E-mail : biswajit.mukherjee@jadavpuruniversity.in
biswajit55@yahoo.com

To

Date; 29/01/2021

Manisheetta Roy

128/1, Satyen Roy Road

Behala, Kolkata -700034

Dear Miss Roy,

I have pleasure to inform that you have selected as Research Assistant for Dr. V. Ravichandran Center for Advanced Research in Pharmaceutical Sciences (CARPS, JU) through an interview held on 28th January, 2021. You will get consolidated 15,000/month as fellowship. If you agree, you may join and report to Prof. Biswajit Mukherjee, Coordinator, CARPS, JU, within 10 days of date of receipt of letter.

Thanking you,

Prof. Biswajit Mukherjee

Coordinator, CARPS, JU

Prof. Dr. Biswajit Mukherjee

Coordinator
Centre for Advanced Research in Pharmaceutical Sciences (CARPS)
(V. Ravi Chandran Centre for Pharmaceutical Sciences)
Dept. of Pharmaceutical Technology
Jadavpur University
Kolkata-700 032, India

Prof. Dr. Biswajit Mukherjee

Coordinator
Centre for Advanced Research in Pharmaceutical Sciences (CARPS)
(V. Ravi Chandran Centre for Pharmaceutical Sciences)
Dept. of Pharmaceutical Tech.
Jadavpur University
Kolkata-700 032, India



Institutional Animal Ethics Committee (IAEC)

Department of Pharmaceutical Technology

Jadavpur University

Kolkata- 700032


RefNo: AEC/PHARM/1705/04A/2020

Date: 05/03/2020

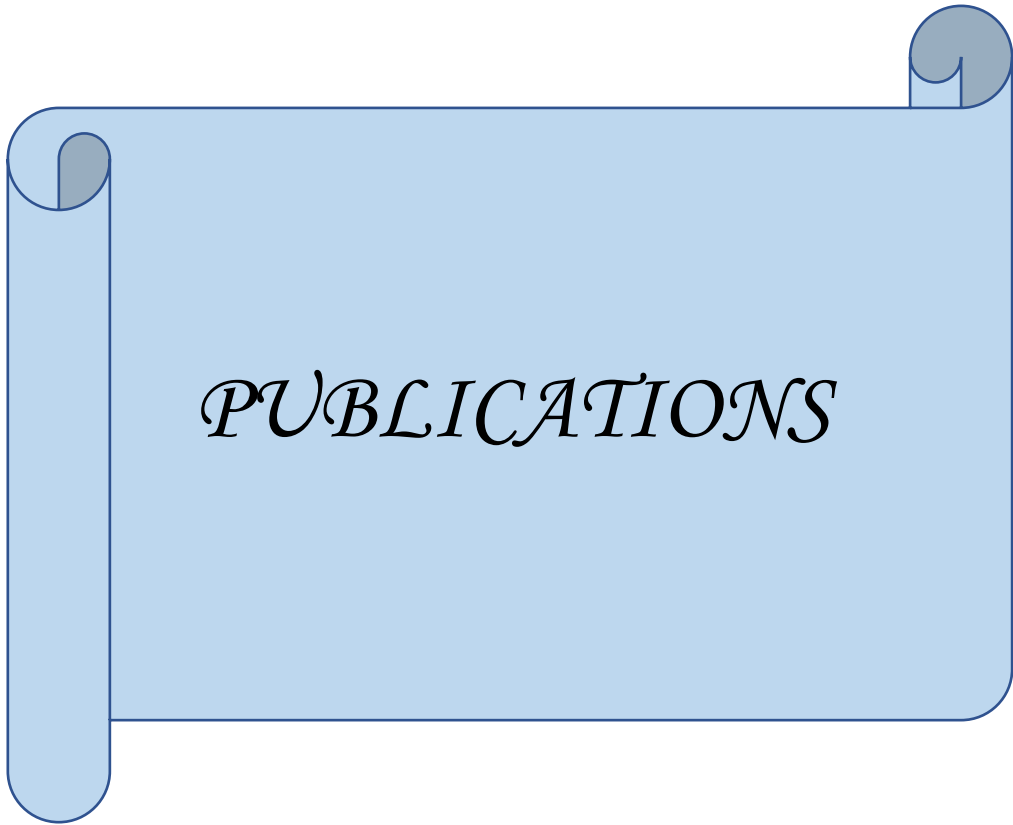
This is to certify that the project titled “Nucleoside Analogue Containing Nanoparticle for Therapeutic Management of Leukemia” has been approved by the Institutional Animal Ethical Committee (IAEC), Jadavpur University in the meeting held on 3rd March, 2020.

Prof. (Dr.) Biswajit Mukherjee

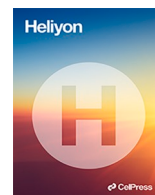
Chairman/Member Secretary IAEC


Signature with date 05/03/2020

Chairman
Institutional Animal Ethics Committee
Jadavpur University
Kolkata-700032



PUBLICATIONS



Research article

Clofarabine-loaded aptamer-conjugated biodegradable nanoparticle successfully targeted CD117 overexpressed HL60 cells and potentially induced apoptosis

Manisheeta Ray^{a,c}, Ashique Al Hoque^a, Saptarshi Chatterjee^b, Sourav Adhikary^c, Samrat Paul^b, Biswajit Mukherjee^{a,*}, Amitava Bhattacharya^a

^a Department of Pharmaceutical Technology, Jadavpur University, 188, Raja S. C. Mullick Road, Jadavpur, Kolkata 700032, India

^b BIRAC E-Yuva Centre, Adamas University, Adamas Knowledge City, Barackpore Main Rd, Barbaria, Kolkata, West Bengal 700126, India

^c School of Materials Science and Nanotechnology, Jadavpur University, Kolkata, India

ARTICLE INFO

Keywords:

Acute myeloid leukemia (AML)

DNA aptamer

Targeted delivery

Nanoparticles

Biomarker CD117

ABSTRACT

Acute Myeloid Leukemia (AML) is a rapidly progressing malignancy characterized by the proliferation of abnormal neutrophils, leading to severe symptoms and complications. Current widely used treatment options include chemotherapy and radiotherapy, which often result in suffering from systemic toxicity and drug resistance. To mitigate systemic toxicity and off-target side effects, a targeted therapeutic strategy is one of the remarkably successful options. For targeting AML cells, we have chosen a single-strand DNA aptamer (Apt), which is specific for the biomarker CD117, overexpressing AML cells. This study introduces explicitly a novel therapeutic approach employing aptamer-conjugated clofarabine-loaded PLGA nanoparticles (Apt-CNP) targeting the CD117 receptor on HL60 leukemia cells. Clofarabine, a potent nucleoside analogue, disrupts DNA synthesis and induces cancer cell death but is limited by its toxicity and resistance. Encapsulation in PLGA nanoparticles enables sustained drug release, maintaining therapeutic concentrations and potentially reducing drug resistance. Our findings demonstrate that Apt-CNP effectively targets HL60 leukemia cells, thereby improving drug delivery and reducing adverse effects on healthy cells. This targeted approach may open a new avenue for more specific drug delivery to mobile and floated blood cells, including AML (HL60 leukemia) cells, and overcome the limitations of traditional AML treatments.

1. Introduction

Acute myeloid leukemia (AML) is a bone marrow and blood malignancy characterized by the rapid growth of abnormal myeloblasts, precursors of granulocytes, which also hinder the production of healthy red blood cells [1]. Symptoms include weakness, fatigue, fever, easy bruising or bleeding, and recurrent infections. Treatment options include radiation, chemotherapy, stem cell transplantation, and targeted therapy based on patient health, age, and leukemia cell characteristics [2].

Clofarabine, a nucleoside analogue, inhibits ribonucleotide reductase, disrupting DNA synthesis and causing death to cancer cells, although leading to toxicity to normal healthy cells, too [3,4]. Clinical trials highlight clofarabine's efficacy against leukemia but also

* Corresponding author.

E-mail addresses: biswajit.mukherjee@jadavpuruniversity.in, biswajit55@yahoo.com (B. Mukherjee).

note limitations such as drug resistance and toxicity [5]. Targeted nanocarrier therapy, using drug-loaded biodegradable (The United States Food and Drug Administration (US-FDA) approved polymer) poly (lactic-co-glycolic acid) (PLGA) nanoparticles, through systemic administration can enhance drug delivery and minimize adverse effects [6–8].

Ligand-conjugated delivery, involving ligands like antibodies and aptamers, offers precise targeting of cells, including AML cells, enhancing therapeutic efficacy and reducing toxicity [9]. Aptamers (also called synthetic monoclonal antibodies) are stable, cost-effective, less immunogenic compounds to monoclonal antibodies, highly target-specific, and ideal for targeted drug delivery [10, 11].

This study introduces aptamer-conjugated clofarabine-loaded PLGA nanoparticles (Apt-CNP) targeting the CD117 (c-KIT) over-expressed receptor on the cell surface of the majority of AML cells, including HL60 AML cells. This approach aims to minimize adverse effects by specifically delivering clofarabine to leukemia cells, enhancing treatment efficacy, and reducing systemic toxicity [9]. PLGA nanoparticles ensure sustained drug release and prolonged blood levels, which would potentially reduce drug resistance [7].

The novelty of this work lies in the development of Apt-CNP as a targeted drug delivery system for floated acute myeloid leukemia cells. The hypothesis driving this study is that conjugating a CD117-specific aptamer to clofarabine-loaded PLGA nanoparticles will significantly enhance the therapeutic efficacy of clofarabine by selectively targeting AML cells, such as HL60 while reducing systemic toxicity and minimizing off-target effects. This novel approach combines the target specificity of aptamers with the sustained drug release capabilities of PLGA nanoparticles, addressing limitations like drug resistance and adverse effects associated with conventional AML therapies.

2. Experimental

2.1. Materials

Clofarabine was procured from TCI Chemicals India Pvt Ltd, Telangana. PLGA (MW 4,000–15,000; lactide to glycolide ratio 75:25) was sourced from Sigma-Aldrich Chemicals Pvt. Ltd., Bangalore. Polyvinyl alcohol (PVA, MW 125,000) was purchased from S.D. Fine-Chem Ltd., Mumbai. Fluorescein isothiocyanate (FITC) was obtained from Himedia Lab Pvt. Ltd., Mumbai. Acetone, acetonitrile, and dichloromethane (DCM) were procured from E. Merck (India) Ltd., Mumbai. All other chemicals were analytical grade, ensuring high purity.

HL60 cells were procured from National Centre for Cell Science (NCCS), Pune.

U937 cells were procured from Dr. Amitava Sengupta, Senior Principal Scientist and Associate Professor of biological sciences, CSIR, Indian Institute of Chemical Biology (IICB-TRUE).

PBMC were isolated from anticoagulated blood (blood with anticoagulant).

2.2. Selection of aptamer

We selected a single-stranded DNA aptamer specific for the CD117 biomarker [12]. The DNA aptamer sequence was 5'-GAGGCATACCAGCTTATTATTGGGGCCGGGGCAAGGGGGGGGTACCGTGGTAGGACAGATAGTAAGTGCAATCTGCGAA-3' with K_d value of 4.24 nM, indicating a strong affinity between the aptamer and its target molecule [9].

2.3. Method

2.4. Preparation of clofarabine encapsulated PLGA nanoparticles (CNP)

PLGA nanoparticles were synthesized using a modified multiple-emulsion solvent evaporation method [13,14]. PLGA with a 75:25 lactic acid to glycolic acid ratio (50 mg) was dissolved in 3 mL of a dichloromethane (DCM) and acetone mixture (1:1 v/v). PVA solutions were prepared at 1.5 % and 2.5 % (w/v) by dissolving PVA in Milli-Q water with continuous stirring and heating at 50 °C. Clofarabine (5 mg), the drug of interest, was added to the 2.5 % PVA solution to create a drug-loaded aqueous phase. The emulsification process was initiated by homogenizing the PLGA organic solution into 2.5 % PVA solution at 6000 rpm for 3 min using an Ultra-Turrax homogenizer (IKA Laboratory Equipment, Germany), forming a primary water-in-oil (W/O) emulsion. This primary emulsion was added to 1.5 % PVA solution and homogenized for 8 min to create a water-in-oil-in-water (W/O/W) double emulsion. To improve particle stability and reduce droplet size, the secondary emulsion was then sonicated for 30 min and stirred overnight. Large particles and aggregates were separated by an initial centrifugation step at 5000 rpm, ensuring that only fine particles remained in the supernatant. This supernatant was centrifuged at 16,000 rpm for 45 min to isolate the nanoparticles. To remove residual PVA, the nanoparticle pellet was washed three times by resuspending it in deionized water, followed by repeated centrifugation at 16,000 rpm for 10 min each. The nanoparticles were then pre-frozen at -20 °C for 9 h to prevent aggregation and structural compromise and lyophilized for 8 h using a freeze dryer (Instrumentation India, Kolkata, India) to obtain dry, stable nanoparticles for further characterization and applications. This method ensures efficient drug encapsulation and high nanoparticle stability, making it suitable for advanced drug delivery systems.

FITC-tagged nanoparticles were prepared following the same protocol as previously described. Specifically, 100 μ l of a FITC solution in ethanol (0.4 % w/v) was added to the organic phase containing the polymer and drug before the homogenization step. All

subsequent procedures remained unchanged.

2.5. Drug-excipient interaction study using Fourier Transform Infrared spectroscopy (FTIR)

This study investigates potential interactions between clofarabine and various excipients utilizing Fourier Transform Infrared (FTIR) spectroscopy, a robust analytical technique to identify changes in chemical bonds and functional groups. FTIR spectroscopy is a critical tool for assessing chemical compatibility in pharmaceutical formulations. By comparing FTIR spectra of pure components, physical mixtures, and nanoparticles, any alterations or shifts in characteristic absorption bands indicate interactions. Pure clofarabine, PVA, PLGA, physical mixtures, drug-loaded nanoparticles, blank nanoparticles, and aptamer-conjugated nanoparticles were evaluated under an inert atmosphere using an FTIR spectrophotometer (Model: Prestige 22, Shimadzu, Japan) within the wave number range of 4000-400 cm^{-1} , using KBr pellets [15].

2.6. Analysis of aptamer and CD117 (c-KIT) interactions by molecular docking

For the molecular docking study, we selected CD117 (c-KIT), to which the aptamer can specifically bind *in silico*. The receptor's crystal structure (6GQJ) was retrieved from the RCSB (Research Collaboratory for Structural Bioinformatics) protein data bank (PDB) [16], and the DNA aptamer structure was created by adding the 79 base pair DNA sequence in Discovery Studio Visualizer 2021 and converting it to PDB format. The receptor was prepared by removing water molecules and adding polar hydrogen atoms and charges. The ligand molecule was also prepared for docking analysis using Discovery Studio Visualizer 2021. HDockLite blind docking software was used to examine interactions between the aptamer and tyrosine-protein kinase KIT protein [17]. The docking analysis and interactions were visualized through Biovia Discovery Studio 2021 (BIOVIA Discovery Studio - BIOVIA - Dassault Systèmes®, Vélizy-Villacoublay, France).

2.7. Aptamer conjugation on the surface of nanoparticles (Apt-CNP)

A 3' amino and phosphorothioate backbone-modified aptamer was conjugated onto clofarabine-containing PLGA nanoparticle formulation using the well-established EDC/NHS method [18]. The clofarabine nanoparticle (CNP) was dissolved in deionized water at 5 mg/ml and incubated with 200 mM EDC and 100 mM NHS for 30 min at 25 °C. Excess EDC/NHS was removed by rinsing with DNase-RNase-free water. The aptamer, at 2.50 μM , was denatured and renatured by heating at 85 °C for 10 min and cooling for 10 min. This aptamer was combined with the activated CNP and reacted under rotation for 6 h. To ensure the purity of the resulting aptamer-CNP bioconjugates, the product was thoroughly washed with deionized water, effectively removing any unbound aptamer or residual reactants. This conjugation process yielded a stable and functional aptamer-nanoparticle complex suitable for further characterization and application in targeted drug delivery systems.

2.8. Agarose gel electrophoresis

Agarose gel electrophoresis offers a quick qualitative assessment of aptamer conjugation by observing shifts of aptamer in gel [16, 19]. Compared to controls (non-conjugated nanoparticles and free aptamers), successful aptamer attachment to nanoparticles results in a shift. CNP conjugated with aptamer, aptamer non-conjugated nanoparticles and free aptamer were subjected to agarose gel electrophoresis. Samples included DNA ladder, Apt-CNP, free aptamer, and drug-loaded NP. The electrophoresis was run at 100V for 30 min with 0.5 mg/ml ethidium bromide to visualize base pairs (bp) on a 2 % agarose gel.

2.9. Drug loading and entrapment efficiency study

To evaluate % drug loading, 2 mg of the nanoformulation was mixed in 2 ml of acetonitrile and water (80:20) and incubated for 3–4 h in a shaker (Somax Incubator Shaker, China). Drug loading and entrapment efficiency were calculated as follows:

$$\text{Drug loading (Practical) (\%)} = \frac{\text{Quantity of drug present in nanoparticles} \times 100}{\text{Quantity of nanoparticles taken}}$$

$$\text{Entrapment efficiency (\%)} = \frac{\text{Practical drug loading} \times 100}{\text{Theoretical drug loading}}$$

2.10. Atomic force microscopy (AFM)

The atomic force microscopy (AFM) study provides detailed surface characterization at the nanometer scale. Samples were dissolved in Milli-Q water, vortexed, sonicated, cast on coverslips, and air-dried for 8 h. The transparent layer was visualized using AFM (5500 Agilent Technologies, USA) in tapping mode [20].

2.11. *In vitro drug release study*

In vitro drug release study indicates how drugs would be released from the particles in physiological conditions, providing a realistic assessment of how the drug-loaded nanoparticles could behave in the body [21]. The study was performed thrice using phosphate buffer saline (PBS) at pH 7.4 over 30 days. Accurately weighed nanoparticles were incubated in 2 ml PBS at $37^{\circ} \pm 0.5^{\circ}\text{C}$ in an incubator shaker. Pre-labeled samples taken at various intervals were centrifuged at 16,000 rpm for 30 min, and supernatants were analyzed at 263 nm [22] using UV-Vis spectroscopy.

The data from this study were plotted to test various kinetic models, namely, zero-order ($C = k_0t$), first-order ($\log C = \log C_0 - k_1t/2.303$), Higuchi ($Q = k\sqrt{t}$), and Korsmeyer-Peppas ($M_t/M_{\infty} = Kt^n$) [23]. The zero-order model indicates drug release independent of drug concentration, promoting slow release. The first-order model shows the release rate linearly related to the remaining drug concentration. The Higuchi model explains drug release regulated by diffusion from a drug matrix. The Korsmeyer-Peppas model's "n" values characterize the release mechanism: $n \leq 0.45$ (Fickian diffusion), $0.45 < n < 0.89$ (non-Fickian diffusion), $n = 0.89$ (case II transport), and $n > 0.89$ (super case II transport) [24].

2.12. *Particle size distribution and zeta potential*

Particle size distribution and zeta potential analyses are crucial for nanoparticle characterization, providing insights into their physical and chemical properties [13]. Uniform particle size ensures consistent performance and stability, especially in drug delivery. Zeta Potential measured surface charge, indicating electrostatic repulsion between particles in their suspension. The average particle size and zeta potential of CNP and Apt-CNP were evaluated using a Malvern Zetasizer Nano-ZS 90 (Malvern Instruments, UK). Samples were dispersed in Milli-Q water, vortexed, and sonicated before analysis.

2.13. *Field emissions scanning electron microscopy (FESEM)*

Particle morphology was examined using a field emission scanning electron microscope, which offers ultra-high-resolution imaging in the nanometer range. This enables precise examination of surface morphology, particle size, shape, and distribution [25]. FESEM's lower accelerating voltages minimize the risk of damaging delicate nanoparticles, making it ideal for imaging soft materials and biological samples without compromising their integrity. The nanoformulation was deposited on carbon tape on a stub, coated with a 5 nm layer of platinum using a platinum coater, and visualized under a field emission scanning electron microscope (FESEM, JEOL JSM-7600F, Japan).

2.13.1. *Stability study of the nanoparticles*

In this study, we proceeded stability with the Apt-CNP only, as this was the formulation of our experimental interest. We have evaluated the particle surface morphology using FESEM of the Apt-CNP nanoformulation after storage at $4-8^{\circ}\text{C}$ in a refrigerator, and at 30°C with 75 % relative humidity (RH) and at 40°C with 75 % RH for 45 days, by particle size analysis for the samples stored at 30°C and 40°C , and FESEM analysis for all the three samples. Drug loading was also checked.

2.14. *High-resolution Transmission electron microscopy (HR-TEM)*

HR-TEM is an advanced imaging technique enables detailed visualization of the nanoparticle structure, providing critical perceptions into the internal morphology, surface characteristics, and the distribution of the encapsulated drug within the polymeric matrix. The HR-TEM analysis facilitated a deeper understanding of the structural integrity and homogeneity of the nanoparticle formulations, which are essential for evaluating their suitability for targeted drug delivery applications. HR-TEM was used to analyze internal morphology and drug distribution within the particles. Nanoparticles were suspended in Milli-Q water, dropped on a copper grid (300 mesh), and air-dried for 12 h. Samples were analyzed using HR-TEM (JEOL JEM 2100 HR, Tokyo, Japan) [15].

2.15. *In vitro Cell cytotoxicity assay*

AML cells, HL-60, were cultured under controlled conditions to maintain optimal growth and experimental reproducibility. The cells were supplemented with 10 % fetal bovine serum (FBS), 50 $\mu\text{g}/\text{ml}$ streptomycin, and 50 IU/ml penicillin G in RPMI 1640 medium at 37°C in a humidified incubator with a 5 % CO_2 atmosphere. Subculturing was performed every 72 h to ensure continuous exponential growth and cell viability. Similarly, Peripheral Blood Mononuclear Cells (PBMC) (PBMC were isolated from anticoagulated blood from human volunteers) and U937 cells were treated and analyzed under identical conditions in RPMI 1640. PBMC were isolated from anticoagulated blood. An equal volume of Ficoll-Hypaque was mixed with the anticoagulated blood and centrifuged at $400\times g$ for 30 min [16]. The PBMCs were carefully collected from the interface between the two liquid layers, washed with PBS, and then resuspended in RPMI 1640 medium. Approximately $1.0-1.20 \times 10^4$ cells were cultured in 96-well plates with 100 μl RPMI 1640 media and incubated for 48 h with each formulation. After treatment, 20 μl MTT solution (5 mg/ml in PBS) was added and incubated for 4 h. Formazan crystals were dissolved in 100 μl DMSO, and optical densities were measured at 540 nm using an ELISA reader (Bio-Rad, CA, USA).

$$\text{Mean percentage viability} = \frac{\text{Mean specific absorbance of treated cells} \times 100}{\text{Mean specific absorbance of untreated cells}}$$

IC₅₀ values were determined using OriginPro software, with experiments conducted in triplicate [15,26].

2.16. *In vitro* cellular uptake study

Cells were cultured under controlled conditions to maintain optimal growth and experimental reproducibility. This study provided the cellular uptake of drug-loaded nanoparticles (CNP) and aptamer-conjugated nanoparticles (Apt-CNP) by HL-60/U937 cells to evaluate the potential of targeted drug delivery. Since the formulations did not show cytotoxicity in PBMC in the experimental concentration range, the cell type was not considered for further study. Using flow cytometry, the internalization of fluorescent FITC-labeled nanoparticles was quantified. HL-60 cells treated with CNP and Apt-CNP were incubated for 12 and 24 h, collected by centrifugation, washed with ice-cold PBS, resuspended in PBS, and analyzed by a flow cytometer to measure nanoparticle uptake. U937 cells were cultured under the same conditions as HL-60 cells and treated with fluorescently labeled CNP and Apt-CNP for 24 h. After incubation, the cells were collected by centrifugation, washed with ice-cold PBS, resuspended in PBS, and analyzed by flow cytometry to evaluate nanoparticle uptake. The uptake results for U937 cells were used to compare the internalization efficiency between the two cell lines. Flow cytometry allows precise quantification of cellular internalization, providing crucial insights into the efficacy of targeted drug delivery [15,16,27].

2.17. Cellular apoptosis assay

The Annexin V FITC detects and quantifies apoptosis by tracking phosphatidylserine (PS) movement to the outer plasma membrane. Annexin V binds to PS and is labeled with FITC for fluorescence detection. HL60 cells (2.8×10^5 /ml) were treated with IC₅₀ concentrations of the free drug, CNP, and Apt-CNP for 24 h at 37 °C. Post-treatment, cells were centrifuged, counted to 10^5 in 100 µl of binding buffer, and incubated with 5 µl of Annexin V-FITC for 15 min in the dark. Cells were then diluted to 500 µl, 5 µl of propidium iodide was added, and they were analyzed using the FACS instrument with FITC (B530-A) and propidium iodide (YG586-A) channels. Similarly, U937 cells were treated and analyzed under identical conditions in RPMI 1640 to compare apoptosis induction between two cell lines. The data were presented in a four-quadrant plot to distinguish between live, early apoptotic, late apoptotic, and dead cells [28,29].

2.18. Mitochondrial membrane depolarization study by JC-1

Investigating mitochondrial membrane depolarization using JC-1 dye assesses changes in mitochondrial membrane potential [30]. JC-1 dye accumulates in mitochondria and exhibits potential-dependent fluorescence red at high membrane potential (J aggregates form) and green at low membrane potential (for monomers). During apoptosis, the mitochondrial membrane potential decreases, shifting from red to green fluorescence, indicating depolarization.

Apt-CNP was observed most effective in HL60 cells. Hence, HL60 cells were selected only for this investigation. HL60 cells (2.8×10^5 /ml) were treated with IC₅₀ concentrations of the free drug, CNP, and Apt-CNP for 24 h at 37 °C. After treatment, cells were washed with ice-cold PBS, incubated with JC-1 for 20 min, collected by centrifugation, and analyzed using FACS Diva software [16,31].

2.18.1. Statistical analysis

All the experiments were conducted in triplicate, and the data were presented as mean values with standard deviations. Statistical analysis was performed using one-way ANOVA and Student's t-test. Graphs and images were created using software tools like Origin 2021 and BIOVIA Discovery Studio Visualizer (BIOVIA—Dassault Systèmes®, Vélizy-Villacoublay, France). The graphical abstract was designed using [Biorender.com](https://www.biorender.com).

3. Results

3.1. Drug-excipients interaction study by FTIR

FTIR studies were conducted to identify potential chemical interactions between the drug clofarabine and the excipients (PVA, PLGA) (Supplementary file: [Figure S1 A](#)). The analysis revealed distinct absorption peaks for PLGA at 3650 cm⁻¹ (O–H stretching), 2935 cm⁻¹ (asymmetric stretching of –CH₂), and 1735 cm⁻¹ (C=O stretching of the carboxylic acid group). Pure clofarabine exhibited peaks at 3466.08 cm⁻¹ (O–H stretching), 3113.19 cm⁻¹ (N–H stretching), 1624.06 cm⁻¹ (C=C stretching), 1581.62 cm⁻¹ (C=N stretching), 1066.35 cm⁻¹ (C–O stretching), 1244.08 cm⁻¹ (C–N stretching), and 704.01 cm⁻¹ (C–Cl stretching). The FTIR spectra of drug-loaded nanoparticles (CNP) and drug-loaded aptamer-conjugated nanoparticles (Apt-CNP) showed the characteristic peaks of clofarabine, indicating that the drug's chemical structure remained intact within these formulations. Additionally, new peaks corresponding to the constituting polymers were observed in the spectra of these nanoformulations, confirming their presence. Notably, the Apt-CNP exhibited a peak at 1635 cm⁻¹, signifying the binding of the aptamer to the nanoparticle surface through amide bond formation.

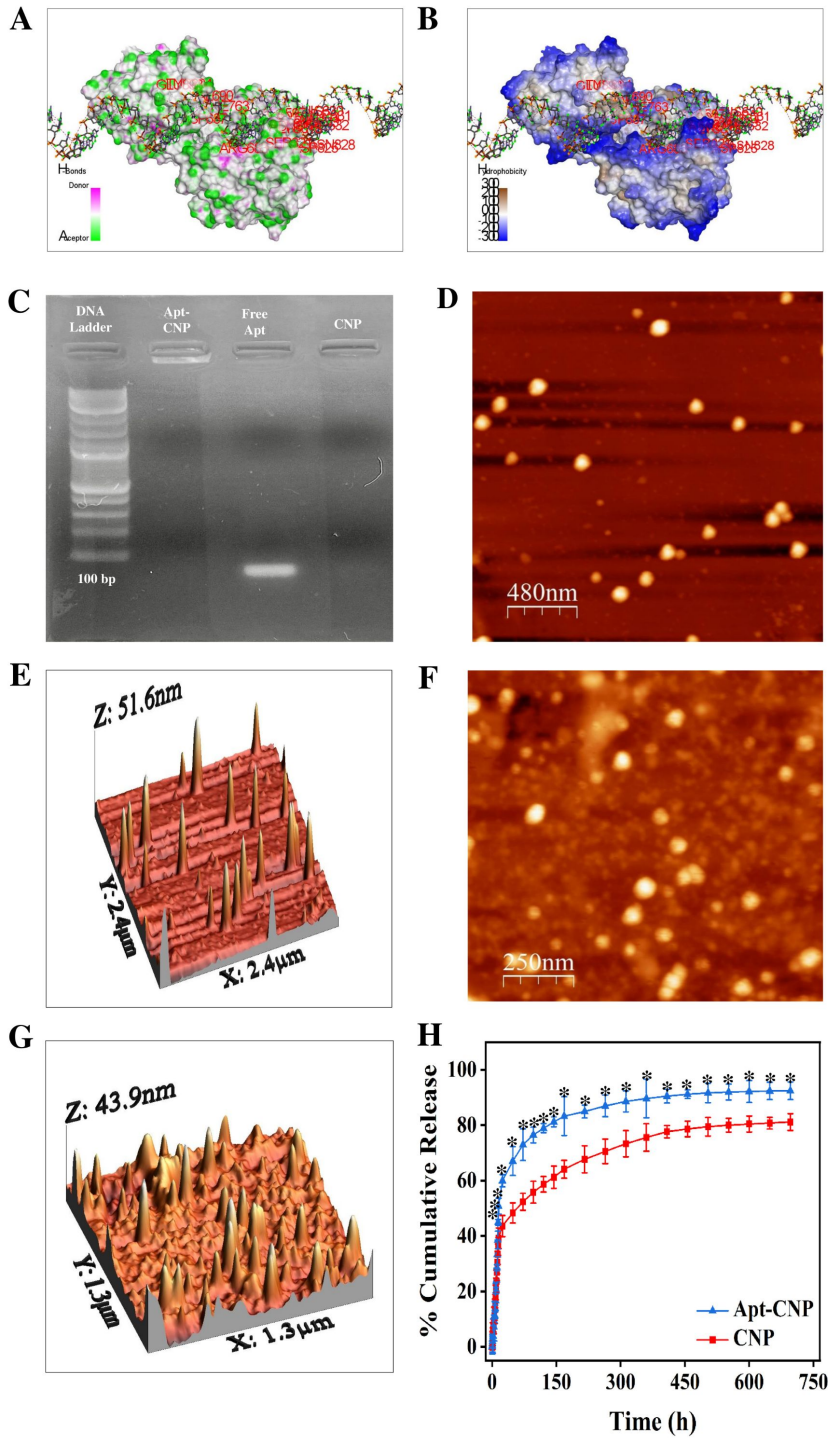


Fig. 1. Aptamer-tyrosine-protein kinase KIT, CD117 interactions by molecular docking, Aptamer conjugation with nanoparticles, In vitro drug release study, Atomic force microscopic evaluation of CNP and Apt-CNP (A) Aptamer-CD117 receptor interactions by hydrogen bonding through in silico molecular docking (B) Aptamer-CD117 receptor hydrophobic interactions through in silico molecular docking (C) Agarose gel electrophoresis confirming the conjugation of aptamer to the drug-loaded nanoparticle. (D), (E) AFM image of CNP. (F), (G) AFM image of Apt-CNP. (H) In vitro drug release of Apt-CNP and CNP. (data show mean \pm SD, n = 3; * indicates p < 0.05 when compared with CNP treated group).

3.2. Analysis of aptamer-CD117 (c-KIT) interactions by molecular docking

A molecular docking study was conducted to assess the affinity and interactions between the 79 bp DNA aptamer and CD117 (c-KIT) protein. The results indicate that the nucleotide bases of the aptamer effectively bond with various amino acid residues (Fig. 1A and Fig. 1B). Various types of interactions (Table 1), including electrostatic, hydrophobic, and hydrogen bonding, were observed between different nucleotide bases of the DNA aptamer and different residue numbers such as guanine (DG 38), guanine (DG 39), guanine (DG 40), guanine (DG 41), guanine (DG 42), guanine (DG 43), adenine (DA 46), adenine (DA 47), cytosine (DC 48), guanine (DG 49), guanine (DG 50), guanine (DG 51), guanine (DG 57), guanine (DG 58), thymine (DT 59), and thymine (DT 60). These interactions occurred with various amino acid residues of the receptor protein, such as threonine (THR 594), leucine (LEU 595), glycine (GLY 596), alanine (ALA 597), glycine (GLY 598), alanine (ALA 599), lysine (LYS 626), histidine (HIS 630), serine (SER 631), threonine (THR 632), glutamic acid (GLU 633), arginine (ARG 634), asparagine (ASN 680), arginine (ARG 683), aspartic acid (ASP 816), lysine (LYS 818), asparagine (ASN 819), aspartic acid (ASP 820), serine (SER 821), aspartic acid (ASP 825), glycine (GLY 827), asparagine (ASN 828), alanine (ALA 829), arginine (ARG 686), aspartic acid (ASP 687), glutamic acid (GLU 688), phenylalanine (PHE 689), valine (VAL 690), proline (PRO 691), phenylalanine (PHE 763), glutamic acid (GLU 893), and tyrosine (TYR 894). The docking score revealed a value of -250.95 , suggesting a strong binding affinity between the ligand and receptor.

3.3. Attachment of aptamer to the surface of nanoparticles

An agarose gel electrophoresis verified the attachment of CD-117 specific DNA aptamer to the nanoparticle surface. Fig. 1C shows that the 79-base pair aptamer migrated through the gel, aligning with the 100-bp marker on the conventional DNA ladder. In contrast, Apt-CNP remained in the loading well, as indicated by fluorescence. Notably, the unconjugated nanoparticles (CNP) did not produce any significant band in the well due to the absence of aptamer. For Apt-CNP, the image confirmed successful aptamer conjugation on the nanoparticle surface (Apt-CNP), supported by the earlier FTIR data, too.

3.4. Percentage of encapsulation efficiency and average drug loading of the formulation

The average drug loading of the CNP formulation was $23.63 \pm 0.593\%$, with an encapsulation efficiency of 70.92% . The Apt-CNP mean drug loading was $21.78 \pm 0.482\%$, and the encapsulation efficiency was 69.86% . Upon storing the formulations, Apt-CNP, at $4-8\text{ }^{\circ}\text{C}$ in a refrigerator, and at $30\text{ }^{\circ}\text{C}$ and $40\text{ }^{\circ}\text{C}$ with 75% relative humidity (RH) for 45 days did not vary drug loading significantly. Apt-CNP had drug loading $22.99 \pm 0.671\%$ in the refrigerated condition, and the values of $21.27 \pm 0.358\%$ and $20.96 \pm 0.432\%$ at $30\text{ }^{\circ}\text{C}$ and $40\text{ }^{\circ}\text{C}$, respectively.

3.5. Atomic force microscopy (AFM)

We observed the atomic force microscopy imaging of CNP (Fig. 1D and Fig. 1E) and Apt-CNP (Fig. 1F and Fig. 1G). AFM images were acquired in both flattened topography and three-dimensional modes. The AFM data revealed that the conjugated nanoparticles maintained a spherical shape with a smooth surface.

3.6. In vitro drug release study

In vitro clofarabine release from CNP and Apt-CNP was conducted using phosphate buffer saline (PBS, pH 7.4) as it closely mimics the pH of human blood and extracellular fluid, facilitating a relevant environment to those in the human body [21]. The cumulative percentages of drug release for CNP and Apt-CNP were found to be 81.15 ± 3.036 and 92.45 ± 3.208 , respectively, in 680 h of the study (Fig. 1H). The drug release data from the nanoparticles were evaluated using various kinetic models, including zero-order, first-order, Higuchi, and Korsmeyer–Peppas [32]. The regression coefficient (R^2) for each model and release exponent (n) values for the Korsmeyer–Peppas model were tabulated. The R^2 values (Table 2) indicate that drug release adhered to the Korsmeyer–Peppas model in the case of both formulations. In addition, the n -values suggested that the drug release followed the Fickian mechanism.

3.7. Measurement of particle size distribution and zeta potential and stability data of the nanoparticles

The zeta potential and particle size distribution were assessed using the dynamic light scattering method. The average hydrodynamic radius (dH) values for CNP and Apt-CNP were 154.7 nm and 175.2 nm , respectively (Fig. 2A). However, the aptamer conjugation resulted in an approximate 20% increase in the size of the APT-CNP. The zeta potential values for CNP and Apt-CNP were -10.9 mV and -15.9 mV , respectively (Fig. 2B and Fig. 2C).

In this study, we proceeded with Apt-CNP only as it is the formulation of experimental interest and there has been no significant morphological change between the two formulations at $4-8\text{ }^{\circ}\text{C}$ (Supplementary file: Figure S1 B). The formulations (Apt-CNP) stored at $30\text{ }^{\circ}\text{C}$ and $40\text{ }^{\circ}\text{C}$ with 75% relative humidity (RH) (Fig. 2D and Fig. 2E) for 45 days exhibited enhancement of dH, and it might be due to particle agglomeration and deformation.

Table 1
Aptamer-CD117 (c-KIT) binding using molecular docking technique.

Name of the receptor	Protein Data Bank (PDB) code	DNA aptamer sequence	Docking score	Interacting residues	Interaction type
CD117 receptor, tyrosine-protein kinase KIT	6GQJ	5'-GAGGCATACC AGCTTATTATTGGGGCCGGGGCAAGGGGGGGGTACCGTGGTAGGACAGATAGTAAGTGC AATCTGCCGAA-3'	-250.95	THR 594, LEU 595, GLY 596, ALA 597, GLY 598, ALA 599, LYS 626, HIS 630, SER 631, THR 632, GLU 633, ARG 634, ASN 680, ARG 683, ASP 816, LYS 818, ASN 819, ASP 820, SER 821, ASP 825, GLY 827, ASN 828, ALA 829, ARG 686, ASP 687, GLU 688, PHE 689, VAL 690, PRO 691, PHE 763, GLU 893 and TYR 894.	electrostatic, hydrophobic interactions, hydrogen bonding

Table 2
Regression coefficient (R^2) values of in vitro drug release data employed in various kinetic models.

Kinetic Models	Formulations	
	CNP	Apt-CNP
Zero Order	$R^2 = 0.8594$	$R^2 = 0.7309$
First Order	$R^2 = 0.9309$	$R^2 = 0.8901$
Higuchi Model	$R^2 = 0.9554$	$R^2 = 0.8668$
Korsmeyer-Peppas Model	$R^2 = 0.9899$	$R^2 = 0.9576$
	$n = 0.2$	$n = 0.12$

R^2 = regression coefficient and n = release exponent (slope of Korsmeyer-Peppas).

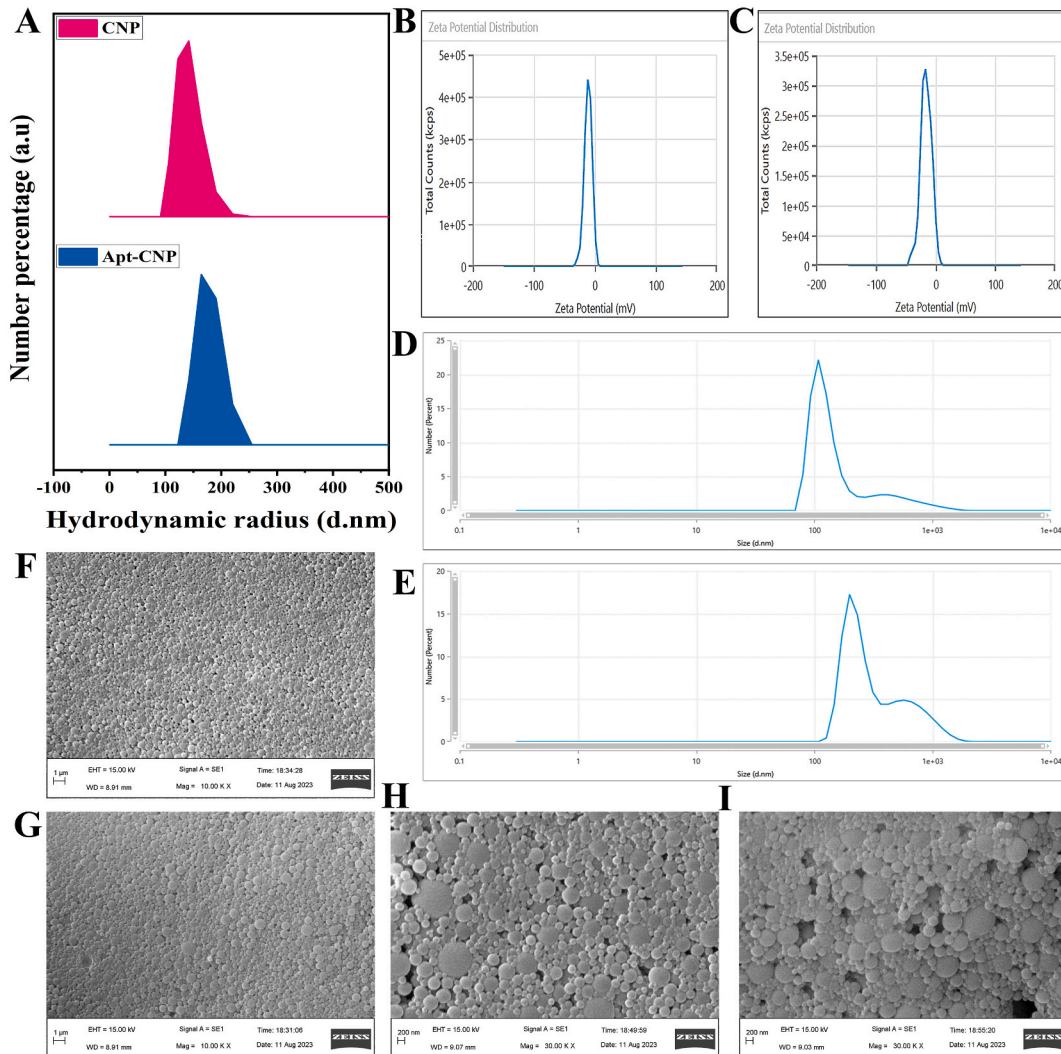


Fig. 2. Particle size and zeta potential of CNP and Apt-CNP, respectively, and stability-related particle size data of Apt-CNP stored at 30 °C and 40 °C with 75 % RH for 45 days, Electron microscopic imaging (FESEM) of CNP and Apt-CNP, Stability related FESEM of Apt-CNP stored at 30 °C with 75 % RH for 45 days. (A) Particle size of CNP and Apt-CNP. (B), (C) Zeta potential values of CNP and Apt-CNP, respectively. (D) Particle size distribution of Apt-CNP at 30 °C with 75 % RH for 45 days. (E) Particle size distribution of Apt-CNP at 40 °C with 75 % RH for 45 days. (F) FESEM image of freshly prepared CNP. (G) FESEM image of freshly prepared Apt-CNP. (H) FESEM image of Apt-CNP stored at 30 °C with 75 % RH for 45 days. (I) FESEM image of Apt-CNP stored at 40 °C with 75 % RH for 45 days.

3.8. Surface morphology of nanoparticle by field emissions scanning electron microscopy (FESEM)

FESEM analysis of the CNP and Apt-CNP nanoparticles demonstrated that both formulations exhibited smooth, spherical surfaces and closely distributed, with a mean hydrodynamic diameter of 100–250 nm, respectively (Fig. 2F and Fig. 2G). Aptamer-conjugation enhanced the size of the particles.

CNP and Apt-CNP stored at 30 °C and 40 °C with 75 % relative humidity (RH) for 45 days exhibited morphological changes with deformation and nanoparticle aggregation that might be due to polymer softening (Fig. 2H and Fig. 2I).

3.9. Internal morphology by transmission electron microscopy (HR-TEM)

We have studied the internal morphology of both CNP and Apt-CNP formulations through HR-TEM. Both the formulations revealed dark, spherical nanoparticles with a homogeneous internal structure (Supplementary file: Fig. S1 C and D), suggesting a homogenous distribution of the drug in the matrix.

3.10. Apt-CNP had variable IC₅₀ values in HL60 and U937 cells, and non-toxic to Peripheral Blood Mononuclear Cells (PBMC)

The cell viability percentage of HL60 cells treated with clofarabine and experimental nanoparticles was evaluated using an MTT assay. Apt-CNP showed the highest toxicity to the HL60 cells (Fig. 3A) with the lowest IC₅₀ value. The IC₅₀ value of clofarabine was found to be 2.14 μM. The values were predominantly reduced in the nanoformulations, CNP, and Apt-CNP. The values were 1.30 μM and 1.07 μM in HL60 cells, respectively, upon CNP and Apt-CNP treatments. In U937 cells, the IC₅₀ values for clofarabine, CNP, and Apt-CNP were 2.31 μM, 1.81 μM, and 1.77 μM, respectively (Fig. 3B). When compared with HL60 cells, a similar trend is expected, but the extent of improvement with Apt-CNP may depend on the CD117 expression levels. The lack of significant enhancement in cytotoxicity with Apt-CNP compared to CNP suggests that the aptamer does not provide a targeting advantage in U937 cells, likely due to

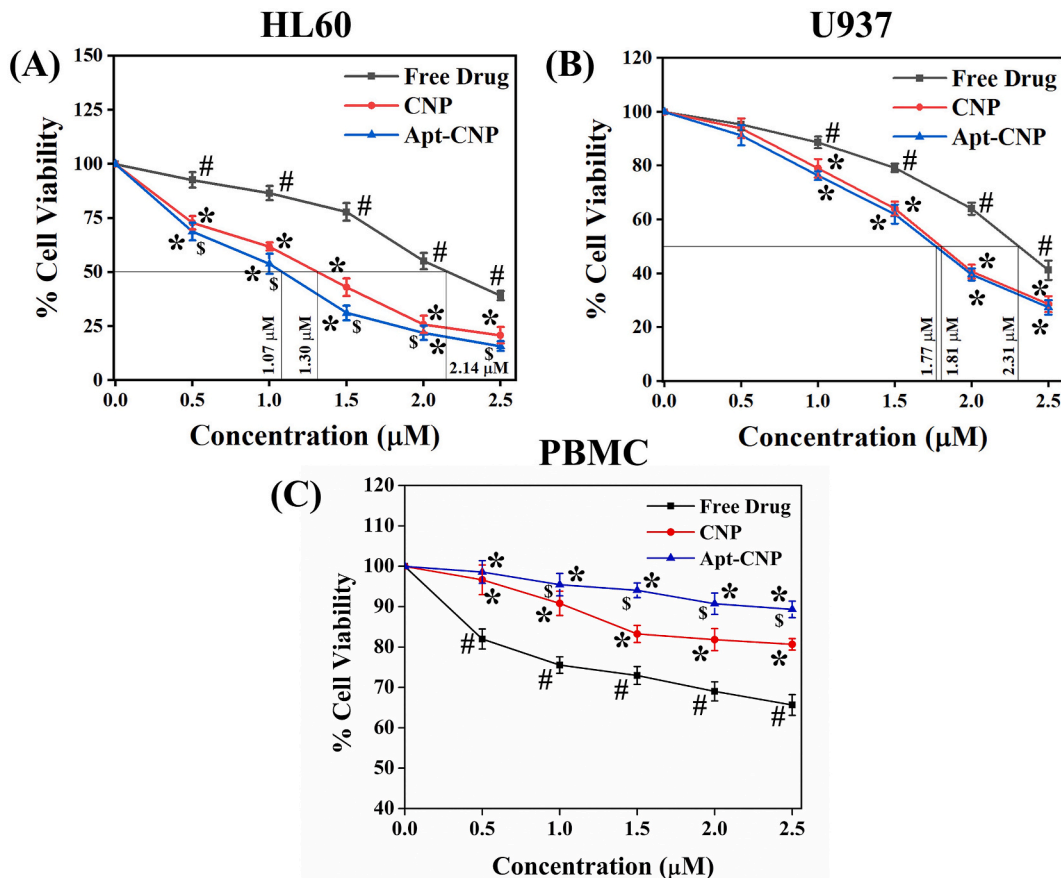


Fig. 3. In vitro cell cytotoxicity assay of the experimental nanoformulations on HL60 cells, U937 cells, and Peripheral Blood Mononuclear Cells (PBMC). (A) MTT assay data of the experimental nanoparticles on HL60 cells. (B) MTT assay data of the experimental nanoparticles on U937 cells. (C) MTT assay data of the experimental nanoparticles on PBMC cells (data show mean ± SD, n = 3; * indicates p < 0.05 when compared with the free drug-treated group, \$ indicates p < 0.05 when compared with the CNP-treated group).

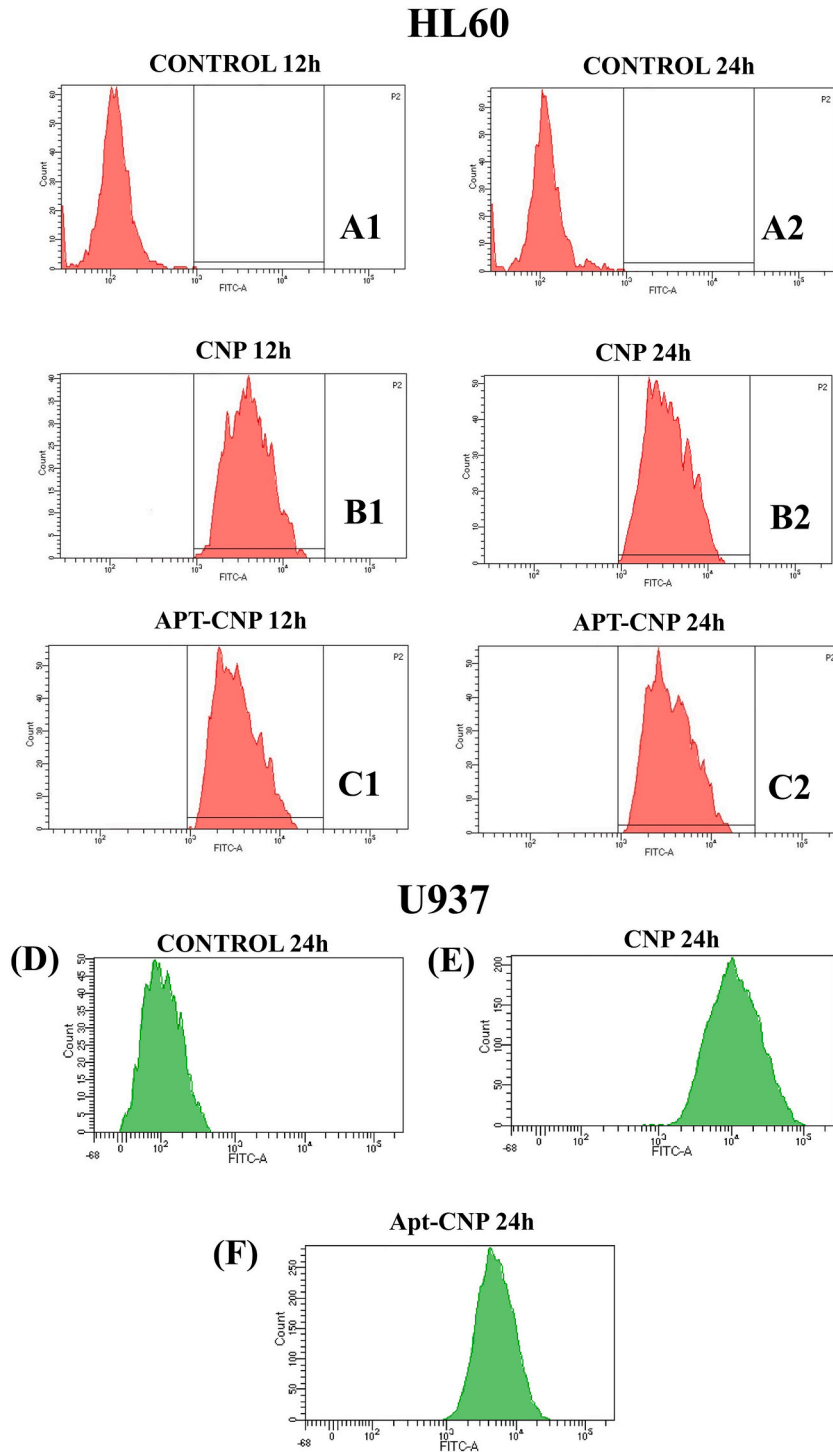


Fig. 4. In vitro HL60/U937 cellular uptake of the experimental formulations. **A1** and **A2** represent untreated control HL60 cells for 12 and 24 h, respectively. **B1** and **B2** represent CNP data for 12 and 24-h treatment, respectively. **C1** and **C2** represent data of Apt-CNP treatment for 12 and 24 h, respectively. **D** U937 control cells without treatment at 24 h. **E** U937 cells received CNP treatment for 24 h. **F** U937 cells received Apt-CNP treatment for 24 h.

the absence of the specific biomarker (CD117). In contrast, the cell viability assay conducted on normal cells (Peripheral Blood Mononuclear Cells, PBMC) did not yield IC₅₀ values (Fig. 3C) for any of the formulations, suggesting minimal cytotoxicity and indicating a favorable safety profile of the formulations in non-cancerous cells.

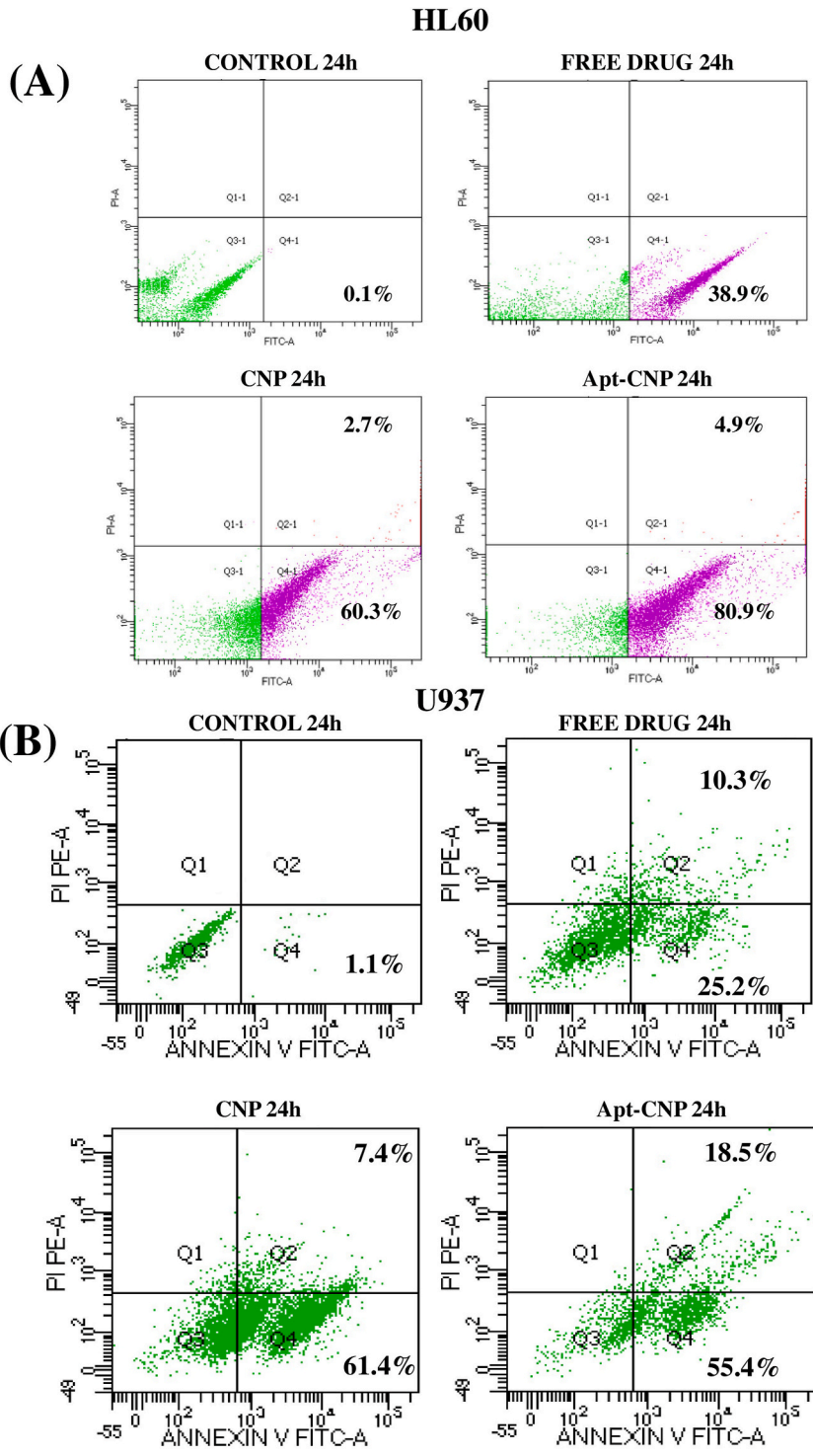


Fig. 5. Cellular apoptosis and cellular internalization of the experimental treatments on HL 60/U937 cells using flow cytometer. (A) In vitro cellular apoptosis study through Annexin V-FITC/PI on HL60 cells. (B) In vitro cellular apoptosis study through Annexin V-FITC/PI on U937 cells.

3.11. FITC-Apt-CNP showed maximum cellular internalization in vitro among the treatment groups

In vitro cellular uptake studies were conducted using flow cytometry to assess the internalization efficiency of FITC-labeled nanoformulations, CNP, and Apt-CNP in HL60 and U937 cells. HL60 is a human promyelocytic leukemia cell line extensively used in biomedical research, especially in studying hematopoiesis, myeloid leukemia, and cell differentiation [30]. These cells are known for their rapid proliferation in suspension culture. This rapid proliferation rate makes them an essential model for exploring the mechanisms of differentiation, apoptosis, drug resistance, and targeted drug delivery in leukemia research. U937, derived from human histiocytic lymphoma, is a widely recognized leukemia and monocytic differentiation study model [33]. Following treatment of HL60 cells with FITC-labeled CNP and Apt-CNP for 12 and 24 h, a significant enhancement in cellular uptake was observed with Apt-CNP compared to CNP. The analysis showed a substantial increase in cellular uptake for Apt-CNP formulations compared to nontreated control cells (Fig. 4 A1 and Fig. 4A2). The uptake of CNP reached 73.2 % (Fig. 4 B1), while Apt-CNP exhibited cellular uptake of 90.6 % (Fig. 4 C1) for 12 h. Again, in the case of 24 h, the uptake of CNP showed 82.9 % (Fig. 4B2), while Apt-CNP showed 95.6 % (Fig. 4C2). This marked increase in uptake for Apt-CNP compared to CNP highlights the significant role of the aptamer in enhancing the internalization of the nanoformulation in HL60 cells. Conversely, analysis in U937 cells showed 88.4 % uptake for CNP and 86.2 % for Apt-CNP (Fig. 4, D-F) after 24 h (though the difference of the data values were statistically non-significant) (Supplementary file: Fig. S2), indicating nonspecific uptake due to the absence of CD117 overexpression.

3.12. Apt-CNP treatment showed maximum cellular apoptosis in HL60 cells

The cellular apoptosis assay was performed using the Annexin V-FITC/PI dual staining method to evaluate the apoptosis-inducing potential of the free drug, CNP, and Apt-CNP in HL60 and U937 cells. After 24 h of treatment with free drug, CNP, and Apt-CNP, the early apoptotic populations in HL60 cells were 38.9 % early for free drug, 60.3 % for CNP, and 80.9 % for Apt-CNP. The late apoptosis in the Apt-CNP case was 4.4 %, the maximum among the treated groups (Fig. 5A). The results demonstrated a significant enhancement

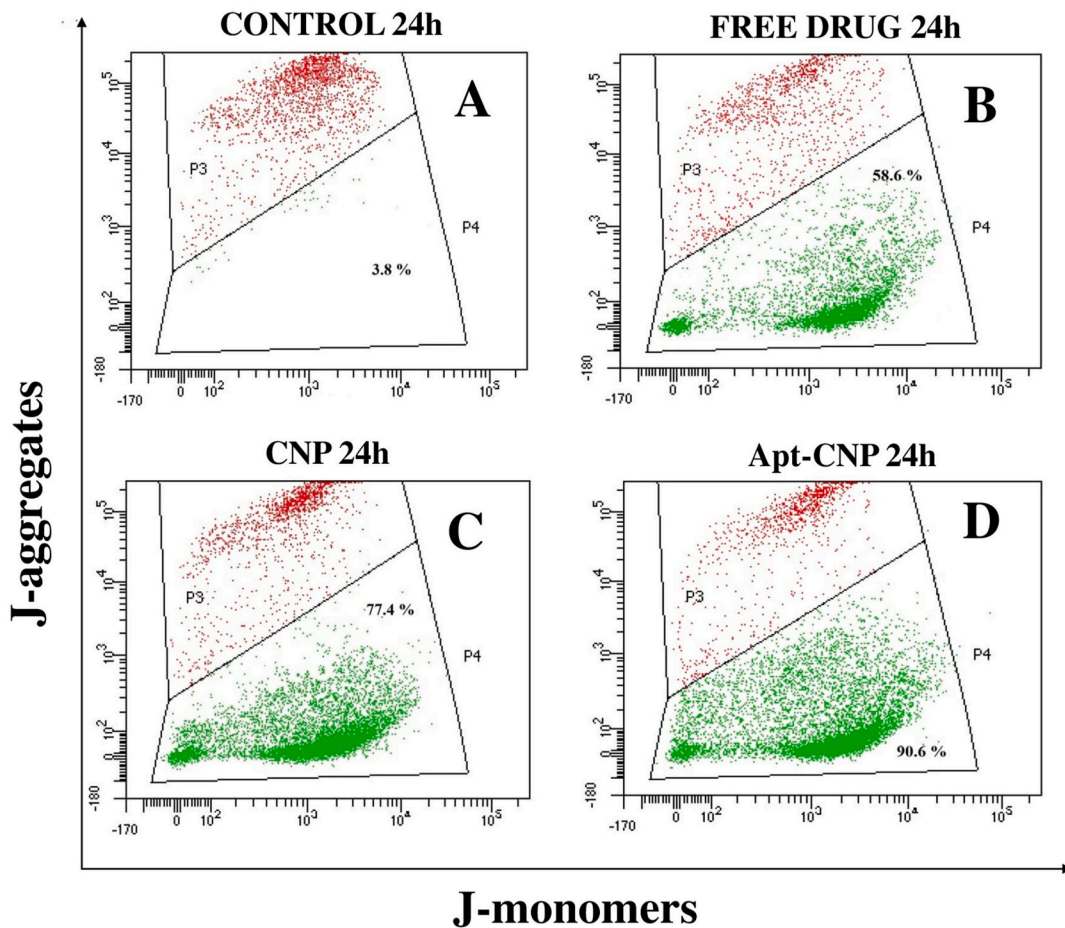


Fig. 6. Cellular mitochondrial membrane depolarization of HL60 cells, receiving experimental treatments using a flow cytometer. A Control B Free drug treatment for 24 h C CNP treatment for 24 h D Apt-CNP treatment for 24 h.

in apoptosis induction by Apt-CNP, highlighting its potential as an effective chemotherapeutic agent in HL60 cells. In contrast, U937 cells showed early and late apoptotic populations of 25.2 % and 10.3 % for the free drug, 61.4 % and 7.4 % for CNP, and 55.4 % and 18.5 % for Apt-CNP (Fig. 5B). Similar trends were expected, but the extent of apoptosis may vary depending on CD117 expression. These findings underscore the ability of Apt-CNP to selectively and efficiently induce apoptosis in CD117-positive leukemia cells (HL60), while minimizing off-target effects in non-target cells (U937), making it a promising candidate for targeted AML therapy.

3.13. Apt-CNP treatment predominantly enhanced mitochondrial membrane depolarization

Apt-CNP was found to be predominantly effective in HL60 cells compared to U937 cells. Hence, we have investigated effect of Apt-CNP on mitochondrial membrane polarization only in HL60 cells. The percentages of JC-1 monomer, which emitted green fluorescence, were 58.6 % for clofarabine, 77.4 % in the case of CNP, and 90.6 % for Apt-CNP after 24 h of treatment in HL60 cells (Fig. 6, A-D). The depolarized mitochondrial cell population predominantly increased for cells receiving Apt-CNP, clearly denoting its potency in higher apoptosis in HL60 cells. The data also correlate well with the cellular apoptosis data.

4. Discussion

We chose a biocompatible, biodegradable, US-FDA-approved polymer (PLGA) and a non-toxic, minimally immunogenic short nucleotide DNA aptamer [12,13]. This strategy aimed to ensure effective targeted drug delivery in vitro while reducing cytotoxicity to normal healthy cells due to less or no uptake of the targeted formulation. The approach focused on preferential accumulation of Apt-CNP in CD117 overexpressed AML cancer cells. HL60 cells were specifically chosen for this study due to their well-established use as a model for acute myeloid leukemia, providing a relevant and reliable system to assess the efficacy of the targeted delivery approach [26]. CD117 is overexpressed by about 70 % of AML varieties. They include HL60 cells. It is expressed in some normal cells too, although not overexpressed. Here, since a majority of AML variety overexpresses CD117, we have selected the protein as a target. Upon success of the formulation, this can work on the AML varieties those overexpress CD117. Secondly, this can be useful for targeting other expressed proteins on AML, by changing the protein specific aptamer.

Fourier-transform infrared (FTIR) spectroscopy was employed to investigate potential chemical interactions between the drug and the excipients [15], and the results indicate that no significant chemical interactions occurred between clofarabine and the excipients, ensuring the drug's stability and integrity within the nanoparticles. The stretching frequencies of the various functional groups of clofarabine-loaded nanoparticles (CNP) and aptamer-conjugated clofarabine-loaded nanoparticles (Apt-CNP) revealed the existence of the characteristic peaks of clofarabine, indicating that the drug's chemical structure remained unaltered in these formulations. Additionally, the spectra of these nanoformulations displayed drug peaks with the polymers, confirming drug incorporation. A peak at 1635 cm^{-1} in the Apt-CNP formulation signified the aptamer's attachment to the nanoparticle surface via amide bond formation. Therefore, the excipients used in the formulations are chemically compatible with the drug, making them suitable for drug delivery systems. The aptamer binding peak in Apt-CNP further validates the successful conjugation of the aptamer to the nanoparticles, which is crucial for targeted drug delivery applications.

The molecular docking study assessed the affinity and interactions between the DNA aptamer and CD117 (c-KIT), providing valuable insights into the binding dynamics and specificity of the aptamer. The findings indicate that the nucleotide bases of the aptamer formed strong bonds with various amino acid residues of the CD117 receptor. These interactions encompassed electrostatic, hydrophobic, and weak hydrogen bonding, underscoring the complexity and robustness of the binding mechanism. The amino acid residues involved in these interactions were not limited to the receptor's binding pocket but extended to other significant regions of the receptor, indicating a broad range of contact points between the aptamer and CD117. This extensive interaction network contributes to the aptamer's high binding affinity, as evidenced by the docking score of -250.95 . Such a robust binding score suggests a highly stable complex, confirming the aptamer's potential for selective binding to the CD117 biomarker on AML cells (HL60). The selective binding of aptamer-conjugated nanoparticles to the CD117 receptor implies that these nanoparticles can effectively target AML cells, ensuring that the drug molecules are delivered directly to the cancer cells. This targeted delivery mechanism increases the drug concentration at the intended site and minimizes off-target effects, thereby enhancing the therapeutic index and reducing potential side effects [16].

Agarose gel electrophoresis was utilized to verify the attachment of the CD117-specific DNA aptamer to the nanoparticle surface. This method has confirmed the successful conjugation of the aptamer to nanoparticles [13]. The fluorescence observed in the Apt-CNP loading well confirms the DNA aptamer's presence on the heavier nanoparticle surface compared to the free aptamer. This finding is further supported by Fourier-transform infrared spectroscopy (FTIR) data, which provides additional evidence of the chemical bonds formed between the aptamer and the nanoparticles.

The average drug loading and percentage encapsulation efficiency results indicate that both formulations achieved substantial drug loading and good encapsulation efficiency, demonstrating their effectiveness in delivering the drug [21].

We have performed the in vitro drug release study of CNP and Apt-CNP using phosphate-buffered saline (PBS), pH 7.4, as a drug release medium. This setup ensures a relevant environment for studying the release of the drug in vitro under conditions similar to those in the human body [34]. Over 680 h, the cumulative drug release percentage from Apt-CNP was higher than that of CNP. Both the nanoparticles showed initial drug release followed by sustained drug release. Drug molecules near the surface might release the drug quicker initially, followed by sustained drug release from the core of the particles. The presence of aptamers on the surface of PLGA nanoparticles might reduce the binding affinity between the drug and the polymer matrix, facilitating comparatively faster drug diffusion out of the nanoparticles.

The FESEM analysis of CNP and Apt-CNP revealed that both types of nanoparticles displayed spherical and smooth surface

morphologies. The smooth surface appearance suggests that the synthesis and surface modification processes did not cause significant surface roughness or irregularities, which is often crucial for enhancing biocompatibility and reducing nonspecific interactions in biological environments [24]. The HR-TEM images demonstrated that the drug is present within the nanoparticles, confirming the uniformity of the internal morphology. The three-dimensional AFM images showed that the nanoparticles were well-separated and within a range of narrow size distribution. Additionally, these images confirmed the absence of pinholes on the nanoparticles.

The dynamic light scattering (DLS) technique was utilized to evaluate both the zeta potential and the particle size distribution of the nanoparticles. Analysis revealed an approximately 20 % size increase for aptamer-conjugated nanoparticles.

The zeta potential values provide insight into the stability of the nanoparticle suspensions. The negative values obtained suggest that both nanoparticle types possessed a moderate electrostatic repulsion that maintained their suspension in aqueous solutions over an extended period. As reported earlier, zeta potential values greater than ± 30 mV are typically associated with highly stable suspensions due to stronger electrostatic repulsion [35]. Consequently, to ensure optimal stability and prevent aggregation, the nanoparticles should be stored in powder form at 2–8 °C (refrigerated condition) and suspended in water before injection.

The stability study of CNP and Apt-CNP revealed that samples stored at 4–8 °C retained their morphology and drug content consistently throughout the study. Conversely, samples stored at 30 °C with 75 % relative humidity (RH) and at 40 °C with 75 % RH for 30 and 45 days exhibited significant morphological alterations.

Higher temperatures induced morphological deformation and an increase in particle size due to polymer softening and nanoparticle aggregation. Stability was compromised at temperatures exceeding 30 °C, which underscores the necessity of maintaining storage temperatures between 2 and 8 °C (refrigerated) to preserve nanoparticle integrity [16,21].

After treating HL60 cells with FITC-labeled CNP and FITC-Apt-CNP for 12 and 24 h, the substantial increase of Apt-CNP uptake in HL60 leukemia cells compared to CNP treatment underscores the significant role of the aptamer in enhancing the internalization of the nanoformulation. The aptamer, designed to target the CD117 receptor on HL60 leukemia cells, effectively facilitated the targeted delivery and internalization of the nanoparticles. On the other hand, the significantly less uptake in U937 cells compared to HL60 cells highlights the specificity of the aptamer for CD117, a biomarker overexpressed in HL60 cells. Significantly less uptake in U937 cells was observed. This marked uptake data difference between HL60 and U937 cells confirms the specificity of aptamer-mediated targeting in CD117-overexpressing HL60 cells, emphasizing the potential of Apt-CNP for precise and effective drug delivery in CD117-overexpressing acute myeloid leukemia therapy. Compared to non-targeted CNP, these results underscore the enhanced efficacy of Apt-CNP in delivering the therapeutic formulation directly to CD117-overexpressed leukemia cells. Interestingly, floating, mobile neutrophils (HL60 cells) were very effectively targeted by Apt-CNP. It may be that the neutrophils which had a predominant role in phagocytosis could detect the Apt-CNP more effectively due to the binding of aptamer and the cell surface receptor CD117, and closed proximity might internalize more Apt-CNP in HL60 leukemia cells. This targeted approach improved the cellular uptake of the drug and potentially enhanced its therapeutic effects while minimizing off-target effects.

IC₅₀, or the half-maximal inhibitory concentration, is a crucial pharmacological indicator that quantifies the concentration of a substance required to inhibit a specific biological process or target by 50 %. In evaluating the cytotoxicity of a compound in cancer cells, a lower IC₅₀ value indicates a greater potency. The MTT assay is the minimal amount of a substance necessary to achieve a 50 % reduction in cell viability or function, underscoring its efficacy at lower doses. Here, the MTT assay results highlight the superior therapeutic efficacy of Apt-CNP in HL60 cells, proving its potential as a targeted drug delivery system for CD117-overexpressing AML cells. The study investigated the effects of a free drug and experimental nanoparticles on the viability of HL60 cells, U937 cells, and normal PBMC cells. The Apt-CNP nanoparticles demonstrated the highest toxicity towards HL60 cells, with the lowest IC₅₀ value. The IC₅₀ was 1.30 μ M for the CNP formulation, and for the Apt-CNP formulation, it was reduced to 1.07 μ M in HL60 cells. In U937 cells, the absence of substantial improvement in cytotoxicity with Apt-CNP over CNP confirms the lack of specificity of the aptamer-mediated delivery system, to U937 cells, which lack CD117 expression. This reinforces the targeted nature of the formulation, which is tailored to exploit CD117 overexpression in HL60 cells. Moreover, the lack of cytotoxicity in PBMC cells underscores the safety profile of the nanoformulation, demonstrating its potential to minimize off-target effects and preserve normal cell viability [36]. This indicates that the nanoformulation, Apt-CNP, was more effective in reducing cell viability in HL60 cells and provides a promising strategy for selective AML therapy.

Apoptosis, the body's programmed cell death, is a crucial action for anticancer agents [37]. The apoptosis-inducing effects of clofarabine, CNP, and Apt-CNP were assessed here. The results emphasize the selective efficacy of Apt-CNP in inducing apoptosis in CD117-overexpressing HL60 cells. Apt-CNP was notably more effective in inducing apoptosis compared to clofarabine and CNP. The present findings highlight the superior apoptotic efficacy of Apt-CNP, with the highest proportion of cells undergoing early apoptosis and a notable percentage also progressing to late apoptosis. This suggests that Apt-CNP is highly effective in triggering apoptotic cell death in HL60 cells, reinforcing its potential as a potent chemotherapeutic agent with a strong cytotoxic impact. U937 cells lack CD117 overexpression and showed the absence of substantial enhancement in apoptotic induction by Apt-CNP compared to CNP. It further reinforces the specificity of the aptamer-mediated targeting mechanism. This selectivity improves therapeutic precision and minimizes off-target effects, a key requirement for effective cancer therapy. The enhanced apoptosis induction by Apt-CNP emphasizes its promising role in targeting CD117 receptors, making it a valuable candidate for further development and clinical testing in cancer therapy.

JC-1, a cationic dye, is a critical tool for evaluating alteration of mitochondrial membrane potential [38]. When JC-1 accumulates in mitochondria at high mitochondrial membrane potentials, it forms J-aggregates that emit red fluorescence. In contrast, depolarized or significantly less polarized mitochondria remain in their monomeric form in the cytosol, emitting green fluorescence [30]. Apt-CNP maximally depolarized mitochondrial membrane potential, leading to mitochondrial dysfunction and apoptosis in HL60 cells compared to free drug and CNP treatments. The enhanced mitochondrial depolarization observed with Apt-CNP underscores its

potential as a more effective therapeutic agent in inducing apoptosis [13], thus offering valuable insights for future therapeutic strategies targeting mitochondrial dysfunction in cancer cells.

Based on the data obtained from U937 cells, a clear pattern emerges, highlighting the nonspecific interaction of the formulations because of the absence of CD117 expression. While U937 cells showed some uptake of both CNP and Apt-CNP, as well as moderate cytotoxicity and apoptosis induction, the differences between these formulations are relatively minor. This lack of significant targeting for Apt-CNP in U937 cells accentuates the specificity of the aptamer for CD117-positive cells, such as HL60. Hence, no further study was conducted with U937 cells to investigate mitochondrial membrane potential. The lack of a JC-1 assay for U937 cells does not undermine the overall conclusions, as the current data clearly illustrate the selective targeting efficiency of Apt-CNP.

Due to constraints in experimental conditions, we could not explore the targeting of AML through in vivo experiments. It is worthwhile to investigate in vivo animal models such as xenograft techniques. Additionally, in vitro cell culture experiments can be enhanced by incorporating normal blood cells alongside AML cancer cells, providing a more comprehensive understanding of the targeted delivery to leukemic cells.

5. Conclusion

In conclusion, compared to non-conjugated formulations, CD117-specific aptamer conjugated clofarabine-loaded PLGA nanoparticles significantly improved cellular internalization in floated HL60 leukemia cells overexpressing CD117. This aptamer-nanoparticle formulation (Apt-CNP) enabled targeted drug delivery, resulting in superior in vitro therapeutic efficacy. These findings highlight the potential of aptamer-coupled nanoparticulate systems for targeted AML therapy. This novel nanoplatform not only showcases the significant potential for improving AML treatment outcomes but also opens avenues for developing targeted therapies for other hematologic malignancies. Further studies are warranted.

CRedit authorship contribution statement

Manisheeta Ray: Data curation, Formal analysis, Investigation, Methodology, Writing – original draft. **Ashique Al Hoque:** Software, Validation, Visualization, Writing – review & editing. **Saptarshi Chatterjee:** Investigation, Methodology. **Sourav Adhikary:** Software, Visualization. **Samrat Paul:** Data curation, Resources. **Biswajit Mukherjee:** Conceptualization, Funding acquisition, Project administration, Supervision, Visualization, Writing – review & editing. **Amitava Bhattacharya:** Resources, Supervision.

Funding

This study was supported by Dr. V. Ravichandran Center for Advanced Research in Pharmaceutical Sciences (CARPS), Jadavpur University. Grant no. CARPS/RA/01/2021. MR received the CARPS research fellowship.

Declaration of competing interest

The authors declare that they have no known competing financial interests or personal relationships that could have appeared to influence the work reported in this paper.

Acknowledgements

We also express our heartfelt gratitude to Dr. Amitava Sengupta, Senior Principal Scientist and Associate Professor of biological sciences, AcSIR, specializing in Cancer Biology and Inflammatory Disorders, for generously providing us with U937 cell line essential for our study.

Abbreviations:

CNP	Clofarabine nanoparticles
Apt-CNP	Aptamer conjugated clofarabine nanoparticles
PLGA	Poly (lactic-co-glycolic acid)
FESEM	Field Emission Scanning Electron Microscopy
HR-TEM	High-Resolution Transmission Electron Microscopy
FTIR	Fourier Transform Infrared Spectroscopy
AFM	Atomic Force Microscopy
FITC	Fluorescein isothiocyanate
PI	Propidium Iodide

Appendix A. Supplementary data

Supplementary data to this article can be found online at <https://doi.org/10.1016/j.heliyon.2025.e42450>.

References

- [1] M.S. Shafat, B. Gnanewaran, K.M. Bowles, S.A. Rushworth, The bone marrow microenvironment – home of the leukemic blasts, *Blood*, Rev. 31 (2017) 277–286, <https://doi.org/10.1016/j.blre.2017.03.004>.
- [2] E.I. Obeagu, Q. Babar, Acute myeloid leukaemia (AML): the good, the bad, and the ugly. <https://doi.org/10.22192/ijcrms.2021.07.07.004>, 2021.
- [3] W.B. Parker, V. Gandhi, Clofarabine: structure, mechanism of action, and clinical pharmacology, in: *Chemotherapy for Leukemia: Novel Drugs and Treatment*, Springer Singapore, 2017, pp. 261–286, https://doi.org/10.1007/978-981-10-3332-2_16.
- [4] P.L. Bonate, L. Arthaud, W.R. Cantrell, K. Stephenson, J.A. Secrist, S. Weitman, Discovery and development of clofarabine: a nucleoside analogue for treating cancer, *Nat. Rev. Drug Discov.* 5 (2006) 855–863, <https://doi.org/10.1038/nrd2055>.
- [5] M.J. Mauro, M.W. Deininger, Management of drug toxicities in chronic myeloid leukaemia, *Best Pract. Res. Clin. Haematol.* 22 (2009) 409–429, <https://doi.org/10.1016/j.beha.2009.06.001>.
- [6] S. Correa, E.C. Dreaden, L. Gu, P.T. Hammond, Engineering nanolayered particles for modular drug delivery, *J. Control. Release.* 240 (2016) 364–386, <https://doi.org/10.1016/j.jconrel.2016.01.040>.
- [7] F. Danhier, E. Ansorena, J.M. Silva, R. Coco, A. Le Breton, V. Préat, PLGA-based nanoparticles: an overview of biomedical applications, *J. Control. Release.* 161 (2012) 505–522, <https://doi.org/10.1016/j.jconrel.2012.01.043>.
- [8] J.M. Anderson, M.S. Shive, *Biodegradation and Biocompatibility of PLA and PLGA Microspheres*, 1997.
- [9] Y. Nur, S. Gaffar, Y.W. Hartati, T. Subroto, Applications of electrochemical biosensor of aptamers-based (APTASENSOR) for the detection of leukemia biomarker, *Sens. Biosensing. Res.* 32 (2021), <https://doi.org/10.1016/j.sbsr.2021.100416>.
- [10] J. Zhou, J. Rossi, Aptamers as targeted therapeutics: current potential and challenges, *Nat. Rev. Drug Discov.* 16 (2017) 181–202, <https://doi.org/10.1038/nrd.2016.199>.
- [11] A.D. Keefe, S. Pai, A. Ellington, Aptamers as therapeutics, *Nat. Rev. Drug Discov.* 9 (2010) 537–550, <https://doi.org/10.1038/nrd3141>.
- [12] N. Zhao, S.N. Pei, J. Qi, Z. Zeng, S.P. Iyer, P. Lin, C.H. Tung, Y. Zu, Oligonucleotide aptamer-drug conjugates for targeted therapy of acute myeloid leukemia, *Biomaterials* 67 (2015) 42–51, <https://doi.org/10.1016/j.biomaterials.2015.07.025>.
- [13] S. Chakraborty, Z.Y. Dlie, S. Chakraborty, S. Roy, B. Mukherjee, S.E. Besra, S. Dewanjee, A. Mukherjee, P.K. Ojha, V. Kumar, R. Sen, Aptamer-Functionalized drug nanocarrier improves hepatocellular carcinoma toward normal by targeting neoplastic hepatocytes, *Mol. Ther. Nucleic Acids* 20 (2020) 34–49, <https://doi.org/10.1016/j.omtn.2020.01.034>.
- [14] M. Iqbal, N. Zafar, H. Fessi, A. Elaissari, Double emulsion solvent evaporation techniques used for drug encapsulation, *Int. J. Pharm.* 496 (2015) 173–190, <https://doi.org/10.1016/j.ijpharm.2015.10.057>.
- [15] D. Dutta, A. Chakraborty, B. Mukherjee, S. Gupta, Aptamer-conjugated apigenin nanoparticles to target colorectal carcinoma: a promising safe alternative of colorectal cancer chemotherapy, *ACS Appl. Bio Mater.* 1 (2018) 1538–1556, <https://doi.org/10.1021/acsbm.8b00441>.
- [16] A. Al Hoque, D. Dutta, B. Paul, L. Kumari, I. Ehsan, M. Dhara, B. Mukherjee, M. Quadir, B.A. Kaipparettu, S. Laha, S. Ganguly, ΔPSap4#5 surface-functionalized abiraterone-loaded nanoparticle successfully inhibits carcinogen-induced prostate cancer in mice: a mechanistic investigation, *Cancer. Nanotechnol* 14 (2023), <https://doi.org/10.1186/s12645-023-00223-5>.
- [17] Y. Yan, H. Tao, J. He, S.Y. Huang, The HDock server for integrated protein–protein docking, *Nat. Protoc.* 15 (2020) 1829–1852, <https://doi.org/10.1038/s41596-020-0312-x>.
- [18] O.C. Farokhzad, J. Cheng, B.A. Teply, I. Sherifi, S. Jon, P.W. Kantoff, J.P. Richie, R. Langer, Targeted nanoparticle-aptamer-biocomplexes for cancer chemotherapy *in vivo*. www.pnas.org/cgi/doi/10.1073/pnas.0601755103, 2006.
- [19] M. Shahriari, S.M. Taghdisi, K. Abnous, M. Ramezani, M. Alibolandi, Self-targeted polymersomal co-formulation of doxorubicin, camptothecin and FOXM1 aptamer for efficient treatment of non-small cell lung cancer, *J. Control. Release.* 335 (2021) 369–388, <https://doi.org/10.1016/j.jconrel.2021.05.039>.
- [20] Y. Herdiana, N. Wathoni, S. Shamsuddin, M. Mughtaridi, Drug release study of the chitosan-based nanoparticles, *Heliyon* 8 (2022) e08674, <https://doi.org/10.1016/j.heliyon.2021.e08674>.
- [21] L. Kumari, I. Ehsan, A. Mondal, A. Al Hoque, B. Mukherjee, P. Choudhury, A. Sengupta, R. Sen, P. Ghosh, Cetuximab-conjugated PLGA nanoparticles as a prospective targeting therapeutics for non-small cell lung cancer, *J. Drug. Target* 31 (2023) 521–536, <https://doi.org/10.1080/1061186X.2023.2199350>.
- [22] A. Shirman, Z.E. Inamdar, H.Y. Patel, N.S. Shaikh, A.I. Manyar, H.A. Siddiqi, A.S. Shaheena, Determination of clofarabine by uv visible spectrophotometer and infra-red spectroscopy, *Int. J. Biol. Pharm. Allied Sci.* 9 (2020) 2085–2089, https://ijbps.com/pdf/2020/August/MS_IJBPA5_2020_5131.pdf.
- [23] G. Pattnaik, B. Sinha, B. Mukherjee, S. Ghosh, S. Mondal, T. Bera, Submicron-size biodegradable polymer-based didanosine particles for treating HIV at early stage: an *in vitro* study, *J. Microencapsul.* 29 (2012) 666–676, <https://doi.org/10.3109/02652048.2012.680509>.
- [24] I. Ehsan, L. Kumari, R. Sen, A. Al Hoque, B. Mukherjee, A. Mukherjee, P. Ghosh, S. Bhattacharya, J591 functionalized paclitaxel-loaded PLGA nanoparticles successfully inhibited PSMA overexpressing LNCaP cells, *J. Drug Deliv. Sci. Technol.* 75 (2022) 103689, <https://doi.org/10.1016/j.jddst.2022.103689>.
- [25] B.S. Satapathy, B. Mukherjee, R. Baishya, M.C. Debnath, N.S. Dey, R. Maji, Lipid nanocarrier-based transport of docetaxel across the blood brain barrier, *RSC Adv.* 6 (2016) 85261–85274, <https://doi.org/10.1039/c6ra16426a>.
- [26] A. Aravind, S.H. Varghese, S. Veeranarayanan, A. Mathew, Y. Nagaoka, S. Iwai, T. Fukuda, T. Hasumura, Y. Yoshida, T. Maekawa, D.S. Kumar, Aptamer-labeled PLGA nanoparticles for targeting cancer cells, *Cancer. Nanotechnol* 3 (2012) 1–12, <https://doi.org/10.1007/s12645-011-0024-6>.
- [27] E. Manthri, S. Azarbad, R. Farahzadi, S. Javanmardi, I. Vietor, Effect of rat bone marrow derived-mesenchymal stem cells on granulocyte differentiation of mononuclear cells as preclinical agent in cell based therapy, *Curr. Gene Ther.* 22 (2021) 152–161, <https://doi.org/10.2174/1566523221666210519111933>.
- [28] N. Jan, A. Madni, M.A. Rahim, N.U. Khan, T. Jamshaid, A. Khan, A. Jabar, S. Khan, H. Shah, *In vitro* anti-leukemic assessment and sustained release behaviour of cytarabine loaded biodegradable polymer based nanoparticles, *Life Sci.* 267 (2021), <https://doi.org/10.1016/j.lfs.2020.118971>.
- [29] R. Farahzadi, Z. Sanaat, A.A. Movassaghpour-Akbari, E. Fathi, S. Montazersaheb, Investigation of L-carnitine effects on CD44+ cancer stem cells from MDA-MB-231 breast cancer cell line as anticancer therapy, *Regen. Ther.* 24 (2023) 219–226, <https://doi.org/10.1016/j.reth.2023.06.014>.
- [30] D. Dutta, A. Al Hoque, B. Paul, J.H. Park, C. Chowdhury, M. Quadir, S. Banerjee, A. Choudhury, S. Laha, N. Sepay, P. Boro, B.A. Kaipparettu, B. Mukherjee, EpCAM-targeted betulinic acid analogue nanotherapy improves therapeutic efficacy and induces anti-tumorigenic immune response in colorectal cancer tumor microenvironment, *J. Biomed. Sci.* 31 (2024), <https://doi.org/10.1186/s12929-024-01069-8>.
- [31] J. Chen, X. Zhang, T. Singleton, F. Kiechle, Mitochondrial membrane potential change induced by Hoechst 33342 in myelogenous leukemia cell line HL-60, *Ann. Clin. Lab. Sci.* 34 (2004) 458–466.
- [32] B. Sinha, B. Mukherjee, G. Pattnaik, Poly-lactide-co-glycolide nanoparticles containing voriconazole for pulmonary delivery: *in vitro* and *in vivo* study, *Nanomedicine* 9 (2013) 94–104, <https://doi.org/10.1016/j.nano.2012.04.005>.
- [33] P. Harris, P. Ralph, Human leukemic models of myelomonocytic development: a review of the HL-60 and U937 cell lines, *J. Leukoc. Biol.* 37 (1985) 407–422, <https://doi.org/10.1002/jlb.37.4.407>.
- [34] M. Dhara, A. Al Hoque, R. Sen, D. Dutta, B. Mukherjee, B. Paul, S. Laha, Phosphorothioated amino-AS1411 aptamer functionalized stealth nanoliposome accelerates bio-therapeutic threshold of apigenin in neoplastic rat liver: a mechanistic approach, *J. Nanobiotechnology.* 21 (2023), <https://doi.org/10.1186/s12951-022-01764-4>.
- [35] J.A. Champion, Y.K. Katara, S. Mitragotri, Particle shape: a new design parameter for micro- and nanoscale drug delivery carriers, *J. Control. Release.* 121 (2007) 3–9, <https://doi.org/10.1016/j.jconrel.2007.03.022>.
- [36] V.V. Veselov, A.E. Nosyrev, L. Jicsinsky, R.N. Alyautdin, G. Cravotto, Targeted delivery methods for anticancer drugs, *Cancers* 14 (2022) 622, <https://doi.org/10.3390/cancers14030622>.
- [37] C. Yedjou, P. Tchounwou, J. Jenkins, R. McMurray, Basic mechanisms of arsenic trioxide (ATO)-induced apoptosis in human leukemia (HL-60) cells, *J. Hematol. Oncol.* 3 (2010) 28, <https://doi.org/10.1186/1756-8722-3-28>.
- [38] A. Mathur, Y. Hong, B.K. Kemp, A.A. Barrientos, J.D. Erusalimsky, Evaluation of fluorescent dyes for the detection of mitochondrial membrane potential changes in cultured cardiomyocytes a b c. www.elsevier.com/locate/cardioresearch.elsevier.nl/locate/cardioresearch, 2000.



Tailored Transdermal Drug Delivery System for Pain Management: Development and Evaluation of Clonidine Hydrochloride/Sodium Montmorillonite Composite Patch

Sourav Adhikary¹ · Ashique Al Hoque^{2,3} · Manisheeta Ray^{1,2} · Pritha Pal¹ · Mahua Ghosh Chaudhuri¹ · Rajib Dey⁴

Accepted: 9 April 2024

© The Author(s), under exclusive licence to Springer Science+Business Media, LLC, part of Springer Nature 2024

Abstract

Researchers are always coming up with new techniques and methods to ensure that drug delivery systems are secure, therapeutically efficient, and patient-compliant. Clay minerals are nanolayered silicates considered potential nanomaterials in medical research. They have been widely used as both active agents and excipients since ancient times for the treatment of various illnesses. Owing to their remarkable characteristics of high biocompatibility, loading capacity, retention capacity, rheological and swelling properties, and affordable price, they can be used as advanced carriers for the effective delivery of drugs by varying their release rate, boosting their stability, and improving their dissolution profile. Nowadays, drug delivery through the skin has received attention as an alternative to the oral route because the skin is a potential route to deliver local and systemic drugs as nanoparticles. In this research work, clonidine hydrochloride (CH) was chosen as a model drug that plays a major role in preventing post-operative pain (both acute and chronic). The epidural solution of clonidine is already available for cancer pain. The transdermal patches of clonidine are also available in different dosages, which are intended to be administered for 7 days to treat neuropathic pain. However, there is no availability of extended-release transdermal patches of clonidine to date for the treatment of several pains mentioned earlier. Therefore, an attempt was made to prepare such transdermal patches. The intercalation of CH into the interlayers of sodium montmorillonite (Na-MMT) nanoclay via three different methods was demonstrated. Freshly prepared CH/Na-MMT composites were utilized to fabricate the transdermal patches to examine the analgesic activity of the drug for an extended period in a single dose or not after entering systemic circulation via skin barriers. The composites and patches were characterized by Fourier-transform infrared (FTIR) spectroscopy, scanning electron microscopy (SEM), transmission electron microscopy (TEM), and X-ray diffraction (XRD). Sustained release of CH from CH/Na-MMT composites was observed for nearly 1 month during the *in vitro* release experiment. The results obtained from the *ex vivo* skin permeation study, as well as *in vivo* analgesic activity using those patches, corroborated the outcomes of the *in vitro* release study. Different kinetic models were applied to the *ex vivo* dissolution data to determine the best-fit kinetic model accompanied by drug release in both burst and sustained release periods.

Keywords Nanoclay · Transdermal patch · Sustained release · Skin permeation · Analgesic activity

✉ Sourav Adhikary
souravadhikary906@gmail.com

✉ Mahua Ghosh Chaudhuri
mahua.ghosh@jadavpuruniversity.in

✉ Rajib Dey
rajib.dey@gmail.com

¹ School of Materials Science and Nanotechnology, Jadavpur University, 700032 Kolkata, India

² Department of Pharmaceutical Technology, Jadavpur University, 700032 Kolkata, India

³ Department of Coatings and Polymeric Materials, North Dakota State University, Fargo, ND 58108, USA

⁴ Metallurgical and Material Engineering Department, Jadavpur University, 700032 Kolkata, India



Investigation of Paracetamol Entrapped Nanoporous Silica Nanoparticles in Transdermal Drug Delivery System

Sourav Adhikary¹ · Ashique Al Hoque^{2,3} · Manisheetta Ray² · Swastik Paul⁴ · Akbar Hossain⁵ · Subrata Goswami⁶ · Rajib Dey⁷

Accepted: 24 May 2023

© The Author(s), under exclusive licence to Springer Science+Business Media, LLC, part of Springer Nature 2023

Abstract

An effort was made to administer paracetamol drug through transdermal patch, as no such formulation of this drug has been developed yet. The primary cause for the lack of such formulations is paracetamol's poor aqueous solubility. As a result, the current research concentrated on preparing nanomedicines, or drug-loaded nanoparticles, for delivery via transdermal formulations. Nanoparticles can improve the solubility of weakly aqueous soluble or even aqueous insoluble drugs by changing the crystalline structure of loaded medicines to an amorphous state and serving as drug permeation boosters. Silica nanoparticles (SNPs) were synthesized through sol-gel technique to achieve the aforementioned goal. DLS data revealed that the average particle size was around 100–200 nm, which was sufficient to penetrate the skin barrier. XRD analysis showed that the SNPs were amorphous, and the drug molecules lost their crystallinity after encapsulation into the nanoparticles, causing the enhancement of dissolution of drug molecules in physiological pH (pH=7.4). Different kinetic models were employed for the *ex vivo* dissolution data to evaluate the suitable kinetic model followed by the drug release in both burst and sustained phase. *In vivo* analgesic study was executed on mice applying each of the transdermal formulations to examine the performances of the patches.

Keywords Silica nanoparticles · Transdermal patch · Sustained release · Skin permeation · Analgesic activity

✉ Sourav Adhikary
SOURAVADHIKARY906@GMAIL.COM

¹ School of Materials Science and Nanotechnology, Jadavpur University, Kolkata, India

² Department of Pharmaceutical Technology, Jadavpur University, Kolkata, India

³ Department of Coatings and Polymeric Materials, North Dakota State University, Fargo, ND 58108, USA

⁴ Department of Chemical Engineering, University of Calcutta, Kolkata, India

⁵ Department of Chemistry, Jadavpur University, Kolkata, India

⁶ Department of Labour, ESI Institute of Pain Management, Kolkata, India

⁷ Metallurgical and Material Engineering Department, Jadavpur University, Kolkata, India



Nanocosmeceuticals

Innovation, Application, and Safety

2022, Pages 327-345

Chapter 12 - Nonionic surfactant nanovesicles for cosmeceutical applications

Biswajit Mukherjee^a, Lopamudra Dutta^{b, *}, Leena Kumari^a, Manasadeepa Rajagopalan^c,
Sanchari Bhattacharya^d, Manisheeta Ray^a, Shreyasi Chakraborty^e

Show more ▾

☰ Outline | 🔗 Share 🗣️ Cite

<https://doi.org/10.1016/B978-0-323-91077-4.00015-6> ↗

[Get rights and content](#) ↗

Abstract

Cosmeceutical is considered one of the most promising areas, and its use has been increased drastically in the past few years due to personal awareness. Nanotechnology is the recent progress of the cosmeceutical industry and has been observed as a safe delivery system for active pharmaceutical ingredients. Because of the unique physical and chemical properties, nanostructured substances gained recognition and attention. Nonionic surfactant-based nanovesicles, i.e., niosome, are primarily composed of cholesterol and a nonionic surfactant such as polysorbate 80. Niosome is the area of interest for the cosmeceutical industry because of its better dermal penetration property, biocompatibility, nontoxicity, etc. Niosome is found to be useful in various conditions related to pigmentation, wrinkles, aging of the skin, hair loss, and nail care. Few formulations and patents are available still now though many are in research. This chapter outlines a brief idea about surfactant-based nanosize liposome, mainly nonionic surfactant-based liposome (niosome), the advantages and disadvantages of niosomal cosmeceuticals, their applications, and also some related available patents, and marketed cosmeceuticals.

[Recommended articles](#)

References (0)

Hepatocellular Carcinoma: Diagnosis, Molecular Pathogenesis, Biomarkers, and Conventional Therapy

Biswajit Mukherjee^{*},¹, Manasadeepa Rajagopalan², Samrat Chakraborty¹, Prasanta Ghosh¹, Manisheetta Ray¹, Ramkrishna Sen¹ and Iman Ehsan¹

¹ *Department of Pharmaceutical Technology, Jadavpur University, Kolkata 700032, India*

² *East West College of Pharmacy, Bangalore, Karnataka 560091, India*

Abstract: Hepatocellular carcinoma (HCC), the most common liver malignancy, has been a significant cause of cancer-related deaths worldwide. Cirrhosis, hepatic viral infections, fatty liver, and alcohol consumption are notable risk factors associated with HCC. Furthermore, a crucial challenge in the therapeutic management of HCC patients is the late-stage diagnosis, primarily due to the asymptomatic early stage. Despite the availability of various preventive techniques, diagnoses, and several treatment options, the mortality rate persists. Ongoing investigation on exploring molecular pathogenesis of HCC and identifying different prognostic and diagnostic markers may intervene in the conventional mode of treatment option for better therapeutic management of the disease. Subsequently, tumor site and its size, extrahepatic spread, and liver function are the underlying fundamental factors in treating treatment modality. The development in both surgical and non-surgical methods has resulted in admirable benefits in the survival rates. Understanding the mechanism(s) of tumor progression and the ability of the tumor cells to develop resistance against drugs is extremely important for designing future therapy concerning HCC. This chapter has accumulated the current literature and provided a vivid description of HCC based on its classification, risk factors, stage-based diagnosis systems, molecular pathogenesis, prognostic/diagnostic markers, and the existing conventional treatment approaches.

Keywords: Cellular signaling pathway, Cirrhosis, HCC molecular pathogenesis, HCC- prognostic/diagnostic markers, HCC risk factors, Hepatocellular carcinoma (HCC), cell signaling during HCC development, Ongoing therapy against HCC, Stage-based diagnosis, Tumor microenvironment.

^{*} **Corresponding author Biswajit Mukherjee:** Department of Pharmaceutical Technology, Jadavpur University, Kolkata 700032, India; Tel/Fax: +913324146677; Emails: biswajit55@yahoo.com, biswajit.mukherjee@jadavpuruniversity.in



Biopolymer-Based Nanomaterials in Drug Delivery and Biomedical Applications

2021, Pages 143-164

Chapter 6 - Guar gum-based nanomaterials in drug delivery and biomedical applications

Biswajit Mukherjee, Leena Kumari, Iman Ehsan, Prasanta Ghosh, Soumyabrata Banerjee, Samrat Chakraborty, Manisheeta Ray, Ashique Al Hoque, Ratan Sahoo

Show more ▾

☰ Outline | 🔗 Share 🗣️ Cite

<https://doi.org/10.1016/B978-0-12-820874-8.00016-6> ↗

[Get rights and content](#) ↗

Abstract

Guar gum is a natural polymer possessing various unique features such as biodegradability, biocompatibility, biosafety, etc. and it is widely used in various biomedical industries. However, the native form of guar gum exhibits difficulties in formulating biomedical devices due to its excessive swelling ability, instability, and likelihood of microbial contamination. These drawbacks could be overcome by tailoring the functional groups of guar gum to accomplish its derivatives with improved physicochemical properties. The various derivatizations of guar gum include cross-linking, carboxymethylation, amination, and grafting with other natural, synthetic, or semisynthetic polymers. Recently, various modified forms of guar gum are exploited to develop an array of nanomaterials for biomedical applications. In this book chapter, we have summarized the source and physicochemical properties of guar gum, its modification approaches, and its utilization in nanomaterial fabrication for drug delivery and biomedical applications. The limitations and future scopes of such nanomaterials are also discussed.

[Recommended articles](#)

References (0)

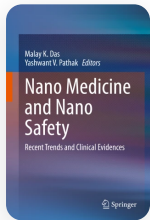
Cited by (8)

[Home](#) > [Nano Medicine and Nano Safety](#) > Chapter

Transdermal Nanomedicines for Reduction of Dose and Site-Specific Drug Delivery

| Chapter | First Online: 10 December 2020

| pp 175–211 | [Cite this chapter](#)



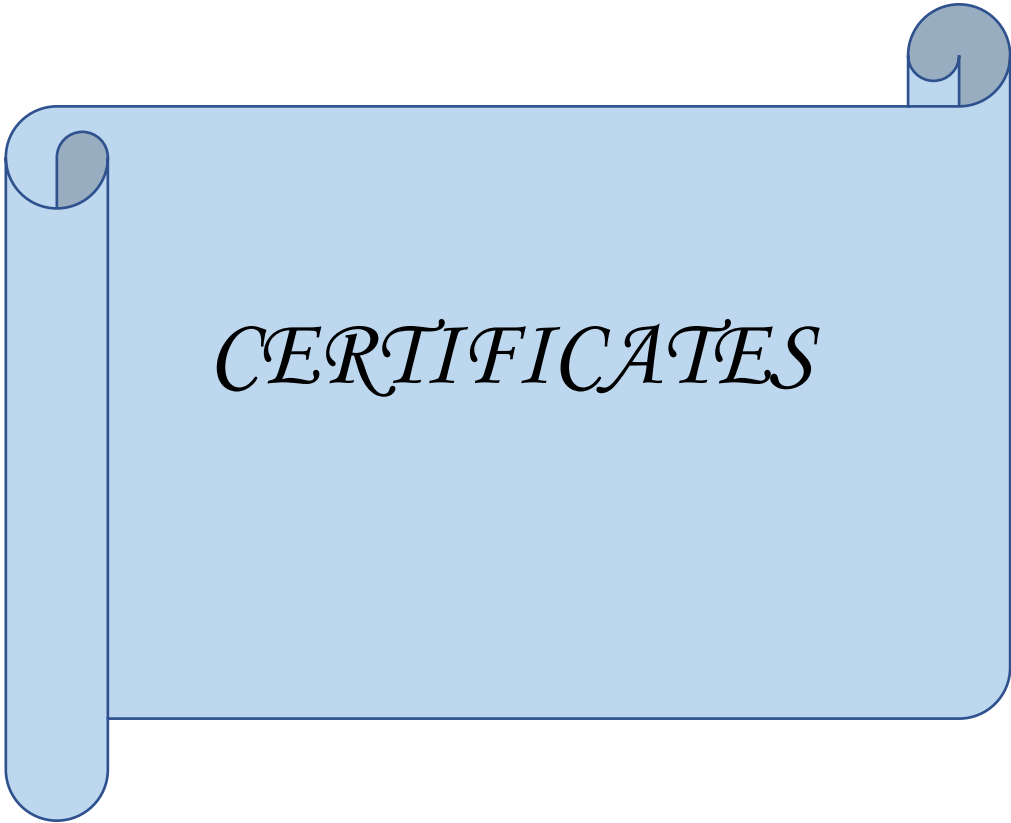
Nano Medicine and Nano Safety

[Biswajit Mukherjee](#), [Soma Sengupta](#), [Soumyabrata Banerjee](#), [Moumita Dhara](#), [Ashique Al Hoque](#), [Leena Kumari](#), [Manisheet Ray](#), [Iman Ehsan](#) & [Alankar Mukherjee](#)

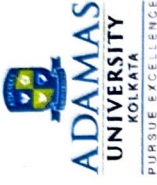
 565 Accesses

Abstract

The emergence of new technologies provides unique opportunities to exploit novel approaches in drug delivery. Transdermal drug delivery systems (TDDS) are one of the imperative technologies of increasing interest with the benefits of sustained/controlled drug delivery leading to patient convenience and compliance. By definition, TDDS are topically administered medications, for example, patches or semisolids, which permeate the active ingredient through the intact skin for systemic effects in a sustained manner. Transdermal drug deliveries, therefore, are the noninvasive administration of active ingredients from the skin surface across its layers, to the systemic circulation.



CERTIFICATES



HEALTHMEDICON 2025
INTERNATIONAL CONFERENCE
ON

**UNVEILING OPPORTUNITIES IN GLOBAL HEALTHCARE LANDSCAPE: SCIENTIFIC
ADVANCEMENTS, INNOVATIONS & RECENT TRENDS**

ORGANIZED BY

**SCHOOL OF HEALTH & MEDICAL SCIENCES, ADAMAS UNIVERSITY, KOLKATA, INDIA IN
COLLABORATION WITH UNIVERSITI TEKNOLOGI MARA (UITM), MALAYSIA**

CERTIFICATE OF AWARD



This is to certify that Prof./ Dr./ Mr./ Ms *Manishketa Ray*..... has been awarded the best **Oral/Poster** from *Dept. of Pharmaceutical Technology, Jadavpur University*..... presentation in 4th INTERNATIONAL CONFERENCE (HEALTHMEDICON 2025) held on 30- 31 January, 2025 organized by School of Health and Medical Sciences, Adamas University, Kolkata, India.

Rudra Prasad Saha

Prof. (Dr.) Rudra Prasad Saha
Dean (Officiating), SoHMS
Adamas University
CHAIRMAN, HEALTHMEDICON 2025

Wong Tin Wui

Prof.(Dr.) Wong Tin Wui
Professor
Department of Pharmacy
Universiti Teknologi MARA - Malaysia

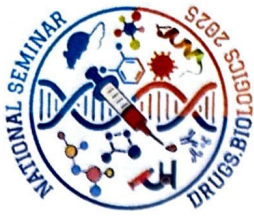
Biswajit Basu

Prof. (Dr.) Biswajit Basu
Professor, SoHMS
Adamas University
CONVENER, HEALTHMEDICON 2025



CENTRAL UNIVERSITY OF KERALA

DEPARTMENT OF BIOCHEMISTRY AND MOLECULAR BIOLOGY,
PERIYE, KASARAGOD-671325



NATIONAL SEMINAR ON DRUGS AND BIOLOGICS: DISCOVERY, DEVELOPMENT AND CLINICAL EVALUATION

Certificate

This is to certify that Mr./Ms.*Manisheetta Ray*..... has been conferred the **Best Poster/ Oral presentation award** during the **NATIONAL SEMINAR** on **'DRUGS AND BIOLOGICS: DISCOVERY, DEVELOPMENT AND CLINICAL EVALUATION'** held at Central University of Kerala, Periyee on March 24 & 25, 2025


Prof. R. Aswati Nair
Convener

Head, Department of Biochemistry and Molecular Biology
Central University of Kerala, Kasaragod


Prof. Sudha Kappalli
Chairperson

Dean, School of Biological Sciences
Central University of Kerala, Kasaragod


Prof. Rajendra Pilankatta
Organizing Secretary

Department of Biochemistry and Molecular
Biology, Central University of Kerala, Kasaragod

**INTERNATIONAL SEMINAR on
"MODERN MEDICINE AND RATIONAL USE OF MEDICINE-A CHALLENGE"**
*Dr. Triguna Sen Memorial Hall, Jadavpur University, Kolkata, India
17th January, 2025*

Certificate

Prof. / Dr. / Mr. / Mrs. / Miss *Manisheta Ray*

has attended the INTERNATIONAL CONFERENCE 2025 on "MODERN MEDICINE AND RATIONAL USE OF MEDICINE-A CHALLENGE" as a STUDENT/RESEARCH SCHOLAR/IAPST MEMBER/DELEGATE/FACULTY/INDUSTRY /ACCOMPANIED PERSON and presented a SCIENTIFIC (ORAL/POSTER) PRESENTATION

Jointly organized by:



INDIAN ASSOCIATION OF
PHARMACEUTICAL SCIENTISTS AND
TECHNOLOGISTS (IAPST), KOLKATA,
INDIA

Prof. N. Udupa
President
IAPST



COMMUNITY DEVELOPMENT
MEDICINAL UNIT (CDMU),
KOLKATA & ODISHA, INDIA

Dr. Ketaki Das
Secretary
CDMU



DR. V. RAVICHANDRAN CENTER FOR ADVANCED
RESEARCH IN PHARMACEUTICAL SCIENCES,
JADAVPUR UNIVERSITY (CARPS), KOLKATA, INDIA

Prof. Biswajit Mukherjee
Coordinator
CARPS



WEST BENGAL VOLUNTARY
HEALTH ASSOCIATION
Working together for Health, Education &
Livelihood towards attaining values of life.
WEST BENGAL VOLUNTARY
HEALTH ASSOCIATION (WBVHA),
KOLKATA, INDIA

Mr. Biswanath Basu
Project Director
WBVHA



M. 2024

CERTIFICATE OF PARTICIPATION

This is to award Mr. / Ms. **MANISHĒTA RAY**.....
from **JADAVPUR UNIVERSITY**.....
with the certificate of participation in the event(s) **SCROLL (PAPER
PRESENTATION)** held under the auspices of METALLIX'24, the annual
national symposium for Metallurgical and Material Engineering students at
Jadavpur University, organized on 15th and 16th March, 2024.

Md Basiruddin Sk

Dr. Md. Basiruddin. Sk
Convener, Metallix 2024
Dept. of Met & Mat Engg.
Jadavpur University

Sathi Banerjee

Dr. S. Banerjee
Jt Convener, Metallix 2024
Dept. of Met & Mat Engg.
Jadavpur University



NATIONAL SEMINAR
"Advancing Healthcare Through Pharmaceutical and Biomedical Application"
Jadavpur University, Kolkata

19th January, 2024



CERTIFICATE

This is to certify that has attended the National Seminar on "Advancing Healthcare Through Pharmaceutical and Biomedical Application" as a Delegate / Resource Person / Chairperson of a Session / Co-Chairperson of a session / presented a scientific Poster / Oral presentation organised by Dr. N. Ravi Chandran Centre for Advanced Research in Pharmaceutical Sciences, IIT & Indian Association of Pharmaceutical Scientists and Technologists, Kolkata, at Dr. H. L. Roy Auditorium, Jadavpur University, Kolkata

(Signature)

Prof. N Udupa
President
IAPST, Kolkata

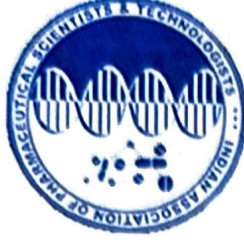
(Signature)

Prof. (Dr.) Biswajit Mukherjee
Secretary, Organising Committee

Professor, Department of Pharm. Tech., Jadavpur University

INTERNATIONAL SEMINAR ON

"EMERGING FIELDS OF RESEARCH IN BIOTECHNOLOGY & BIOMEDICINE"



CERTIFICATE OF APPRECIATION

THIS CERTIFICATE RECOGNIZES THE CONTRIBUTION OF

Prof/Dr./Mr./Ms./Miss

as Invited Speaker/Chair Person/Co-Chair Person/Evaluator/Delegate/Presenter(Oral/Poster)
In the International Seminar Jointly Organized by Dr. V. Ravi Chandran Centre for Advanced
Research in Pharmaceutical Sciences, Jadavpur University, Kolkata, India &
Indian Association of Pharmaceutical Scientists and Technologists (IAPST), Kolkata, India.
held at Jadavpur University, Kolkata, India on 16 November 2022.

Prof. Dr. Biswajit Mukherjee
Coordinator,
Dr. V. Ravi Chandran Centre for
Advanced Research in
Pharmaceutical Sciences, Jadavpur
University, Kolkata, India.



Dr. N. Udupa
President,
Indian Association of
Pharmaceutical Scientists
and Technologists (IAPST),
Kolkata, India.

PhD Thesis of Manisheeta Ray

ORIGINALITY REPORT

5%

SIMILARITY INDEX

PRIMARY SOURCES

- | | | |
|---|--|------------------|
| 1 | cancer-nano.biomedcentral.com
Internet | 127 words — < 1% |
| 2 | serval.unil.ch
Internet | 75 words — < 1% |
| 3 | Leena Kumari, Iman Ehsan, Arunima Mondal, Ashique Al Hoque et al. "Cetuximab-conjugated PLGA nanoparticles as a prospective targeting therapeutics for non-small cell lung cancer", Journal of Drug Targeting, 2023
Crossref | 57 words — < 1% |
| 4 | www.ingentaconnect.com
Internet | 56 words — < 1% |
| 5 | Debasmita Dutta, Apala Chakraborty, Biswajit Mukherjee, Sreya Gupta. "Aptamer-Conjugated Apigenin Nanoparticles To Target Colorectal Carcinoma: A Promising Safe Alternative of Colorectal Cancer Chemotherapy", ACS Applied Bio Materials, 2018
Crossref | 51 words — < 1% |
| 6 | www.mdpi.com
Internet | 51 words — < 1% |
| 7 | Sourav Adhikary, Ashique Al Hoque, Manisheeta Ray, Pritha Pal, Mahua Ghosh Chaudhuri, Rajib Dey. "Tailored Transdermal Drug Delivery System for Pain Management: Development and Evaluation of Clonidine | 43 words — < 1% |